A HOLISTIC FRAMEWORK FOR EVALUATING THE SUSTAINABILITY OF THE WATER-ENERGY-FOOD-ECOSYSTEM NEXUS UNDER MULTIPLE SOCIOECONOMIC AND CLIMATE CHANGE CONDITIONS

A THESIS SUBMITTED TO
THE GRADUATE SCHOOL OF NATURAL AND APPLIED SCIENCES
OF
MIDDLE EAST TECHNICAL UNIVERSITY

BY

ZEYNEP ÖZCAN

IN PARTIAL FULFILLMENT OF THE REQUIREMENTS
FOR
THE DEGREE OF DOCTOR OF PHILOSOPHY
IN
ENVIRONMENTAL ENGINEERING

JUNE 2023

Approval of the thesis:

A HOLISTIC FRAMEWORK FOR EVALUATING THE SUSTAINABILITY OF THE WATER-ENERGY-FOOD-ECOSYSTEM NEXUS UNDER MULTIPLE SOCIOECONOMIC AND CLIMATE CHANGE CONDITIONS

submitted by **ZEYNEP ÖZCAN** in partial fulfillment of the requirements for the degree of **Doctor of Philosophy in Environmental Engineering, Middle East Technical University** by,

Prof. Dr. Halil Kalıpçılar
Dean, Graduate School of **Natural and Applied Sciences** _____

Prof. Dr. Bülent İçgen
Head of the Department, **Environmental Engineering** _____

Assoc. Prof. Dr. Emre Alp
Supervisor, **Environmental Engineering, METU** _____

Examining Committee Members:

Prof. Dr. Ayşegül Aksoy
Environmental Engineering, METU _____

Assoc. Prof. Dr. Emre Alp
Environmental Engineering, METU _____

Prof. Dr. Elçin Kentel Erdoğan
Civil Engineering, METU _____

Prof. Dr. Cevza Melek Kazezyılmaz Alhan
Civil Engineering, İstanbul Uni.- Cerrahpaşa _____

Prof. Dr. M. Levent Kavvas
Civil and Environmental Eng., UC Davis _____

Date: 05.06.2023

I hereby declare that all information in this document has been obtained and presented in accordance with academic rules and ethical conduct. I also declare that, as required by these rules and conduct, I have fully cited and referenced all material and results that are not original to this work.

Name Last name: Zeynep Özcan

Signature:

ABSTRACT

A HOLISTIC FRAMEWORK FOR EVALUATING THE SUSTAINABILITY OF THE WATER-ENERGY-FOOD-ECOSYSTEM NEXUS UNDER MULTIPLE SOCIOECONOMIC AND CLIMATE CHANGE CONDITIONS

Özcan, Zeynep
Doctor of Philosophy, Environmental Engineering
Supervisor: Assoc. Prof. Dr. Emre Alp

June 2023, 341 pages

Water scarcity, energy demand, declining crop yields, and environmental damage present interconnected challenges in the 21st century. This study addresses these issues through the Water-Energy-Food (WEF) nexus framework, focusing on the Sakarya Basin in Türkiye. The objective is to develop a methodology for evaluating the Water-Energy-Food-Ecosystem (WEFE) nexus under evolving climatic and socioeconomic conditions, while emphasizing the often-ignored ecosystem component. The proposed methodology incorporates cutting-edge climate projections and socioeconomic scenarios, employing dynamical downscaling and integrating them into a coupled water-energy systems model (WEAP-LEAP). The future climate projections were downscaled to 18 km resolution using the WRF model. Socioeconomic changes were captured through the application of the Shared Socioeconomic Pathways (SSPs) scenarios (SSP1, SSP2, and SSP5). The ecosystem component was assessed using a methodology inspired by the Index of Hydrologic Alteration (IHA) and Range of Variability Approach (RVA). Three scenarios (RCP4.5_SSP1, RCP4.5_SSP2, RCP8.5_SSP5) were developed to evaluate the impacts on WEFE nexus sectors. The overall WEFE Nexus Index values and pillar scores were calculated for the seven subbasins of the Sakarya Basin. The results indicate challenges in agricultural irrigation across almost all subbasins, regardless of the scenario. The tradeoff between the ecosystem and food pillars within the

WEFE Nexus is noteworthy, while the energy pillar consistently falls short of targets such as the Paris Agreement and renewable energy utilization. Limited utilization of hydropower potential exacerbates this issue. Prioritization based on subbasin characteristics is crucial, e.g., with a focus on sustainable agricultural strategies in agricultural subbasins, which can be further examined through smaller-scale studies. The developed WEFE Nexus Index can serve as a valuable tool for policy-making and public communication, enhancing understanding of the sustainability and security of the WEFE Nexus.

Keywords: Water-Energy-Food-Ecosystem Nexus, Climate Change, Sustainability, WEFE Nexus Index

ÖZ

SU-ENERJİ-GIDA-EKOSİSTEM BAĞININ SÜRDÜRÜLEBİLİRLİĞİNİN ÇOKLU SOSYOEKONOMİK VE İKLİM DEĞİŞİKLİĞİ KOŞULLARINDA DEĞERLENDİRİLMESİNE YÖNELİK BÜTÜNSEL BİR ÇERÇEVE

Özcan, Zeynep
Doktora, Çevre Mühendisliği
Tez Yöneticisi: Doç. Dr. Emre Alp

Haziran 2023, 341 sayfa

Su kıtlığı, enerji talebi, düşen mahsul verimleri ve çevresel hasar, 21. yüzyılın birbirine bağlı zorluklarıdır. Bu çalışma, Türkiye'deki Sakarya Havzası'na odaklanarak, bu sorunları Su-Enerji-Gıda (SEG) Bağı çerçevesinde ele almaktadır. Amaç, değişen iklimsel ve sosyoekonomik koşullar altında Su-Enerji-Gıda-Ekosistem (SEGE) Bağı'nı değerlendirmek için bir metodoloji geliştirmek ve bu değerlendirmeyi sıklıkla göz ardı edilen ekosistem bileşenini de dahil ederek yapmaktır. Önerilen metodoloji, iklim projeksiyonları ve sosyoekonomik senaryoları içermektedir. Ölçeği dinamik olarak küçültülen iklim projeksiyonları, su-enerji sistemleri modeline (WEAP-LEAP) entegre edilmiştir. Geleceğe yönelik iklim projeksiyonları, WRF modeli kullanılarak 18 km çözünürlüğe ölçeklendirilmiştir. Sosyoekonomik değişimler, Paylaşılan Sosyoekonomik Yollar (SSP) senaryoları (SSP1, SSP2 ve SSP5) uygulanarak ele alınmıştır. Ekosistem bileşeni, Hidrolojik Değişiklik Göstergeleri (HDG) ve Değişkenlik Aralığı Yaklaşımı (DAY) metodolojisinden esinlenerek değerlendirilmiştir. SEGE Bağı sektörleri üzerindeki etkileri değerlendirmek için üç senaryo (RCP4.5_SSP1, RCP4.5_SSP2, RCP8.5_SSP5) geliştirilmiştir. Sakarya Havzası'nın yedi alt havzası için genel SEGE Bağı İndeksi değerleri ve bileşenlerin puanları hesaplanmıştır. Sonuçlar, senaryo fark etmeksizin neredeyse tüm alt havzalarda tarımsal sulama konusunda zorluklar yaşanacağını göstermektedir. Ayrıca, SEGE Bağı içinde ekosistem ve gıda bileşenleri arasındaki ödünleşim dikkate değerdir. Enerji bileşeni ise Paris

Anlaşması ve yenilenebilir enerji kullanımı gibi hedeflere ulaşmada sürekli olarak eksik kalmaktadır. Hidroelektrik potansiyelinin sınırlı kullanımı bu sorunu daha da kötüleştirmektedir. Tarımsal alt havzalarda sürdürülebilir tarımsal stratejilere odaklanılması ve bunların etkinliğinin daha küçük ölçekli çalışmalarla daha ayrıntılı olarak incelenmesi gibi, alt havza özelliklerine dayalı olarak yönetim alternatiflerinin önceliklendirilmesi oldukça önemlidir. Geliştirilen SEGE Bağı İndeksi, politika oluşturma ve kamu ile iletişimde değerli bir araç olarak hizmet edebilir ve SEGE Bağı'nın sürdürülebilirliği ve güvenliği konusundaki anlayışı artırabilir.

Anahtar Kelimeler: Su-Enerji-Gıda-Ekosistem Bağı, İklim Değişikliği, Sürdürülebilirlik, SEGE Bağı İndeksi

To my mom and dad

ACKNOWLEDGMENTS

I would like to express my sincere appreciation and gratitude to the individuals who have provided their invaluable support and guidance throughout the completion of this thesis. First and foremost, I extend my deepest thanks to my advisor, Assoc. Prof. Dr. Emre Alp, for his motivating comments, insightful feedback, and continuous encouragement during my graduate study. I am also grateful to my dissertation committee members, Prof. Dr. Ayşegül Aksoy, Prof. Dr. Elçin Kentel Erdoğan, Prof. Dr. Cevza Melek Kazezyılmaz Alhan, and Prof. Dr. M. Levent Kavvas, for their valuable feedback and constructive suggestions.

I would like to acknowledge the Scientific and Technological Research Council of Türkiye (TÜBİTAK) for providing funding for the projects under grant numbers 116Y166 and 121R014.

I would like to express my gratitude to the Turkish Fulbright Commission for granting me the opportunity to complete a significant portion of my research on climate change as a Visiting Student Researcher at the University of California, Davis. Additionally, I would like to extend my thanks to Assoc. Prof. Dr. Ali Ercan, Dr. Tuan Trinh, Dr. Yoshihiko Iseri, and Dr. Yusuke Hiraga, with whom I had the privilege to collaborate at the Hydrologic Research Lab at UC Davis.

I extend my heartfelt appreciation to all my friends who accompanied me throughout this journey, providing support and assisting me in numerous ways. Their presence and assistance have been invaluable to me.

I am immensely grateful to my family, whose unwavering belief in me and constant encouragement have been instrumental throughout my life. I owe them my deepest gratitude, as none of my achievements would have been possible without their boundless love and patience.

TABLE OF CONTENTS

LIST OF TABLES

TABLES

LIST OF FIGURES

FIGURES

LIST OF ABBREVIATIONS

ABBREVIATIONS

DSİ: State Hydraulic Works

ET: Evapotranspiration

LAI: Leaf Area Index

LEAP: Low Emissions Analysis Platform

LULC: Land Use Land Cover

MGM: Turkish State Meteorological Service

OIZ: Organized Industrial Zones

RCP: Representative Concentration Pathway

RRF: Runoff Resistance Factor

RVA: Range of Variability Approach

SDGs: Sustainable Development Goals

SSPs: Shared Socioeconomic Pathways

SYGM: General Directorate of Water Management

TÜİK: Turkish Statistical Institute

WEAP: Water Evaluation and Planning System

WEFE: Water Energy Food Ecosystem

CHAPTER 1

INTRODUCTION

Water scarcity, soaring energy demand, and declining crop yields due to climate change threaten our ability to feed and support a growing global population sustainably. By 2050, it is estimated that worldwide water demand will increase by 55% (OECD, 2012). Furthermore, freshwater supplies are being depleted at an alarming rate. In the past 50 years, there has been an 83% decrease in global freshwater aquatic life, with freshwater fish populations experiencing a decline of 76% from 1970 to 2016 (WWF, 2022). Meanwhile, The Energy Information Administration's (EIA) International Energy Outlook 2021 forecasts that global energy consumption will increase by almost 50% from 2020 to 2050 if current policy and technological developments persist (IEA, 2021). And with crop yields projected to decline by up to 25% by 2050, food shortages and higher prices loom on the horizon (Mbow et al., 2019). It is clear that urgent action is needed to address these interconnected challenges and ensure a livable future for all.

The sustainable development goals (SDGs) set by the United Nations in 2015 aim to address urgent global challenges (United Nations, 2018). Water, energy, and food are three crucial resources that are essential for human well-being and sustainable development. Ensuring access to these resources is critical not only for individual livelihoods but also for achieving SDGs. The relationship between water, energy, and food security and the SDGs is multifaceted and complex. These resources are interconnected and interdependent, and their availability and access are affected by

various factors such as climate change, population growth, economic development, and technological change.

Recognizing the importance of the interlinkages between water, energy, and food security, the Water Energy Food (WEF) nexus approach has emerged as a new paradigm for sustainable resource management (Bazilian et al., 2011; Hoff, 2011). The WEF nexus approach acknowledges that the three resources are interconnected and cannot be managed in isolation. The WEF nexus approach has increasingly been adopted as a framework for research, technology, and policy to manage complex socio-environmental issues that demand enhanced scientific comprehension of feedback loops and interactions between human and natural systems. By aiming to comprehend the interconnections among these three systems, the WEF Nexus concept seeks to clarify the reasons and consequences of changes within and across these aspects (Jones et al., 2017). However, despite increasing recognition of its importance, significant challenges and knowledge gaps persist, such as inadequate data and information sharing, poor institutional coordination, and ineffective governance and financing mechanisms for WEF nexus initiatives. Furthermore, ecosystem services, which are essential for human well-being, are often excluded from nexus assessments. Urgent action is needed to address these challenges and ensure the WEF nexus approach is applied effectively and holistically to safeguard human and environmental well-being.

After conducting a comprehensive review of existing literature on WEF nexus assessment, it becomes evident that the significance of ecosystems is often undervalued (details in Chapter 2 in Section 2.3). It is crucial to highlight the essentiality of incorporating knowledge about ecosystem services into the analysis for ensuring the sustainability and security of WEF nexus components. The literature review shows that most studies in the field of WEF nexus fail to adopt a holistic perspective in this sense. Furthermore, there is a scarcity of studies that include

ecosystems as the fourth pillar of the nexus. Given these limitations, the objective of this PhD study is to conduct a thorough evaluation that encompasses all aspects of the nexus while acknowledging the pivotal role of ecosystem services. Therefore, this study places the ecosystem component at the core of the WEF nexus framework, leading the use of the term WEFE Nexus instead of WEF nexus.

To address these pressing issues and contribute to the development of effective solutions, this thesis study aims to develop a novel methodology that can effectively evaluate the WEFE Nexus in watersheds under evolving climatic and socioeconomic conditions of the 21st century. In addition, it aims to empower decision-makers with a comprehensive understanding of the risks and tradeoffs involved in the WEFE Nexus through the application of the developed methodology. Apart from its overall objective, this study aims to answer the following questions through a case study in the Sakarya Basin in Türkiye.

- How are the current water, energy, food, and ecosystem systems in the basin functioning?

- Can we identify any areas with particularly high water, energy, food, and ecosystem stress within the watershed?

- How will Türkiye's policies impact the Water-Energy-Food-Ecosystem (WEFE) Nexus?

The proposed methodology is designed to tackle the pressing challenges posed by climate change and socioeconomic factors on the intricate interplay of water, energy, food, and ecosystem components of the WEFE Nexus (details in Chapter 3). Unlike other studies that may overlook the importance of ecosystem sustainability, the approach considers every component of the nexus through integrated water-energy system modeling. By utilizing a range of carefully selected indicators, the approach provides a comprehensive evaluation of the sustainability status of each nexus

component. The overall nexus status is evaluated via WEFE Nexus Index which range between 0 and 1, corresponding to unsustainable and sustainable status, respectively. To comprise the uncertainties associated with the future changes in the climatic conditions, and economic and social aspects of the society, three different scenarios, i.e., RCP4.5_SSP1, RCP4.5_SSP2, and RCP8.5_SSP5, are evaluated via the developed methodology.

The remainder of this thesis is structured as follows: Chapter 2 provides background information and literature review, Chapter 3 presents the methodology employed in the study, Chapter 4 provides information on the study area, and Chapter 5 presents the WEAP-LEAP model setup in the Sakarya Basin, Chapter 6 describes the dynamical downscaling of climate projections, Chapter 7 provides the assessment of environmental flows in Sakarya Basin, i.e., the ecosystem nexus component, Chapter 8 describes the methodology followed to build WEAP-LEAP model for the 21st century, Chapter 9 presents the selection, normalization, weighting, and aggregation of WEFE Nexus indicators, and the results. Finally, Chapter 10 provides conclusions and recommendations.

CHAPTER 2

LITERATURE REVIEW

This chapter provides a comphrehensive analysis of the existing body of knowledge relating to the methodology developed within the scope of this study for the evaluation of the WEFE Nexus. The chapter begins with the definition of water, energy, and food security, and their relationship with the sustainable development goals. Then, the Water-Energy-Food nexus concept is described. Additionally, the chapter examines the role of ecosystems as the often ignored fourth pillar of nexus assessment, highlighting their significance in achieving sustainable outcomes. Furthermore, the chapter reviews the key scenarios represented by Representative Concentration Pathways (RCPs) and Shared Socioeconomic Pathways (SSPs) that shape the future of the WEFE Nexus. It also critically assesses various methods and approaches utilized in the assessment of the WEFE Nexus, alongside an exploration of the indicators employed to measure and evaluate its dynamics.

2.1 Water, Energy, and Food Security

Water, energy, and food security are three interrelated concepts that are critical to the well-being of individuals, communities, and societies around the world. Water security refers to the availability, accessibility, and quality of water for human use and consumption (UN Water, 2013). It is the assurance that people have access to sufficient quantities of safe and affordable water for drinking, cooking, and sanitation. Water security also includes the sustainability of water resources over

time, and the protection of water-related ecosystems. Energy security refers to the availability, reliability, and affordability of energy sources and their supply infrastructure (WWAP (United Nations World Water Assessment Programme), 2014). In addition, it means that the energy supply is resilient to external shocks, such as natural disasters or geopolitical conflicts. Energy security also includes the transition to clean and sustainable energy sources to mitigate climate change impacts. Food security refers to the availability, access, utilization, and stability of food for a population. It is the assurance that people have access to sufficient, safe and nutritious food to meet their dietary needs and preferences. Food security also includes the sustainability and resilience of food production systems, and the equitable distribution of food resources. Water, energy and food security are interrelated, as they are all fundamental to human well-being, sustainable development and climate resilience. Ensuring the security of these three resources requires a multi-dimensional and collaborative approach involving policy, planning, investment and innovation, at global, national and local levels (UN Water, 2015).

The Sustainable Development Goals are a set of 17 global goals adopted by the United Nations General Assembly in 2015 as part of the 2030 Agenda for Sustainable Development (United Nations, 2018). The goals are a call to action for all countries, organizations, and individuals to work towards a sustainable and equitable future for all. The SDGs cover a wide range of interconnected issues, including poverty, hunger, health, education, gender equality, clean water and sanitation, renewable energy, sustainable cities and communities, responsible consumption and production, climate action, biodiversity, peace, justice and strong institutions, and partnerships for sustainable development. Each goal is accompanied by a set of specific targets and indicators, designed to measure progress towards achieving the goal. The SDGs are intended to be universal, meaning that they apply to all countries, rich and poor, and are based on the principle of leaving no one behind. The 2030 Agenda for Sustainable Development and the SDGs represent a

bold and ambitious vision for a sustainable and equitable world, and are seen as critical to achieving a range of economic, social, and environmental objectives, as well as promoting peace, justice, and strong institutions (United Nations, 2022).

Water, energy, food security and sustainable development goals are interconnected. The United Nations Sustainable Development Goals (SDGs) provide a framework for understanding the interrelated nature of these issues and their importance for achieving sustainable development.

Water Security and SDGs:

Water security is directly linked to several of the SDGs, including SDG 6, which aims to ensure availability and sustainable management of water and sanitation for all. Water security is also essential for achieving SDGs related to health (SDG 3), food security (SDG 2), climate action (SDG 13) and biodiversity conservation (SDG 14 and 15).

Energy Security and SDGs:

Energy security is critical to achieving a number of SDGs, particularly SDG 7, which aims to ensure access to affordable, reliable, sustainable and modern energy for all. Access to energy is essential for achieving other SDGs, including poverty eradication (SDG 1), health (SDG 3), education (SDG 4), and climate action (SDG 13).

Food Security and SDGs:

Food security is central to achieving several SDGs, particularly SDG 2, which aims to end hunger, achieve food security and improved nutrition, and promote sustainable agriculture. Ensuring access to nutritious and safe food is critical for achieving other SDGs, including health (SDG 3), and poverty reduction (SDG 1).

Overall, the achievement of water, energy, and food security is essential for sustainable development, and these issues are deeply interconnected with a range of

other sustainable development goals. Addressing these issues in an integrated and holistic manner is crucial for achieving sustainable development and creating a more equitable and resilient world.

2.2 Water-Energy-Food (WEF) Nexus

The Water-Energy-Food (WEF) nexus is a concept that highlights the interdependent relationship between water, energy, and food. It recognizes that these systems are interconnected and mutually dependent, and that changes in one system can have significant impacts on the others. The WEF nexus approach seeks to understand and manage these interdependencies in a more integrated and holistic way, recognizing the trade-offs and synergies between water, energy, food, and ecosystems. It emphasizes the need for coordinated policies and management strategies that address these interconnections, enhance the resilience and sustainability of these systems, and promote more equitable and efficient resource use.

The WEF nexus concept emerged in response to debates and concerns about water and food crises, the perspectives of climate change, and the volatility of food and energy prices in the late 2000s. The concept was first introduced in the World Economic Forum in 2008 when prominent business leaders issued a “call to action” on the ways in which resource security across a WEF nexus and climate is linked to economic growth (Lazaro et al., 2022). The WEF nexus research agenda has drawn increasing attention since the 2011 Bonn conference, which highlighted the need to develop policies, strategies, and investments to maximize synergies and mitigate trade-offs, thus improving governance across nexus sectors (Hoff, 2011). Nexus thinking and resource management are imperative for achieving the United Nations Sustainable Development Goals.

The WEF nexus is a rapidly evolving and growing field of research, policy and practice, with numerous studies and initiatives being conducted across the world. There is increasing recognition of the need for a more integrated and holistic approach to the management of water, energy and food resources, particularly in the context of growing population, climate change and other global challenges. Many countries, international organizations and research institutions are now incorporating WEF nexus approaches into their policies and programs, and there is a growing emphasis on cross-sectoral collaboration and stakeholder engagement in the planning and implementation of WEF nexus projects. However, there are still significant challenges and knowledge gaps in the field, particularly in terms of data and information sharing, institutional coordination, and the development of effective governance and financing mechanisms for WEF nexus initiatives.

WEF Nexus Frameworks

The WEF Nexus is most commonly examined by constructing a theoretical framework that acknowledges the areas of convergence and conflict between the three systems. As a result, utilizing a Venn diagram is a popular method in WEF Nexus research (Jones et al., 2017). The studies in question consider the subjects that lie within the intersection of all three circles (such as those explored by Daher et al. in 2019 and Rodriguez in 2017) as well as the subjects that fall within the intersection of any two of the circles (for instance, Murrant's work in 2016 and Wang et al.'s research in 2019).

Figure 2-1 shows the conceptual framework developed by Hoff (2011) for the Bonn2011 Nexus Conference on the Water, Energy and Food Security Nexus. Hoff's framework places water at the center of the nexus and considers it as both a state and control variable. Water availability determines the availability of food and energy resources, and global trends such as urbanization, population growth and climate change impact water resources. The framework identifies finance, governance, and

innovation as key factors to enable progress towards water, energy, and food security for all, equitable and sustainable growth, and a resilient and productive environment. The framework focuses on society, economy and environment as action fields that can achieve these goals.

Figure 2-2 illustrates the approach to the nexus proposed by the World Economic Forum in 2011 (World Economic Forum WEF, 2011). The WEF systems are interconnected through the utilization of water and energy, and there are tradeoffs involved in the use of each system. Social changes such as population and economic growth, as well as environmental pressures, affect the nexus. The food system is also affected by the impacts of the nexus. The primary objective of the framework is to identify and communicate the risks associated with the nexus to decision-makers, enabling them to take swift and proactive action.

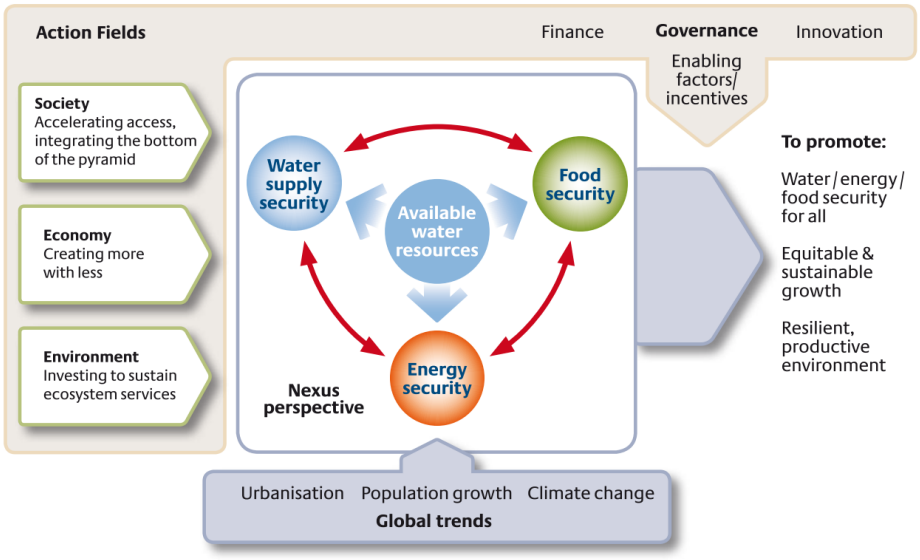

Figure 2-1. The water, energy and food security nexus Hoff (2011)

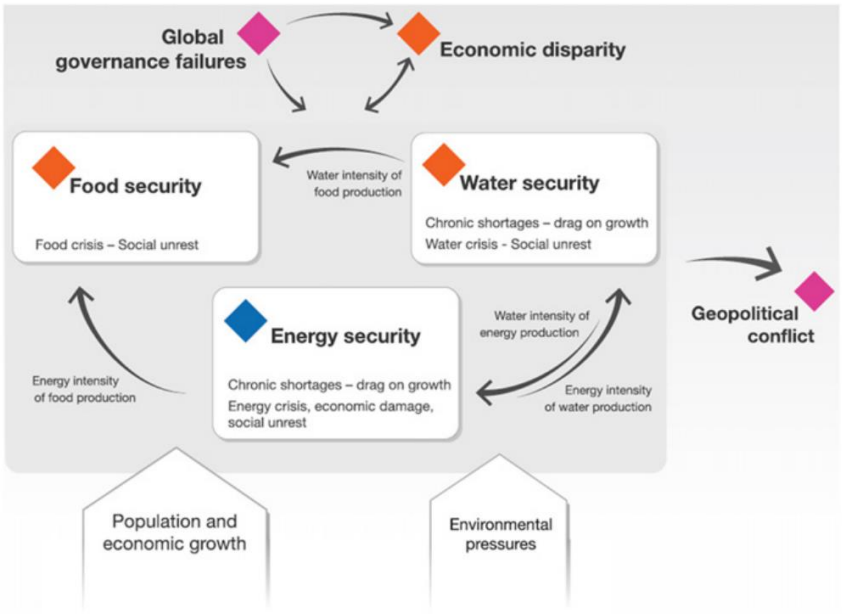

Figure 2-2. WEF nexus framework proposed by the World Economic Forum in 2011

Figure 2-3 shows the conceptual framework examined by Mohtar and Daher (2010). This framework differs from the one presented by Hoff (2011) in that none of the three systems is positioned at the nexus center. Furthermore, it differs from the approach articulated by the World Economic Forum (2011) in that all three systems are influenced and impacted by the nexus. The framework also highlights the relationships and tradeoffs between any two of the three systems through various human activities and decisions. Additionally, the framework identifies the external factors that influence the nexus, such as emerging economies, climate change, international trade, governance, and global population.

The final conceptual framework (Figure 2-4) is taken from Bizikova et al. (2013). Among the three conceptual frameworks mentioned, the one presented by Bizikova et al. (2013) is the most comprehensive. It was created by reviewing and synthesizing of numerous WEF Nexus conceptual models. The core elements of the framework

are the water, energy and food security. These independent securities are further divided into three aspects as utilization, access and availability. Then, the concentric rings which represent natural (e.g., riparian buffer management, wetlands for water purification etc.) and built (e.g., water treatment plants, constructed wetlands) systems are added to the framework. The natural and built systems affect access and the constant supply of water, energy and food. The final ring, institutions and governance, is the broadest one. It embraces all the other rings and it involves community networks, financial services, education, disaster recovery plans etc.

All of the WEF Nexus frameworks mentioned so far are similar to each other in terms of presenting a systems approach to find out the interconnections, overlaps and tradeoffs between the three systems. Governance, for instance, plays a critical role in all of the frameworks by affecting the all parts of the systems. In addition, global trends such as climate change and population growth are placed among the external factors influencing the nexus. However, there are also some differences. For instance, the core elements of the nexus are not always the same in these frameworks. While the availability of the water is located at the center of the nexus in Hoff's (2011) study, this is not the case for the others. Moreover, the framework presented by the World Economic Forum ignores the food for water and food for energy interconnections of the nexus, and elaborates the food system as the one impacted from the nexus. On the contrary, the others discuss all of the three systems by considering the fact that all of them both affect and are affected from the nexus.

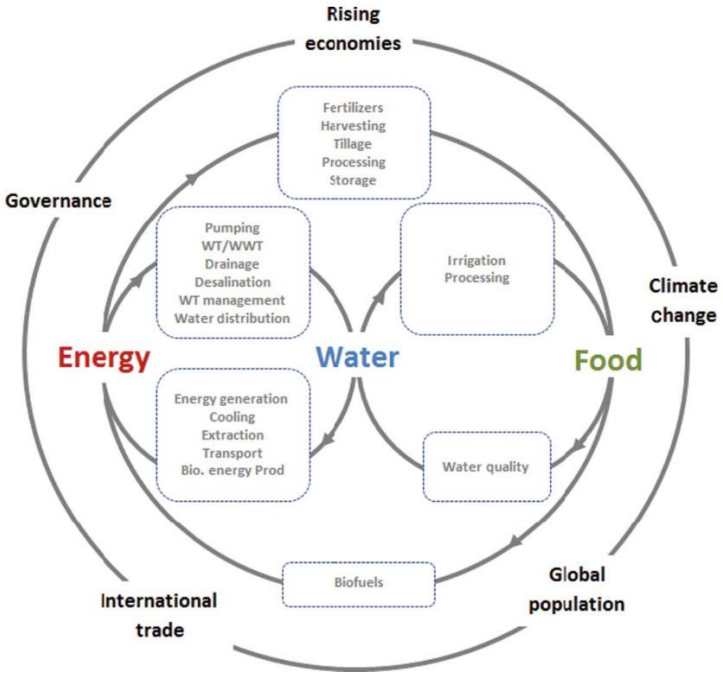

Figure 2-3. Water-energy-food nexus with effecting parameters (Mohtar and Daher, 2010)

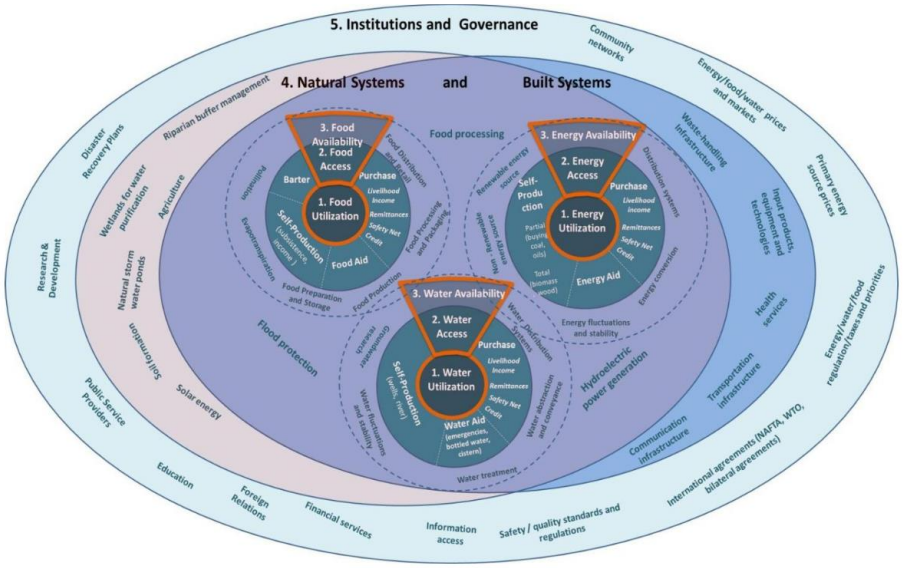

Figure 2-4. Overview of the framework linking water, food and energy security (Bizikova et al., 2013)

2.3 Ecosystem as a Fourth Pillar of the Nexus Assessments

Water-Energy-Food systems are interconnected. There are complex interrelations and interdependences between these three systems. Water-Energy-Food (WEF) nexus is a way to understand these complex interconnections so that the stakeholders' view of resources as individual assets is overcome. It is important to acknowledge that the current and future challenges on water-energy-food systems cannot be tackled by acting from the perspective of individual sectors. Although this idea is being acknowledged more and more, there are some discrepancies between the WEF Nexus related statements and practice. Moreover, ecosystems which provide essential services called ecosystem services are often not included in the nexus assessment.

Although ecosystem services are not among the pillars of the nexus assessment commonly, it is a major nexus component. The water sector benefits the ecosystem services provided by rivers, lakes, wetlands, and aquifers as the sources of freshwater as well as the sink for pollution from domestic and industrial usages. The agricultural sector profits from the ecosystem services, e.g., in terms of irrigation water and land use, and it affects them through changes in land use. Furthermore, the ecosystem services provide both the sources of energy such as fossil fuels and bioenergy and sinks for pollution, e.g., cooling water, air. There are a few studies which address ecosystem services as a fourth component other than water, energy and food in the nexus approach. Karabulut et al. (2019) developed Ecosystem Water Food Energy (EWFE) nexus concept in which the ecosystems and their services are defined as the fourth component of the nexus assessment which is compatible with the expression of Aichi Biodiversity targets. Hanes et al. (2018) emphasize that the continuity of the WEF nexus related activities depend on the maintenance of the efficiency of the ecosystem services and the prevention of the ecological degradation. They aim to design a system for co-producing food and energy under constraints on ecological

sustainability. To value the ecological sustainability, the agricultural, technological and ecological land uses are included in the co-production system superstructure. Garcia et al. (2019) integrated the ecosystem service valuation methods into the WEF nexus framework so that the bioenergy systems are designed in a way that the ecological damage is minimized and ecological restoration is maximized. Karabulut et al., (2016) map and evaluate water provisioning services and associated benefits to support the ecosystem-water-food-energy nexus. They include the environmental flow requirements for riverine ecosystem in order to take into account the role of ecosystems in the nexus. Momblanch et al. (2018) aim to develop and test a framework in order to analyze the effects of global change on the water-food-energy-environment nexus and to help the development of the adaptation policies for water resource management. The environment component of the nexus includes the environmental flow requirements.

The studies mentioned in the previous paragraph are the most current and some of the few studies in the literature in the field of water-energy-food nexus. The literature shows that the number of the studies addressing the ecosystems as the fourth component of the WEF nexus is very few. Moreover, the studies which address the ecosystems as the fourth pillar of the nexus only partially address. Among these studies it is a very common approach to include the environmental flow requirements in the nexus so that the role of ecosystems is revealed. Some of the studies include the changes in land use/land cover and the land area requirements as the representation of the impact of ecosystems. Furthermore, water quality which is a significant concern in the water provisioning services is not a concern in any of the mentioned studies.

Based on the literature survey in the field of WEF nexus assessment, it can be concluded that the role of ecosystems does not get enough appreciation. It is important to emphasize that the sustainability and the security of WEF nexus

components depends on the integration of the knowledge on the ecosystem services in the analysis. As it is also stated by Bidoglio and Brander (2016), most of the studies in WEF nexus field lack the full nexus perspective. The number of studies including the ecosystems as the fourth pillar of the nexus are even very rare. Considering these shortcomings in the nexus field, this PhD study aims to provide a full nexus evaluation without ignoring the role of ecosystem services. For this reason, Ecosystem is included as the fourth pillar of the nexus assessment and is even placed at the heart of the WEFE Nexus framework. The details of the methodology followed is given in Chapter 3.

2.4 Representative Concentration Pathways (RCPs), Shared Socioeconomic Pathways (SSPs) and WEFE Nexus

In the late 2000s, researchers began developing new scenarios to explore how the world might change over the rest of the 21st century. Earlier efforts during the 1990s had developed the "SRES" scenarios (IPCC, 2000), which were becoming outdated, so a group of researchers developed the "Representative Concentration Pathways" (RCPs) to describe different levels of greenhouse gases that might occur in the future (van Vuuren et al., 2011). These scenarios range from a low-emissions future (RCP2.6) to a high-emissions future (RCP8.5) with varying levels of warming by the end of the century. Another group of researchers developed the "Shared Socioeconomic Pathways" (SSPs) to model how socioeconomic factors may change over the next century (O'Neill et al., 2014). The two efforts were designed to be complementary, with the RCPs setting pathways for greenhouse gas concentrations and the SSPs setting the stage on which reductions in emissions will – or will not – be achieved. The SSPs feature multiple baseline worlds because underlying factors could lead to different future emissions and warming outcomes, even without climate

policy. The RCPs were used in the IPCC Fifth Assessment Report, while the SSPs were published in 2016 and are now being used in the next round of climate modelling (Hausfather, 2018). More information about RCPs and SSPs can be found in Chapter 6 and Chapter 8, respectively.

The Water-Energy-Food-Ecosystem (WEFE) nexus is affected by a range of pressures, including climate change, population growth, economic development, and technological change. The Representative Concentration Pathways (RCPs) and Shared Socioeconomic Pathways (SSPs) are two sets of scenarios that are commonly used to explore how these pressures might affect the WEFE Nexus. Climate change is a major pressure on the WEFE Nexus, and the RCPs are used to model the potential impacts of climate change on water availability, food production, and energy generation. The SSPs are used to model the potential impacts of population growth, economic growth, education, urbanization, and technological development on the WEFE Nexus. By combining RCPs and SSPs, researchers can explore a wide range of possible future scenarios for the WEFE Nexus. For example, a study might use the RCPs to model the impacts of climate change on water availability, and the SSPs to explore how different socioeconomic factors might affect water demand. These scenarios can help policymakers and stakeholders better understand the risks and opportunities associated with different development pathways, and identify potential strategies for sustainable development.

Researchers have employed a variety of methods and models to investigate the implications of different RCP-SSP combinations on the WEFE Nexus, resulting in a growing body of literature on this topic. Han et al. (2022), for instance, conducted a systematic review and meta-analysis of 97 studies to evaluate the effects of climate change and socio-economic development on the water-energy-food nexus. The study found that the most serious impact of climate change on food yield occurred under the RCP8.5 scenario, with an average decrease of 1.73%, 4.17%, and 4.56% in the

2020s, 2050s, and 2080s, respectively. The study also found that increases in population and GDP were positively correlated with power generation and water withdrawal. The paper advocates for the adoption of innovative technologies and a coordinated strategy for adaptation to ensure the security and stability of the water-energy-food nexus. K. Wang et al. (2021) applied an integrated management model to quantify the combined impacts of climate change and socio-economic development on the Food, Energy, and Water (FEW) Nexus in the Mekong River Delta. Results showed that rice yields will be vulnerable to extreme climate events, power generation will increase sharply due to socio-economic development, and the average total water withdrawal in 2050 will increase by 40% compared to that in the 2016 drought year. Pastor et al. (2019) examines the impact of climate change and socioeconomic factors on land use, water consumption, and food trade under different water regulation policies. The researchers used the Global Biosphere Management Model and simulated water availability, environmental flow requirements, and water use from agriculture, industry, and households. Momblanch et al. (2018) highlights the importance of holistic water management approaches in achieving inter-disciplinary societal goals such as the Sustainable Development Goals (SDGs) of clean water, hunger eradication, clean energy and life on land. Using a systems modelling approach, the study explores global change impacts on the water-food-energy-environment (WEFE) nexus in a complex western Himalayan water resource system in India under a range of climate change and alternative socio-economic development scenarios. Wada et al. (2016) highlights the challenges of managing global water use, which has increased nearly 6 times over the last 100 years to sustain growing food demand and increasing standards of living. The Water Futures and Solutions (WFaS) initiative aims to establish a consistent set of new global water scenarios based on the SSPs and RCPs.

By combining RCPs and SSPs, researchers can gain a more comprehensive understanding of the complex interactions between climate change and socio-

economic development on the WEFE Nexus, which is crucial for developing effective policies and strategies to ensure a sustainable future. Overall, the growing literature on combining RCPs and SSPs to evaluate the WEFE Nexus highlights the importance of integrated assessments to inform sustainable development policies for the future.

2.5 Review of Methods for WEFE Nexus Assessment

The Water-Energy-Food-Ecosystem (WEFE) nexus is an approach that highlights the interdependence and interconnectedness of water, energy, food, and ecosystem. The evaluation methods used to assess the WEFE Nexus aim to provide a comprehensive understanding of the complex interactions between these systems and help identify opportunities for sustainable management and development. In this review, an overview of the main evaluation methods used in WEFE Nexus research is provided. For this purpose, the following three review studies were particularly useful: Albrecht et al. (2018); Keairns et al. (2016); Semertzidis, (2015).

Albrecht et al. (2018) discusses the various analytical approaches used for evaluating the WEF nexus. The review reveals that numerous and diverse analytical tools have been used or proposed for examining the WEF nexus, and many studies combined multiple methods. The most commonly utilized methods were from the fields of environmental management and economics. Social science methods were also used, such as institutional analysis, Delphi technique, agent-based modeling, and participatory workshops. Most studies utilized multiple tools, often closely related, and approaches most commonly featured a combination of tools from the areas of environmental management, economics, indicators, statistics, and integrated models. The article notes a preference for quantitative methods, with only a small percentage relying on qualitative methods alone. Keairns et al. (2016) states that the WEF nexus recognizes the earth as a large, interconnected system consisting of many smaller

systems linked through flows of information, matter, and energy. To deal with specific applications, it is useful to quantify flows of energy and materials, estimate costs, and make numerical predictions. FAO (2014) stresses the role of rapid appraisal based on appropriate indicators and readily available information, while Bazilian et al. (2011) point to the need to develop new and robust analytical tools, conceptual models, algorithms, and data sets. According to Keairns et al. (2016), nexus modelling studies have been made at an aggregated scale for use at regional or global levels, i.e., large-scale system models, or the energy, water, and food supply chains have been modelled separately, i.e., life cycle and supply chain approaches, depending on the nature of the issues being addressed. Semertzidis (2015) discusses the concept of the resource nexus, which highlights the interlinkages between various resources such as energy, water, food, land, and minerals. It argues that a systems-thinking approach is needed to address the potential shortages of these resources and their impacts on global warming. However, existing energy systems modeling tools have limitations in dealing holistically with all interlinkages between resources. The article categorizes these tools into top-down and bottom-up models and further categorizes them into various types. It presents specific tools that have been used to address the resource nexus, such as OSeMOSYS, MARKAL/TIMES, and LEAP, and highlights the importance of data availability and identifying the problem at hand when choosing the right tool. The article concludes that with the right modifications, existing energy systems modeling tools could be used to successfully address the resource nexus.

The literature review show that the methods used in WEFE Nexus evaluations can be grouped under three main headings as: (i) Quantitative Methods, (ii) Qualitative Methods, (iii) Mixed Methods. *Quantitative methods* refer to methods that employ numerical data and models to assess the WEFE Nexus. Life cycle assessment (Al-Ansari et al., 2015; De Laurentiis et al., 2016; Irabien & Darton, 2016; King and Carbajales-Dale, 2016), foot printing (Daccache et al., 2014; Damerau et al., 2016;

Heckl et al., 2015; Irabien and Darton, 2016; Vlotman and Ballard, 2014), integrated assessment modeling (Bonsch et al., 2016; Howells et al., 2013; Karlberg et al., 2015; Ringler et al., 2016; van Vuuren et al., 2015), and indicators, metrics, or indices (Abbott et al., 2017; El-Gafy, 2017; Hua et al., 2020; Qin et al., 2022; Venghaus and Dieken, 2019; Willis et al., 2016) are some examples of quantitative methods that can be used to evaluate WEFE systems. *Qualitative methods* rely on expert judgment and stakeholder engagement to evaluate the WEFE Nexus. Examples of qualitative methods include scenario analysis, multi-criteria decision analysis, and participatory approaches (Foran, 2015; Halbe et al., 2015; Howarth and Monasterolo, 2016; Villamayor-Tomas et al., 2015). These methods provide a more holistic understanding of the social and political dimensions of the WEFE Nexus and can help decision-makers identify potential risks and opportunities and develop more robust strategies. *Mixed methods* combine both quantitative and qualitative approaches to evaluate the WEF nexus (De Strasser et al., 2016; Endo et al., 2015; Guillaume et al., 2015; Stucki and Sojamo, 2012; Wolfe et al., 2016). Mixed methods can provide a more comprehensive understanding of the WEF nexus, as they combine the strengths of both quantitative and qualitative methods.

2.6 WEFE Nexus Indicators

Indicators are methods used to quantitatively describe and operationalize any system regardless of how inherently complex it is (Endo et al., 2015). As Yi et al. (2020) states, indicator selection is always the first step to initiate the assessment of sustainability. Many social and environmental characteristics of a system can be represented via indicators. In order to create such indicators, measurable variables are used so that the overall characteristics of a systems can be quantified. However, it is difficult to create common indicators for different environments since these indicators should be strongly related to the issue, and adjusted specifically for the

study area. Giupponi and Gain (2017) state that a concise index developed from the aggregation of multiple indicators can contribute greatly to enhance the transformation of scientific evidence into effective information for policy/decision making. Within the scope of the WEF nexus security and sustainability assessment studies, the most relevant indicators in terms of availability, affordability, accessibility, quality and safety are selected. In this way the status and security of WEF nexus components are analyzed (Endo et al., 2015; Giupponi & Gain, 2017; Momblanch et al., 2018).

Resource availability, accessibility, self-sufficiency and productivity are the major drivers of the securities of water, energy and food from where indicators are defined. Thus, Nhamo et al. (2019) emphasizes that indicators which are not related to these drivers should be excluded from the list of WEF nexus indicators. According to Saladini et al. (2018), the selected indicators for the assessment of water, energy and food securities should cover most sustainable development goals (SDGs), consider biophysical limits, highlight the linkages among all nexus components, consider both national and sectoral systems, and be limited in number. In addition, data availability should be guaranteed frequently enough to be meaningful in the desired time horizon. Moreover, as Endo et al. (2015) states, the indicators should be strongly linked to the issue and objective for measurement and tailored specifically for the research area.

Numerous studies used indicator-based approach for the assessment of WEF nexus security. In these studies, the components of WEF nexus, the scale of the studies, and the number of indicators used for each nexus component differ from each other. The literature review on the studies following indicator-based approach is summarized in Table 2-1, Table 2-2, Table 2-3, and Table 2-4. As it can be seen these tables, several different indicators were used for each nexus component. Some of these studies (e.g. Giupponi and Gain (2017); Hua et al. (2020); Yuan and Lo

(2020)) referred to the global framework for SDGs which was developed by the Inter-Agency and Expert Group on SDG Indicators (IAEG-SDGs) (*SDG Indicators*, 2021) while selecting the nexus indicators. The global indicator framework includes total of 231 unique indicators for 17 SDGs.

Table 2-4 shows that among the studies using indicator-based approach for nexus evaluation, the number of studies putting ecosystem as the fourth pillar of the WEF nexus framework is limited. Furthermore, the number and variety of indicators used for the ecosystem component are not as large as they are in other nexus component indicators, i.e., water, energy and food. Among the reviewed studies, the only study which put land as a nexus component is the one carried out by Kebede et al. (2021).

Table 2-1. Summary of literature review on the studies using indicator-based approach to evaluate WEFE Nexus: Water component

Nexus Component	Nexus Indicators	Unit	Scale	Source
WATER	Drinking water supply as % of demand met	%	River Basin	(Momblanch et al., 2018)
	Abatement capacity of reservoirs	%	River Basin	(Momblanch et al., 2018)
	Proportion of available freshwater resources per capita (availability)	m^3/capita	Country	(Nhamo et al., 2019)
	Proportion of crops produced per unit of water used (productivity)	US$/$m^3$	Country	(Nhamo et al., 2019)
	Crop water productivity	kg/m^3	Country; Europe; Province	(Saladini et al., 2018); (United Nations, 2015); (Yi et al., 2020)
	Annual freshwater withdrawal for agriculture	%	Country	(Saladini et al., 2018)
	Population using safely managed water services (rural)	%	Country	(Saladini et al., 2018); (Hua et al., 2020)
	Population using safely managed sanitation services (rural)	%	Country	(Saladini et al., 2018); (Hua et al., 2020)
	Total internal renewable water resources per capita	m^3 per inhabitant per year	River Basin; Province	(Giupponi and Gain, 2017); (Yi et al., 2020)
	Access to sanitation	%	River Basin; Europe	(Giupponi and Gain, 2017); (United Nations, 2015)
	Access to drinking water	%	River Basin; Europe	(Giupponi and Gain, 2017); (United Nations, 2015)
	Groundwater depletion rate	million m^3/year; m^3/year/capita	River Basin; Country	(Giupponi and Gain, 2017); (Hua et al., 2020)
	Drought Index (DI)	-	River Basin	(Giupponi & Gain, 2017)
	People using at least basic drinking water services	%	Country	(Yuan and Lo, 2020); (Hua et al., 2020)
	People using at least basic sanitation services	%	Country	(Yuan and Lo, 2020); (Hua et al., 2020)
	Renewable internal freshwater resources	m^3/capita	Country	(Yuan and Lo, 2020)
	Water body extent	% of total land area	Country	(Yuan and Lo, 2020)
	Total actual renewable water resources (TARWR) per capita	m^3 per year per capita	Transboundary River Basin	(United Nations, 2015)
	Storage capacity per person	m^3 per year per capita	Transboundary River Basin	(United Nations, 2015)
	Intensity of use of actual water resources (percentage of withdrawals from TARWR)	%	Transboundary River Basin	(United Nations, 2015)
	Water use by different sectors	m^3/year	Transboundary River Basin	(United Nations, 2015)
	Indicators of flow variability, occurrence of extreme hydrological events	-	Transboundary River Basin	(United Nations, 2015)

Table 2-1 (continued)

WATER	Energy-intensity of water provision (withdrawal, treatment, conveyance; special attention to the use of methods with high-energy requirements like desalination)	-	Transboundary River Basin	(United Nations, 2015)
	Access to modern electricity		Transboundary River Basin	(United Nations, 2015)
	Hydropower potential and level of development	-	Transboundary River Basin	(United Nations, 2015)
	People flooded in 100-year event	Number of people	Europe	(Kebede et al., 2021)
	Water exploitation index	-	Europe	(Kebede et al., 2021)
	Freshwater withdrawal as % total renewable water resources	%	Country	(Hua et al., 2020)
	Water consumed per unit of GDP	-	Province	(Yi et al., 2020)
	Water function area monitoring compliance rate	%	Province	(Yi et al., 2020)
	Pumping per unit of power consumption	m^3/kWh	Province	(Yi et al., 2020)
	Water consumption per unit of irrigated area	-	Province	(Yi et al., 2020)

Table 2-2. Summary of literature review on the studies using indicator-based approach to evaluate WEFE Nexus: Energy component

Nexus Component	Nexus Indicators	Unit	Scale	Source
ENERGY	Energy production as % of maximum generation capacity	%	River Basin	(Momblanch et al., 2018)
	Proportion of the population with access to electricity (accessibility)	%	Country	(Nhamo et al., 2019); (Yuan and Lo, 2020); (Hua et al., 2020)
	Energy intensity measured in terms of primary energy and GDP (productivity)	MJ/GDP	Country	(Nhamo et al., 2019)
	Aggregated energy availability	-	River Basin	(Giupponi and Gain, 2017)
	Aggregated energy affordability	-	River Basin	(Giupponi and Gain, 2017)
	Environmental sustainability	-	River Basin	(Giupponi and Gain, 2017)
	Political strength	-	River Basin	(Giupponi and Gain, 2017)
	Social strength	-	River Basin	(Giupponi and Gain, 2017)
	Access to clean fuels and technologies for cooking	%	Country	(Yuan and Lo, 2020); (Hua et al., 2020)
	Energy use	constant 2011 PPP $ per kg of oil equivalent	Country	(Yuan and Lo, 2020)
	Renewable energy share	%	Country	(Yuan and Lo, 2020)
	Primary energy mix	-	Transboundary River Basin	(United Nations, 2015)
	Energy dependence	-	Transboundary River Basin	(United Nations, 2015)
	Power sharing arrangements	-	Transboundary River Basin	(United Nations, 2015)
	Energy-intensity of production, industries etc.	-	Transboundary River Basin	(United Nations, 2015)
	Total average annual energy from all dams in gigawatt hour per year	GWh/year	River Basin	(Geressu et al., 2020)
	Firm annual energy	GWh/year	River Basin	(Geressu et al., 2020)
	Firm monthly energy	GWh/month	River Basin	(Geressu et al., 2020)
	Fossil energy use per unit of GDP	-	Province	(Yi et al., 2020)
	Energy self-sufficiency rate	%	Province	(Yi et al., 2020)
	Contribution of fossil energy to energy supply	%	Province	(Yi et al., 2020)
	Hydroelectric power generation	-	Province	(Yi et al., 2020)
	Energy consumption of agricultural production per unit of agricultural output value	tons coal/yen	Province	(Yi et al., 2020)

Table 2-3. Summary of literature review on the studies using indicator-based approach to evaluate WEFE Nexus: Food component

Nexus Component	Nexus Indicators	Unit	Scale	Source
FOOD	Irrigated crop production as % of maximum potential production	%	River Basin	(Momblanch et al., 2018)
	Prevalence of moderate or severe food insecurity in the population (self- sufficiency)	%	Country	(Nhamo et al., 2019)
	Proportion of sustainable agricultural production per unit area (cereal productivity)	kg/ha	Country	(Nhamo et al., 2019)
	Cereal yield	kg/ha	Country	(Saladini et al., 2018); (Yuan and Lo, 2020); (Hua et al., 2020)
	Agriculture value added	US$/worker	Country	(Saladini et al., 2018)
	Fertilizer consumption	$kg/ha_{arable\ land}$	Country; Europe	(Saladini et al., 2018); (United Nations, 2015)
	Amount of agricultural residues used for energy purpose	T	Country	(Saladini et al., 2018)
	Average food supply	kcal/capita/day	River Basin	(Giupponi and Gain, 2017)
	Volatility on agricultural production	-	River Basin	(Giupponi and Gain, 2017)
	Food loss	%	River Basin	(Giupponi and Gain, 2017)
	Poverty	%	River Basin	(Giupponi and Gain, 2017)
	Prevalence of undernourishment (% of people)	%	River Basin; Country; Country	(Giupponi and Gain, 2017); (Yuan and Lo, 2020); (Hua et al., 2020)
	Diet diversification	%	River Basin	(Giupponi and Gain, 2017)
	Protein quality	gr	River Basin	(Giupponi and Gain, 2017)
	Prevalence of obesity (% of people)	%	River Basin	(Giupponi and Gain, 2017)
	Arable land	%	Country	(Yuan and Lo, 2020)
	Proportion of local breeds being at risk	%	Country	(Yuan and Lo, 2020)
	Share of rain-fed agriculture, irrigated	%	Transboundary River Basin	(United Nations, 2015)
	Degree of cultivation of arable land	%	Transboundary River Basin	(United Nations, 2015)
	Energy-intensity of agriculture (reflecting mechanization etc.)	-	Transboundary River Basin	(United Nations, 2015)
	Crops & livestock	-	Transboundary River Basin	(United Nations, 2015)
	Prevalence of organic agriculture	-	Transboundary River Basin	(United Nations, 2015)
	Food production	-	Europe	(Kebede et al., 2021)
	Total irrigation area	ha	River Basin	(Geressu et al., 2020)
	Irrigation water supply demand deficit	MCM/year	River Basin	(Geressu et al., 2020)
	Net export of agricultural products, food and live animals per capita	-	Province	(Yi et al., 2020)
	Arable land occupied by construction	-	Province	(Yi et al., 2020)
	Grain production per unit of farmland area	tons per ha	Province	(Yi et al., 2020)
	Grain production per unit of power consumption	ton/kWh	Province	(Yi et al., 2020)

Table 2-4. Summary of literature review on the studies using indicator-based approach to evaluate WEFE Nexus: Ecosystem and Land components

Nexus Component	Nexus Indicators	Unit	Scale	Source
ECOSYSTEM	Natural flow maintenance	%	River Basin	(Momblanch et al., 2018)
	GHG Emissions	$t\ CO_{2e}$	Country	(Saladini et al., 2018)
	Water Quality Index	-	River Basin	(Giupponi and Gain, 2017)
	Protected ecosystems in the basin	-	Transboundary River Basin	(United Nations, 2015)
	Main ecosystems services provided	-	Transboundary River Basin	(United Nations, 2015)
	Biodiversity vulnerability index	-	Europe	(Kebede et al., 2021)
	Timber production	-	Europe	(Kebede et al., 2021)
	CO2 emissions from fuel combustion / electricity output	MtCO2/TWh	Country	(Hua et al., 2020)
	Area flooded by the Julius Nyerere Hydropower Project reservoir	ha	River Basin	(Geressu et al., 2020)
	Lower Rufiji flow disruption	-	River Basin	(Geressu et al., 2020)
LAND	Artificial surfaces	%	Europe	(Kebede et al., 2021)
	Land use diversity	-	Europe	(Kebede et al., 2021)

CHAPTER 3

METHODOLOGY

The Water-Energy-Food-Ecosystem (WEFE) nexus is a complex system requiring a robust and dynamic evaluation methodology. In this study, the proposed methodology not only takes into account the interconnectivity of the WEFE Nexus but also incorporates cutting-edge dynamically downscaled climate projections and socioeconomic pathway scenarios. The proposed WEFE Nexus evaluation methodology is embedded in a Pressure-State-Response (PSR) framework. The PSR framework is a widely used framework for evaluating complex systems such as the WEFE Nexus. In this framework, the system is evaluated based on three components: the pressures on the system, the state of the system, and the responses to the pressures and state of the system (Waheed et al., 2009). Figure 3-1 illustrates the circular relationship between Pressure, State, and Response. The following paragraphs discuss each step of the methodology in detail.

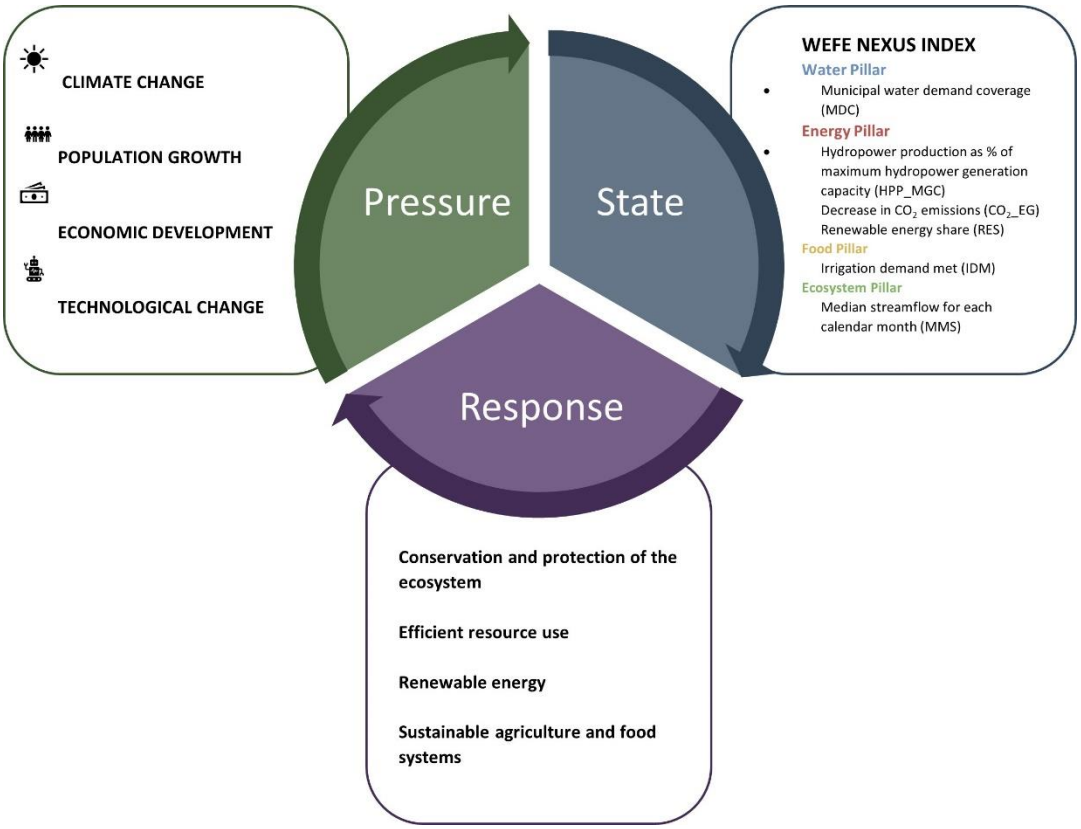

Figure 3-1. Circular relationship between Pressure, State, and Response: Diagram depicting the dynamic interactions among pressure, state, and response in WEFE Nexus

In order to ensure the long-term sustainability of water, energy, food, and ecosystem, it is important to indentify the root causes of environmental problems and develop effective strategies to address them. Incorporating WEFE Nexus evaluation in the PSR framework can provide a comphrenensive approach to understand the complex interactions between human activities and the natural environment. Figure 3-2 summarizes the methodology adopted in this study. The figure represents the steps involved in the proposed WEFE Nexus evaluation methodology, highlighting the importance of incorporating climate projections, socioeconomic scenarios, and ecosystem services into the analysis. The figure also emphasizes the use of a PSR

framework to guide the analysis and identify strategies for promoting sustainable development and enhancing the resilience of the WEFE Nexus.

First, the *pressures* on the WEFE Nexus are identified (Figure 3-2 a). These pressures may include climate change, population growth, economic development, technological change, and other drivers that may affect the WEFE Nexus. By identifying these pressures, the potential impacts on the WEFE Nexus can be assessed, and areas for intervention can be prioritized. Next, the *state* of the WEFE Nexus is evaluated (Figure 3-2 (b-1) and (b-2)). This involves assessing the current status of the water, energy, food, and ecosystem components of the nexus. A coupled water-energy systems model is used to obtain WEFE Nexus indicators that provide insight into the state of the nexus. Finally, the *responses* to the pressures and state of the WEFE Nexus are evaluated (Figure 3-2 c). This involves identifying policies, strategies, and interventions that can help promote sustainable development and enhance the resilience of the WEFE Nexus.

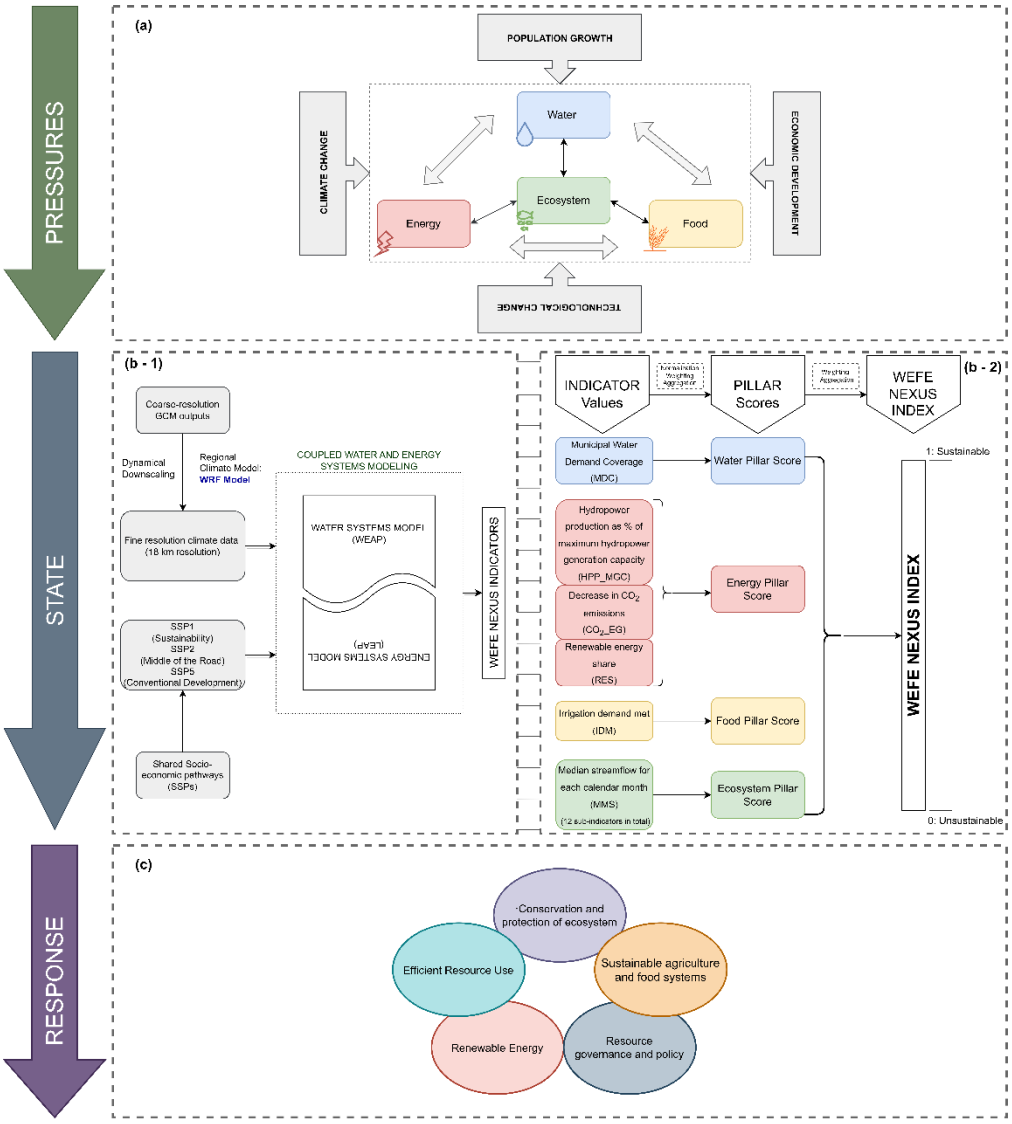

Figure 3-2. Assessing the WEFE Nexus: A comprehensive methodology for evaluating water, energy, food, and ecosystems in the context of climate change and socioeconomic pressures

Pressures (Figure 3-2 (a))

The developed methodology recognizes that the ecosystem plays a crucial role in the WEFE Nexus and should not be overlooked. This is why the ecosystem has been

included as the fourth pillar of the WEFE Nexus framework, with a focus on ecosystem services. Chapter 2.3 of this study discusses the importance of incorporating ecosystem services into the evaluation of the WEFE Nexus. Ecosystem services refer to the direct and indirect benefits that society derive from ecosystems, such as clean air and water, pollination, and nutrient cycling (FAO, 2023). These services are essential for the functioning of the WEFE Nexus, as they underpin the production of food and energy, as well as the provision of clean water. By incorporating ecosystem services into the evaluation framework, it is ensured that the role of the ecosystem is given appropriate consideration in decision-making processes. This helps to avoid undervaluing the importance of the ecosystem and its services, which can have negative consequences for the sustainability and resilience of the WEFE Nexus. Therefore, the proposed methodology aims to create a comprehensive and integrated evaluation of the WEFE Nexus by including the ecosystem as the fourth pillar of the nexus framework.

The proposed WEFE Nexus framework is subject to various pressures that can significantly impact the sustainability and resilience of the nexus. These pressures include:

(i) *Climate change*: Climate change is one of the most significant pressures on the WEFE Nexus. It affects water availability, energy demand, food production, and ecosystem services. Changes in temperature and precipitation patterns can alter the availability and quality of water resources, impacting agriculture, energy production, and other sectors. Climate change also affects the availability of energy resources, such as hydropower, which is sensitive to changes in water availability.

(ii) *Population growth*: The increasing population puts pressure on the WEFE Nexus, as more people require access to water, energy, and food. Population growth also leads to increased demand for land, which can impact ecosystem

services and biodiversity. As the population continues to grow, there is a need for sustainable development strategies to ensure that the demands of future generations can be met.

(iii) Economic development: Economic development can pressure the WEFE Nexus through increased demand for energy and water resources. Economic growth often increases energy consumption, exacerbating climate change and further stressing sources. Economic development can also lead to changes in land-use patterns, affecting ecosystems and biodiversity.

(iv) Technological change: Technological change can both positively and negatively affect the WEFE Nexus. Advancements in technology can lead to more efficient use of resources, such as water and energy, and increase food production. However, technological change can also have negative impacts, such as increased pollution and ecosystem degradation.

State: Integrated Modeling (Figure 3-2 (b-1))

This part of Figure 3-2 shows the methodology followed to assess the nexus status. As mentioned in the description of Figure 3-2 a, there are four main pressures on the nexus, i.e., climate change, population growth, economic development, and technological change. The future climate projections were obtained by dynamical downscaling to be fed into a coupled water-energy systems model. The impacts of the rest of the pressures, all of which correspond to socioeconomic parameters, were reflected in the water-energy model based on the Shared-Socioeconomic-Pathways (SSPs).

The WRF model was used for the downscaling of the climate projections. The WRF model was first used to reconstruct the historical climatic variables over the basin by dynamically downscaling the ERA-Interim reanalysis dataset. The model was calibrated for the year 2010 before reconstructing the historical atmospheric data over the whole historical period (2009 – 2018). Four distinct future climate

projections over the Sakarya Basin were dynamically downscaled to a finely tuned resolution of 18 km using a calibrated and validated WRF model, which is more appropriate for the hydrologic modeling of the basin. The details of the dynamical downscaling of the climate projections are given in Chapter 6.

Socio-economic parameters are the other external factors affecting the WEFE Nexus. The effects of socioeconomic changes were reflected in the water-energy model based on the Shared Socioeconomic Pathways (SSPs), specifically SSP1 (Sustainability), SSP2 (Middle of the Road), and SSP5 (Conventional Development). SSPs investigate how the world might change without climate policies and to what extent climate change targets could be achieved when RCP mitigation targets of RCPs are combined with the SSPs. Thus, the RCPs and the SSPs are complementary to each other. Based on the qualitative and quantitative results of the SSPs, some key parameters under the data categories, such as land use areas, municipal and industrial water demand, and energy demand, were modified to build a WEAP-LEAP model for the future period under the evolving socio-economic conditions (details in Chapter 8).

Based on the methodology followed to evaluate the impacts of future climatic and socio-economic conditions, there are two main scenarios within the scope of this study, i.e. RCP 4.5 (Low Emission Climate Change Scenario) and RCP 8.5 (High Emission Climate Change Scenario). The socio-economic scenarios are created under these climate change scenarios according to the consistency of RCP and SSP scenarios. Thus, the socio-economic scenarios have the same climate data as the climate change scenario they are under. The details of the scenario development are given in Chapter 8.

State: WEFE Nexus Index Development (Figure 3-2(b-2))

Utilizing the coupled water-energy systems model, i.e., WEAP-LEAP model, key indicators are derived to provide valuable insights into the performance of the

system. Incorporating climate projections and socio-economic parameters into the model results in a holistic understanding of how the system will behave under different scenarios. The resulting indicators bring the data to life, painting a vivid picture of what the future may hold for this complex and dynamic system. Once the WEFE Nexus indicators are obtained, they are normalized to ensure comparability across different indicators. This ensures that each indicator is given a fair chance of contribution in the final calculation of the WEFE Nexus index. These normalized indicators are then weighted and aggregated into a WEFE Nexus index. The index value ranges between 0 and 1, corresponding to the unsustainable and sustainable WEFE Nexus index. This provides a comprehensive and integrated view of the WEFE Nexus, enabling decision-makers to prioritize interventions and policies that can help promote sustainable development (details in Chapter 9).

Response (Figure 3-2 – c)

The responses to the proposed WEFE Nexus evaluation methodology are based on the sustainability status of the nexus as determined by the WEFE Nexus index. Depending on the value of the WEFE Nexus index, different responses may be necessary to promote sustainable development and enhance the resilience of the nexus.The responsens may involve conservation and protection of the ecosystem, efficient resource use, sustainable agriculture and food systems, renewable energy, and resource governance and policy.

If the WEFE Nexus index indicates a high level of sustainability and resilience, the responses may focus on maintaining the status quo and ensuring that current policies and practices are sustained. For example, efforts may be made to promote the conservation and sustainable management of water and energy resources, support sustainable agriculture practices, and protect and restore ecosystems. However, if the WEFE Nexus index indicates a low level of sustainability and resilience, more significant responses may be necessary to address the challenges facing the nexus.

These responses may include policy interventions, technological innovations, and changes in behavior and consumption patterns.

By using the WEFE Nexus index to guide responses, decision-makers can prioritize interventions that promote sustainable development and enhance the resilience of the WEFE Nexus. This can help to ensure that the WEFE Nexus can continue to meet the needs of current and future generations in a sustainable and equitable manner.

CHAPTER 4

STUDY AREA

This section presents information on the Sakarya Basin's geographical and topographical features, land use/land cover, climatic characteristics, agricultural and industrial practices, as well as energy production characteristics.

4.1 Geographic and Topographic Features

The Sakarya Basin is located in northwest Türkiye. It constitutes approximately 7% of Türkiye's surface area, with a drainage area of about 63,000 km^2. Sakarya River, the main river of the basin, arises from the Çifteler Sakaryabaşı springs at 800 m elevation in the south of Eskişehir province. Sakarya River flows into the Black Sea in the Karasu district of Sakarya province. It is fed by many tributaries and streams, such as Porsuk, Ankara, Karasu, Çarksuyu, and Mudurnu until it empties into the sea. The total length of the Sakarya River is 720 km, and the Sakarya Basin has approximately 3.4% of the total water potential of Türkiye (DSİ, 2017). The total population of the basin is around 7.5 million (DSİ, 2017) and corresponds to approximately 9% of the total population of Türkiye. The entire area of Eskişehir and Sakarya provinces, almost the whole of Bilecik province (97.2%), about 70% of the Ankara province, 42% of Bolu, 35% of Kütahya with its center, 23% of Afyonkarahisar, about 20% of Konya, 17% of Bursa, 10% of Kocaeli, and less than 2% of Düzce, Çankırı, and Uşak provinces are located within the boundaries of the basin. 7.3% of the population lives in villages, and the rest of the population lives in municipalities (Alp et al., 2020). Sakarya Basin has a wide elevation band. It ranges from 0 elevations on the Western Black Sea cost to 2510 m elevations at Uludağ.

The location of the Sakarya Basin in Türkiye, the borders of the provinces within the basin, and the digital elevation map of the basin are shown in Figure 4-1. Sakarya Basin is divided into seven subbasins, considering the basin's hydrological and topographic condition, the river network, and the studies carried out by the relevant institutions. These subbasins are from upstream to downstream: Upper Sakarya, Porsuk, Ankara, Kirmir, Middle Sakarya, Göksu, and Lower Sakarya. The boundaries of these subbasins are shown in Figure 4-2.

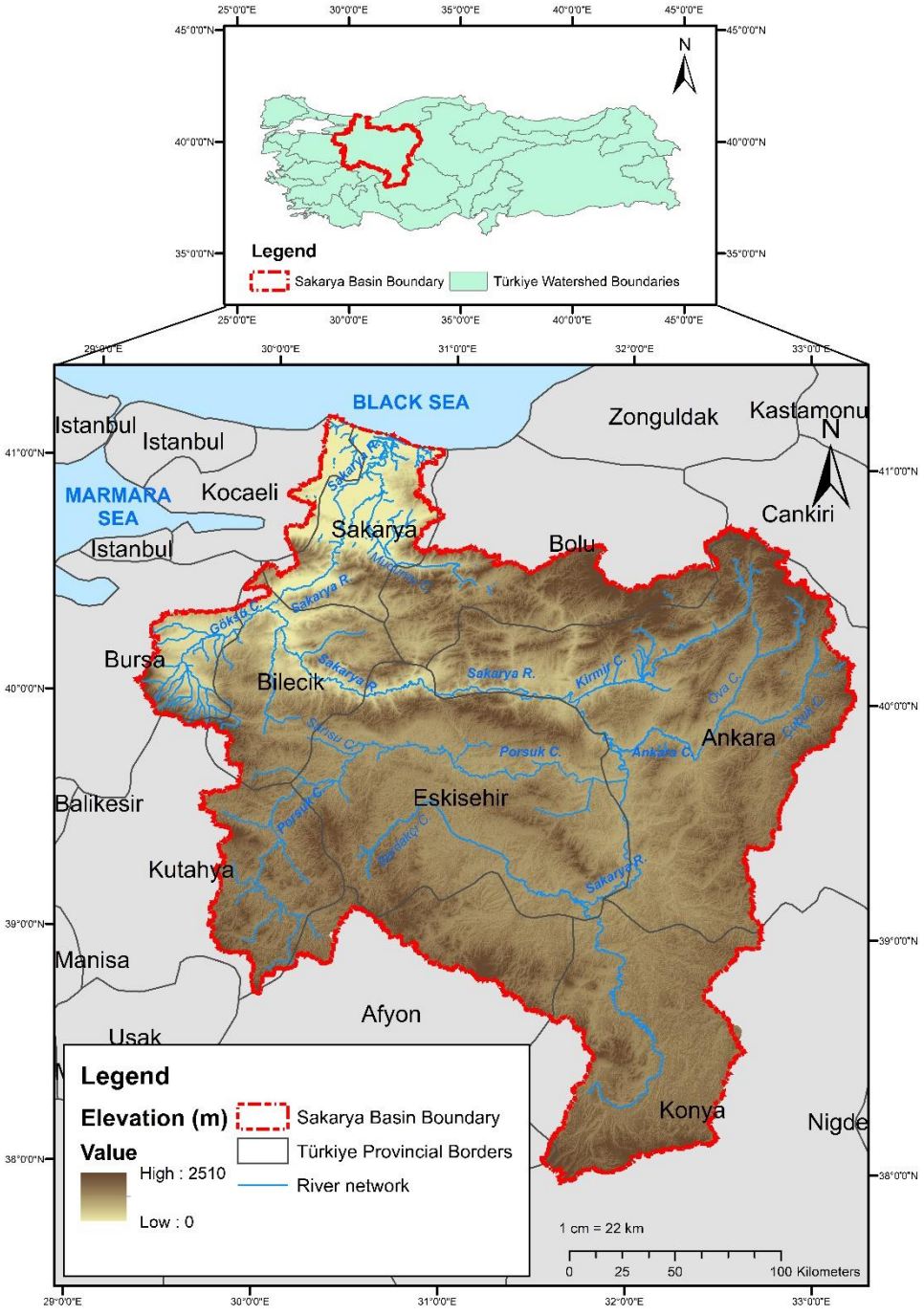

Figure 4-1. Location of Sakarya Basin in Türkiye, borders of provinces and digital elevation map

4.2 Land Use/Land Cover

The land use/land cover map of the Sakarya Basin is given in Figure 4-2. According to CORINE 2018 data, 53% of the Sakarya Basin consists of agricultural areas. Forest and semi-natural areas account for approximately 44%. Artificial surfaces, on the other hand, constitute only about 3% of the total area. The map (Figure 4-2) shows that the subbasin with the highest agricultural land area is the Upper Sakarya subbasin. Agricultural areas in this subbasin constitute approximately 70% of the entire subbasin. The Upper Sakarya subbasin is followed by Ankara (64%), Porsuk (50%), Lower Sakarya (50%), Göksu (49%), Kirmir (32%), and Middle Sakarya (32%) subbasins, respectively. The largest artificial surfaces area belongs to the Ankara subbasin with an areal percentage of approximately 10%. In other subbasins, this percentage varies between 1% and 3%. The Middle Sakarya subbasin ranks first in terms of the size of the forest and semi-natural areas. Detailed numerical information about the distribution of land use in the subbasins is given in Table A. 1 in the Appendix A.

Figure 4-2. CORINE 2018 Sakarya Basin Land Use Land Cover

4.3 Climate

There are four basins in Türkiye with an average rainfall of less than 500 mm. Sakarya Basin is one of these four basins with an average annual precipitation of 479 mm. On the other hand, considering the total annual precipitation, it is one of the basins receiving the highest precipitation with 32 billion m^3. Sakarya Basin, which is one of the basins with the highest flow value with an annual flow of 12 billion m^3, is one of the basins with the lowest rainfall per capita (4,437 m^3/person) due to its high population (SYGM, 2022).

The subbasins of Sakarya Basin show differences in terms of climatic characteristics. Upper Sakarya subbasin has continental climate characteristics. Winters are cold and rainy; summers are hot and dry. Day and night temperature differences are high. The coldest month is January and the hottest is July. It is the subbasin with the lowest precipitation with 380 mm annual average precipitation calculated within the scope of this current study. The average temperature is 12.2 ˚C. The Porsuk subbasin is in the transition zone from the moderate climate of the Western Black Sea, Aegean and Marmara regions to the continental climate of Central Anatolia. Winters are harsh, long and rainy; summers are hot and dry. Day and night temperature differences are high. Within the scope of this study, the annual average precipitation and annual average temperature were calculated as 479 mm and 11.8˚C, respectively. Ankara and Kirmir subbasins are located in the Central Anatolia Region. Therefore, they have continental climate characteristics. In Ankara, where the climate is steppe in the south and mild and rainy in the north, winters are generally cold and less rainy, and summers are hot and dry. There is little temperature difference between day and night. Within the scope of this study, the annual average precipitation was calculated as 417 mm. This is the second lowest amount of precipitation among all subbasins. The annual average temperature value is 12.4˚C. Middle Sakarya subbasin is located within the borders of Türkiye's Central Anatolia, Black Sea and Marmara Regions.

In the Central Anatolia Region, in accordance with the typical continental climate characteristics, summers are hot and dry, and winters are cold and rainy. In the Black Sea and Marmara Regions, the Black Sea climate is dominant, with warm and rainy summers and cold and snowy winters. The annual average precipitation and temperature values calculated within the scope of this study are 496 mm and 13.1˚C, respectively. Göksu subbasin is close to the Marmara basin and is in the transition zone from the moderate continental climate of Central Anatolia to the rainy climate of the Marmara. The precipitation average is above the average of the Sakarya Basin. The climate is closer to the temperate climate of Marmara. It is hot and less rainy. Winter months are cold and rainy. The annual average precipitation and temperature values calculated within the scope of this study are 531 mm and 13.5˚C, respectively. The Lower Sakarya Basin is located within the Marmara Region and the Black Sea Region. For this reason, Black Sea climate is observed in the north and east of the subbasin, and Marmara climate characteristics are observed in the west and south. It has the highest annual average precipitation value among all subbasins. The annual average precipitation and temperature values calculated within the scope of this study are 733 mm and 15.9 degrees, respectively.

4.4 Hydrological Structures

There are many dams and ponds built for irrigation, drinking water or energy purposes in the Sakarya Basin. Sarıyar Hasan Polatkan dam and hydroelectric power plant, which is the oldest hydroelectric power plant in Türkiye and the construction of which started in 1953, is located in the Sakarya Basin. In addition, Çubuk I dam, the first dam of the Republic of Türkiye, is in the Sakarya Basin. Ankara, Eskişehir and Sakarya are the three important provinces in terms of water allocations. The municipal water demand of Ankara is approximately 486 hm^3/y. The drinking water requirement of the province is supplied from the six dams in the basin (Çamlıdere,

Eğrekkaya, Kurtboğazı, Kavşakkaya, Akyar, and Çubuk II), the Kesikköprü Dam built on the Kızılırmak river (Ankara 1st stage drinking water project) and the Gerede system (Ankara 2nd stage drinking water project) (Governorship of Ankara, 2022). Sapanca Lake is another important drinking water source in the Sakarya Basin. Approximately 60% of the drinking water need of Sakarya province is met from Sapanca Lake (Governorship of Sakarya, 2021). In Eskişehir, a significant part of the drinking water need is provided from the Porsuk Dam. Around 100 hm^3 of water is allocated annually for drinking water from the Porsuk Dam (Governorship of Eskişehir, 2022). The total number of ponds in the operation built by DSİ in the Sakarya basin is 65 (TÜBİTAK MAM, 2013). Their total surface area is calculated as 1424 ha. The physical characteristics of the reservoirs and the ponds included in this study are given in Chapter 5 in Section 5.4.

4.5 Agriculture, Irrigated Agricultural Lands, and Livestock

The agricultural sector is of great importance for the economic and social life in the Sakarya Basin. Sakarya Basin is still an agricultural basin despite the increasing industrialization. Livestock and agricultural activities are carried out intensively throughout the basin. The cultivation of field crops is predominantly practiced in various areas across the basin. Specifically, the Kütahya Altıntaş Plain, Eskişehir's Çifteler and Mahmudiye districts, Ankara's Polatlı Plain and Beyzaparı district, and Bursa's Yenişehir Plain, Pamukova, and Adapazarı Plain are the regions characterized by the highest agricultural activity levels (TÜBİTAK MAM, 2013).

The total size of the irrigation areas established by DSİ in the Sakarya Basin, where agriculture has a significant share, is 125,470 ha (The Ministry of Forestry and Water Affairs, 2016). Therefore, agricultural irrigation is one of the most important sources of water consumption in the basin. Approximately 20% of the Sakarya Basin's total water potential is used for irrigation, while 80% is allocated for activities other than

irrigation (municipal water demand, industry etc.). About 40% of the irrigation areas established by DSİ in the basin are located in the Upper Sakarya subbasin (The Ministry of Forestry and Water Affairs, 2016). The locations of the irrigated agricultural lands are shown in Figure 4-3.

There is an intense livestock activity in some parts of the Sakarya Basin. Cattle breeding in Ankara and Sakarya provinces, sheep and goat breeding in Ankara and Eskişehir provinces, and poultry breeding in Bolu and Sakarya provinces is more intense compared to other provinces.

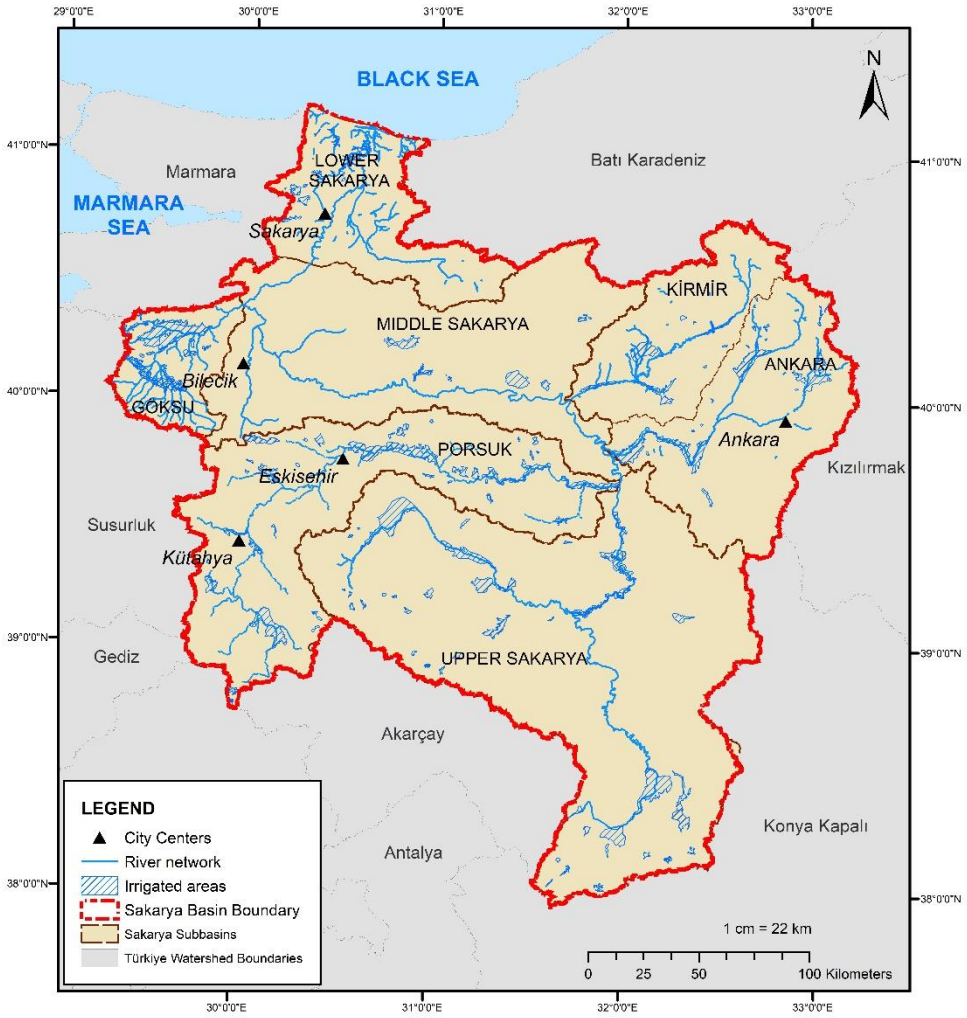

Figure 4-3. Sakarya Basin irrigated agricultural lands

4.6 Industry

Sakarya Basin is one of the basins where industrial activity is intense in Türkiye. Industrial establishments from many different sectors operate in almost all of the basin, especially in Ankara, Eskişehir and Sakarya provinces. In addition, there are 20 organized industrial zones (OIZs) in the basin that are currently operating (Table

4-1). The machinery manufacturing industry and metal goods industry dominate in Eskişehir. In Kütahya, there are industrial facilities based on ceramics, porcelain, mining, forest products, agriculture and livestock, depending on surface and underground resources. Machinery and metal industry has an important place in Ankara. The food industry stands out in Bolu. Textile, woodworking and furniture sectors have an important place among industrial activities in İnegöl district of Bursa province. In Sakarya province, there are facilities that produce in the automotive, food and textile sectors.

Table 4-1. Sakarya Basin OIZs (TÜBİTAK MAM, 2013)

OIZ Name	Subbasin	Province	Activity Status	Sector	Size (ha)	Number of Companies
Emirdağ	Upper Sakarya	Afyon.	Active	Food	104	3
Polatlı	Upper Sakarya	Ankara	Active	Machinery	267	13
Eskişehir	Porsuk	Eskişehir	Active	Metal	2980	386
Sivrihisar	Porsuk	Eskişehir	Not active	-	218	0
Beylikova Besi İh.	Porsuk	Eskişehir	Not active	Stock	143	0
Kütahya	Porsuk	Kütahya	Active	Mining	215	57
Kütahya Merkez II	Porsuk	Kütahya	Not active	-	320	0
Ostim	Ankara	Ankara	Active	Machinery	476	4748
İvedik	Ankara	Ankara	Active	Machinery	477	6103
ASO I	Ankara	Ankara	Active	Machinery	955	216
ASO II	Ankara	Ankara	Partially act.	-	620	15
Başkent	Ankara	Ankara	Active	Machinery	1014	33
Çubuk Hay. İh.	Ankara	Ankara	Not active	Livestock	255	0
Dökümcüler	Ankara	Ankara	Active	Casting	240	0
Beypazarı	Middle Sakarya	Ankara	Not active	-	300	0
Bilecik I	Göksu	Bilecik	Active	Marble	110	36
Bilecik II	Göksu	Bilecik	Active	Marble	194	15
Bozüyük	Göksu	Bilecik	Active	Metal	550	7
Osmaneli	Göksu	Bilecik	Active	Ceramic	97	0
Pazaryeri	Göksu	Bilecik	Active	Ceramic	145	3
Söğüt	Göksu	Bilecik	Not active	-	140	0
İnegöl	Göksu	Bursa	Active	Textile	300	86
İnegöl Mob. İh.	Göksu	Bursa	Not active	Furniture	410	0
Yenişehir	Göksu	Bursa	Active	Glass	173	2
Sakarya I	Lower Sakarya	Sakarya	Active	Automotive	161	59
Sakarya II	Lower Sakarya	Sakarya	Active	Automotive	350	23
Sakarya III	Lower Sakarya	Sakarya	Active	Food	254	25
Karasu	Lower Sakarya	Sakarya	Not active	Iron and Steel	44	0
Ferizli	Lower Sakarya	Sakarya	Not active	-	-	-
Kaynarca	Lower Sakarya	Sakarya	Not active	-	-	-

4.7 Power Plants

Sakarya Basin is a basin with high electricity demand and electricity production. There are nearly 100 power plants in the basin. The annual total electricity production of these power plants, calculated within the scope of this current study, amounts to approximately 35,464 GWh. Approximately 65% of the total electricity production is realized by natural gas, 28% by coal/lignite fired thermal power plants and 5% by hydroelectric power plants. Enka Gebze Thermal Power Plant, Türkiye's 4th largest thermal power plant, is located in the Sakarya Basin. Other important thermal power plants in the basin are Baymina Ankara Natural Gas Power Plant (798 MW), Çayırhan Thermal Power Plant (620 MW) in Ankara; Seyitömer Thermal Power Plant (600 MW), and Tunçbilek Thermal Power Plant (365 MW) in Kütahya. The most important hydroelectric power plants in the basin are Sarıyar (160 MW), Gökçekaya (278 MW) and Yenice (38 MW) HPPs. The distribution of the power plants according to their type, total number, electricity generation and water consumption is given in Table 4-2.

Due to the Enka Gebze thermal power plant, approximately 46% of the total electricity generation in the Sakarya Basin is realized in the Lower Sakarya subbasin. Middle Sakarya is responsible for 23% of the total electricity production and most of the power plants are located in this subbasin. In addition, all of the important hydroelectric power plants are located in this subbasin. Middle Sakarya subbasin is followed by Ankara (18%) and Porsuk (11%) subbasins, respectively, in terms of their share in total electricity production. Electricity generation in Upper Sakarya and Göksu subbasins is quite low compared to other subbasins. There are no power plants in the Kirmir subbasin. The distribution of electricity generation by subbasins in the Sakarya Basin is given in Table 4-3. The location of the power plants evaluated within the scope of this study is given in Figure 4-4.

Table 4-2. The distribution of power plants based on their number, installed capacity, electricity generation and water consumption in the Sakarya Basin

Power Plant Type	Total Number of Plants	Total Installed Capacity (MW)	Annual Total Electricity Generation (GWh)	Percentage (%)	Total Water Consumption (m^3/y)	Water Intensity (m^3/GWh)	Capacity Factor
Natural gas	24	3408.9	23154.5	65.3	5356695	231.3	0.79
Lignite/Coal	8	1687.6	9775.6	27.6	23952568	2561.2	0.66
Hydropower	24	683.6	1686.3	4.8	28706210	17023.0	0.42
Biogas	10	71.2	329.6	0.9	255770	776.0	0.50
Fuel Oil	2	36.0	262.3	0.7	1993	7.6	0.83
Wind	2	39.1	105.1	0.3	0	0.0	0.30
LPG	1	9.6	79.0	0.2	600	7.6	0.94
Coal	1	10.0	56.9	0.2	5535	97.2	0.66
Solar	26	30.5	44.9	0.1	170	3.8	0.17
Waste heat	1	6.0	26.3	0.1	200	7.6	0.50
Total	**98**	**5972.4**	**35463.5**	**100**	**58274206**	**1643.2**	

Table 4-3. The distribution of electricity generation by subbasins in the Sakarya Basin

	HPP (GWh)	TPP (GWh)	Wind (GWh)	Solar (GWh)	Biomass (GWh)	Total (GWh)	Percentage (%)
Upper Sakarya	-	198.0	-	11.1	6.3	215.4	0.6
Porsuk	-	4,008.5	-	4.7	8.8	4021.9	11.4
Ankara	-	6,140.5	-	44.5	288.4	6473.4	18.3
Kirmir	-	-	-	-	-	-	-
Middle Sakarya	1,388.1	6,633.4	105.1	0.01	12.4	8,139.0	23.0
Göksu	125.6	179.3	-	0.03	-	305.0	0.9
Lower Sakarya	172.6	16,059.0	-	-	-	16,231.6	45.9

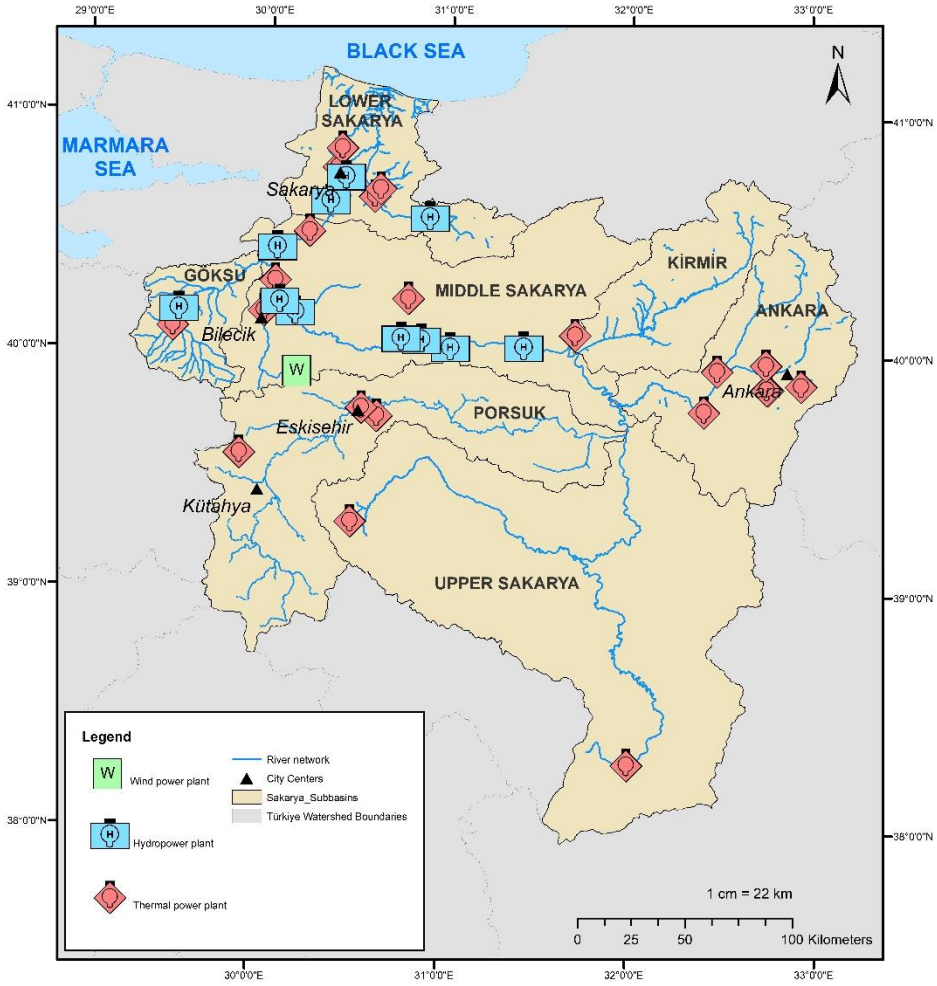

Figure 4-4. Location of the power plants modeled in the baseline period

CHAPTER 5

WEAP LEAP MODEL SETUP IN THE SAKARYA BASIN

In this chapter, theoretical background information about the WEAP and LEAP models; data sources and data collection for the coupled WEAP-LEAP model; WEAP, LEAP, and the integrated model setups; the calibration and the validation of the model will be explained in detail.

5.1 WEAP Model Theoretical Background

The Water Evaluation and Planning System (WEAP; Yates et al., 2005) is a hydrological conceptual model. It operates on the basic principle of a water balance and can be applied to municipal and agricultural systems, a single watershed, or complex transboundary river basin systems. WEAP was developed by Stockholm Environment Institute (SEI), and it is a tool for integrated water resources planning. WEAP can solve multi-sectoral water allocation problems based on demand priority and supply preferences. Water resources, i.e., surface water, including snow and glacier runoff and groundwater; water demand, i.e., urban, hydropower, irrigation, and environmental flows; and water infrastructures, i.e., reservoirs, canals, and wells, can be represented by WEAP.

The WEAP model is used to study water supply and demand systems, which can be defined as a set of demand sites or a specific water supply system such as a river basin or groundwater aquifer. Another way to define a study area in the WEAP model is to include both a set of demand sites and a specific river system together as

the study area. The model uses a drag-and-drop graphical interface called the Schematic View to visualize the physical features of the system, which consists of demand sites, catchments, rivers, diversions, groundwater, other supplies, transmission links, runoff/infiltration links, return flow links, waste water treatment plants, and priorities for water allocation. GIS layers can be added to the schematic for clarity (Sieber and Purkey, 2015). The starting point for all activities in WEAP is the Schematic View. Figure 5-1 and Figure 5-2 depicts various screenshots of the schematic view of the WEAP model developed in the context of this study. Information about WEAP schematic components defined within the scope of this study is given in the subsections of this section.

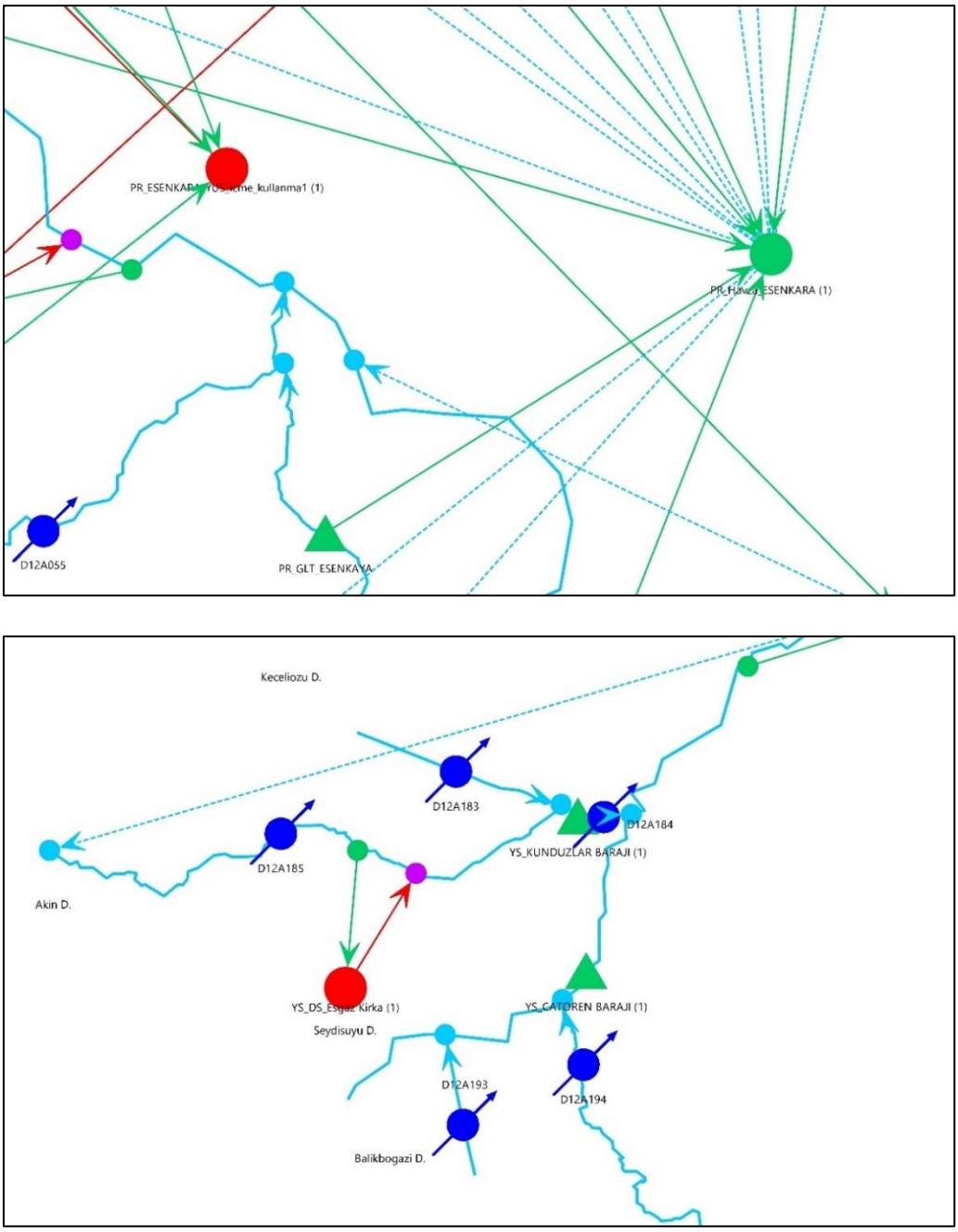

Figure 5-1. Schematic views from the WEAP model: Upper and lower figure are zoom into parts of Porsuk and Upper Sakarya subbasins, respectively

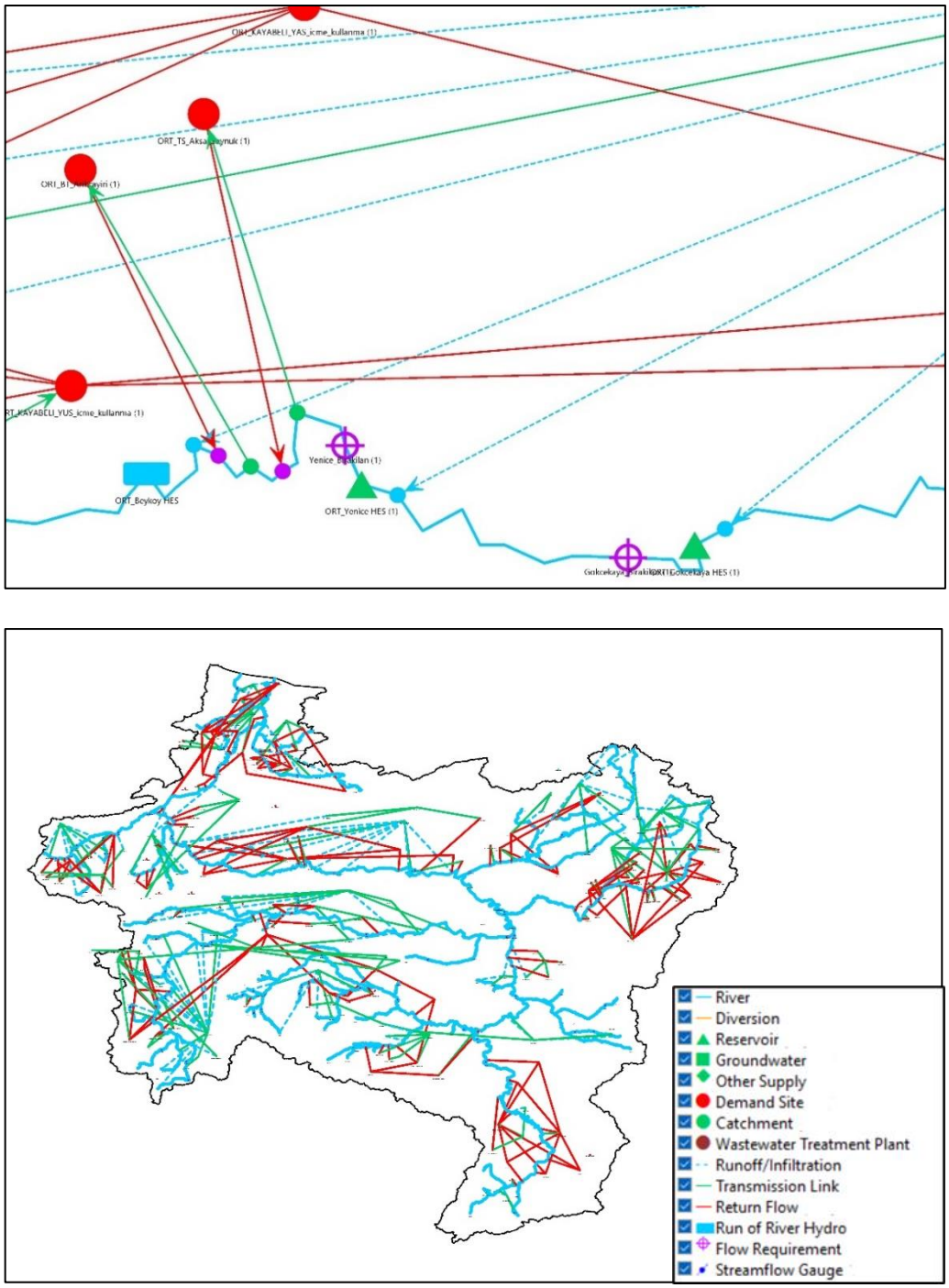

Figure 5-2. Schematic views from the WEAP model: Upper figure is zoom into a part of Middle Sakarya subbasin. Lower figure is the complete WEAP model schematic view

WEAP is a modeling tool that calculates water and pollution mass balance for each node and link in a system on a monthly time step. It dispatches water to meet different requirements subject to constraints such as demand priorities, supply preferences, and mass balance. The calculations follow a specific order each month, which includes determining annual demand and monthly supply requirements, calculating inflows and outflows of water, generating hydropower, estimating costs and benefits, and accounting for pollution generation and treatment. The time scale is relatively long, so all flows are assumed to occur instantaneously within a month. Additionally, if a MODFLOW model is linked, WEAP results will be loaded into the MODFLOW input files, and MODFLOW will be run for one time step before its results are read into WEAP (Sieber and Purkey, 2015).

In the WEAP model, the processes such as precipitation, evapotranspiration, runoff, and irrigation are computed in a user-defined area called a catchment. There are five different methods to simulate catchment processes: (i) Irrigation Demands Only Method (Simplified Coefficient Method), (ii) Rainfall-Runoff Method (Simplified Coefficient Method), (iii) Rainfall-Runoff Method (Soil Moisture Method), (iv) MABIA Method (FAO 56, Dual Kc, Daily), and (v) Plant Growth Method (PGM). The method chosen varies depending on data availability, the purpose of the study, and how detailed the watershed processes are to be modeled (Sieber and Purkey, 2015). Within the scope of this thesis, the Soil Moisture method was used to model catchment processes. The main reason for this is that the Soil Moisture method can model the effects of different land use and soil properties, vegetation types, and weather conditions on soil moisture dynamics. Thus, it provides a detailed understanding of the water balance in the soil, which is essential for managing water resources. However, for these reasons, it requires much more detailed climate and soil parameterization than either version of the Simplified Coefficient Method. The MABIA method is a daily simulation of transpiration, evaporation, irrigation requirements, scheduling, crop growth and yields. It also includes modules for

estimating reference evapotranspiration and soil water capacity. This method uses the dual Kc method. PGM method simulates plant growth, water use, and yield using a daily time step. It was developed to provide a method to study the impacts of altered atmospheric CO_2 concentration, temperature stress, season length variability, and water stress on plant water use and crop yields (Sieber and Purkey, 2015). The choice of method in the WEAP model depends on the specific focus of the analysis and the data available. The Soil Moisture method is a simple and effective way to simulate catchment processes, and it is well-suited to the specific purpose of this study. Since there is no need to perform daily simulations within the scope of this study, there is no need for the additional complexity of the PGM or MABIA methods. The Soil Moisture method provides a good balance between accuracy and simplicity. In summary, the Soil Moisture method is the best choice for this study because it meets the specific needs and provides the necessary level of detail without unnecessary complexity.

The Soil Moisture method uses a one-dimensional, two-layer soil moisture dynamic accounting system with empirical functions to partition water into evapotranspiration (ET), surface runoff, sub-surface runoff (interflow), and deep percolation (Figure 5-3). The catchment processes such as evapotranspiration, surface runoff, percolation, and interflow are simulated in the upper soil layer. Base flow routing the river and soil moisture changes are computed in the lower soil layer. The empirical functions that describe the processes in each soil compartment can be seen in Figure 5-3. Climate data, including precipitation, temperature, relative humidity, and wind speed, is an important input for the method, and each subbasin/catchment unit has a unique climate dataset. The subbasin/catchment unit is divided into fractional areas with independent land use/land cover (LULC) classes, and each fractional area's LULC values are summed to reflect the lumped hydrologic response (Abera Abdi and Ayenew, 2021). Surface runoff, interflow, and base flow are linked to a river feature, while ET is lost from the system. ET is calculated by the Penman-

Monteith method. A water balance is computed for each fractional area, and the deep percolation can be transmitted to a surface water body as baseflow or directly to groundwater storage by linking the subbasin unit node to a groundwater node. The empirical equation for the water balance is calculated as follows (Equation 5.1) (Sieber and Purkey, 2015):

$$Rd_j \frac{dZ_{1,j}}{dt} = P_e(t) - ET_0(t)K_{c,j}(t)\left(\frac{5Z_{1,j} - 2Z_{1,j}^2}{3}\right) - P_e(t)Z_{1,j}^{RRF_j} - f_j k_{s,j} Z_{1,j}^2 - (1 - f_j)K_{s,j}Z_{1,j}^2 \quad 5.1$$

where

$Z_{1,j}$= [1,0] the relative storage given as a fraction of the total effective storage of the root zone, (mm) for land cover fraction, j,

Rd_j: soil water holding capacity of land use j [mm]

P_e : effective precipitation [mm],

$ET_0(t)$: reference evapotranspiration [mm/day]

$K_{c,j}$: crop/plant coefficient for each fractional land cover, j,

RRF_j: runoff resistance factor for land cover fraction, j,

$P_e(t)Z_{1,j}^{RRF_j}$: surface runoff

$f_j k_{s,j} Z_{1,j}^2$: interflow from the first layer land use

f_j: partitioning coefficient related to the land cover, soil and topography

$K_{s,j}$: the saturated conductivity of the lower storage [mm/time]

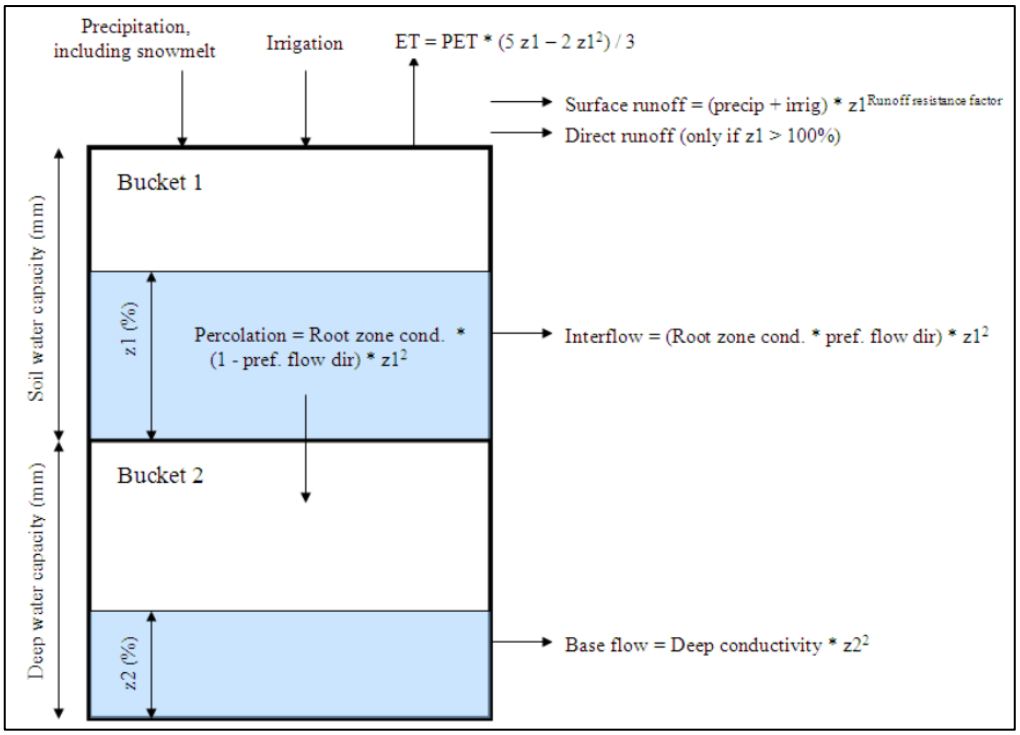

Figure 5-3. Conceptual diagram and equations incorporated in the Soil Moisture method (Sieber and Purkey, 2015)

The WEAP model considers the hydraulic connection between surface water and groundwater in watersheds. Streams can either gain water from or contribute to groundwater recharge, depending on the groundwater level in the aquifer. Groundwater levels are affected by both natural precipitation and irrigation in the watershed. To simulate groundwater interactions with surface water in the WEAP model, there are four options: (i) directly specifying groundwater inflow to a river, (ii) modeling interactions using a groundwater "wedge" connected to a river, (iii) modeling interactions using a deep soil layer of the Soil Moisture method catchment, or (iv) linking WEAP to MODFLOW (Sieber and Purkey, 2015). In this study, groundwater-surface water interactions were specified directly; they were not modeled.

5.2 LEAP Model Theoretical Background

The Low Emissions Analysis Platform (LEAP) is a software tool for quantitative modeling of energy systems, energy sector and non-energy sector greenhouse gas (GHG) emissions, cost-benefit analysis of different energy portfolios together with their environmental impacts, health impacts, and sustainable development indicators (Lazarus et al., 1995). LEAP is not for the modeling of a specific energy system but it is a tool to generate models for different energy systems. LEAP was created by SEI to support sustainable development by informing decision-making and allowing stakeholders to perform their analyses. It is a well-suited tool for medium and long-term planning.

LEAP allows the user to embed simulation and optimization methods into an accounting framework that accounts for energy, emissions, costs, and natural resources. Moreover, it is a scenario-based tool and hence the impacts of different policies, assumptions, and analytical questions can be evaluated and compared with LEAP. LEAP can be used to develop models at numerous scales such as national, subnational, regional, and global. LEAP has libraries of default data for conversion units, the physical characteristics of pollutants and fuels, and emission factors. LEAP has an annual time step with seasonal/time-of-day details (SEI, 2005).

The structure of a representative LEAP analysis is shown in Figure 5-4. LEAP was originally built as an energy systems model. However, today it can also be used for purposes such as cost-benefit analysis and determination of SDG indicators. LEAP models final energy demand which is often premised on exogenous demographics and macroeconomics, and the supply side responds to the final energy demands. Furthermore, LEAP models the transformation from one form of energy to another. There are special modules for the extraction of primary resources, land-use change, and land-based resources. LEAP also includes statistical differences in stock changes

which are accounting conventions used in energy balances. In addition to all of these capabilities, LEAP allows users to model pollutant emissions, carry out an integrated cost-benefit analysis, and assess the impact of air pollution on mortality, crop losses, and temperature change. In the most recent version of LEAP, it is possible to evaluate the impact of different climate mitigation pathways on sustainable development indicators (Veysey and Wagner, 2021).

Within the scope of this thesis, energy demand analysis was not performed with LEAP. For all scenarios, annual total energy values were calculated externally and entered into the LEAP model during the simulation period (details in Section 5.5). By using Transformation Analysis, one of the analyzes that form the backbone of the LEAP model, answers to the questions such as whether the total electricity need can be met, how the distribution of electricity generation will be on a plant basis in different scenarios, and how CO_2 emissions will change were obtained. In the Transformation Analysis, the "Electricity Generation" module was created and electricity production “Processes" and "Output Fuel" were defined under this module. In LEAP, each power plant where electricity is produced was defined separately. "Output fuel" was selected as electricity. The details of the LEAP model setup are given in Section 5.5.

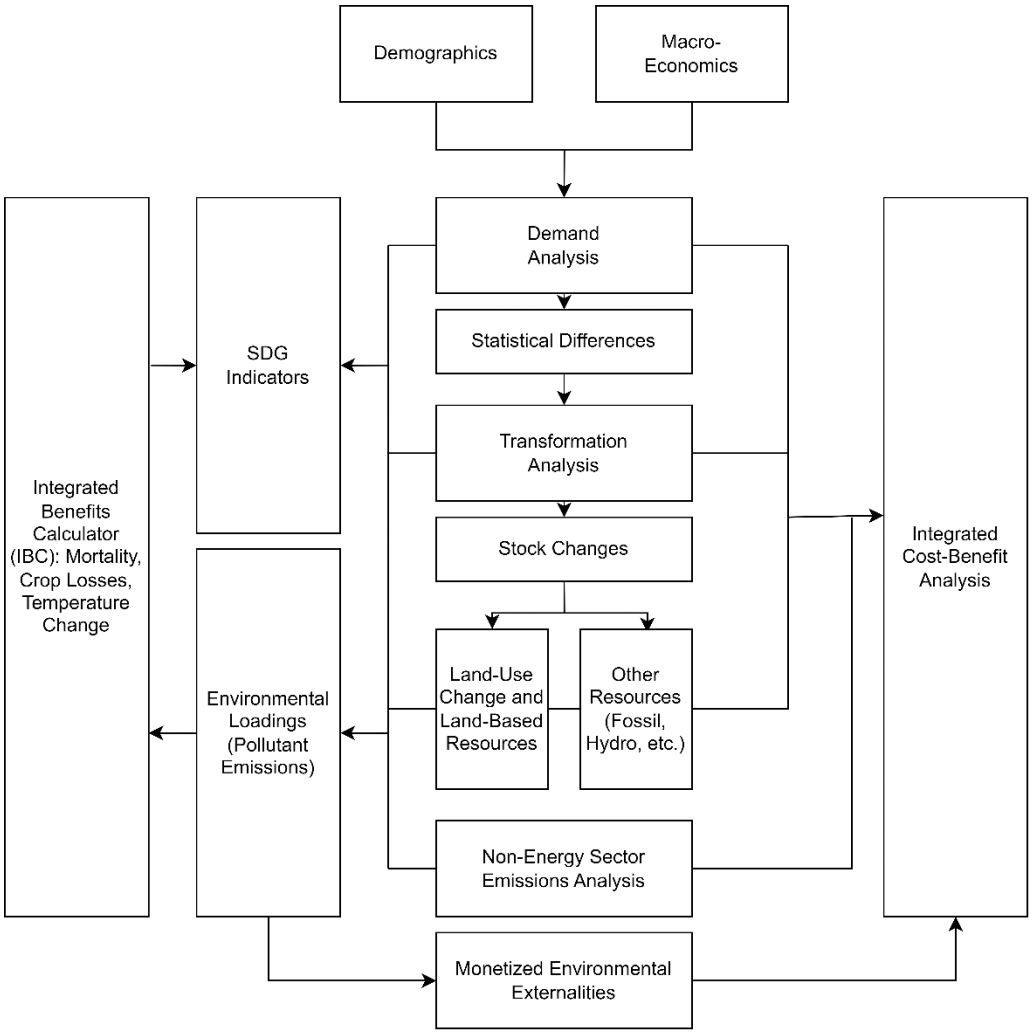

Figure 5-4. Structure of a representative LEAP analysis (Veysey and Wagner, 2021)

5.3 Data Sources and Data Collection

WEAP model inputs and data sources are given in Table 5-1. Some information about the demand sites, especially power plants was obtained through field studies.

The remaining data that need to be entered into the model were either obtained from the relevant institutions or open literature.

LEAP's data requirements are relatively simple compared to WEAP. The LEAP tree branches and the related inputs and sources are listed in Table 5-2. In LEAP, data describing the percentage of the maximum availability of each power plant, which means the highest percentage of hours that process is available in each dispatch period, is required. In this study, since WEAP and LEAP models are used in a coupled way, this data is calculated based on the information coming from WEAP. Detailed information about the integration of WEAP and LEAP models is given in Section 5.6.

Table 5-1. WEAP Model Inputs and Data Sources

	Data	Source
Basic Data	Topography	Shuttle Radar Topography Mission (SRTM)
	Land use/Land cover	CORINE 2018 LULC map and State Hydraulic Works (DSİ)
	Meteorological Data	General Directorate of Meteorology
Demand Sites and Catchment Data	Urban	Sakarya Basin Protection Action Plan, DSİ and TÜİK
	Industry	Field study and literature
	Energy	Energy and Natural Resources Ministry, Energy Market Regulatory Authority (EPDK) and field study
	Agriculture	TÜİK, DSİ, Ministry of Agriculture and Forestry, Directorate of Agriculture, Irrigation Cooperatives
Sources and Allocations	Rivers	DSİ
	Groundwater	DSİ and literature
	Reservoirs/Dams/Ponds	DSİ and field study
	Transmission Links	DSİ
	Return Flow	DSİ

Table 5-2. LEAP Model Inputs and Data Sources.

Tree Branches in LEAP	Data	Source
Demand	Yearly electricity demand	Turkish Energy Exchange (EPİAŞ)
Transformation	Electricity generation processes: • Installed capacities of power plants, • Average energy efficiencies of power plants • Costs, i.e., capital ($/MW), fixed ($/MW) and variable ($/MWh) operating and maintenance and fuel costs ($/GJ) of each power plant*, • The seasonal load shape for the electric system e.g., MW hourly peak load shape, • Maximum availability of each type of power plant**, • Feedstock fuels	EPİAŞ, Energy Market Regulatory Authority (EPDK), field surveys, literature survey
Resources	Fuel characteristics, e.g., energy content, chemical composition etc.	Electricity generation company (EÜAŞ), Field surveys, literature survey

*Within the scope of this study, electricity generation optimization was not made according to the cost. However, in case of the possibility of developing such a scenario in the future, this information was entered into the model. **This parameter is calculated based on the information coming from WEAP in this study.

5.4 WEAP Model Setup

In the Sakarya Basin, WEAP model simulation period was selected as 2004 – 2017, and the model was run on a monthly time-step. This period was determined based on the availability of data. The study area was divided into seven subbasins. These subbasins are Upper Sakarya, Porsuk, Ankara, Kirmir, Middle Sakarya, Göksu and Lower Sakarya. These subbasins are further divided into ‘catchments’ based on the location and data availability of gauging stations to allow calibration. These catchments are shown in Figure 5-5. The information on all of the stream gages used for model setup is given in Table 5-3. All these stations were not used in the calibration, but their information was checked during the selection of the stations to be used for calibration and during the creation of the 'catchments'. The stations in bold in Table 5-3 are the stations used in the calibration and validation phases. The

locations of the gauging stations used in the model calibration are provided in Figure 5-5.

In the following subsections, information on the Land Use/Land Cover and climate data required by the Soil Moisture method, two important parameters of this method: Kc and RRF, water supply and resources, and demand sites are given.

Table 5-3. Information on gauging stations.

Subbasin	Name	Station Code	Monitoring Period	Drainage Area (km^2)	Altitude (m)
Lower Sakarya	Dinsiz Ç. - Yağbasan	E12A019	1953-1968; 1971-2011	410.8	25
	Mudurnu Ç. – Dokurcun	E12A037	1956-2011 2013-2014	1073.4	286
	Mudurnu Ç. – Gebeş	D12A136	1978-1983; 2003-2004; 2006-2008	1521	25
	Sakarya N. – Adatepe	**E12A057**	**2002-2011; 2014-2015; 2018**	**56224.4**	**6**
Göksu Middle Sakarya	Sakarya N.-Doğançay	E12A021	1953-2011; 2015-2016	52531.6	41
	Kocasu - Rüstümköy	**E12A022**	**1953-2014;**	**2021.6**	**198**
	Sakarya N.-Kayabeli	**E12A058**	**2004-2011; 2013-2016**	**46334.9**	**114**
Kirmir	Kirmir C. - Yeşilöz Köprüsü	D12A244	2004-2007	2239	680
	Kara D.- Endil Boğazı	**D12A243**	**2003-2008**	**5.9**	**910**
Ankara	**Ankara Ç. - Meşecik**	**E12A026**	**1963-2011; 2015**	**7140**	**635**
	Mera Ç. - Uğurlu	**D12A242**	**2003-2015**	**121**	**1015**
Porsuk	Porsuk Çiftliği	D12A033	1962-1984; 1987; 1989; 1991-2008 2010-2016	2432	951
	Çalça (Y.Bosna)	D12A181	1986-1995; 1997; 1999-2009 2011-2016	3810.5	912
	Porsuk Barajı Çıkış	D12A034	1963-2005; 2007-2016	4655	842
	Eşenkara	D12A054	1964-2004; 2006-2016	5169	807
	Parsibey	D12A215	2012-2016	867.1	750
	Kıranharmanı	**E12A051**	**1989-2010; 2015**	**10955.4**	**676**
	Beşdeğirmen	**E12A003**	**2003-2011**	**3938**	**855**
Upper Sakarya	Aktaş	E12A024	1963-2011; 2013-2016	4342.2	837
	Aydınlı	D12A159	1982-2008; 2011 2015-2016	2117.2	790
	Ayvalı Yaylası	**E12A052**	**1989-2008; 2010-2011; 2013-2016**	**19839**	**709**

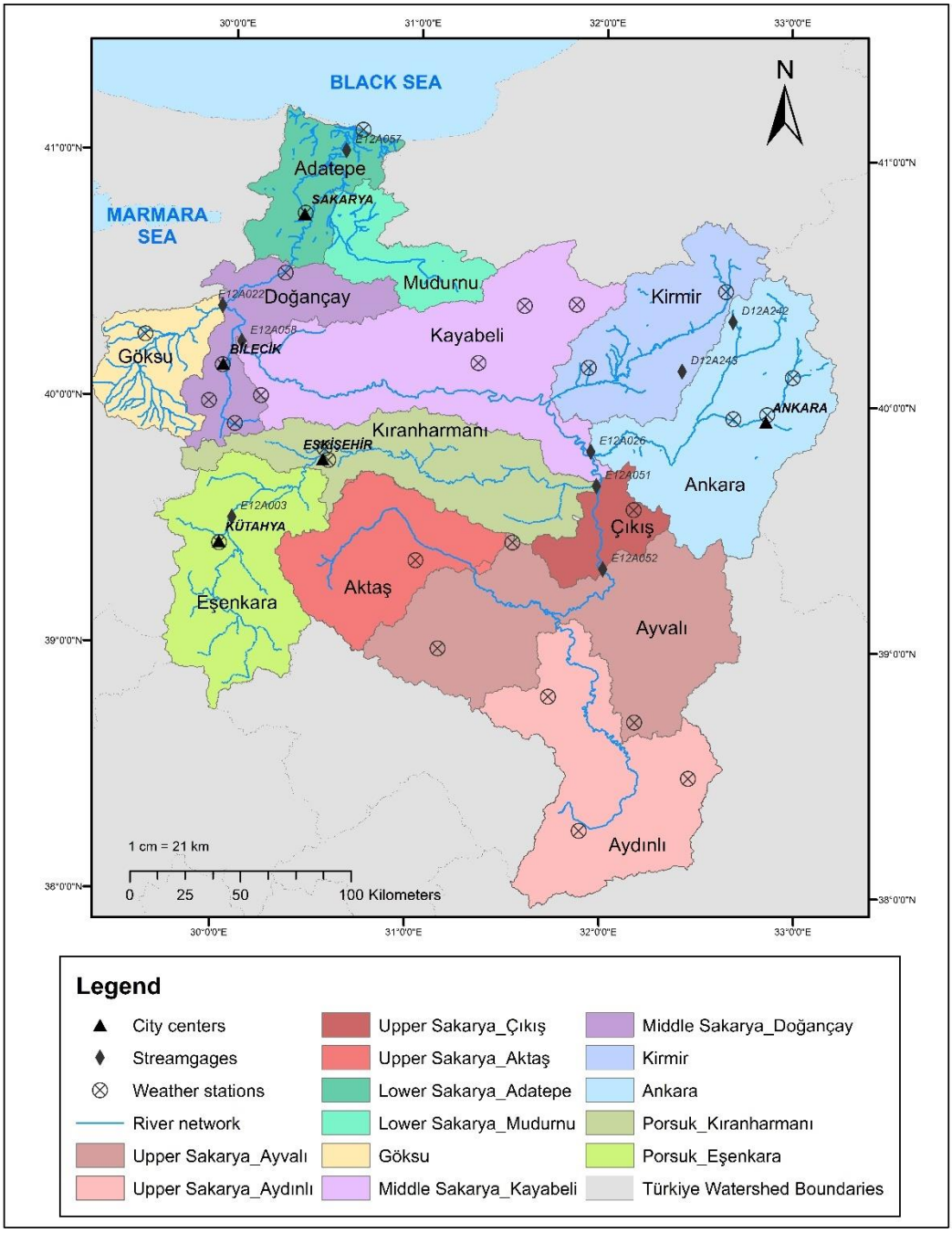

Figure 5-5. WEAP catchments, locations of weather stations used for the model setup, and the locations of streamgages used in the model calibration

5.4.1 Land Use/Land Cover

WEAP model inputs and data sources were previously summarized in Table 5-1. Land use and land cover (LULC) information of the basin was obtained by using the Coordination of Information on the Environment (CORINE) 2018 data. In the WEAP model, agricultural area and forest and semi-natural area subclasses were defined according to CORINE Level 3, while artificial areas were not divided into subclasses, but they were defined as the sum of all artificial area subclasses. The areas and percentage distribution of CORINE land use classes in each subbasin and catchments are given in Table A. 1 in the Appendix A. In addition, the crop pattern was defined in non-irrigated and irrigated farming lands. However, data for non-irrigated and irrigated land use classes do not belong to CORINE 2018. They were collected from DSİ (State Hydraulic Works) reports and the Turkish Statistical Institute (TuskStat). The permanently irrigated agriculture area changes year by year. The crop pattern of permanently irrigated lands was assumed to be constant throughout the simulation period. The difference between the CORINE land use classes areas and the areas obtained from DSİ and TurkStat was distributed to other selected land use classes according to their areal proportion. The land uses where the difference was distributed are the classes called pastures, complex cultivation patterns, and land principally occupied by agriculture, with significant areas of natural vegetation, which are under the "Agricultural areas" class.

In the WEAP model, a separate catchment component was created for agricultural lands irrigated with groundwater in each unit in each subbasin. The crop pattern of these catchments, therefore, reflects the crop pattern of areas irrigated with groundwater only.

5.4.2 The Crop Coefficients (Kc) and Runoff Resistance Factor (RRF)

The crop coefficients, Kc values, represent the crop type and the development of the crop. There may be several Kc values for a single crop depending on the crop's stage of development (Figure 5-6). In the WEAP/Soil Moisture model, Kc values have to be defined for each land use class and the crops/plants. For the Kc values of the crops, the report named “Evapotranspiration of irrigated plants in Türkiye” which was prepared by TAGEM and DSİ (2017) was used. For the land use classes the Kc values given in Table 5-4 were used. The Kc values of the crops and land use classes were not calibrated.

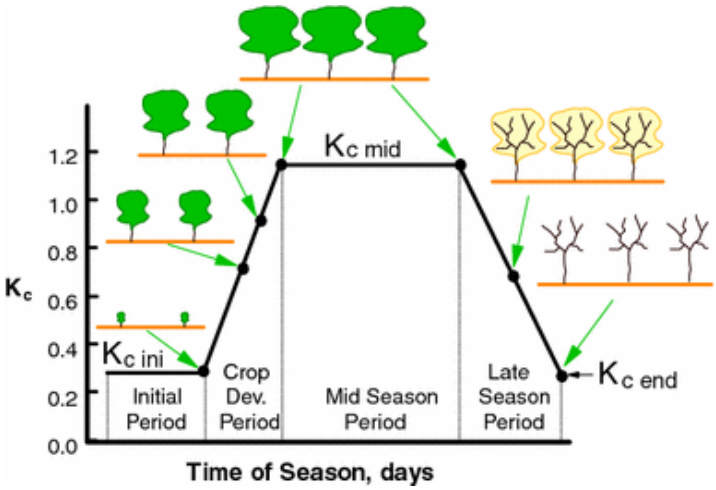

Figure 5-6. FAO segmented crop coefficient curve and four growing stages (Allen and Pereira, 2009)

Runoff Resistance Factor (RRF) is used to control surface runoff response. It is related to factors such as leaf area index (LAI) and land slope. In the model, it ranges from 0 to 1000, and runoff will tend to decrease with higher values of RRF. Since RRF is correlated with LAI, LAI values determined for similar land use classes

(Ingol-Blanco and McKinney, 2012) were used for Sakarya Basin as initial calibration values for RRF.

Table 5-4. Kc values and RRF initial calibration values for land use classes.

Land Use Class	**Kc** (Amato et al., 2006)	**LAI** (Ingol-Blanco and McKinney, 2012)
Artificial Surfaces	0.77	8.00
Non-irrigated/Irrigated Agricultural Lands	-	4.22
Pastures	0.46	2.50
Forests	0.35	5.18
Semi Natural Areas	0.30-0.46	1.31-2.50
Wetlands	0.90	6.34
Water Bodies	1	0.10

5.4.3 Climate Data

Thiessen Polygon method was used to obtain catchment precipitation data in each subbasin. For this purpose, 27 different meteorology stations located in and around the Sakarya subbasins were used. The location of meteorological stations can be seen in Figure 5-5. For the data of temperature, humidity, and wind speed, the meteorology station with the largest Thiessen polygon area in the relevant subbasin was used, because it would better represent the subbasin. The Thiessen polygons are shown in Figure 5-7. The climate input data of the catchment components in the WEAP model are given in the Appendix A in Figure A. 1, Figure A. 2, Figure A. 3, Figure A. 4, Figure A. 5, Figure A. 6, Figure A. 7 for each subbasin, respectively.

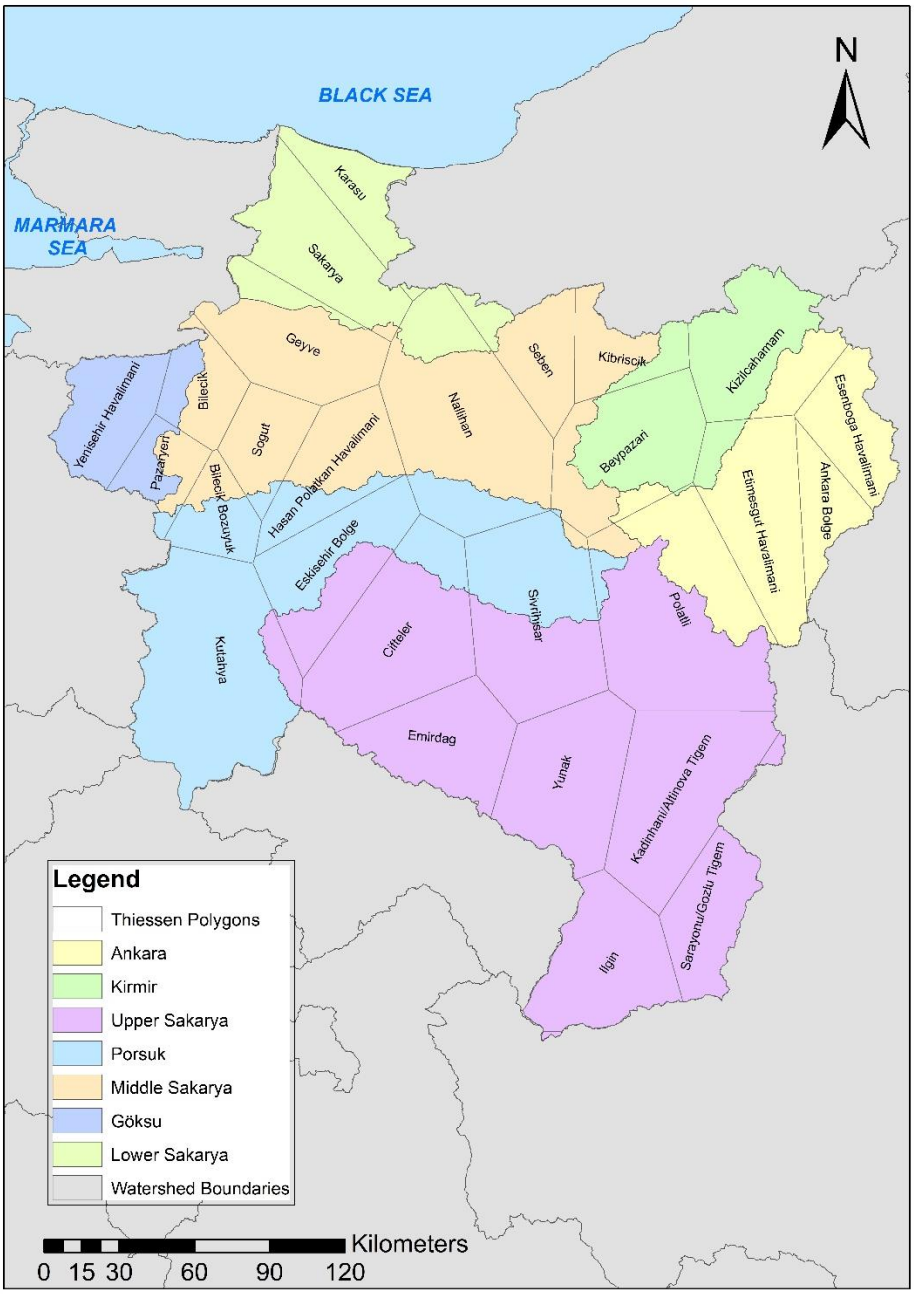

Figure 5-7. Thiessen polygons used to obtain climate data of catchment components in the WEAP model

5.4.4 Supply and Resources

In the WEAP model, the Supply and Resources section determines the amounts, availability and allocation of supplies, simulates monthly river flows, including surface/groundwater interactions and instream flow requirements, hydropower generation, and tracks reservoir and groundwater storage (Sieber and Purkey, 2015). The Supply and Resources section consists of the following subsections: (i) Transmission Link, (ii) Rivers and Diversions, (iii) Groundwater, (iv) Local Reservoirs, (v) Other Supplies. Water supply to demand sites is provided via transmission links, and the amount of water loss and physical capacities of these links can be defined. Surface inflows to rivers, properties, and operation of reservoirs and run-of-river hydropower facilities, instream flow requirements, surface water-groundwater interaction, and streamflow gauges are defined under the Rivers and Diversions subsection. Groundwater subsection includes aquifer properties, storage capacities, and natural recharge. Local Reservoirs refer to the reservoirs which are not on a river. Surface sources that are not modeled in the WEAP, such as inter-basin transfers, are defined under Other Supplies subsection. The return flows subsection is for routing of wastewater from demand sites to the wastewater treatment plants, or routing of treated effluent from wastewater treatment plants to one or more rivers, groundwater nodes, or other supply sources (Sieber and Purkey, 2015). In the following subsections, the supply and resources defined in this study are explained.

Transmission Links

Transmission links transport water from surface water, groundwater and other supplies to satisfy final demand at demand sites. In the WEAP model, water is allocated to the demand sites according to their demand priorities. In this study, it is assumed that all transmission links have equal demand priority in the baseline simulation period.

Rivers and Diversions

In this study, the Sakarya Basin was divided into seven subbasins, and these subbasins are further divided into catchments by using the streamflow monitoring gauges. Runoff calculated by the Soil Moisture method in catchments was distributed to the rivers according to the drainage areas of the important dams in the subbasin. For this purpose, first, the percentage of the drainage areas of dams based on the total catchment area was calculated. Then, instead of having a single runoff/infiltration link, the link was divided into several links based on the number and location of the dams. Thus, the runoff fraction that needs to be defined in these runoff/infiltration links was set according to the drainage area of the dams. Consequently, both realistic inflow values were sent to the dams and accurate streamflow values were obtained in streamflow gauging stations determined as pour points.

Groundwater

The characteristics of the groundwater basins, i.e., initial storage (hm^3) and annual total natural recharge (hm^3/yr), in the Sakarya Basin were obtained from the master plan prepared by DSİ (DSİ, 2017). In the WEAP model, the groundwater sources and their physical characteristics were created in each subbasin accordingly (Table 5-5). Thus, groundwater-surface water interactions were specified directly; they were not modeled.

Table 5-5. Groundwater sources and their characteristics defined in the WEAP model

Subbasin	GW Source	Initial Storage (hm^3)	Natural Recharge (hm^3/yr)
Upper Sakarya	Aktaş	174	186
	Aydınlı	360	287
	Ayvalı	170	378
	Çıkış	27	63
Porsuk	Eşenkara	137	186
	Kıranharmanı	222	174
Ankara	Ankara	130	125
Kirmir	Kirmir	42	81
Middle Sakarya	Kayabeli	68	107
	Doğançay	56	97
Göksu	Göksu	112	140.4
Lower Sakarya	Mudurnu	78	94
	Adatepe	211	277

Reservoirs and Ponds

There are many reservoirs and ponds in the Sakarya Basin that are used for different purposes. The reservoirs in the subbasins were individually defined in the model. However, one reservoir component was created and placed at the location of the largest pond in each subbasin, to represent all the ponds in the relevant subbasin. The characteristics of this pond, representing all the ponds, were calculated by summing up the total, active, and inactive volumes of the smaller ponds. The surface runoff fraction of the runoff/infiltration link was determined based on the total drainage areas of the ponds. This link was connected to the upstream of the largest pond. Similarly, the inflows of the reservoirs were obtained by distributing the surface runoff formed in the relevant catchment according to the drainage area ratios of the reservoirs. The physical characteristics of the reservoirs and the ponds are given in the Appendix A in Table A. 2. Top of conservation and top of buffer volumes were assumed to be equal to the storage capacity and the inactive volume, respectively.

Net evaporation in the reservoirs was calculated via the Pan Evaporation method. For this purpose, open surface evaporation data were obtained from Turkish State

Meteorological Service (MGM). This data was not available for all MGM stations located in the basin. The monitoring period of the available data was 2016-2017. To calculate the net evaporation in the reservoirs, firstly, the correlation between temperature and evaporation data of the meteorology station was found. Then, the elevation difference between the reservoir lake and the meteorological station where evaporation and temperature are measured was found to correct temperature. This elevation difference was multiplied by the default value used in temperature correction, thus the temperature values in the reservoir were calculated. Evaporation from the reservoir lake was calculated by using the reservoir site temperature values in the correlation equation between temperature and evaporation. Finally, since the model requires net evaporation data, the precipitation values were subtracted from the evaporation data. The monthly average net evaporation values in the reservoirs during the simulation period are given in the Appendix A in Table A. 3.

5.4.5 Demand Sites

The demand sites in the Sakarya Basin consist of districts, industries, and power plants. The yearly water consumption amounts of these demand sites were defined in the model except fossil fuel power plants since their water consumption is calculated based on the electricity generation value calculated by the LEAP model. For each sector, i.e., using/drinking and industry, demand sites were created separately based on the sources of water, i.e., groundwater and surface water. The water consumption percentage has to be defined for each demand site in the model. Thus, urban water consumption percentages were defined on a provincial basis by calculating the difference between the statistics of the Daily Water Withdrawn per Capita (liters/person-day) and Daily Wastewater Discharged in Municipalities (liters/person-day). These values were obtained from TÜİK. The consumption percentage of industrial demand sites were accepted as 25% unless otherwise stated.

The annual average water use amount of the demand sites in the baseline simulation period is given in Table A. 4 in the Appendix A.

5.5 LEAP Model Setup

To use WEAP and LEAP models in an integrated manner, both models' simulation period has to be the same. For this reason, the simulation period was selected as 2004 – 2017. Thus, the total electricity demand of these years has to be entered into the model. Also, data on plant characteristics and fuel type of electricity generation processes should also be entered into the model. Within the scope of the study, twelve HPPs, twenty-three different thermal (coal/lignite, natural gas, or biomass fueled) power plants and a wind power plant were defined in the baseline simulation period. Power plants with an installed capacity of less than 7 MW were not taken into consideration. The installed power, water withdrawal and consumption factor, year of commissioning of these power plants are given in Table A. 5 in the Appendix A, and their location is given in Chapter 4 in Figure 4-4.

In order to calculate the annual electricity demand during the simulation period, the monthly electricity generation data of each power plant was obtained from EPİAŞ (Turkish Energy Exchange). For the power plants whose monthly electricity generation data were not available, different sources, e.g., webpages, were used. Annual average electricity generation values were used for power plants for which electricity generation information could not be obtained separately for each year. The electricity generation information obtained was entered into the model as electricity demand. The calculated total electricity demand is given in Figure 5-8.

The LEAP modeling approach requires information on the seasonal and hourly profiles of electricity production. For this purpose, the hourly electricity generation of Türkiye in 2017 was obtained from the Load Dispatch Information system. In the

next step, the monthly Electricity Market Sector Reports for the provinces within the borders of the Sakarya Basin in 2017 were obtained from Energy Market Regulatory Authority (EMRA). The weighted total electricity generation of each province was estimated using the area percentages of the provinces that fall into the Sakarya Basin. The resulting total electricity generation of the study area was then proportioned to the total electricity generation of Türkiye. These percentages are used to determine the hourly load curve of the Sakarya Basin based on the hourly load profile of Türkiye in 2017. This load curve is also assumed to be valid throughout the simulation period. The obtained load curve for the Sakarya Basin is given in Figure 5-9.

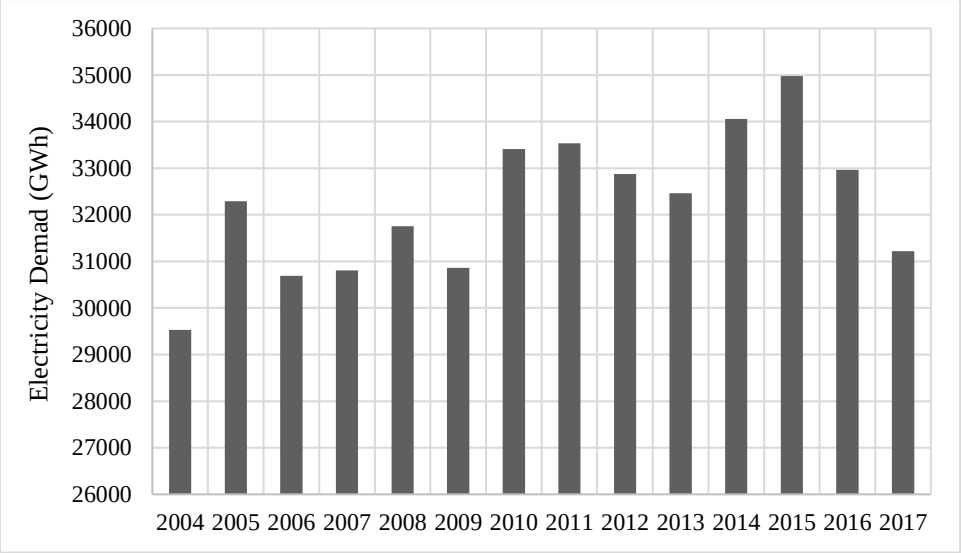

Figure 5-8. Sakarya Basin annual total electricity demand in the baseline period

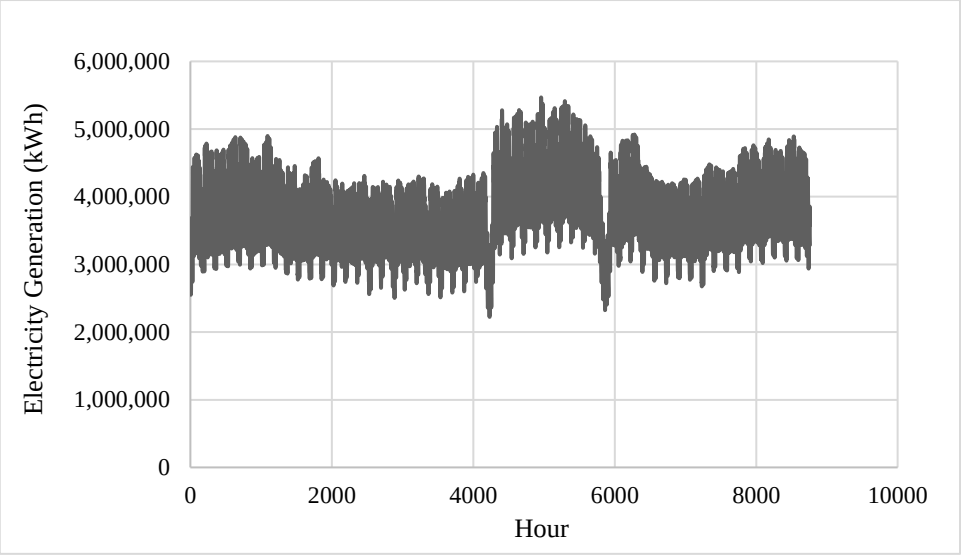

Figure 5-9. Sakarya Basin hourly load curve

5.6 Integrated WEAP-LEAP Model Setup

When WEAP and LEAP models are linked to each other, the models can transfer information to each other. Hydropower generation is calculated directly by WEAP. LEAP takes this information. The maximum availabilities of hydropower plants are calculated in LEAP by dividing the hydropower generation (in terms of MW) to the exogenous capacity (in terms of MW). Similarly, the maximum availabilities of fossil fuel power plants are calculated based on the cooling water demand coverage (%) information coming from WEAP. WEAP calculates the water demand of the plants by multiplying the average power dispatched value coming from LEAP with the cooling water requirements which are provided to WEAP. The cooling water demand coverage is calculated accordingly. Figure 5-10 shows the conceptual representation of WEAP-LEAP model integration with broadly categorized inputs of both models.

WEAPValue function is used for information transfer from WEAP to LEAP, and *LEAPValue* function is used for information transfer from LEAP to WEAP. Hydroelectric is modeled in WEAP and it is fed into LEAP model (Step 1 in Figure 5-10). In order to feed the hydroelectric modeled in WEAP into LEAP model, *WEAPValue* function is used. For example, the exact form of the function written in the Maximum Availability variable in LEAP is as follows for Plant A (Function 5.1):

*100*Min(1, WEAPValue (Supply and Resources\Reservoirs\Plant_A:Hydropower Generation[MW]/Exogenous Capacity[MW])* 5.1

LEAP makes a power distribution based on the capacities of hydroelectric and fossil-fueled power plants modeled in WEAP (Step 2 in Figure 5-10). This information is sent back to WEAP. WEAP calculates the cooling water requirement of fossil fuel power plants. Function 5.2 is entered under Water Use variable in WEAP:

*LEAPValue(Transformation\Electricity Generation\Processes\Plant_E:Average Power Dispatched[MW])*Days*24*Key\Cooling Water Requirements per MWh_Lignite_Wet[m^3]* 5.2

Accordingly, the information on how much of the water demand of the power plants is covered is calculated by WEAP and sent to LEAP (Step 3 in Figure 5-10). The exact version of the function (Function 5.3) written under the Maximum Availability variable in LEAP is as follows:

WEAPValue(Demand Sites and Catchments\Plant_E:Coverage[%]) 5.3

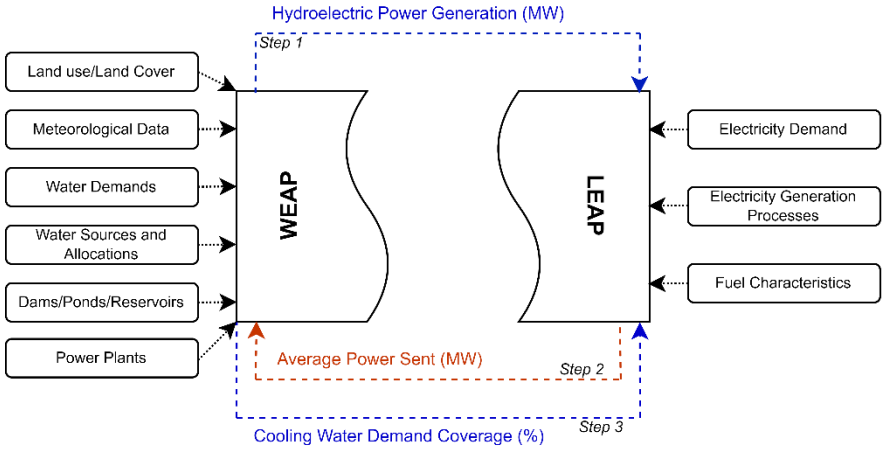

Figure 5-10. Conceptual representation of WEAP-LEAP integration

5.7 Model Calibration and Validation

Model calibration and validation were performed based on streamflow values. Reservoir volumes and the electricity generation were also evaluated throughout the calibration process. The gauging stations at the outlet of the each subbasin were used for calibration if the data is available. If not, alternative gauging stations were used. The characteristics of the streamflow monitoring stations used in the WEAP-LEAP model calibration are given in Table 5-3 in Section 5.4. The model calibration period was Oct. 2003 – Sept. 2008 except for Kirmir subbasin. In Kirmir subbasin the calibration period was selected as Oct. 2004 – Sept. 2009 due to data availability. The model validation period is different in almost all subbasins based on the availability of data. The list of calibration parameters is given in Table 5-6.

Table 5-6. The list of calibration parameters used in the WEAP model calibration

Name of the Parameter	Land Use Class	Default Value	Unit	Calibration Range
Soil Water Capacity	Artificial surfaces	1000	mm	0 - 10000
	Non-irrigated arable land	1000	mm	0 - 10000
	Permanently irrigated land	1000	mm	0 - 10000
	Vineyards	1000	mm	0 - 10000
	Fruit trees and berry plantations	1000	mm	0 - 10000
	Pastures	1000	mm	0 - 10000
	Complex cultivation patterns	1000	mm	0 - 10000
	Land princ. occup. by agr., with signf. areas of natural veg.	1000	mm	0 - 10000
	Forests	1000	mm	0 - 10000
	Natural grasslands	1000	mm	0 - 10000
	Sclerophyllous vegetation	1000	mm	0 - 10000
	Transitional woodland-shrub	1000	mm	0 - 10000
	Bare rocks	1000	mm	0 - 10000
	Sparsely vegetated areas	1000	mm	0 - 10000
	Wetlands	1000	mm	0 - 10000
	Water bodies	1000	mm	0 - 10000
Runoff Resistance Factor (RRF)	Artificial surfaces	8.00	-	0 - 100
	Non-irrigated arable land	4.22	-	0 - 100
	Permanently irrigated land	4.22	-	0 - 100
	Vineyards	4.22	-	0 - 100
	Fruit trees and berry plantations	4.22	-	0 - 100
	Pastures	2.50	-	0 - 100
	Complex cultivation patterns	4.22	-	0 - 100
	Land princ. occup. by agr., with signf. areas of natural veg.	4.22	-	0 - 100
	Forests	5.18	-	0 - 100
	Natural grasslands	2.50	-	0 - 100
	Sclerophyllous vegetation	2.08	-	0 - 100
	Transitional woodland-shrub	2.08	-	0 - 100
	Bare rocks	1.31	-	0 - 100
	Sparsely vegetated areas	1.31	-	0 - 100
	Wetlands	6.34	-	0 - 100
	Water bodies	0.1	-	0 - 100
Preferred Flow Direction	Artificial surfaces	0.15	-	0 - 1
	Non-irrigated arable land	0.15	-	0 - 1
	Permanently irrigated land	0.15	-	0 - 1
	Vineyards	0.15	-	0 - 1
	Fruit trees and berry plantations	0.15	-	0 - 1
	Pastures	0.15	-	0 - 1
	Complex cultivation patterns	0.15	-	0 - 1
	Land princ. occup. by agr., with signf. areas of natural veg.	0.15	-	0 - 1
	Forests	0.15	-	0 - 1
	Natural grasslands	0.15	-	0 - 1
	Sclerophyllous vegetation	0.15	-	0 - 1
	Transitional woodland-shrub	0.15	-	0 - 1
	Bare rocks	0.15	-	0 - 1
	Sparsely vegetated areas	0.15	-	0 - 1
	Wetlands	0.15	-	0 - 1
	Water bodies	0.15	-	0 - 1

Table 5-6 (continued)

Root Zone Conductivity	Artificial surfaces	20	mm/month	0 - 1000
	Non-irrigated arable land	20	mm/month	0 - 1000
	Permanently irrigated land	20	mm/month	0 - 1000
	Vineyards	20	mm/month	0 - 1000
	Fruit trees and berry plantations	20	mm/month	0 - 1000
	Pastures	20	mm/month	0 - 1000
	Complex cultivation patterns	20	mm/month	0 - 1000
	Land princ. occup. by agr., with signf. areas of natural veg.	20	mm/month	0 - 1000
	Forests	20	mm/month	0 - 1000
	Natural grasslands	20	mm/month	0 - 1000
	Sclerophyllous vegetation	20	mm/month	0 - 1000
	Transitional woodland-shrub	20	mm/month	0 - 1000
	Bare rocks	20	mm/month	0 - 1000
	Sparsely vegetated areas	20	mm/month	0 - 1000
	Wetlands	20	mm/month	0 - 1000
	Water bodies	20	mm/month	0 - 1000
Deep Water Capacity	-	10000	mm	0 - 300000
Deep Conductivity	-	20	mm/month	0.1 - 150
Initial_Z2	-	30	%	0 - 100
Freezing Point	-	-5	ºC	-20 - +20
Melting Point	-	+5	ºC	-20 - +20

The WEAP-LEAP model performance was evaluated based on R^2, Nash Sutcliffe Efficiency (NSE), and Percent Bias (PBIAS) according to the general performance ratings for a monthly time step (Moriasi et al., 2007). The observed average monthly streamflow and the corresponding simulated streamflow at the selected streamflow gauging stations at each subbasin were compared. The results for each subbasin are provided in Figure 5-11, Figure 5-12, Figure 5-13, Figure 5-14, Figure 5-15, Figure 5-16, and Figure 5-17. The performance statistics for each streamflow gauging stations are given below the relevant figures.

The results show that the model was able to simulate the observed average monthly streamflow data satisfactorily during the calibration period in each gauging station except Porsuk and Ankara subbasins according to general performance ratings (Moriasi et al., 2007). As expected, the performance statistics obtained during the validation period are generally lower than for calibration. The degree of collinearity between simulated and observed data is acceptable, i.e., $R^2 \geq 0.5$, at most streamflow monitoring stations.

Calibration results in Porsuk and Ankara subbasins were evaluated at two different streamflow monitoring stations (Figure 5-12 and Figure 5-13). E12A051 in the Porsuk and E12A026 in the Ankara are the closest stations to the outlets of these subbasins (Figure 5-5). However, the statistics obtained from these two stations (E12A051 and E12A026) indicate poor model performance. Porsuk subbasin is a subbasin where both agricultural and industrial activities are intense. During the field studies carried out within the scope of the project named "Evaluation of Water, Energy and Food Nexus in Sakarya Watershed" (Alp et al., 2020), the authorities stated that there are many illegal wells used for agricultural irrigation in the region. Figure 5-12 and PBIAS value indicate that the model overestimates the streamflow at E12A051. It can be said that the reason for this bias is the amount of water used for agricultural irrigation from illegal wells, which cannot be reflected in the model. For this reason, the model results were also evaluated using the data of station E12A003, which is relatively less affected by agricultural water withdrawals compared to station E12A051, which is upstream of the Porsuk Dam, and it has been observed that the results improve significantly. This proves the negative effect of illegal wells on the model results. In the Ankara subbasin, unlike the Porsuk subbasin, the model underestimates the streamflow. In the Ankara subbasin, there are lots of industries withdrawing and discharging water. In the WEAP model, these industries were not defined individually, and the annual total water requirement originating from all these industries was calculated and entered into the model as a single demand site. The WEAP model divides this annual total water requirement into monthly shares in proportion to the number of days in the month. Therefore, this may be the reason why the model did not perform satisfactorily. In order to check whether the WEAP Soil Moisture method can simulate the catchment processes correctly, the model results were also evaluated at the station D12A242 (Figure 5-5), which was affected as little as possible by all water withdrawals and discharges. As can be seen in Figure 5-13, the model performance is satisfactory. This indicates that

the model is successful in simulating catchment processes, and poor model performance is most likely due to industrial discharges.

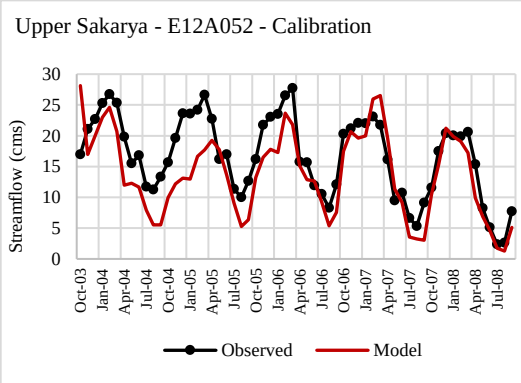

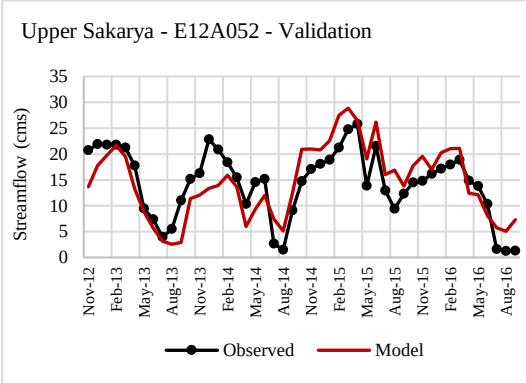

Calibration		***Validation***	
NSE	: 0.57	NSE	: 0.62
PBIAS	: 17.4	PBIAS	: -1.7
R^2	: 0.73	R^2	: 0.64

Figure 5-11. Upper Sakarya subbasin: Comparisons of the observed average monthly streamflow and the corresponding simulated streamflow at the Ayvalı Yaylası (E12A052) gauging station for the calibration and validation of the WEAP-LEAP model over the Sakarya Basin

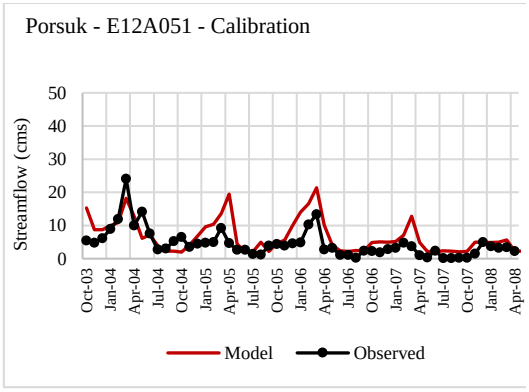

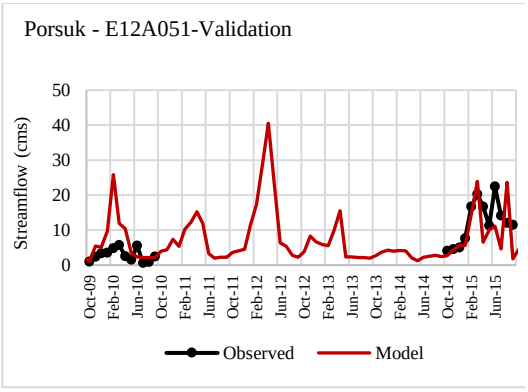

Calibration		***Validation***	
NSE	: -0.07	NSE	: -0.22
PBIAS	: -48.3	PBIAS	: -8.7
R^2	: 0.46	R^2	: 0.22

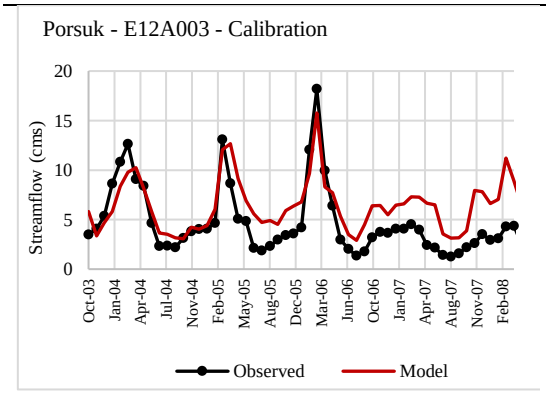

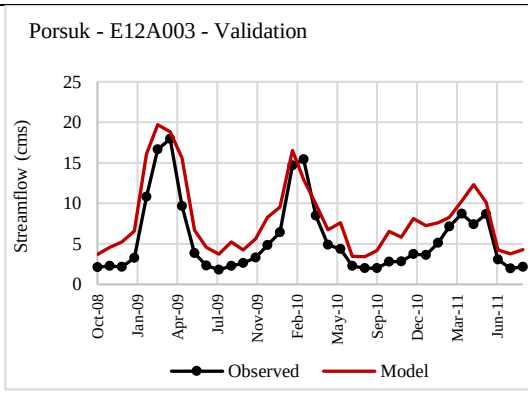

Calibration		***Validation***	
NSE	: 0.36	NSE	: 0.60
PBIAS	: -31.6	PBIAS	: -48.3
R^2	: 0.64	R^2	: 0.90

Figure 5-12. Porsuk subbasin: Comparisons of the observed average monthly streamflow and the corresponding simulated streamflow at the Kıranharmanı (E12A051) and Beşdeğirmen (E12A003) gauging stations for the calibration and validation of the WEAP-LEAP model over the Sakarya Basin

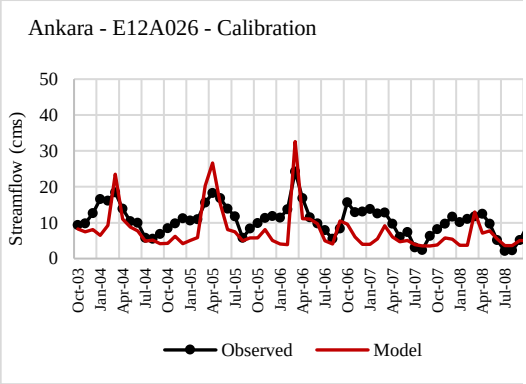

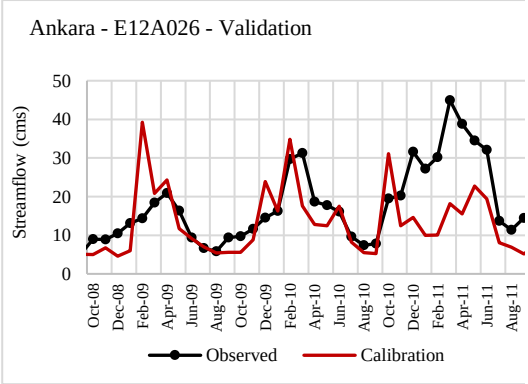

Calibration		***Validation***	
NSE	: -0.30	NSE	: -0.15
PBIAS	: 27.0	PBIAS	: 25.0
R^2	: 0.50	R^2	: 0.23

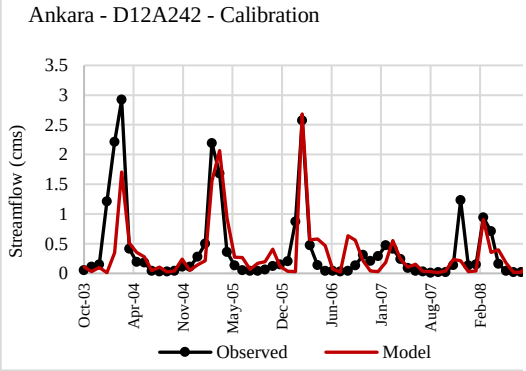

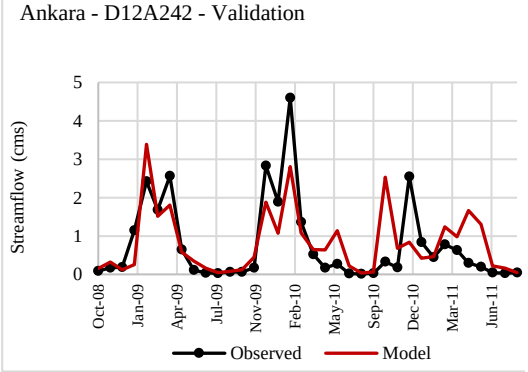

Calibration		***Validation***	
NSE	: 0.57	NSE	: 0.49
PBIAS	: 14.5	PBIAS	: -7.1
R^2	: 0.58	R^2	: 0.50

Figure 5-13. Ankara subbasin: Comparisons of the observed average monthly streamflow and the corresponding simulated streamflow at the Meşecik (E12A026) and Uğurlu (D12A242) gauging stations for the calibration and validation of the WEAP-LEAP model over the Sakarya Basin

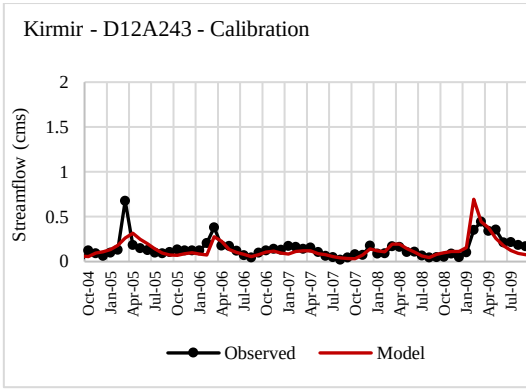

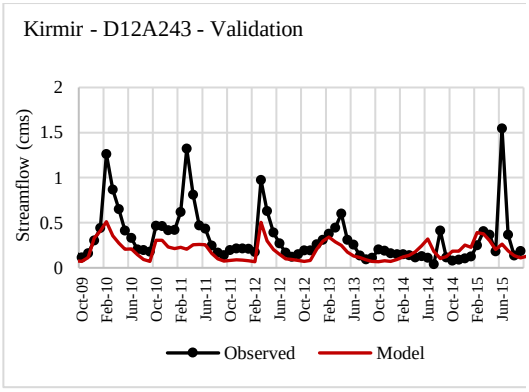

Calibration		***Validation***	
NSE	: 0.46	NSE	: 0.07
PBIAS	: 5.3	PBIAS	: 41.7
R^2	: 0.47	R^2	: 0.35

Figure 5-14. Kirmir subbasin: Comparisons of the observed average monthly streamflow and the corresponding simulated streamflow at the Endil Boğazı (D12A243) gauging station for the calibration and validation of the WEAP-LEAP model over the Sakarya Basin

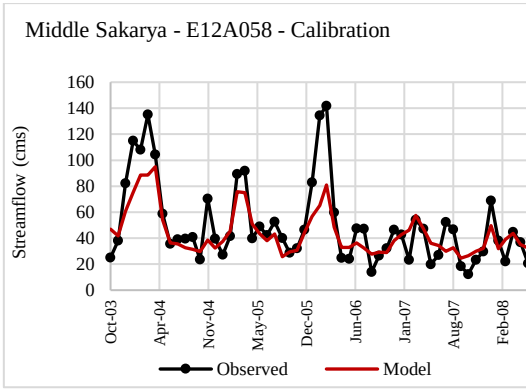

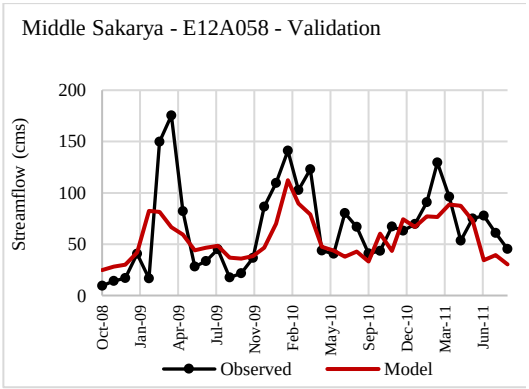

Calibration		***Validation***	
NSE	: 0.62	NSE	: 0.35
PBIAS	: 12.5	PBIAS	: 15.6
R^2	: 0.76	R^2	: 0.43

Figure 5-15. Middle Sakarya subbasin: Comparisons of the observed average monthly streamflow and the corresponding simulated streamflow at the Kayabeli (E12A058) gauging station for the calibration and validation of the WEAP-LEAP model over the Sakarya Basin

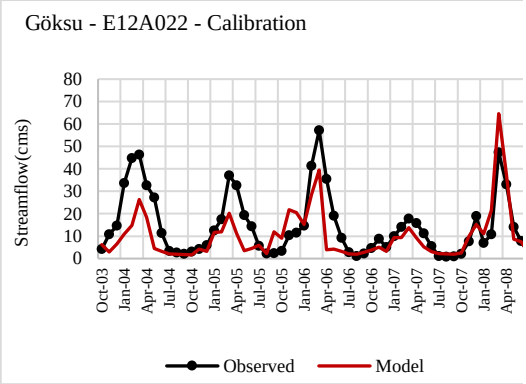

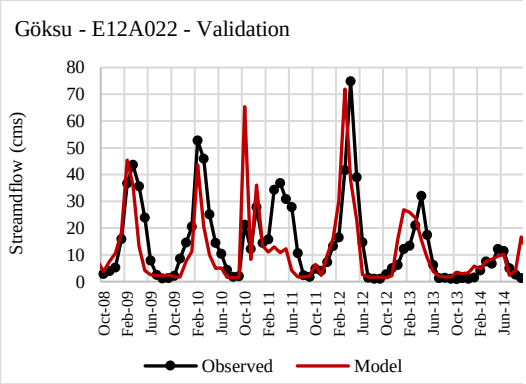

Calibration		***Validation***	
NSE	: 0.43	NSE	: 0.35
PBIAS	: 28.8	PBIAS	: 15.6
R^2	: 0.52	R^2	: 0.45

Figure 5-16. Göksu subbasin: Comparisons of the observed average monthly streamflow and the corresponding simulated streamflow at the Rüstümköy (E12A022) gauging station for the calibration and validation of the WEAP-LEAP model over the Sakarya Basin

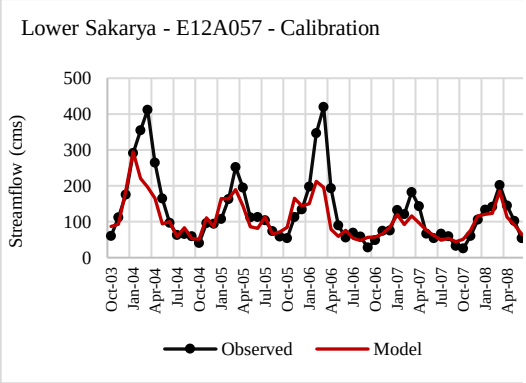

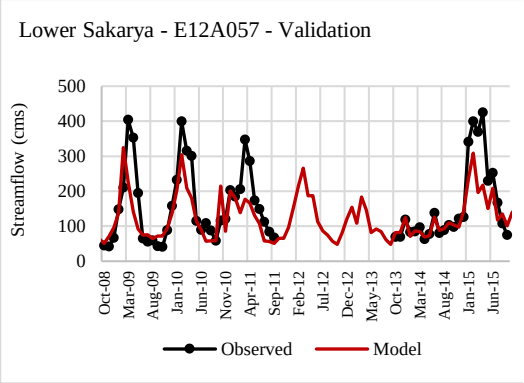

Calibration		***Validation***	
NSE	: 0.61	NSE	: 0.55
PBIAS	: 15.7	PBIAS	: 19.2
R^2	: 0.72	R^2	: 0.68

Figure 5-17. Lower Sakarya subbasin: Comparisons of the observed average monthly streamflow and the corresponding simulated streamflow at the Rüstümköy (E12A022) gauging station for the calibration and validation of the WEAP-LEAP model over the Sakarya Basin

The comparison of the total electricity generation by the LEAP model and the observed data is given in Figure 5-18. Modeled total electricity generation was calculated by summing up the electricity generation of each power plant modeled in the LEAP model. As it can be seen from Figure 5-18, the LEAP model can successfully simulate total electricity generation.

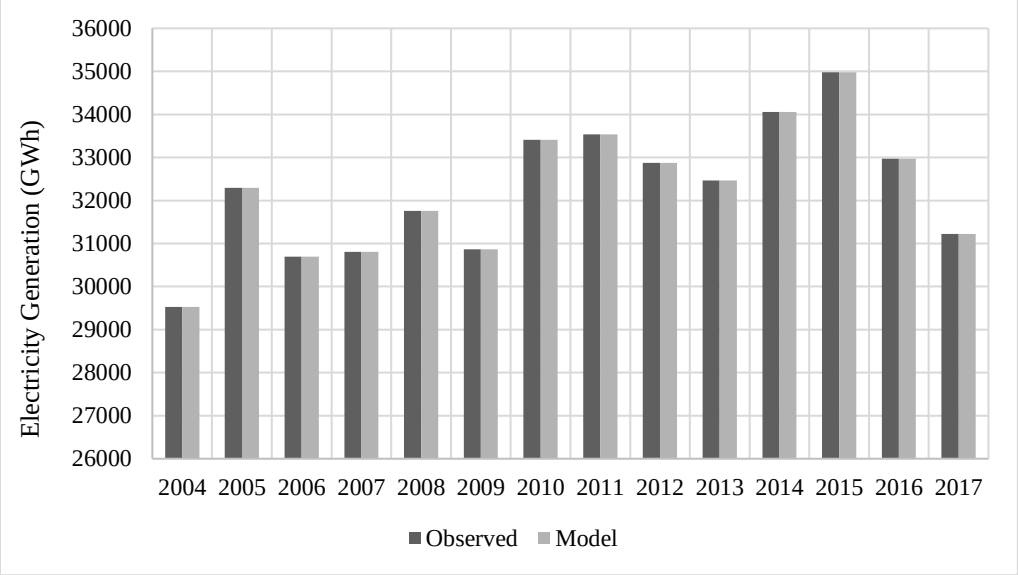

Figure 5-18. Comparison of the observed and modeled total electricity generation over the Sakarya Basin

The calibration and validation results show that although the model performs satisfactorily at most streamflow monitoring stations, there are also stations where typically accepted performance statistic ratings cannot be obtained. At this point, the question arises whether the model performance is sufficient for this study. The purpose of using models in modeling studies can be divided into three general categories as Exploratory, Planning and Regulatory/Legal. Moving from the Exploratory category to the Regulatory/Legal category, more strict model

performance ratings are sought (Figure 5-19). The main purpose of studies in the category of Exploratory is to make initial and approximate comparisons (Harmel et al., 2014). In these studies, evaluations are made about the potential consequences, possible opportunities and risks related to alternative management strategies (Arabi et al., 2012). Therefore, strict model performance ratings are not sought in these studies (Moriasi et al., 2007). The overall aim of this thesis is to develop a methodology that enables the assessment of the sustainability of and the security provision for the WEFE Nexus components. In this context, answers are sought to questions such as how the safety of the nexus and its components will be affected under different climatic and socioeconomic conditions, and whether the sustainability of these components is in danger (details in Chapter 3). Therefore, within the scope of this study, it is not aimed to plan for the implementation of different management alternatives, or to develop regulations. Therefore, it can be concluded that the model performance is suitable for the study purpose. However, if it is aimed to evaluate the management alternatives that are planned to be implemented by following the same methodology, a modeling tool with higher performance ratings should be used.

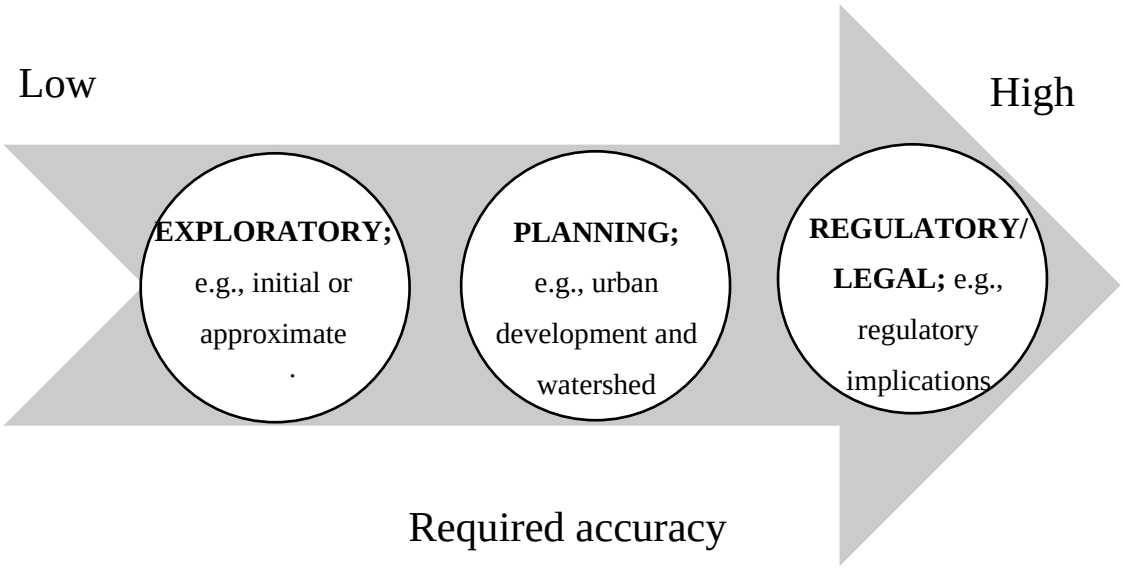

Figure 5-19. Continuum of model's intended use from least model performance accuracy to most required accuracy (Özcan, 2016; Özcan et al., 2017)

CHAPTER 6

DYNAMICAL DOWNSCALING OF CLIMATE PROJECTIONS IN THE SAKARYA BASIN

This section explains the method of obtaining the climate data needed to evaluate how the WEFE Nexus index will change in different scenarios in the 21st century. The future climate data were obtained by dynamical downscaling with WRF, a regional climate model. Figure 6-1 shows the flow diagram of the methodology followed to obtain the fine-resolution future climate data in the Sakarya Basin. As can be seen from the figure, the WRF model needs to be calibrated first before downscaling the GCM outputs to the desired resolution. For this purpose, first, ERA-Interim reanalysis data with a spatial resolution of 80 km were obtained. Then, ERA-Interim reanalysis data were downscaled in different model configurations until the satisfactory model performance was obtained. Whether the model performance is satisfactory or not was evaluated by comparing the basin-average values of the downscaled ERA-Interim data and the basin-average values of the observed data. When satisfactory model performance is achieved, the calibrated and validated WRF model was used to downscale the GCM outputs to 18 km resolution, a suitable resolution for hydrological modeling. After correcting the bias in the downscaled GCM outputs, the future climate data took its final form to be input to the integrated WEAP-LEAP model. In this chapter, firstly, the data used and model implementation are explained. Then, the calibration and verification of the WRF model, bias correction, and finally the results are given.

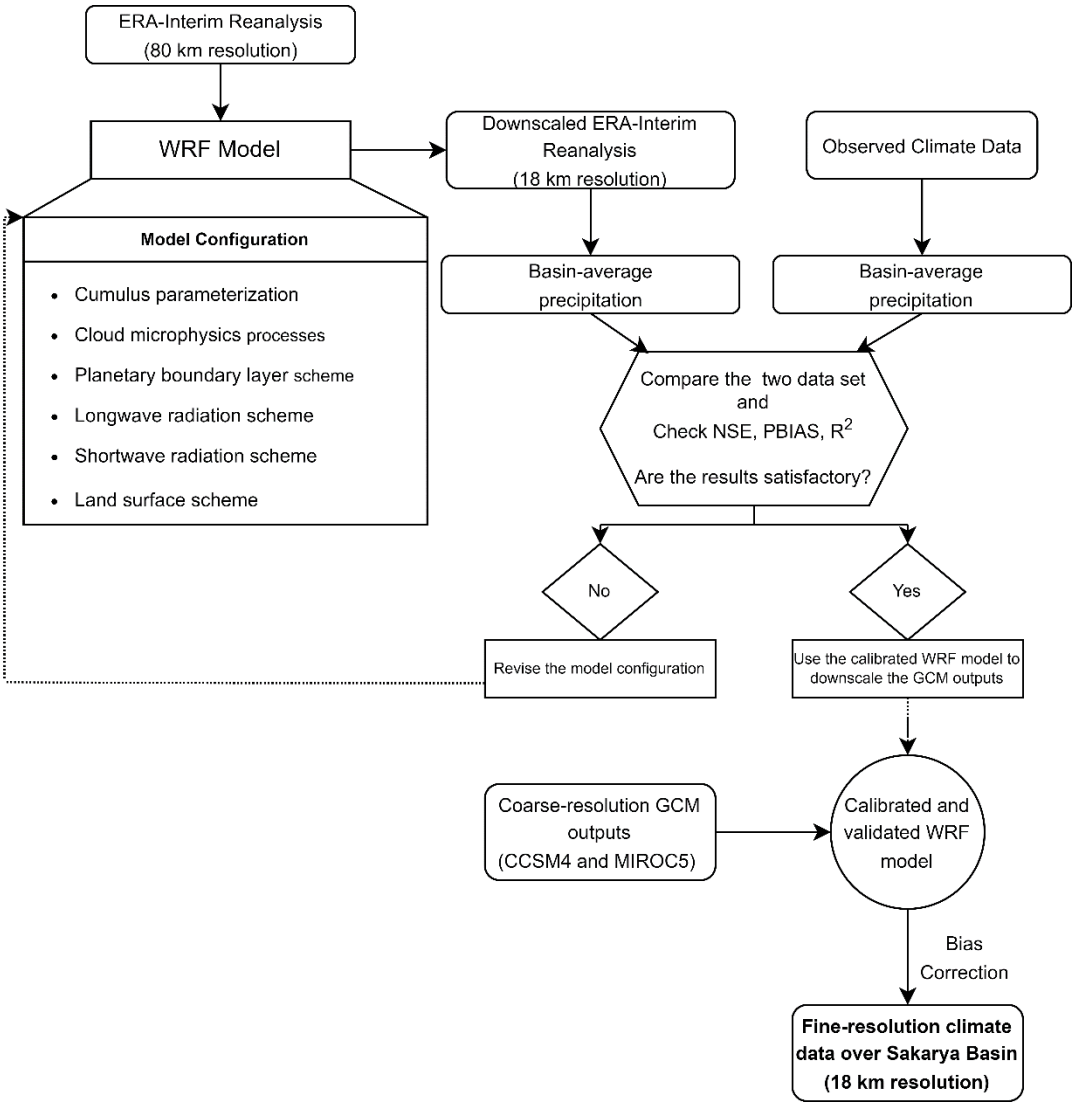

Figure 6-1. Flow diagram of the method followed in obtaining fine resolution climate data in Sakarya Basin

6.1 Data and Model Implementation

This study uses four different future climate projection realizations from two general circulation models (GCMs: CCSM4 and MIROC5) based on two emission scenarios

(RCP 4.5 and RCP 8.5). CCSM4 is the fourth version of the Community Climate System Model (CCSM4) (Gent et al., 2011). The model was developed by the National Center for Atmospheric Research, United States. It has a spatial resolution of 0.9º x 1.25º. MIROC5 is the latest version of the Model for Interdisciplinary Research on Climate which was cooperatively produced by the Japanese research community (Watanabe et al., 2010). The model has a spatial resolution of 1.4° × 1.4°. The two emission scenarios selected were RCP 4.5 and RCP 8.5. RCP 4.5 is a scenario that stabilizes radiative forcing at 4.5 W m^{-2} in the year 2100 without ever exceeding that value (Thomson et al., 2011). On the other hand, the greenhouse gas emissions and concentrations in the RCP 8.5 scenario increase considerably over time, leading to a radiative forcing of 8.5 W/m^2 at the end of the century. RCP 8.5 corresponds to the pathway with the highest greenhouse gas emissions compared to the total set of RCPs (Riahi et al., 2011).

It is necessary to downscale the GCM results to finer spatial resolutions for a reliable assessment of the regional impact of climate change on precipitation and temperature. Dynamical downscaling is one of the techniques, and it requires the usage of a regional climate model (RCM). In this study, the Weather Research and Forecasting (WRF) model is used to dynamically downscale future climate projection realizations. WRF model is a mesoscale numerical weather prediction system designed for both atmospheric research and operational forecasting applications. It is a fully compressible and non-hydrostatic model. It was developed by multiple agencies collaboratively (Skamarock et al., 2008).

In this study, the future projection period ranges from 2020 to 2100. The future climate projection realizations were downscaled to 18-km resolution grids over Sakarya Basin for a period of 30 years (2020 – 2030; 2055 – 2065; 2090 – 2100). The realizations were downscaled as 10-yr segments due to the high computational cost of the regional model and time constraints. The historical atmospheric data used

in this study is from September 2009 to September 2018 based on the availability of the data at the meteorological stations located in the study basin. Observed daily total precipitation and temperature data from 20 different meteorological stations within the Sakarya Basin were obtained from the Turkish State Meteorological Service (MGM). The locations of these stations are shown in Figure 5-5. The coordinates and measurement periods of these stations are listed in Table 6-1.

Table 6-1. Details of the meteorological stations in the Sakarya Basin used in this study

Station Number	Station Name	Latitude	Longitude	Automatic Measurement Period
17753	BAYAT	38.9715	30.9179	2005-2018
17798	YUNAK	38.8205	31.7258	2009-2018
17680	BEYPAZARI	40.1608	31.9172	2005-2018
17662	GEYVE	40.5214	30.296	2005-2018
17644	KARASU	41.1113	30.6901	2006-2018
17155	KUTAHYA	39.4171	29.9891	2005-2018
17723	CIFTELER	39.3659	31.0209	2005-2018
17752	EMIRDAG	39.0098	31.1463	2005-2018
17832	ILGIN	38.2763	31.894	2009-2018
17728	POLATLI	39.5834	32.1624	2005-2018
17733	HAYMANATARIM	39.613	32.672	2005-2018
17128	ANKARA ESENBOGA	40.124	32.9992	2005-2018
17693	SEBEN	40.4088	31.573	2005-2018
17664	KIZILCAHAMAM	40.4729	32.6441	2005-2018
17130	ANKARABOLGE	39.9727	32.8637	2005-2018
17118	BURSA YENISEHIR	40.2552	29.5624	2009-2018
17069	SAKARYA	40.7676	30.3934	2005-2018
17126	ESKISEHIR BOLGE	39.7656	30.5502	2005-2018
17120	BILECIK	40.1414	29.9772	2005-2018
17679	NALLIHAN	40.1733	31.332	2005-2018

6.2 WRF Model Calibration and Validation

Before downscaling the future climate projections, the WRF model needs to be calibrated. ERA-Interim reanalysis data was used for the calibration of the model. ERA-Interim is one of the best reanalyses of its generation and has been extensively used for downscaling with WRF. It is a common practice to use ERA-Interim driven WRF simulations to evaluate the ability of WRF model to simulate observed fields (Gorguner et al., 2019). For this purpose, reanalysis data for the years between 2009

and 2018 was obtained. ERA-Interim data set with a six-hour temporal resolution was obtained from the Research Data Archieve (RDA) at NCAR. The spatial resolution of the data set is approximately 80 km on 60 levels in the vertical from the surface up to 0.1 hPa.

Before downscaling the ERA-Interim reanalysis for the whole historical period, the WRF model was first calibrated for the year 2010 by comparing its results to the observed total monthly precipitation data. The observed data from 20 different meteorological stations were used to calculate the basin's average total monthly precipitation. For this purpose, the Thiessen polygon method was used. Two two-way nested domains were set up for the WRF dynamical downscaling, as shown in Figure 6-2. The outer domain (D01) has 31 x 33 horizontal grid points at a 54-km resolution, and the second domain (D02) has 28 x 25 horizontal grid points at an 18-km resolution with 25 vertical (Eta) levels. The outer domain, D01, comprises southeast Europe, the Black Sea, the Aegean Sea and the eastern Mediterranean Sea. The second domain, D02, comprises the whole Sakarya Basin. In order to find the best combination of physics options, several different combinations of the parameterizations of the WRF model were tested. The model configuration of the WRF model used in this study is shown in Table 6-2.

Table 6-2. WRF model configuration

Cumulus parameterization	Grell-3D Scheme (an improved version of the GD scheme) (Grell and Dévényi, 2002)
Cloud microphysics processes	Kessler (Kessler, 1969)
Planetary boundary layer scheme	Yonsei University (Hong et al., 2006)
Longwave radiation scheme	RRTM scheme (Mlawer et al., 1997)
Shortwave radiation scheme	Dudhia (Dudhia, 1989)
Land surface scheme	Rapid Update Cycle (RUC) land surface model (Smirnova et al., 1997)

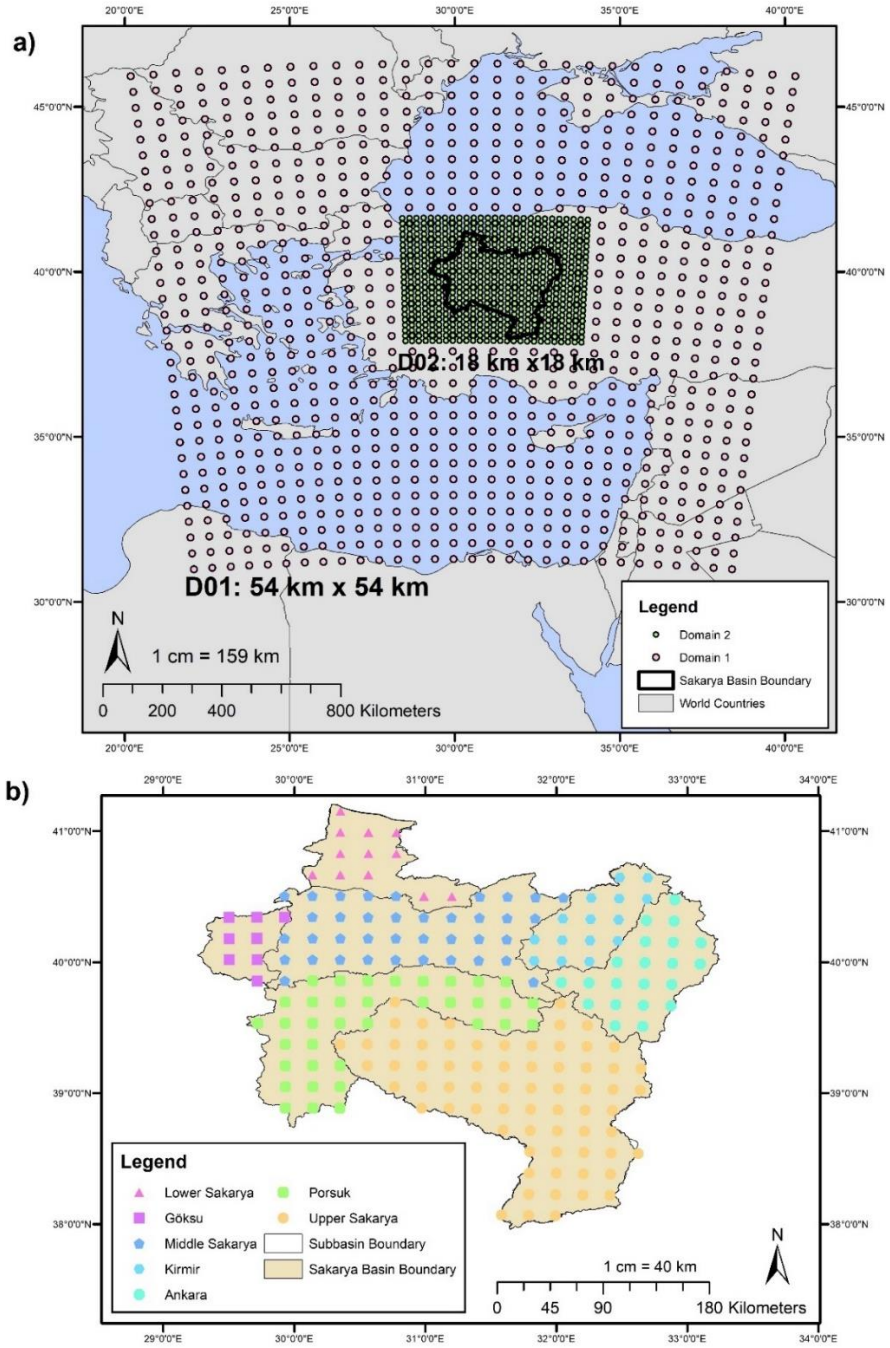

Figure 6-2. a) Nested domain configuration over the Sakarya Basin b) Grid points used to calculate the basin average precipitation and temperature values for each subbasin

After the WRF model was calibrated for the year 2010 (Figure 6-3), the model was validated for the years from 2009 through 2018 by comparing the total monthly precipitation to the observed values. This comparison is done for the basin average values. A statistical summary of the calibration and validation results are listed in Table 6-3. For the assessment of model performance, the Nash-Sutcliffe model efficiency (NSE), Percent Bias (PBIAS), and coefficient of determination (R^2) were employed. A graphical comparison of the observed and downscaled precipitation data through the validation period is given in Figure 6-4. As it can be seen from Table 6-3, the NSE, PBIAS and R^2 values indicate satisfactory model simulations. The calibrated and validated WRF model was then used to downscale the climate projections of CCSM4 and MIROC5 under RCP 4.5 and RCP 8.5 scenarios to a much finer spatial resolution of 18 km.

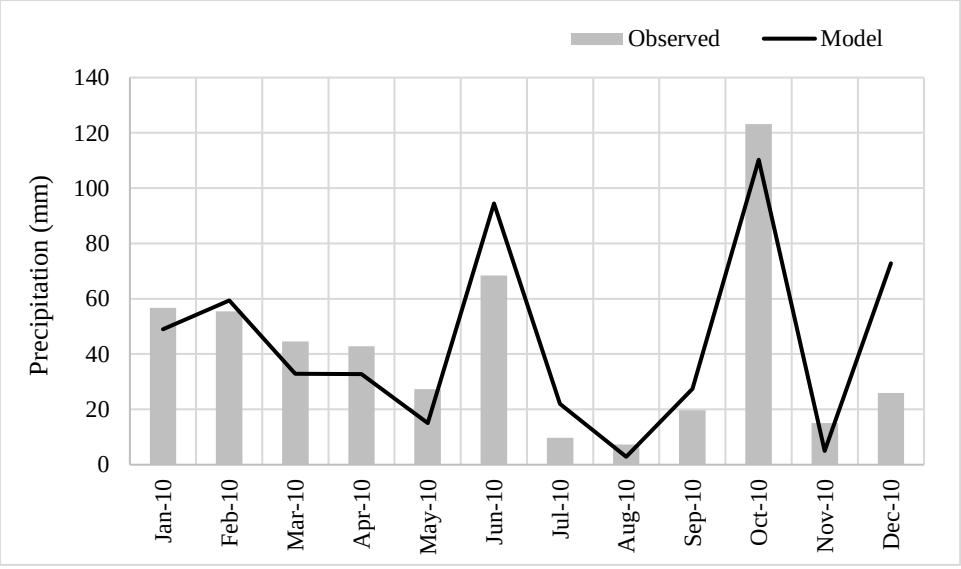

Figure 6-3. Calibration results for the WRF model for the year 2010

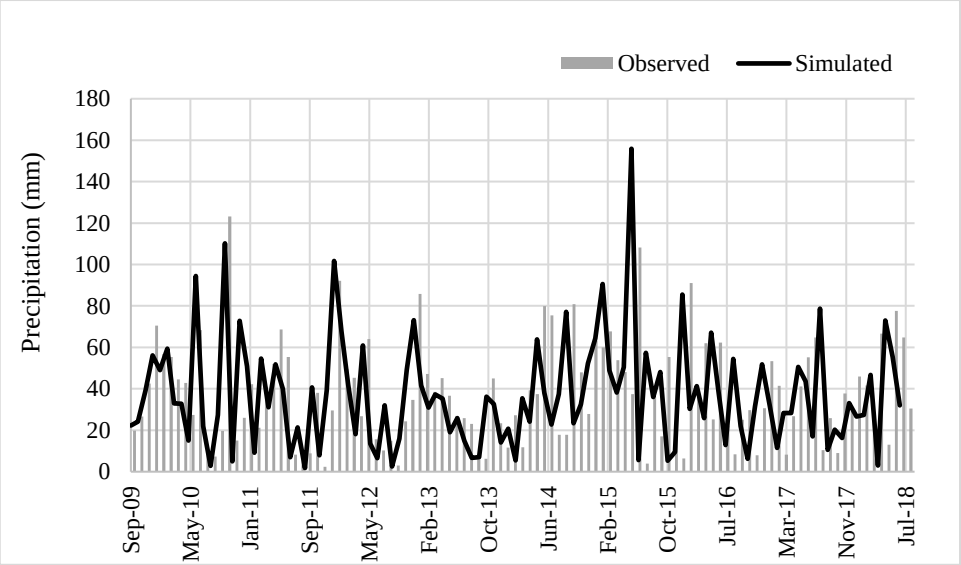

Figure 6-4. Validation results for the WRF model showing the time series of the observed and simulated basin average monthly precipitation values

Table 6-3. Summary statistics for the model calibration and validation

	Model Calibration	Model Validation
NSE	0.67	0.66
PBIAS	-5.62	2.2
R^2	0.72	0.71

6.3 Bias Correction

To correct biases, delta change method was used. It is the simplest approach for bias correction. In this approach, a time series of future climate is generated as (Maraun, 2016):

$$x_{i,corr}^{f} = x_{i,raw}^{f} - Bias\ (\mu^{p}) = x_{i,raw}^{f} - \left(\bar{x}_{i}^{p} - \bar{y}_{i}^{p}\right) \quad 6.1$$

or equivalent for precipitation:

$$x_{i,corr}^{f} = \frac{x_{i,raw}^{f}}{Rel.Bias\ (\mu^{p})} = x_{i,raw}^{f} x\ \frac{\bar{y}_{i}^{p}}{\bar{x}_{i}^{p}} \quad 6.2$$

where

x_i^p: a simulated present-day model (predictor) time series of length N

y_i^p: the corresponding observed (predictand) time series

$x_{i,corr}^f$: corrected future simulations

$x_{i,raw}^f$: raw future simulations

The GCM's (CCSM4 and MIROC5) precipitation and temperature projections from September 2009 to July 2018 were downscaled. This period was determined based on the availability of observed data in the monitoring stations. The observed and downscaled basin average monthly precipitation and temperature values between September 2009 and July 2018 were calculated. Then, the Equations 6.1 and 6.2 were used to correct biases in temperature and precipitation, respectively.

6.4 Results and Discussion

In this study, climate change was analyzed in terms of the projected changes and trends in the basin's average annual total precipitation depths and basin average

temperatures over the seven study subbasins in Sakarya Basin in the 21st century. The future period was divided into three segments as near century (2020 – 2030), mid-century (2055 – 2065), and far century (2090 – 2100), and the results were investigated based on the four dynamically downscaled bias-corrected future climate projections accordingly. The results were also evaluated for the entire 21st century for 33 years (2020 – 2030; 2055 – 2065; 2090 – 2100). In addition to the individual assessment of all climate projection realizations, the evaluation was also performed based on the ensemble averages of two emission scenarios (RCP 4.5 and RCP 8.5) and the ensemble average of both GCMs (CCMS4 and MIROC5). Ensemble averages are useful for the assessment of the general trends in the precipitation and temperature, and to take the uncertainties resulting from GCMs and scenarios into account (Ishida et al., 2018).

The least squares regression method and the Mann-Kendall trend test were employed to quantify the trends in the annual basin-average precipitation and temperature. The slopes and the standard errors of the trend lines were calculated through the least-squares regression method. The Mann-Kendall trend test is non-parametric and it is used to determine the significance of the trend for consistently increasing or decreasing trends (Mann, 1945).

In this section, the projected changes and trends in basin average precipitation and temperature in the 21st century are given, respectively.

6.4.1 Projected changes and trends in annual total basin average precipitation in the 21st century

Temporal variability of annual total basin average precipitation over the seven subbasins for all four climate projection realizations, the ensemble averages of RCP 4.5 and RCP 8.5 scenarios, and the ensemble averages of all realizations is shown in

Figure 6-5. As it can be seen from Figure 6-5, no clear significant increasing or decreasing trend is observed for annual total precipitations in the 21st century in all subbasins. However, there are some peaks evident especially in the mid-century. The slopes and standard errors of the least squares' regression line of annual basin-average precipitation depths over the seven study subbasins with p-value of the Mann-Kendall trend test in parentheses are given in Table 6-4, Table 6-5, Table 6-6, and Table 6-7 for the 21st century, near century, mid-century, and far century, respectively. In these tables, the p-values are bolded if the trend is statistically significant at the 95% confidence level.

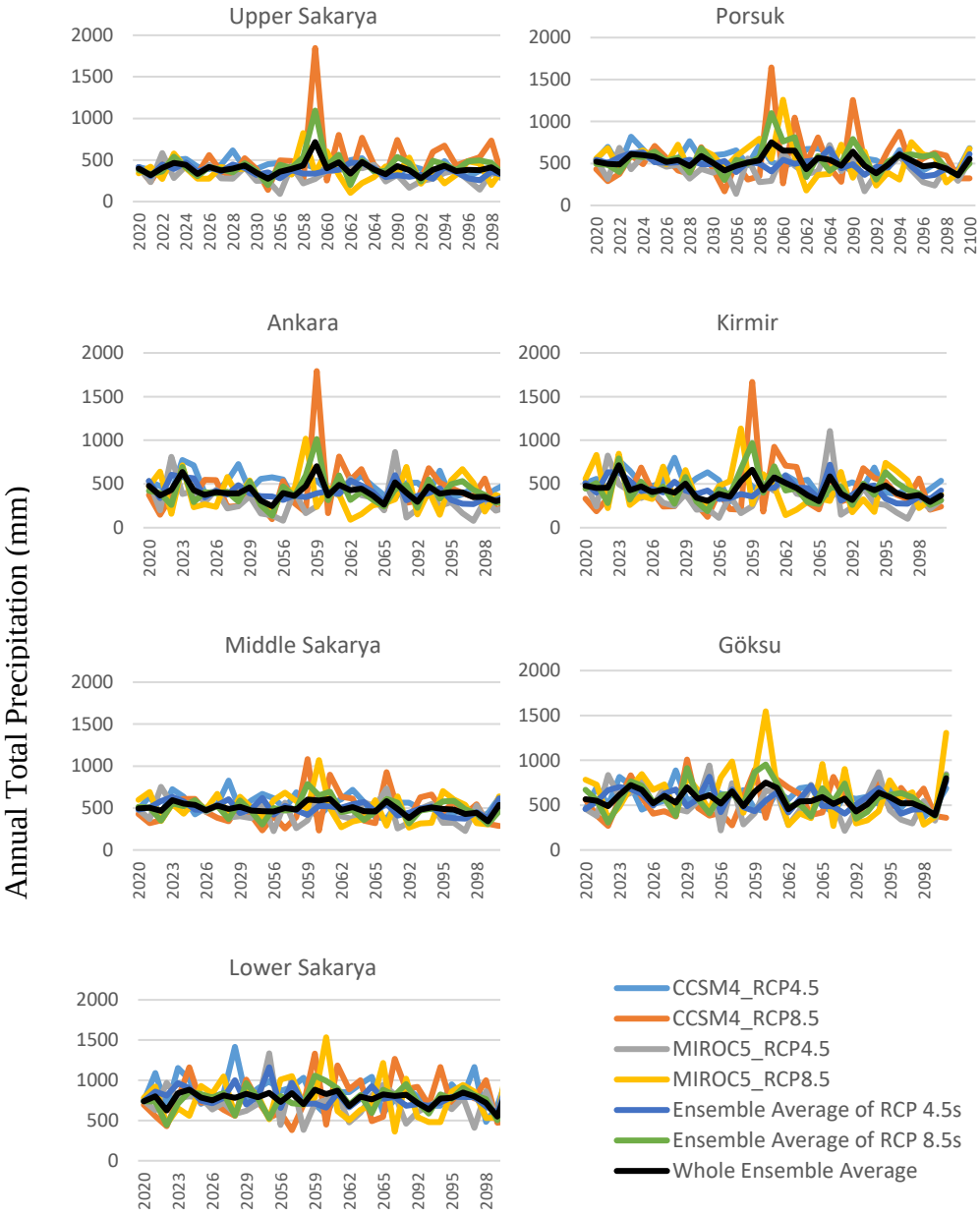

Figure 6-5. Annual total basin average precipitation over the seven subbasins; Upper Sakarya, Porsuk, Ankara, Kirmir, Middle Sakarya, Göksu, Lower Sakarya. All four climate projection realizations, the ensemble averages of RCP 4.5 scenarios, the ensemble averages of RCP 8.5 scenarios, and the ensemble averages of all realizations

Minimum and maximum values of annual total precipitation depths in the historical period as well as in the 21st century and each segment of the future period over the seven study subbasins with the mean value in parentheses are given in Table 6-4, Table 6-5, Table 6-6, and Table 6-7, respectively. Statistical information about the historical period was provided for comparison purposes. In these tables, the mean value shows the average annual total precipitation depth for the related time period. In this way, the changes in the precipitation depths are analyzed by comparing the historical means with the means of each future period segment.

Table 6-4. Entire 21st century (2020 – 2030; 2055 – 2065; 2090 - 2100) (33 years): Summary statistics of annual basin-average precipitation depths

		Upper Sakarya	**Porsuk**	**Ankara**	**Kirmir**	**Middle Sakarya**	**Göksu**	**Lower Sakarya**
Historical Period (2010 – 2017)	Min. - Max. (Mean)	274.6 - 449.3 (380.1)	344.4 - 565.8 (479.21)	292.0 - 520.8 (417.1)	343.0 - 564.2 (458.3)	362.52 - 575.44 (496.15)	387.3 - 711.7 (531.2)	422.4 - 946.5 (733.1)
Entire 21st century (2020 – 2030; 2055 – 2065; 2090 - 2100) (33 years)								
CCSM4_ RCP4.5	Slope ± SE (p_value)	-0.81 ± 0.44 (0.10)	-1.49 ± 0.61 (**0.04**)	-1.39 ± 0.66 (**0.05**)	-1.56 ± 0.65 (**0.03**)	-1.17 ± 0.65 (0.09)	-0.95 ± 0.71 (0.41)	-1.36 ± 1.19 (0.43)
	Min. - Max. (Mean)	298.1 - 616.1 (413.3)	407.2 - 818.5 (569.5)	315.1 - 774.5 (492.7)	301.6 - 800.8 (511.2)	372.3 - 827.3 (540.3)	364.0 - 887.6 (567.2)	482.8 - 1415.8 (868.0)
CCSM4_ RCP8.5	Slope ± SE (p_value)	1.27 ± 1.80 (0.43)	1.43 ± 1.84 (0.51)	0.36 ± 1.85 (0.79)	0.48 ± 1.83 (0.96)	0.75 ± 1.22 (0.91)	0.37 ± 1.15 (0.77)	1.49 ± 1.57 (0.57)
	Min. - Max. (Mean)	140.1 - 1846.9 (486.1)	168.0 - 1644.2 (551.1)	97.3 - 1792.6 (438.6)	123.7 - 1667.8 (444.6)	232.2 - 1083.4 (485.7)	268.6 - 1008.5 (538.7)	380.6 - 1332.0 (768.0)
MIROC5_ RCP4.5	Slope ± SE (p_value)	-1.05 ± 0.60 (0.20)	-1.00 ± 0.84 (0.29)	-1.38 ± 1.09 (0.10)	-1.14 ± 1.23 (0.07)	-0.91 ± 0.83 (0.20)	-1.12 ± 1.20 (0.34)	-0.68 ± 1.21 (0.77)
	Min. - Max. (Mean)	21.8 - 583.4 (295.5)	21.3 - 719.6 (403.1)	16.5 - 865.7 (293.0)	14.1 - 1106.4 (329.6)	20.4 - 752.8 (427.2)	32.3 - 941.9 (502.6)	101.4 - 1335.3 (697.0)
MIROC5_ RCP8.5	Slope ± SE (p_value)	-0.43 ± 0.84 (0.39)	-1.52 ± 1.23 (0.30)	-0.30 ± 1.28 (0.68)	-1.36 ± 1.42 (0.38)	-1.22 ± 1.04 (0.20)	-1.13 ± 1.84 (0.33)	-0.54 ± 1.66 (0.84)
	Min. - Max. (Mean)	104.4 - 823.9 (365.3)	178.2 - 1259.3 (549.0)	91.1 - 1019.3 (385.0)	144.1 - 1135.6 (443.3)	267.0 - 1071.5 (505.4)	268.3 - 1546.3 (638.0)	362.0 - 1534.7 (776.3)
Ensemble RCP 4.5s	Slope ± SE (p_value)	-0.93 ± 0.33 (**0.02**)	-1.24 ± 0.46 (**0.00**)	-1.38 ± 0.53 (**0.02**)	-1.35 ± 0.61 (**0.01**)	-1.04 ± 0.41 (**0.02**)	-1.04 ± 0.69 (0.10)	-1.02 ± 0.75 (0.14)
	Min. - Max. (Mean)	256.1 - 470.3 (363.4)	346.2 - 675.4 (499.4)	270.0 - 606.1 (404.1)	274.4 - 721.4 (432.0)	374.0 - 632.7 (497.2)	296.7 - 817.3 (551.0)	595.0 - 1161.5 (791.3)
Ensemble RCP 8.5s	Slope ± SE (p_value)	0.42 ± 0.93 (0.38)	-0.04 ± 0.98 (0.79)	0.03 ± 1.01 (0.99)	-0.44 ± 1.03 (0.59)	-0.23 ± 0.67 (0.41)	-0.38 ± 1.01 (0.82)	0.48 ± 0.88 (0.55)
	Min. - Max. (Mean)	198.1 - 1094.7 (426.6)	302.6 - 1100.1 (551.4)	136.3 - 1014.9 (412.6)	188.7 - 968.6 (444.8)	303.3 - 786.4 (497.1)	299.4 - 953.2 (588.6)	443.4 - 1058.1 (772.6)
Ensemble All	Slope ± SE (p_value)	-0.26 ± 0.47 (0.36)	-0.64 ± 0.50 (0.16)	-0.68 ± 0.56 (0.08)	-0.90 ± 0.59 (**0.04**)	-0.64 ± 0.34 (0.07)	-0.71 ± 0.57 (0.15)	-0.27 ± 0.50 (0.72)
	Min. - Max. (Mean)	274.3 - 715.9 (398.1)	357.6 - 752.2 (528.0)	247.6 - 703.8 (410.7)	294.7 - 714.8 (440.6)	342.0 - 638.4 (498.8)	361.6 - 800.7 (571.3)	548.9 - 957.2 (782.5)

Table 6-5. Near century (2020 – 2030) (11 years): Summary statistics of annual basin-average precipitation depths

		Upper Sakarya	Porsuk	Ankara	Kirmir	Middle Sakarya	Göksu	Lower Sakarya
Historical Period (2010 – 2017)	Min. - Max. (Mean)	274.6 - 449.3 (380.1)	344.4 - 565.8 (479.21)	292.0 - 520.8 (417.1)	343.0 - 564.2 (458.3)	362.52 - 575.44 (496.15)	387.3 - 711.7 (531.2)	422.4 - 946.5 (733.1)
Near century (2020 – 2030) (11 years)								
CCSM4_ RCP4.5	Slope ± SE	5.91 ± 8.02	-0.96 ± 11.35	1.01 ± 13.95	2.60 ± 12.22	5.40 ± 12.88	4.51 ± 14.79	9.20 ± 22.95
	(p_value)	(0.64)	(0.76)	(0.88)	(0.88)	(0.76)	(0.44)	(0.64)
	Min. - Max. (Mean)	310.7 - 616.1 (434.8)	460.2 - 818.5 (609.1)	398.0 - 774.5 (542.1)	441.9 - 800.8 (569.7)	415.4 - 827.3 (568.7)	450.3 - 887.6 (612.4)	648.0 - 1415.8 (916.3)
CCSM4_ RCP8.5	Slope ± SE	4.19 ± 9.65	12.40 ± 13.13	-1.05 ± 16.45	-2.63 ± 18.18	2.40 ± 10.82	15.12 ± 21.16	15.62 ± 20.05
	(p_value)	(0.88)	(0.53)	(0.76)	(0.88)	(1.00)	(0.64)	(0.44)
	Min. - Max. (Mean)	236.1 - 557.8 (409.8)	287.0 - 710.4 (489.2)	149.8 - 676.5 (388.3)	187.0 - 739.2 (395.0)	320.6 - 610.0 (457.1)	268.6 - 1008.5 (535.5)	430.7 - 1161.7 (727.8)
MIROC5_ RCP4.5	Slope ± SE	-9.43 ± 10.46	-12.98 ± 10.44	-29.22 ± 15.83	-28.38 ± 14.83	-14.16 ± 10.08	-3.56 ± 15.39	-15.08 ± 9.85
	(p_value)	(0.35)	(0.21)	(0.12)	(**0.03**)	(0.16)	(0.88)	(0.16)
	Min. - Max. (Mean)	233.0 - 583.4 (348.6)	315.5 - 686.1 (463.8)	163.1 - 809.7 (353.2)	207.1 - 826.3 (387.1)	370.5 - 752.8 (488.3)	379.8 - 837.9 (587.9)	581.8 - 969.9 (722.5)
MIROC5_ RCP8.5	Slope ± SE	-1.42 ± 8.96	1.96 ± 10.40	-10.44 ± 18.88	-16.82 ± 22.88	-2.40 ± 11.31	3.22 ± 17.13	14.18 ± 18.33
	(p_value)	(0.88)	(0.88)	(1.00)	(0.88)	(0.88)	(1.00)	(0.44)
	Min. - Max. (Mean)	270.9 - 580.3 (373.8)	410.1 - 722.2 (579.8)	159.7 - 712.9 (404.8)	224.4 - 847.9 (491.0)	345.8 - 690.6 (533.6)	343.6 - 847.6 (649.2)	456.1 - 1046.5 (768.8)
Ensemble RCP 4.5s	Slope ± SE	-1.76 ± 5.27	-6.97 ± 4.41	-14.11 ± 9.06	-12.89 ± 8.09	-4.38 ± 6.19	0.48 ± 8.73	-2.94 ± 10.05
	(p_value)	(0.64)	(0.12)	(0.28)	(0.21)	(0.64)	(1.00)	(0.76)
	Min. - Max. (Mean)	305.9 - 470.3 (394.8)	491.1 - 629.9 (540.2)	339.0 - 606.1 (455.9)	386.4 - 636.0 (484.1)	438.4 - 632.7 (528.2)	456.3 - 702.5 (594.2)	700.4 - 998.8 (820.2)
Ensemble RCP 8.5s	Slope ± SE	1.39 ± 6.57	7.18 ± 8.84	-5.75 ± 12.76	-9.72 ± 15.54	0.00 ± 8.03	9.17 ± 16.88	14.90 ± 13.53
	(p_value)	(0.76)	(0.64)	(0.76)	(0.76)	(1.00)	(0.76)	(0.28)
	Min. - Max. (Mean)	304.9 - 541.4 (392.0)	391.7 - 683.4 (534.9)	261.1 - 694.7 (396.9)	274.5 - 793.5 (443.4)	350.3 - 592.2 (495.8)	306.1 - 912.1 (593.0)	443.4 - 965.6 (749.7)
Ensemble All	Slope ± SE	-0.19 ± 4.73	0.11 ± 4.99	-9.93 ± 7.74	-11.30 ± 8.68	-2.19 ± 3.85	4.82 ± 7.58	5.98 ± 6.36
	(p_value)	(1.00)	(0.76)	(0.21)	(0.12)	(0.53)	(0.64)	(0.53)
	Min. - Max. (Mean)	316.8 - 466.7 (393.9)	467.6 - 610.0 (538.1)	311.5 - 637.4 (426.0)	342.6 - 714.8 (464.1)	467.2 - 594.6 (513.5)	487.5 - 722.3 (598.0)	626.2 - 881.7 (787.0)

Table 6-6. Mid-century (2055 – 2065) (11 years): Summary statistics of annual basin-average precipitation depths

		Upper Sakarya	Porsuk	Ankara	Kirmir	Middle Sakarya	Göksu	Lower Sakarya
Historical Period (2010 – 2017)	Min. - Max. (Mean)	274.6 - 449.3 (380.1)	344.4 - 565.8 (479.21)	292.0 - 520.8 (417.1)	343.0 - 564.2 (458.3)	362.5 - 575.4 (496.2)	387.3 - 711.7 (531.2)	422.4 - 946.5 (733.1)
Mid-century (2055 – 2065) (11 years)								
CCSM4_ RCP4.5	Slope ± SE	-2.53 ± 6.47	-2.39 ± 9.42	-5.97 ± 8.98	-6.01 ± 10.43	-8.75 ± 10.72	-4.27 ± 9.89	-12.38 ± 16.00
	(p_value)	(0.64)	(1.00)	(0.28)	(0.53)	(0.44)	(0.88)	(0.64)
	Min. - Max. (Mean)	329.8 - 522.7 (417.6)	464.3 - 718.1 (584.3)	315.1 - 592.4 (481.7)	301.6 - 634.8 (499.5)	396.8 - 718.6 (561.2)	433.5 - 707.8 (598.9)	568.8 - 1044.7 (852.0)
CCSM4_ RCP8.5	Slope ± SE	4.98 ± 47.98	14.38 ± 43.78	8.02 ± 48.36	15.17 ± 46.59	14.29 ± 28.12	11.08 ± 19.73	15.55 ± 31.52
	(p_value)	(0.64)	(0.76)	(0.64)	(0.76)	(0.88)	(0.53)	(0.64)
	Min. - Max. (Mean)	140.1 - 1846.9 (553.4)	168.0 - 1644.1 (574.8)	97.3 - 1792.6 (515.5)	123.7 - 1667.8 (512.1)	232.2 - 1083.3 (492.4)	274.5 - 895.2 (529.7)	380.6 - 1332.0 (737.4)
MIROC5_ RCP4.5	Slope ± SE	16.34 ± 9.99	18.71 ± 15.31	19.25 ± 13.23	22.66 ± 12.46	8.83 ± 13.75	-8.05 ± 22.88	-13.46 ± 27.89
	(p_value)	(0.12)	(0.28)	(0.28)	(0.21)	(0.64)	(1.00)	(0.88)
	Min. - Max. (Mean)	21.8 - 442.9 (265.0)	21.3 - 719.6 (351.6)	16.5 - 561.7 (247.9)	14.1 - 592.2 (276.3)	20.4 - 652.6 (373.1)	32.3 - 941.9 (430.8)	101.4 - 1335.3 (689.2)
MIROC5_ RCP8.5	Slope ± SE	-11.97 ± 19.20	-14.55 ± 28.15	-24.49 ± 23.98	-28.00 ± 26.14	-13.27 ± 21.66	-11.90 ± 37.81	4.01 ± 32.55
	(p_value)	(0.64)	(0.76)	(0.53)	(0.64)	(0.44)	(0.53)	(0.88)
	Min. - Max. (Mean)	104.4 - 823.9 (373.5)	178.2 - 1259.2 (595.0)	91.1 - 1019.3 (354.7)	144.1 - 1135.6 (430.7)	272.5 - 1071.4 (533.2)	278.5 - 1546.3 (701.8)	505.3 - 1534.7 (841.9)
Ensemble RCP 4.5s	Slope ± SE	6.91 ± 5.56	8.16 ± 7.19	6.64 ± 6.88	8.32 ± 7.55	0.04 ± 6.22	-6.16 ± 13.21	-12.92 ± 15.40
	(p_value)	(0.21)	(0.44)	(0.21)	(0.21)	(1.00)	(1.00)	(1.00)
	Min. - Max. (Mean)	278.2 - 467.6 (369.1)	397.7 - 675.3 (506.4)	285.8 - 540.3 (392.1)	329.0 - 596.3 (416.7)	417.1 - 620.9 (507.4)	420.0 - 817.3 (565.0)	656.9 - 1161.5 (803.5)
Ensemble RCP 8.5s	Slope ± SE	-3.49 ± 24.10	-0.08 ± 23.23	-8.23 ± 23.74	-6.42 ± 22.60	0.51 ± 14.44	-0.41 ± 18.55	9.78 ± 16.03
	(p_value)	(0.88)	(0.76)	(0.64)	(0.88)	(0.76)	(1.00)	(0.88)
	Min. - Max. (Mean)	198.1 - 1094.7 (463.5)	302.6 - 1100.1 (584.9)	136.3 - 1014.9 (435.1)	188.7 - 968.6 (471.4)	303.3 - 786.4 (512.8)	373.3 - 953.2 (615.8)	525.8 - 1058.1 (789.7)
Ensemble All	Slope ± SE	1.71 ± 11.71	4.04 ± 10.38	-0.80 ± 12.42	0.95 ± 11.61	0.28 ± 6.02	-3.29 ± 9.12	-1.57 ± 6.87
	(p_value)	(0.76)	(0.44)	(0.88)	(1.00)	(1.00)	(1.00)	(0.53)
	Min. - Max. (Mean)	274.3 - 715.9 (419.7)	415.4 - 752.2 (549.4)	247.6 - 703.8 (416.4)	302.0 - 663.5 (447.6)	457.7 - 638.4 (511.6)	453.2 - 752.1 (590.5)	679.8 - 883.7 (797.6)

Table 6-7. Far century (2090 – 2100) (11 years Summary statistics of annual basin-average precipitation depths

		Upper Sakarya	Porsuk	Ankara	Kirmir	Middle Sakarya	Göksu	Lower Sakarya
Historical Period (2010 – 2017)	Min. - Max. (Mean)	274.6 - 449.3 (380.1)	344.4 - 565.8 (479.21)	292.0 - 520.8 (417.1)	343.0 - 564.2 (458.3)	362.5 - 575.4 (496.2)	387.3 - 711.7 (531.2)	422.4 - 946.5 (733.1)
Far century (2090 – 2100) (11 years)								
CCSM4_ RCP4.5	Slope ± SE (p_value)	4.71 ± 6.96 (0.64)	2.81 ± 9.70 (1.00)	-0.62 ± 9.70 (0.88)	0.58 ± 9.81 (1.00)	1.68 ± 8.00 (0.64)	1.89 ± 10.40 (0.76)	7.84 ± 19.65 (0.88)
	Min. - Max. (Mean)	298.1 - 489.2 (385.0)	407.1 - 681.9 (509.5)	337.4 - 650.9 (450.5)	336.4 - 687.4 (459.6)	372.3 - 625.7 (486.0)	364.0 - 689.0 (490.4)	482.8 - 1165.1 (832.4)
CCSM4_ RCP8.5	Slope ± SE (p_value)	-11.42 ± 16.79 (0.53)	-46.88 ± 22.50 (0.16)	-15.95 ± 14.10 (0.28)	-21.92 ± 14.62 (0.12)	-35.10 ± 14.25 (**0.04**)	-20.52 ± 14.06 (0.12)	-49.09 ± 19.15 (0.06)
	Min. - Max. (Mean)	215.3 - 739.6 (495.3)	299.4 - 1256.4 (589.3)	198.1 - 681.8 (412.1)	205.9 - 682.3 (426.7)	276.7 - 929.0 (507.6)	301.6 - 816.5 (551.0)	470.9 - 1264.7 (838.8)
MIROC5_ RCP4.5	Slope ± SE (p_value)	2.76 ± 7.30 (0.64)	-1.39 ± 14.22 (1.00)	-29.54 ± 18.99 (0.53)	-38.15 ± 24.65 (0.64)	-5.09 ± 16.37 (0.76)	10.30 ± 21.12 (1.00)	9.92 ± 17.24 (0.44)
	Min. - Max. (Mean)	142.6 - 372.7 (277.7)	168.3 - 585.6 (399.3)	78.1 - 865.7 (283.5)	102.0 - 1106.4 (330.5)	225.9 - 734.1 (425.8)	213.8 - 867.4 (496.9)	410.3 - 955.6 (681.4)
MIROC5_ RCP8.5	Slope ± SE (p_value)	-3.43 ± 11.38 (0.76)	14.10 ± 17.81 (0.53)	-4.40 ± 19.42 (0.76)	1.25 ± 20.21 (0.76)	11.56 ± 16.87 (0.53)	34.43 ± 30.78 (0.28)	35.22 ± 26.74 (0.21)
	Min. - Max. (Mean)	199.2 - 530.1 (348.5)	237.1 - 753.2 (472.3)	149.5 - 694.1 (395.4)	177.3 - 741.3 (408.0)	267.0 - 704.1 (449.5)	268.3 - 1308.0 (563.1)	362.0 - 1287.5 (718.1)
Ensemble RCP 4.5s	Slope ± SE (p_value)	3.73 ± 4.97 (0.64)	0.71 ± 9.63 (0.53)	-15.08 ± 8.08 (0.44)	-18.79 ± 11.32 (0.35)	-1.70 ± 8.05 (0.44)	6.09 ± 12.08 (1.00)	8.88 ± 10.72 (1.00)
	Min. - Max. (Mean)	256.1 - 417.0 (326.3)	346.2 - 622.1 (451.6)	270.0 - 601.5 (364.5)	274.4 - 721.4 (395.2)	374.0 - 615.5 (456.2)	296.7 - 768.1 (493.7)	595.0 - 1022.6 (750.1)
Ensemble RCP 8.5s	Slope ± SE (p_value)	-7.43 ± 8.72 (0.35)	-16.39 ± 12.26 (0.44)	-10.17 ± 10.41 (0.35)	-10.34 ± 10.97 (0.44)	-11.77 ± 9.49 (0.16)	6.96 ± 14.73 (0.76)	-6.94 ± 13.30 (0.76)
	Min. - Max. (Mean)	243.0 - 535.3 (424.4)	307.8 - 792.6 (534.4)	229.0 - 550.9 (405.8)	258.8 - 634.1 (419.7)	308.1 - 610.4 (482.6)	299.4 - 833.2 (557.0)	502.8 - 954.4 (778.4)
Ensemble All	Slope ± SE (p_value)	-1.85 ± 4.34 (0.35)	-7.84 ± 8.35 (0.44)	-12.62 ± 5.42 (0.06)	-14.56 ± 6.97 (0.06)	-6.74 ± 6.47 (0.35)	6.52 ± 10.98 (1.00)	0.97 ± 10.92 (1.00)
	Min. - Max. (Mean)	305.1 - 431.7 (380.8)	357.6 - 642.0 (496.5)	301.9 - 520.5 (389.8)	294.7 - 588.8 (410.0)	342.0 - 581.8 (471.3)	361.6 - 800.7 (525.4)	548.9 - 957.2 (762.8)

In the Upper Sakarya subbasin, all climate projection realizations except for CCSM4_RCP8.5 and the ensemble of RCP 8.5 scenarios show decreasing trend in the basin-average precipitation in the 21st century. Among all of the projections, only the trend in ensemble of RCP 4.5 scenarios is statistically significant. In the near century, while all CCSM4 projections and the ensemble of RCP 8.5 scenarios have increasing trend, the rest of the projections have decreasing trend. However, none of the trends is statistically significant. Similar to the trends in the near century, there is no statistically significant trend in the mid-century. Three of the projections, i.e., CCMS4_RCP4.5, MIROC5_RCP8.5 and the ensemble of RCP8.5 scenarios have a decreasing trend while the rest has an increasing trend. Lastly, all RCP 8.5 projections and the ensemble of all projections indicate decreasing trend in the far century. Again, the trends are away from monotonic trend according to the p-value of Mann-Kendall trend test. When the statistics of the historical precipitation is compared to the 21st century, near, mid-, and far century, it can be seen that the mean of the MIROC5 projections and the mean of the ensemble of RCP 4.5 scenarios are

lower compared to the historical period with the only exception of the ensemble of RCP 4.5s in the near century. The lowest mean is projected in the MIROC5_RCP 4.5 in all time periods.

In the Porsuk subbasin, the only projection with an increasing trend in the 21st century is the CCSM4_RCP8.5 but the trend is not monotonic. All of the ensembles, all MIROC5 projections, and the CCSM4_RCP4.5 scenario have a decreasing trend. Furthermore, CCSM4_RCP4.5 and the ensemble of RCP4.5s denote statistically significant decreasing trend. In all of the three segments of the future period, although the trends are either decreasing or increasing depending on the GCM and the RCP involved, there is no significant trend in the time series. From Table 6-4, Table 6-5, Table 6-6 and Table 6-7, it can be seen that the only projection with a lower mean as compared to the historical period is MIROC5_RCP4.5 in all time periods. In the far century, however, the ensemble of RCP 4.5 scenarios also projects a lower mean. Among all projections, the lowest mean in the Porsuk subbasin is projected by MIROC5_RCP4.5 in all time periods.

The Mann-Kendall trend test detected significant downward trend in the CCSM4_RCP4.5 and the ensemble average of RCP 4.5 scenarios in the Ankara subbasin in the 21st century. All of the projections except for CCSM4_RCP4.5 show decreasing trend in the near century. However, none of these trends are statistically significant. Similarly, there is no significant upward or downward trend in the climate projections both in the mid- and far century. Although the trends are either increasing or decreasing in the mid-century, all of the projections indicate decreasing trend in the far century. Table 6-4, Table 6-5, Table 6-6 and Table 6-7 show that the means of the CCSM4_RCP4.5, MIROC5_RCP4.5, MIROC5_RCP8.5, the ensemble of RCP 4.5s, the ensemble of RCP 8.5s and the ensemble of all projections are lower than the mean of the historical period both in the 21st century and the far century. In the near and mid-century, the results are similar to the 21st century and the far century

with the only exception is that the ensemble of RCP 4.5 scenarios project higher mean in comparison to the historical period. The basin average annual total precipitation projected to be in MIROC5_RCP4.5 scenario is the lowest among all other projections in all time periods.

In the Kirmir subbasin, all of the climate projections except for CCSM4_RCP8.5 have a decreasing trend in the 21st century. Moreover, three of these downward trends, i.e., CCSM4_RCP4.5, the ensemble of RCP 4.5s and the ensemble of all projections, are statistically significant. The results in the near century are very similar to the Ankara subbasin. The only difference is that the downward trend in the MIROC5_RCP4.5 scenario is close to the monotonic trend. In fact, this is the only projection which has a statistically significant trend among all projections in all study subbasins in the near century. The number of climate projections with an upward trend in the mid-century are higher compared to the ones with a downward trend. However, none of them has statistically significant p-values. Finally, in the far century, only two of the projections have increasing trend while the rest has a decreasing trend. Again, there is no monotonic trend. When the mean precipitation values of the historical and the future period are compared, it is seen that all of the projections except for CCSM4_RCP4.5 project a lower mean than the historical period in the 21st century and the far century. In the near century, the mean values are lower in the CCMS4_RCP8.5, MIROC5_RCP4.5, the ensemble of RCP 4.5 scenarios and the ensemble of all projections. In the mid-century, the results are similar to near century but the only difference is that the MIROC5_RCP8.5 has also a lower mean as compared to the historical period in the mid-century.

In the Middle Sakarya subbasin, all of the projections except for CCMS4_RCP8.5 have a decreasing trend in the 21st century. Furthermore, the ensemble average of RCP 4.5 scenarios show a statistically significant downward trend. In the near and mid-century there is no statistically significant upward or downward trend. There are

four downward trends in the near century while there is only two in the mid-century. In the far century, on the other hand, CCSM4_RCP.8.5 projection denotes a downward trend with a statistically significant p-value. There is not statistically significant evidence that a trend is present in the other climate projections in the far century. In the 21st century and mid-century, CCSM4_RCP8.5 and MIROC5_RCP4.5 projections have lower means as compared to the historical period. In the near century, the ensemble of RCP 8.5 scenarios is also projected to have a lower mean in addition the CCSM4_RCP8.5 and MIROC5_RCP4.5 projections. Lastly, in the far century, all of the climate projections except for CCSM4_RCP8.5 have lower means than the historical period. The lowest mean among all other projections is projected by MIROC5_RCP4.5 in the 21st century, mid- and far century. In the near century, CCSM4_RCP8.5 has the lowest mean as compared to other projections.

In the Göksu subbasin, none of the climate projections has a significant trend in the 21st century or any segments of the future period. The most remarkable result is that all projections except MIROC5_RCP4.5 are in an increasing trend in the near and far century. Göksu is the only subbasin where almost all of the climate projections indicate an increasing trend in the near and far century but none of them statistically significant. However, in the mid-century, basin-average annual total precipitation depths tend to decrease. In the 21st century, the only projection which has a lower mean than the historical period is MIROC5_RCP4.5. All of the climate projections in the near century project higher means in comparison to the historical mean. In the mid-century, CCSM4_RCP8.5 and MIROC5_RCP4.5 have lower means as compared to the historical period. In the far century, on the other hand, the means of all projections involving the RCP 4.5 scenario and the ensemble of all scenarios are lower than the historical period.

Similar to the Göksu subbasin, the Lower Sakarya subbasin does not have any statistically significant p-value in any future period. Only two out of seven projections are on an upward trend in the 21st century. In the near and far century, however, the number of projections with an increasing trend are higher compared to the ones with a decreasing trend. Unlike near and far century, most of the projections have downward trend in the mid-century. In the 21st century and mid-century, MIROC5_RCP4.5 is the only projection which has a lower mean compared to the historical mean. In the near century, two of the projections, i.e., CCSM4_RCP8.5 and MIROC5_RCP4.5, project lower means than the historical period. Finally, in the far century, all MIROC5 projections indicate lower means than the mean of the historical precipitation. Moreover, MIROC5_RCP4.5 always projects the lowest mean as compared to the other projections in the Lower Sakarya subbasin.

The results show that all the climate projections with a statistically meaningful p-value point out a downward trend in the basin-average annual total precipitation depths overall study subbasins in the 21st century. There is no projection with an upward trend and with a significant p-value. Thus, the precipitation depths tend to decrease in all subbasins in the 21st century. Except for Göksu and Lower Sakarya subbasins, there are at least one or more projections with statistically significant decreasing trends in all other sub-basins. In addition, Göksu and Lower Sakarya have different trends compared to other sub-basins in all segments of the future period. CCSM4_RCP8.5 projection, two MIROC5 projections, and the ensemble averages of the RCP 8.5 scenarios do not have a significant decreasing or increasing trend based on the results of the Mann-Kendall trend test in all subbasins. The p-values of CCSM4_RCP4.5 projection in Porsuk, Ankara and Kirmir subbasins indicate a significant decreasing trend. Similarly, the ensemble averages of RCP 4.5 scenarios point out significant decreasing trend in the basin-average annual total precipitation depths of Upper Sakarya, Porsuk, Ankara, Kirmir and Middle Sakarya subbasins. Lastly, the p-values of the ensemble average of climate projection realizations show

a significant decreasing trend only in Kirmir subbasin. The Mann-Kendall trend test results show neither increasing nor decreasing trend in all projections in two subbasins namely Göksu and Lower Sakarya.

In the near century, only one subbasin, i.e., Kirmir, has a projection with a statistically significant decreasing trend which is MIROC5_RCP4.5. In all sub-basins except for Porsuk, Göksu and Lower Sakarya, the number of projections with a decreasing trend is higher than the number of projections with an increasing trend. In the mid-century, there are no projections with a statistically meaningful p-value. Except for Göksu and Lower Sakarya, the number of projections with an increasing trend is higher than the number of projections with a decreasing trend in all subbasins. Lastly, in the far century, there is only one projection, i.e., CCSM4 RCP8.5, with a statistically significant decreasing trend, and this trend is projected in the Middle Sakarya subbasin.

6.4.2 Projected changes and trends in basin average temperature in the 21st century

Temporal variability of basin-average temperatures based on the annual average temperature time series over the seven subbasins for all four climate projection realizations, the ensemble averages of RCP 4.5 and RCP 8.5 scenarios, and the ensemble averages of all realizations is shown in Figure 6-6. The most obvious conclusion drawn from this figure is that temperatures are on an increasing trend in all subbasins throughout the 21st century. The slopes and standard errors of the least squares regression line of basin-average temperature over the seven study subbasins with p-value of the Mann-Kendall trend test in parentheses are given in Table 6-8, Table 6-9, Table 6-10 and Table 6-11 for the 21st century, near century, mid-century, and far century, respectively. The bolded p-values in these tables mean that the trend is statistically significant at the 95% confidence level.

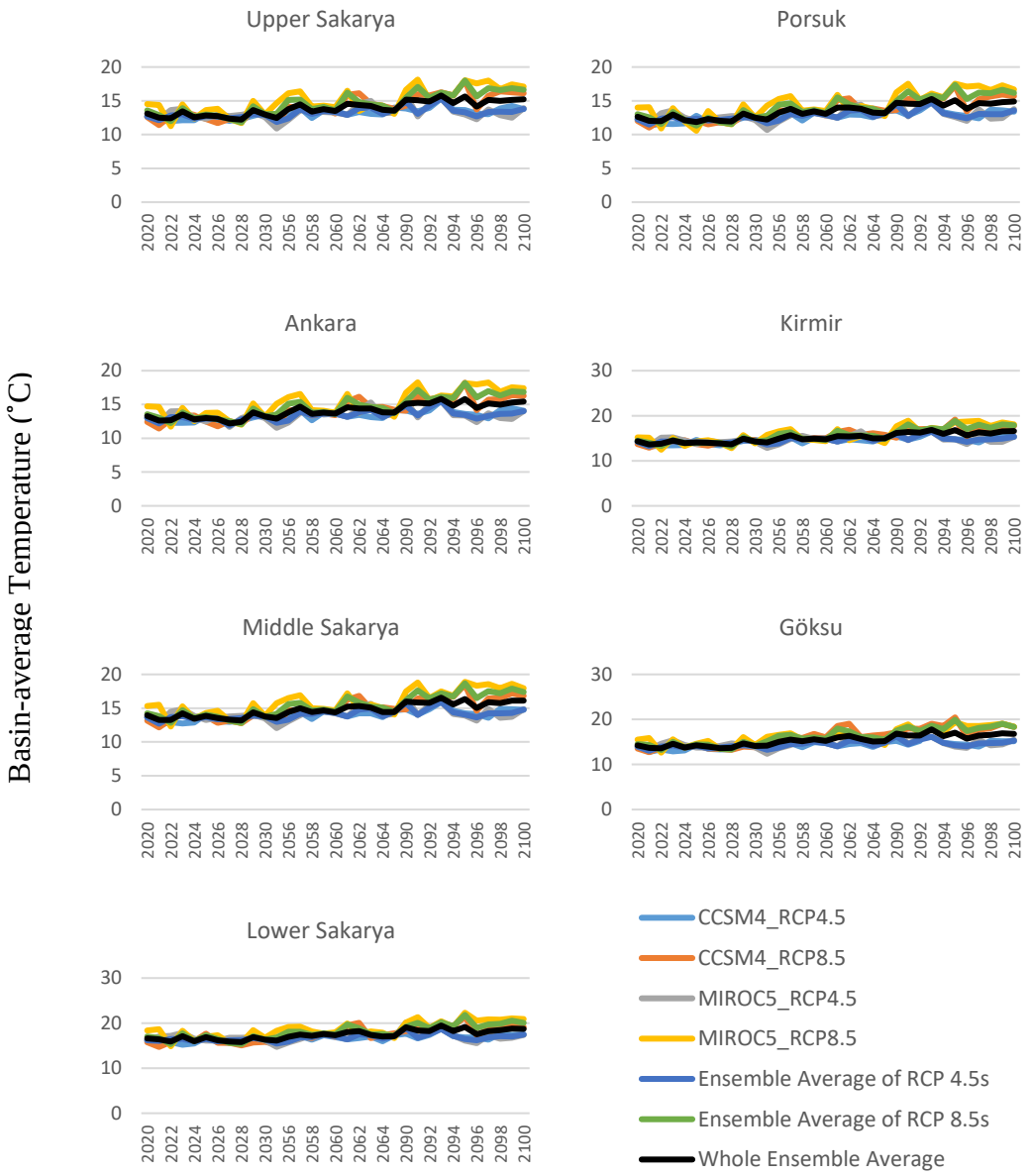

Figure 6-6. Basin average temperature over the seven subbasins; Upper Sakarya, Porsuk, Ankara, Kirmir, Middle Sakarya, Göksu, Lower Sakarya. All four climate projection realizations, the ensemble averages of RCP 4.5 scenarios, the ensemble averages of RCP 8.5 scenarios, and the ensemble averages of all realizations

Minimum and maximum values of basin-average temperature in the historical period as well as in the 21st century and each segment of the future period over the seven study subbasins with the mean value in parentheses are given in Table 6-8, Table 6-9, Table 6-10, and Table 6-11 , respectively. The statistical information about the historical period was provided for comparison purposes. In these tables, the mean value shows the average of the basin-scale temperatures for the related time period. In this way, the changes in the basin-scale temperatures are analyzed by comparing the historical means with the means of each future period segment.

Table 6-8. Entire 21st century (2020 – 2030; 2055 – 2065; 2090 - 2100) (33 years): Summary statistics of the basin-average temperatures based on the annual average temperature time series

		Upper Sakarya	**Porsuk**	**Ankara**	**Kirmir**	**Middle Sakarya**	**Göksu**	**Lower Sakarya**
Historical Period (2010 – 2017)	Min. - Max. (Mean)	10.5 - 13.9 (12.2)	10.5 - 13.3 (11.8)	11.1 - 13.7 (12.4)	12.4 - 15.0 (13.6)	11.9 - 14.1 (13.1)	11.9 - 14.6 (13.5)	14.6 - 16.7 (15.9)
Entire 21st century (2020 – 2030; 2055 – 2065; 2090 - 2100) (33 years)								
CCSM4_ RCP4.5	Slope ± SE (p_value)	0.02 ± 0.00 (**0.00**)	0.02 ± 0.00 (**0.00**)	0.02 ± 0.00 (**0.00**)	0.02 ± 0.00 (**0.00**)	0.02 ± 0.00 (**0.00**)	0.02 ± 0.00 (**0.00**)	0.02 ± 0.00 (**0.00**)
	Min. - Max. (Mean)	12.0 - 14.2 (13.1)	11.4 - 13.7 (12.6)	1.1 - 14.4 (12.9)	13.1 - 15.6 (14.5)	12.6 - 14.9 (13.9)	12.8 - 15.2 (14.2)	15.1 - 17.7 (16.5)
CCSM4_ RCP8.5	Slope ± SE (p_value)	0.05 ± 0.01 (**0.00**)	0.05 ± 0.01 (**0.00**)	0.05 ± 0.01 (**0.00**)	0.05 ± 0.00 (**0.00**)	0.05 ± 0.01 (**0.00**)	0.06 ± 0.01 (**0.00**)	0.05 ± 0.01 (**0.00**)
	Min. - Max. (Mean)	11.4 - 18.0 (14.1)	11.0 - 17.2 (13.7)	11.4 - 18.2 (14.2)	12.9 - 19.2 (15.5)	12.2 - 18.5 (14.9)	12.7 - 20.4 (16.1)	14.7 - 21.3 (17.5)
MIROC5_ RCP4.5	Slope ± SE (p_value)	0.01 ± 0.01 (0.11)	0.01 ± 0.01 (**0.05**)	0.01 ± 0.01 (0.13)	0.01 ± 0.01 (0.07)	0.01 ± 0.01 (0.07)	0.01 ± 0.01 (**0.03**)	0.01 ± 0.01 (0.19)
	Min. - Max. (Mean)	10.9 - 15.9 (13.4)	10.7 - 15.4 (13.0)	11.5 - 15.5 (13.6)	12.9 - 16.6 (14.8)	12.0 - 16.7 (14.3)	12.4 - 17.2 (14.7)	14.7 - 20.1 (17.0)
MIROC5_ RCP8.5	Slope ± SE (p_value)	0.05 ± 0.01 (**0.00**)	0.06 ± 0.01 (**0.00**)	0.05 ± 0.01 (**0.00**)	0.05 ± 0.01 (**0.00**)	0.05 ± 0.01 (**0.00**)	0.05 ± 0.01 (**0.00**)	0.05 ± 0.01 (**0.00**)
	Min. - Max. (Mean)	11.3 - 18.1 (15.1)	10.6 - 17.5 (14.6)	11.7 - 18.3 (15.3)	4.8 - 18.9 (15.6)	12.3 - 18.9 (16.0)	12.6 - 19.4 (16.4)	14.9 - 22.3 (18.7)
Ensemble RCP 4.5s	Slope ± SE (p_value)	0.02 ± 0.00 (**0.00**)	0.02 ± 0.00 (**0.00**)	0.02 ± 0.00 (**0.00**)	0.01 ± 0.00 (**0.00**)	0.02 ± 0.00 (**0.00**)	0.02 ± 0.0 0 (**0.00**)	0.01 ± 0.00 (**0.00**)
	Min. - Max. (Mean)	11.9 - 15.4 (13.2)	11.3 - 17.4 (14.1)	8.3 - 14.8 (13.2)	13.2 - 16.5 (14.6)	12.7 - 15.9 (14.1)	13.0 - 16.2 (14.5)	10.2 - 18.9 (16.5)
Ensemble RCP 8.5s	Slope ± SE (p_value)	0.05 ± 0.00 (**0.00**)	0.05 ± 0.00 (**0.00**)	0.05 ± 0.00 (**0.00**)	0.05 ± 0.00 (**0.00**)	0.05 ± 0.00 (**0.00**)	0.06 ± 0.00 (**0.00**)	0.05 ± 0.01 (**0.00**)
	Min. - Max. (Mean)	11.8 - 18.0 (14.6)	11.5 - 14.7 (12.8)	12.1 - 18.2 (14.7)	9.4 - 18.9 (15.5)	12.8 - 18.7 (15.4)	13.2 - 19.9 (16.2)	15.3 - 21.8 (18.0)
Ensemble All	Slope ± SE (p_value)	0.03 ± 0.00 (**0.00**)	0.03 ± 0.00 (**0.00**)	0.03 ± 0.00 (**0.00**)	0.03 ± 0.00 (**0.00**)	0.03 ± 0.00 (**0.00**)	0.04 ± 13.02 (**0.00**)	0.03 ± 0.00 (**0.00**)
	Min. - Max. (Mean)	12.2 - 15.9 (13.9)	11.8 - 15.4 (13.5)	12.2 - 15.8 (14.0)	10.7 - 17.0 (15.1)	13.1 - 16.8 (14.7)	13.4 - 17.8 (15.4)	15.8 - 19.7 (17.4)

Table 6-9. Near century (2020 – 2030) (11 years): Summary statistics of the basin-average temperatures based on the annual average temperature time series

		Upper Sakarya	Porsuk	Ankara	Kirmir	Middle Sakarya	Göksu	Lower Sakarya
Historical Period (2010 – 2017)	Min. - Max. (Mean)	10.5 - 13.9 (12.2)	10.5 - 13.3 (11.8)	11.1 - 13.7 (12.4)	12.4 - 15.0 (13.6)	11.9 - 14.1 (13.1)	11.9 - 14.6 (13.5)	14.6 - 16.7 (15.9)
Near century (2020 – 2030) (11 years)								
CCSM4_ RCP4.5	Slope ± SE (p_value)	0.06 ± 0.04 (0.09)	0.08 ± 0.04 (**0.03**)	0.06 ± 0.05 (0.12)	0.08 ± 0.05 (0.09)	0.08 ± 0.05 (0.06)	0.08 ± 0.05 (0.09)	0.08 ± 0.05 (0.12)
	Min. - Max. (Mean)	12.0 - 13.2 (12.4)	11.4 - 12.8 (12.0)	12.1 - 13.5 (12.7)	13.1 - 14.6 (13.8)	12.6 - 14.1 (13.3)	12.8 - 14.5 (13.6)	15.1 - 16.8 (15.9)
CCSM4_ RCP8.5	Slope ± SE (p_value)	0.04 ± 0.06 (0.53)	0.05 ± 0.05 (0.53)	0.07 ± 0.06 (0.28)	0.08 ± 0.05 (0.28)	0.05 ± 0.06 (0.64)	0.03 ± 0.05 (0.88)	-0.01 ± 0.08 (1.00)
	Min. - Max. (Mean)	11.4 - 13.4 (12.5)	11.0 - 12.8 (12.1)	11.4 - 13.6 (12.6)	12.9 - 14.8 (14.0)	12.2 - 14.1 (13.3)	12.7 - 14.4 (13.7)	14.7 - 17.7 (15.9)
MIROC5_ RCP4.5	Slope ± SE (p_value)	-0.01 ± 0.05 (0.88)	0.00 ± 0.05 (0.76)	-0.02 ± 0.07 (0.76)	0.01 ± 0.05 (1.00)	0.00 ± 0.06 (0.88)	0.01 ± 0.06 (0.76)	-0.04 ± 0.05 (0.53)
	Min. - Max. (Mean)	12.3 - 13.8 (13.0)	12.0 - 13.6 (12.7)	12.5 - 14.0 (13.3)	13.7 - 15.2 (14.5)	13.2 - 14.9 (13.9)	13.8 - 15.4 (14.3)	16.1 - 17.8 (16.7)
MIROC5_ RCP8.5	Slope ± SE (p_value)	-0.06 ± 0.12 (0.53)	-0.06 ± 0.14 (0.64)	-0.07 ± 0.12 (0.44)	-0.04 ± 0.10 (0.44)	-0.07 ± 0.12 (0.53)	-0.05 ± 0.11 (0.64)	-0.09 ± 0.13 (0.44)
	Min. - Max. (Mean)	11.3 - 15.6 (13.5)	10.6 - 15.0 (12.8)	11.7 - 15.8 (13.7)	4.8 - 15.7 (13.4)	12.3 - 16.4 (14.4)	12.6 - 16.3 (14.8)	14.9 - 19.1 (17.2)
Ensemble RCP 4.5s	Slope ± SE (p_value)	0.03 ± 0.03 (0.44)	0.04 ± 0.03 (0.16)	0.02 ± 0.04 (0.64)	0.04 ± 0.03 (0.53)	0.04 ± 0.03 (0.35)	0.04 ± 0.03 (0.21)	0.02 ± 0.02 (0.53)
	Min. - Max. (Mean)	12.1 - 13.0 (12.7)	11.3 - 13.6 (12.4)	11.9 - 13.3 (12.8)	13.2 - 14.6 (14.1)	12.7 - 13.9 (13.5)	13.0 - 14.3 (13.9)	16.0 - 16.7 (16.3)
Ensemble RCP 8.5s	Slope ± SE (p_value)	-0.01 ± 0.07 (0.88)	-0.01 ± 0.08 (0.88)	0.00 ± 0.07 (0.76)	0.02 ± 0.06 (1.00)	-0.01 ± 0.07 (0.64)	-0.01 ± 0.06 (0.76)	-0.05 ± 0.08 (0.44)
	Min. - Max. (Mean)	11.8 - 14.2 (12.9)	11.5 - 12.6 (12.3)	12.1 - 14.4 (13.1)	9.4 - 15.3 (13.7)	12.8 - 14.9 (13.8)	13.2 - 15.0 (14.1)	15.3 - 17.7 (16.4)
Ensemble All	Slope ± SE (p_value)	0.01 ± 0.05 (1.00)	0.02 ± 0.04 (1.00)	0.01 ± 0.05 (0.88)	0.03 ± 0.04 (0.64)	0.01 ± 0.04 (1.00)	0.02 ± 0.44 (0.64)	-0.02 ± 0.04 (0.44)
	Min. - Max. (Mean)	12.2 - 13.6 (12.8)	11.8 - 13.1 (12.3)	12.2 - 13.8 (13.0)	10.7 - 14.9 (13.8)	13.1 - 14.4 (13.6)	13.4 - 14.6 (14.0)	15.8 - 17.1 (16.4)

Table 6-10. Mid-century (2055 – 2065) (11 years): Summary statistics of the basin-average temperatures based on the annual average temperature time series

		Upper Sakarya	Porsuk	Ankara	Kirmir	Middle Sakarya	Göksu	Lower Sakarya
Historical Period (2010 – 2017)	Min. - Max. (Mean)	10.5 - 13.9 (12.2)	10.5 - 13.3 (11.8)	11.1 - 13.7 (12.4)	12.4 - 15.0 (13.6)	11.9 - 14.1 (13.1)	11.9 - 14.6 (13.5)	14.6 - 16.7 (15.9)
Mid-century (2055 – 2065) (11 years)								
CCSM4_ RCP4.5	Slope ± SE (p_value)	0.05 ± 0.05 (0.44)	0.05 ± 0.04 (0.53)	0.04 ± 0.05 (0.88)	0.05 ± 0.05 (0.64)	0.04 ± 0.04 (0.64)	0.04 ± 0.04 (0.64)	0.04 ± 0.05 (0.44)
	Min. - Max. (Mean)	12.5 - 14.0 (13.2)	11.8 - 13.1 (12.3)	12.7 - 14.2 (13.4)	13.9 - 15.4 (14.6)	13.4 - 14.7 (14.1)	13.8 - 14.9 (14.4)	16.0 - 17.3 (16.7)
CCSM4_ RCP8.5	Slope ± SE (p_value)	0.20 ± 0.11 (0.35)	0.17 ± 0.09 (0.16)	0.20 ± 0.09 (0.06)	0.19 ± 0.07 (0.06)	0.19 ± 0.09 (**0.04**)	0.19 ± 0.11 (0.09)	0.19 ± 0.12 (0.12)
	Min. - Max. (Mean)	11.5 - 16.1 (14.1)	11.3 - 15.4 (13.6)	11.9 - 16.1 (14.2)	13.4 - 16.9 (15.5)	12.6 - 16.8 (14.8)	14.2 - 19.0 (16.5)	15.3 - 20.1 (17.4)
MIROC5_ RCP4.5	Slope ± SE (p_value)	0.19 ± 0.09 (0.28)	0.18 ± 0.08 (0.16)	0.17 ± 0.08 (0.21)	0.16 ± 0.08 (0.12)	0.18 ± 0.08 (0.16)	0.17 ± 0.09 (0.16)	0.19 ± 0.08 (0.16)
	Min. - Max. (Mean)	10.9 - 15.0 (13.3)	10.7 - 14.4 (12.9)	11.5 - 15.3 (13.5)	12.9 - 16.6 (14.8)	12.0 - 15.6 (14.2)	12.4 - 16.1 (14.7)	14.7 - 18.4 (16.9)
MIROC5_ RCP8.5	Slope ± SE (p_value)	-0.19 ± 0.10 (0.16)	-0.14 ± 0.09 (0.28)	-0.19 ± 0.10 (0.09)	-0.17 ± 0.09 (0.12)	-0.15 ± 0.09 (0.16)	-0.12 ± 0.08 (0.28)	-0.14 ± 0.08 (0.09)
	Min. - Max. (Mean)	13.1 - 16.5 (14.7)	12.8 - 15.9 (14.2)	13.2 - 16.6 (14.8)	13.9 - 17.0 (15.4)	14.1 - 17.2 (15.5)	14.3 - 17.4 (15.9)	16.6 - 19.9 (18.2)
Ensemble RCP 4.5s	Slope ± SE (p_value)	0.12 ± 0.05 (0.09)	0.11 ± 0.05 (0.09)	0.10 ± 0.05 (0.12)	0.10 ± 0.05 (0.09)	0.11 ± 0.05 (0.06)	0.11 ± 0.05 (0.06)	0.11 ± 0.05 (0.12)
	Min. - Max. (Mean)	11.9 - 14.0 (13.2)	12.8 - 15.5 (13.9)	12.3 - 14.2 (13.4)	13.6 - 15.5 (14.7)	13.0 - 14.9 (14.1)	13.2 - 15.3 (14.5)	15.5 - 17.5 (16.8)
Ensemble RCP 8.5s	Slope ± SE (p_value)	0.00 ± 0.09 (0.88)	0.02 ± 0.08 (1.00)	0.01 ± 0.08 (1.00)	0.01 ± 0.07 (0.88)	0.02 ± 0.08 (0.88)	0.04 ± 0.08 (1.00)	0.02 ± 0.08 (1.00)
	Min. - Max. (Mean)	13.1 - 16.2 (14.4)	11.7 - 13.7 (12.8)	13.5 - 16.0 (14.5)	14.6 - 16.7 (15.4)	14.1 - 16.7 (15.2)	15.2 - 17.9 (16.2)	16.8 - 19.7 (17.8)
Ensemble All	Slope ± SE (p_value)	0.06 ± 0.06 (0.64)	0.06 ± 0.05 (0.64)	0.05 ± 0.05 (0.53)	0.06 ± 0.04 (0.35)	0.06 ± 0.05 (0.28)	0.07 ± 1.45 (0.16)	0.07 ± 0.05 (0.35)
	Min. - Max. (Mean)	12.5 - 15.1 (13.8)	12.2 - 14.5 (13.4)	12.9 - 15.1 (14.0)	14.1 - 15.9 (15.1)	13.6 - 15.7 (14.7)	14.2 - 16.6 (15.4)	16.1 - 18.6 (17.4)

Table 6-11. Far century (2090 – 2100) (11 years): Summary statistics of the basin-average temperatures based on the annual average temperature time series

		Upper Sakarya	Porsuk	Ankara	Kirmir	Middle Sakarya	Göksu	Lower Sakarya
Historical Period (2010 – 2017)	Min. - Max. (Mean)	10.5 - 13.9 (12.2)	10.5 - 13.3 (11.8)	11.1 - 13.7 (12.4)	12.4 - 15.0 (13.6)	11.9 - 14.1 (13.1)	11.9 - 14.6 (13.5)	14.6 - 16.7 (15.9)
Far century (2090 – 2100) (11 years)								
CCSM4_ RCP4.5	Slope ± SE	-0.03 ± 0.06	-0.03 ± 0.06	-0.02 ± 0.07	-0.01 ± 0.06	-0.02 ± 0.06	-0.02 ± 0.06	-0.02 ± 0.07
	(p_value)	(0.88)	(0.88)	(0.76)	(1.00)	(0.76)	(0.53)	(0.88)
	Min. - Max.	13.0 - 14.2	12.4 - 13.7	1.1 - 14.4	14.1 - 15.6	13.6 - 14.9	13.9 - 15.2	16.3 - 17.7
	(Mean)	(13.7)	(13.2)	(12.7)	(15.0)	(14.5)	(14.8)	(17.1)
CCSM4_ RCP8.5	Slope ± SE	0.08 ± 0.11	0.11 ± 0.10	0.09 ± 0.11	0.12 ± 0.10	0.09 ± 0.10	0.05 ± 0.11	0.05 ± 0.10
	(p_value)	(0.53)	(0.09)	(0.35)	(0.35)	(0.21)	(0.35)	(0.06)
	Min. - Max.	13.7 - 18.0	13.4 - 17.2	14.1 - 18.2	15.1 - 19.2	14.6 - 18.5	16.2 - 20.4	17.3 - 21.3
	(Mean)	(15.9)	(15.3)	(15.8)	(17.0)	(16.5)	(18.2)	(19.1)
MIROC5_ RCP4.5	Slope ± SE	-0.19 ± 0.10	-0.16 ± 0.09	-0.17 ± 0.09	-0.15 ± 0.08	-0.17 ± 0.09	-0.15 ± 0.09	-0.20 ± 0.11
	(p_value)	(0.21)	(0.16)	(0.21)	(0.35)	(0.12)	(0.21)	(0.44)
	Min. - Max.	12.3 - 15.9	12.0 - 15.4	12.4 - 15.5	13.7 - 16.5	13.2 - 16.7	13.7 - 17.2	15.5 - 20.1
	(Mean)	(13.7)	(13.4)	(13.8)	(15.1)	(14.6)	(15.1)	(17.3)
MIROC5_ RCP8.5	Slope ± SE	0.09 ± 0.09	0.09 ± 0.08	0.09 ± 0.09	0.08 ± 0.08	0.09 ± 0.08	0.10 ± 0.07	0.10 ± 0.09
	(p_value)	(0.76)	(0.44)	(0.64)	(0.53)	(0.44)	(0.21)	(0.21)
	Min. - Max.	15.1 - 18.1	15.1 - 17.5	15.6 - 18.3	16.5 - 18.9	16.5 - 18.9	16.9 - 19.4	18.9 - 22.3
	(Mean)	(17.0)	(16.6)	(17.2)	(18.0)	(17.9)	(18.3)	(20.6)
Ensemble RCP 4.5s	Slope ± SE	-0.11 ± 0.07	-0.09 ± 0.07	-0.10 ± 0.07	-0.08 ± 0.06	-0.10 ± 0.07	-0.09 ± 0.07	-0.11 ± 0.08
	(p_value)	(0.64)	(0.44)	(0.53)	(0.76)	(0.76)	(0.64)	(1.00)
	Min. - Max.	12.7 - 15.4	14.9 - 17.4	8.3 - 14.8	14.2 - 16.5	13.6 - 15.9	14.1 - 16.2	10.2 - 18.9
	(Mean)	(13.7)	(16.0)	(13.3)	(15.1)	(14.6)	(15.0)	(16.5)
Ensemble RCP 8.5s	Slope ± SE	0.09 ± 0.07	0.10 ± 0.07	0.09 ± 0.07	0.10 ± 0.07	0.09 ± 0.07	0.08 ± 0.07	0.07 ± 0.08
	(p_value)	(0.28)	(0.16)	(0.21)	(0.12)	(0.16)	(0.44)	(0.76)
	Min. - Max.	15.5 - 18.0	12.4 - 14.7	15.4 - 18.2	16.4 - 18.9	16.2 - 18.7	17.4 - 19.9	18.8 - 21.8
	(Mean)	(16.4)	(13.4)	(16.5)	(17.5)	(17.2)	(18.3)	(19.9)
Ensemble All	Slope ± SE	-0.01 ± 0.04	0.00 ± 0.04	0.00 ± 0.04	0.01 ± 0.04	0.00 ± 0.04	-0.01 ± -0.26	-0.02 ± 0.05
	(p_value)	(1.00)	(0.88)	(0.76)	(0.76)	(1.00)	(1.00)	(1.00)
	Min. - Max.	14.2 - 15.9	13.8 - 15.4	12.2 - 15.8	15.6 - 17.0	15.0 - 16.8	15.7 - 17.8	17.5 - 19.7
	(Mean)	(15.1)	(14.7)	(14.9)	(16.3)	(15.9)	(16.7)	(18.6)

In the Upper Sakarya subbasin, all climate projection realizations show an increasing trend in the 21st century. Moreover, except for MIROC5_RCP4.5 all of these trends are statistically significant. When each 11-year future period segment is analyzed individually, however, none of the trends have statistically meaningful p-values. It is also seen that there are climate projections with a decreasing trend. For instance, MIROC5 and the ensemble average of RCP 8.5 scenarios project a decreasing trend in the near century. In the mid-century, MIROC5_RCP4.5 is the only climate projection with a decreasing trend. Lastly, in the far century, MIROC5_RCP4.5, the ensemble of RCP 4.5 scenarios, and the ensemble of all GCMs have a decreasing trend. When the mean of the historical temperatures is compared to the mean of the future climate projections, it is seen that all future projections have higher means. The increase in the projected annual average temperatures range between 0.25 ˚C and 4.77 ˚C. The largest increase is projected by MIROC5_RCP8.5 in the far century while the lowest belongs to the CCSM4_RCP4.5 projection in the near century.

In the Porsuk subbasin, all climate projections point to rising temperatures in the 21st century. In addition, all these trends are statistically significant. In the near century, the only statistically significant increasing trend belongs to CCSM4_RCP4.5. Moreover, MIROC5_RCP8.5 and the ensemble average of RCP 8.5 scenarios show a decreasing trend. In the mid-century, there is no statistically meaningful trend. One of the climate projections which is MIROC5_RCP8.5 point to a decreasing trend. Similar to mid-century, none of the projections has a statistically important p-value in the far century. Three of these projections namely CCSM4_RCP4.5, MIROC5_RCP4.5 and the ensemble of RCP 4.5 scenarios have a decreasing trend. The average of the basin-scale temperatures for the historical time period is always smaller than the future projections. The increase in the temperatures range between 0.24˚C and 4.86˚C. The lowest and the largest increase in the temperature is projected by CCSM4_RCP4.5 in the near century and MIROC5_RCP8.5 in the far century, respectively.

In the Ankara subbasin, the temperatures are projected to increase in all climate projections in the 21st century. Except for MIROC5_RCP4.5, all climate projections have a significant p-value. In the other future period segments, however, none of the trends are statistically significant. In the near century, all MIROC5 projections show a decreasing trend while all other projections have an increasing trend. In the mid-century, the only projection with a decreasing trend is MIROC5_RCP8.5. Lastly, in the far century, MIROC5_RCP4.5 and the ensemble of RCP 4.5 scenarios have a decreasing trend. The mean values of the all projections are always above the mean of the historical period. The range of the increase is between 0.20˚C and 4.78˚C which are projected by CCSM4_RCP8.5 in the near century and by MIROC5_RCP8.5 in the far century, respectively.

In the Kirmir subbasin, the temperatures show an increasing trend throughout the 21st century. All of the climate projections except MIROC5_RCP4.5 have a trend

line with a statistically significant p-value. In the near, mid-, and far century, none of the projections has a statistically meaningful trend. In the near and mid-century, one of the projections, i.e., MIROC5_RCP8.5, have a decreasing trend. In the far century, CCSM4_RCP4.5, MIROC5_RCP4.5, and the ensemble of RCP 4.5 scenarios show a decreasing trend. The change in the average annual temperatures compared to the historical period ranges between -0.26˚C and 4.33˚C. The only decrease in the mean values is projected by MIROC5_RCP8.5 in the near century. The largest increase, on the other hand, also belongs MIROC5_RCP8.5 but it is projected in the far century.

In the Middle Sakarya subbasin, all of the climate projections point to increasing temperatures in the 21st century. Furthermore, all of them except MIROC5_RCP4.5 have a statistically significant upward trend. In the near century, MIROC5_RCP8.5 and the ensemble average of RCP 8.5 scenarios have downward trends. However, none of the trends are statistically important in this period. In the mid-century, there is only one projection with a significant p-value which is CCSM4_RCP8.5. All of the projections except MIROC5_RCP8.5 have an upward trend. Finally, similar to mid-century, there is no statistically significant trend in the far century. Three of the projections, i.e., CCSM4_RCP4.5, MIROC5_RCP4.5 and the ensemble of RCP 4.5 scenarios, have a downward trend. The mean values of the climate projections are always higher than the mean of the historical temperatures. The change in the mean values range between 0.22˚C and 4.89˚C. The lowest change belongs to CCSM4_RCP4.5 in the near century while the highest is in MIROC5_RCP8.5 in the far century.

In the Göksu subbasin, all climate projections show an upward trend in temperature with statistically significant p-values in the 21st century. Other 11-year future period segments, however, do not have a statistically meaningful upward or downward trend. In the near century, MIROC5_RCP8.5 and the ensemble average of RCP 8.5

scenarios show a decreasing trend. In the mid-century, the only projection having a downward trend is MIROC5_RCP8.5. In the far century, the number of projections with a downward trend is higher as compared to the ones with an upward trend. Although there are projections with a downward trend, the mean values of these projections are always higher than the mean of the historical precipitation. The change ranges between 0.09˚C and 4.86˚C. The smallest and the largest increases belong to CCSM4_RCP4.5 in the near century and MIROC5_RCP8.5 in the far century, respectively.

In the Lower Sakarya subbasin, the basin-average temperature has an increasing trend in the 21st century. All of the trends except MIROC5_RCP4.5 are statistically significant. In the near, mid-, and far century, there is no statistically significant trend. In the near century, almost all of the projections except CCSM4_RCP4.5 and the ensemble average of RCP 4.5 scenarios have a decreasing trend. In the mid-century, however, MIROC5_RCP8.5 is the only projection with a downward trend. In the far century, CCSM4_RCP8.5, MIROC5_RCP8.5 and the ensemble of RCP 8.5 scenarios have an increasing trend. Even though, there are number of projections with a downward trend, the mean values of the projections in any segment of the future period are higher as compared to the historical period. The range of variation in basin-average temperatures is between 0.04˚C and 4.72˚C. As in almost all subbasins, the lowest change increase in the temperature is projected to be in CCSM4_RCP4.5 in the near century while the highest is in MIROC5_RCP8.5 in the far century.

The results show that the temperatures are increasing in all subbasins with significant p-values in most of the time in the 21st century. In the near, mid-, and far century, although the trends are either downward or upward depending on the GCM and the RCP involved, the average of the basin-scale temperatures for all time periods are always higher than the mean of the temperatures in the historical period. The only

exception to that is Kirmir subbasin where the mean of the MIROC5_RCP8.5 projection in the near century is lower compared to the historical mean. Moreover, it is understood that the estimated increases in temperatures in RCP 8.5 scenarios are higher than in RCP 4.5 scenarios. This is most probably due to the fact that RCP 8.5 is a scenario of comparatively high greenhouse gas emissions while RCP 4.5 is an intermediate stabilization emission scenario. In addition, the lowest and highest increases in the temperatures in all subbasins are always projected by CCSM4_RCP4.5 and MIROC5_RCP8.5, respectively.

6.4.3 Wind and Relative Humidity Data

Wind Speed (m/s)

Like precipitation and temperature, future period wind data were also obtained from the WRF model outputs. For this purpose, the WRF model outputs U10 (m/s), i.e., wind speed in the x direction at 10 m above the surface, and V10 (m/s), i.e., wind speed in the y direction at 10 m above the surface, were used. To obtain the wind speed the Pythagorean Theorem was used (Equation 6.3):

$$Wind\ Speed\ (m/s) = sqrt(u^2 + v^2) \qquad 6.3$$

Basin average wind speed data were not investigated separately for each subbasin in Sakarya Basin unlike precipitation and temperature data. It is assumed that the Sakarya Basin average wind values will be valid in each subbasin. The summary statistics for the future wind speed data is given in Table 6-12. Monthly values for all four climate projection realizations, the ensemble averages of RCP 4.5 scenarios,

the ensemble averages of RCP 8.5 scenarios, and the ensemble averages of all realizations of the wind speed are provided in Figure 6-7.

Table 6-12. Statistical results of the wind speed for the historical period and the future period based on monthly average wind speed time series.

	Average Wind Speed (m/s)				Change Compared to the Historical Period (m/s)
	Min	**Max**	**Stdev**	**Average**	
Historical Precipitation (Sept. 2009 - Sept. 2018)	1.54	3.0	0.3	2.2	-
21st Century (2020 - 2100)					
CCSM4_RCP4.5	1.32	3.5	0.4	2.2	-0.01
CCSM4_RCP8.5	0.89	4.7	0.7	2.0	-0.18
MIROC5_RCP4.5	0.92	5.0	0.7	2.0	-0.13
MIROC5_RCP8.5	0.99	3.8	0.5	2.0	-0.15
Ensemble Average of RCP 4.5 Scenarios	1.24	3.6	0.4	3.6	1.48
Ensemble Average of RCP 8.5 Scenarios	1.08	3.5	0.4	2.0	-0.17

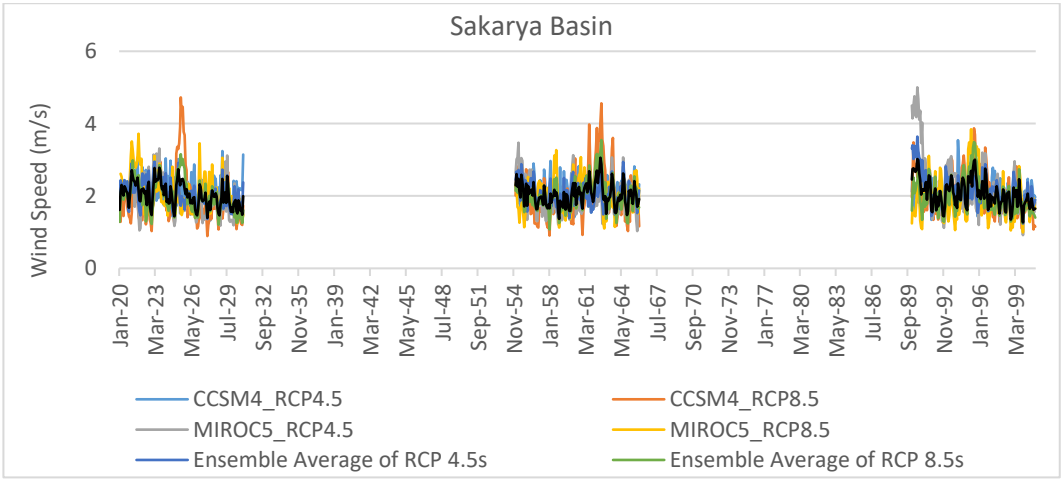

Figure 6-7. Basin average wind speed over the Sakarya Basin: All four climate projection realizations, the ensemble averages of RCP 4.5 scenarios, the ensemble averages of RCP 8.5 scenarios, and the ensemble averages of all realizations

Relative Humidity (%)

Relative humidity data of each catchment in each subbasin for the future period were obtained through linear regression analysis via using the precipitation and temperature data. Thus, in the linear regression model, the dependent variable is relative humidity, and the predictors are temperature and precipitation. The linear regression model summary for each subbasin is provided in Table 6-13. Monthly values for the RCP 4.5 and RCP 8.5 ensemble average of the relative humidity are provided in Figure 6-8 and Figure 6-9, respectively.

Table 6-13. Relative humidity linear regression model summary for each catchment in each subbasin

Subbasin	**R**	**R^2**	**Std. Error of the Estimate**
Lower Sakarya	0.4	0.2	4.7
Göksu	0.7	0.5	5.9
Middle Sakarya-Doğançay	0.8	0.6	4.7
Middle Sakarya-Kayabeli	0.8	0.7	6.9
Ankara	0.9	0.8	5.7
Kirmir	0.9	0.9	5.5
Upper Sakarya-Aktaş	0.9	0.7	7.6
Upper Sakarya-Aydınlı	0.9	0.8	5.2
Upper Sakarya-Ayvalı	0.9	0.8	5.3
Upper Sakarya-Çıkış	0.9	0.9	5.3
Porsuk-Eşenkara	0.8	0.7	5.2
Porsuk-Kıranharmanı	0.7	0.6	7.0

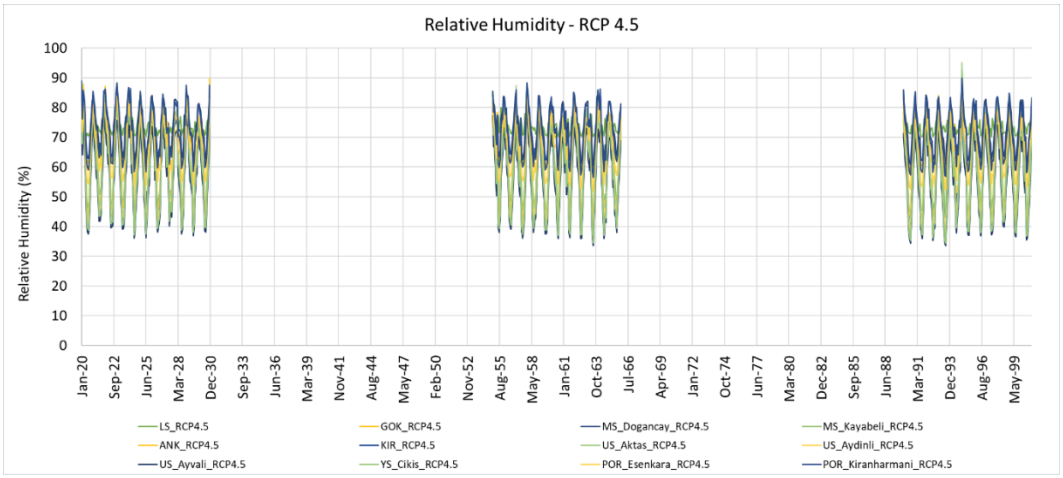

Figure 6-8. Relative humidity: Ensemble average of CCSM4 and MIROC5 GCMs based on RCP 4.5 for each catchment in each subbasin

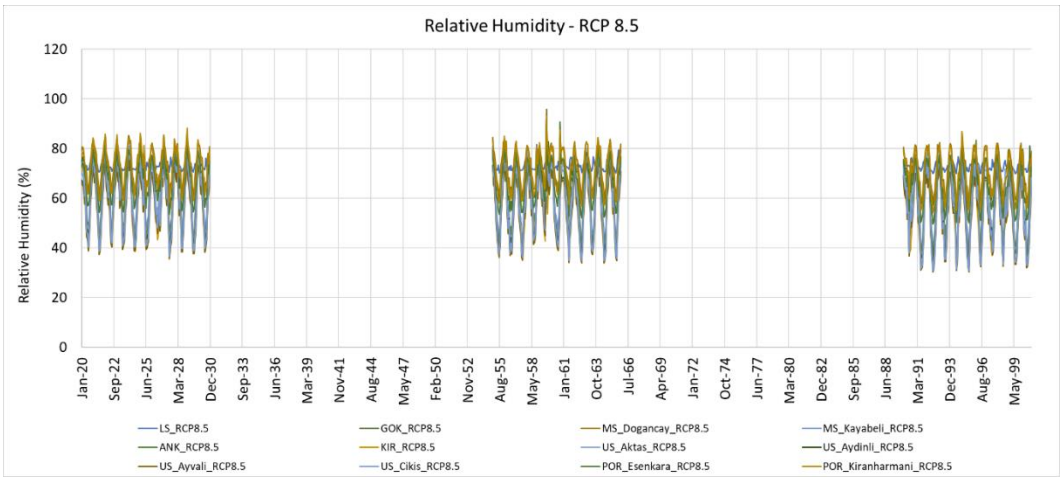

Figure 6-9. Relative humidity: Ensemble average of CCSM4 and MIROC5 GCMs based on RCP 8.5 for each catchment in each subbasin

CHAPTER 7

ASSESSMENT OF ENVIRONMENTAL FLOWS IN SAKARYA BASIN: ECOSYSTEM NEXUS COMPONENT

Studies show that preserving the full range of natural hydrological changes is essential for maintaining the biodiversity and integrity of river ecosystems. River management should aim to accommodate this natural flow paradigm to achieve conservation goals (Richter et al., 1997). There are many definitions of "natural streamflow" or "natural flow regime" in the literature but there is no standard. For example, Novak et al. (2015) states that a stream's natural flow regime is a function of the climate and the physical properties of its unique upstream drainage area. DFO (2013) defines a "natural flow regime" as a flow regime that is only affected by the variability in hydrological inputs and outputs (precipitation, evaporation) and natural water storage (such as groundwater) and for which the response in terms of amplitude, timing, duration and frequency of events is unaltered by human impacts.

Naturalized streamflow is a means of evaluating the degree to which human activities have altered the natural flow regime of a river or stream. Hydrological alteration refers to any change to the quantity, timing, or quality of water in a river system, which can result from human activities such as dam building, water withdrawals, and land use changes. Streamflow naturalization can serve as a benchmark for assessing the extent of hydrological alteration. This can be accomplished by comparing the current flow regime of the river with the naturalized flow regime, and identifying any discrepancies. The assessment of hydrological alteration can then be used to inform river management decisions and guide efforts to restore the ecological health of the river system. In summary, naturalized streamflow can provide a valuable

reference point for evaluating the impacts of human activities on the flow regime of a river and for assessing the effectiveness of efforts to restore the ecological health of the river system.

One of the main purposes of this thesis is to evaluate the nexus without ignoring the Ecosystem component, which is considered much less as a component of the nexus in WEF nexus studies (details in Chapter 2). The literature survey in the field of WEFE Nexus assessment concluded that the role of ecosystems does not receive enough recognition, although the integration of ecosystem services knowledge is crucial for the sustainability and security of the WEFE Nexus components. To address these shortcomings, this study aims to provide a full nexus evaluation by placing the ecosystem component at the center of the framework. Streamflow is a "master variable" that affects the ecological integrity of flowing water systems (Poff et al., 1997). Based on this fact, twelve hydrological regime indicators were selected under the Ecosystem pillar, and hydrological alteration assessment was performed in all scenarios evaluated within the scope of this study. Thus, the sustainability of the Ecosystem pillar was evaluated. The adopted methodology can be roughly divided into 3 parts: determination of naturalized flows and pre-impact condition interannual statistics, i.e., median and interquartile range, for all scenarios (Figure 7-1 - a); determination of monthly streamflow values and interannual statistics in all scenarios in post-impact conditions, i.e., median streamflow (Figure 7-1 - b); Determination of indicator values and total index of hydrological alteration by comparing pre-impact and post-impact conditions statistics in each scenario (Figure 7-1 - c). A detailed description of the methodology is given in Section 7.5.

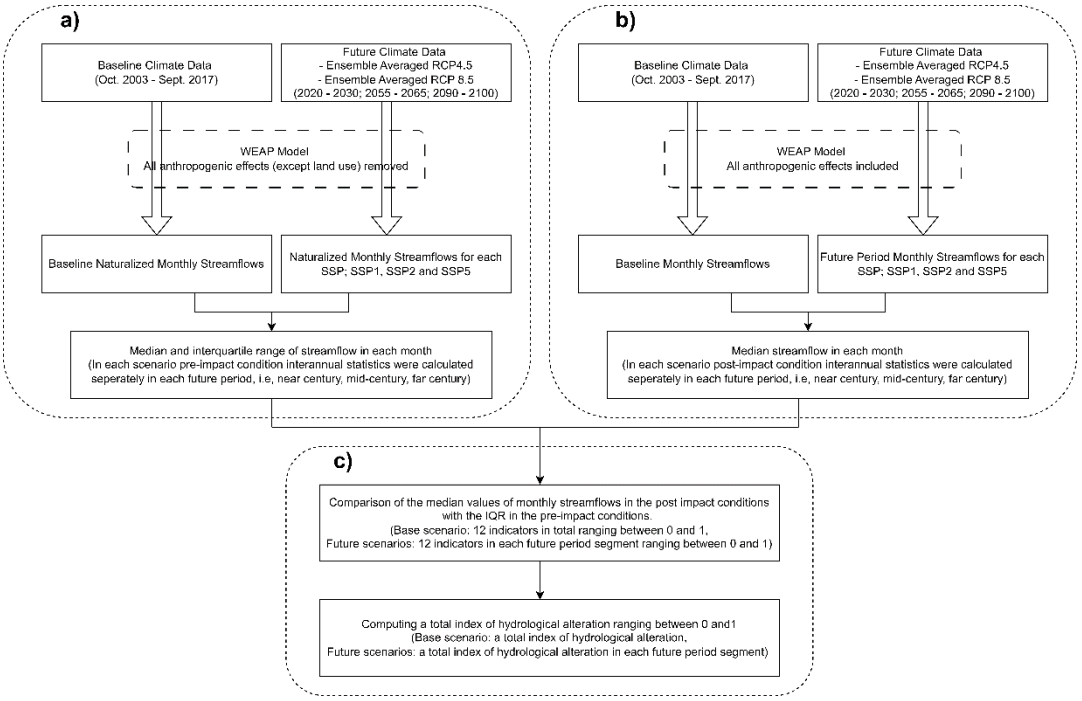

Figure 7-1. Methodology followed to assess hydrological alteration and to develop a total index revealing the status of the Ecosystem component of the WEFE Nexus

This Chapter starts with a discussion of the ecological integrity and hydrological variation relationship (Section 7.1). Then, the methodology for streamflow naturalization (Section 7.2), the streamflow naturalization results for the Sakarya Basin (Section 7.3), the description of the IHA-RVA method (Section 7.4), and lastly, the methodology to assess hydrological alteration (Section 7.5) are given.

7.1 Ecological Integrity vs Hydrological Variation

Ecological integrity refers to the completeness and functionality of an ecosystem and its ecological processes. In river ecosystems, the natural variability of the flow

regime was recognized as a key controlling variable in sustaining ecological integrity. Poff et al. (1997) state that streamflow is a "master variable" that limits the distribution and abundance of riverine species and regulates the ecological integrity of flowing water systems. There are five ecologically relevant components of the flow regime: magnitude, frequency, duration, timing, and rate of change of flows. Magnitude is the amount of water. Frequency is how often a given magnitude occurs. Duration is the period of time during which a magnitude persists. Timing refers to when a given flow occurs within different time scales, and thus it shows the predictability or regularity of the flow level. Lastly, the rate of change refers to how quickly flow levels change from one magnitude to another. All of these components of the flow regime affect the main components of ecological integrity, which are water quality, energy sources, physical habitat, and biotic interactions (Figure 7-2).

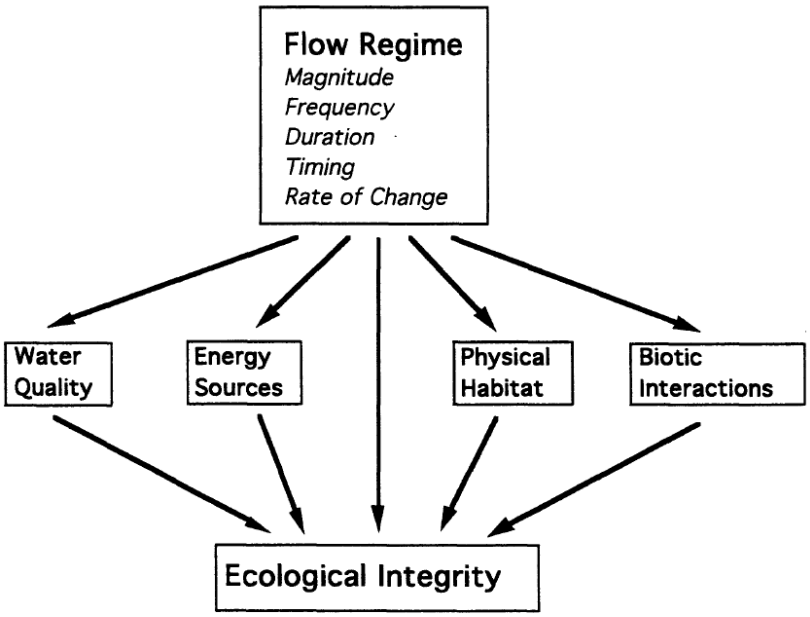

Figure 7-2. The components of the flow regime and the ecological integrity and the relationship among them (Poff et al., 1997)

Natural variability of flows provides the essential in-channel and floodplain conditions and habitats by creating and maintaining their dynamics. River biota has adaptive mechanisms to cope with habitat changes caused by natural flow variability. Furthermore, regular or seasonal changes in the flow regime are necessary for river biota to complete their life cycle (Zeiringer et al., 2018). High- and low-flow events, particularly, present critical stresses and opportunities for many different types of riverine species. Frequent moderately high flows transport sediment through channels, and they provide many ecological benefits by maintaining ecosystem productivity and diversity. Low flows, on the other hand, present recruitment opportunities for riparian plant species in regions where floodplains are frequently inundated. Temporarily dry streams have aquatic and riparian species with special behavioral or physiological adaptations that suit them to these harsh conditions (Poff et al., 1997).

Bunn and Arthington (2002) describe the influences of natural flow regime on aquatic biodiversity with four basic principles (Figure 7-3). Firstly, the relationship between the physical characteristics of the aquatic habitat and the biotic diversity is driven mainly by large events that impact channel form and shape (principle 1). Secondly, life history patterns of aquatic species are influenced by the features of the natural flow regime, such as seasonality and predictability of the overall pattern and the timing of particular flow events (principle 2). Thirdly, the maintenance of natural patterns of longitudinal and lateral connectivity is critical to the viability of populations of many riverine species (principle 3). Lastly, the invasion of exotic species is favored by the altered flow regime (principle 4).

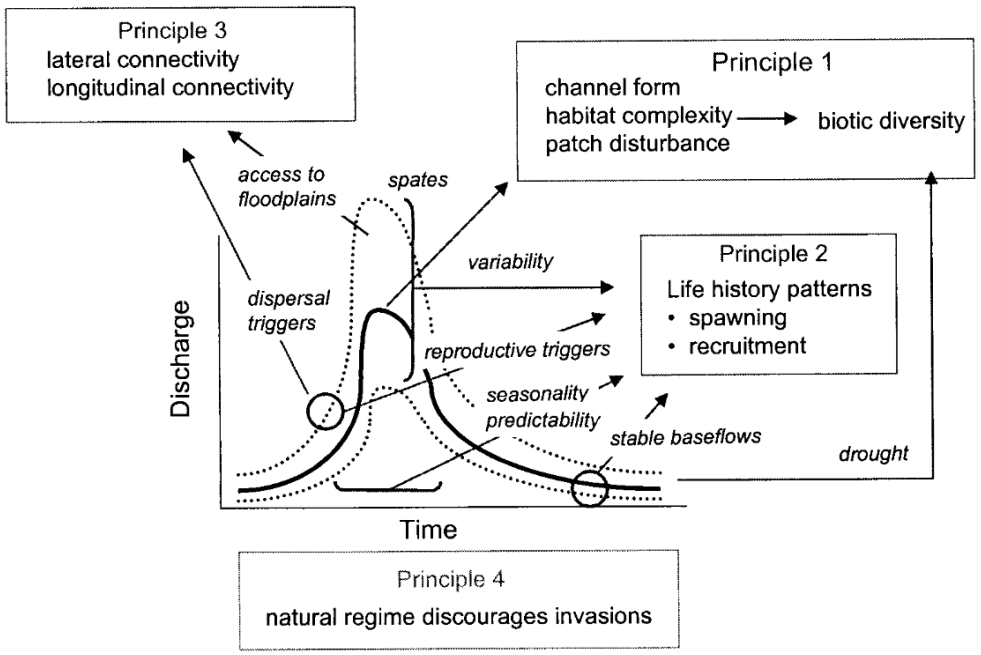

Figure 7-3. The relationship between the natural flow regime and the aquatic biodiversity (Bunn and Arthington, 2002)

Flow regime influences water quality, one of the crucial ecological integrity components, in many ways. It is well known that high flows dilute and flush contaminants. However, it is also possible that high flows transport contaminants into the river due to the washing of rainwater and runoff. Dissolved oxygen, for example, is among the most significant flow-related water quality issues. Low and slow-moving flows create conditions for low oxygen levels, while higher and more turbulent flows promote aeration. On the other hand, initial high-flow pulses may result in the resuspension of large quantities of organic matter that can cause brief but harmful hypoxic or anoxic events (Nilsson and Malm Renofalt, 2008).

As a conclusion, natural flow regime is important in sustaining river environments and aquatic ecosystems. Altered flow regimes modify the distribution and availability of riverine habitat conditions. The modified habitat conditions eventually result in adverse consequences for native biota. A natural flow regime is widely

accepted as a reference for conserving and restoring ecological integrity (Gao et al., 2012; Gao et al., 2021). The ecological state of a river and the anthropogenic influences on it can typically be evaluated by comparing the natural or naturalized flow regime and the observed streamflow (Terrier et al., 2021).

7.2 Streamflow Naturalization

Terrier et al. (2021) identified six main naturalization methods in the literature: (1) reconstitution, (2) water balance, (3) routing, (4) extension, (5) paired catchment and (6) regionalization. The differences between these methods are mainly due to the input data and the underlying models used. The decision on which method to use depends on the availability of data on influences, pre- or post-influenced period, or of regional data. Figure 7-4 shows the diagram of naturalization method selection based on the available input data.

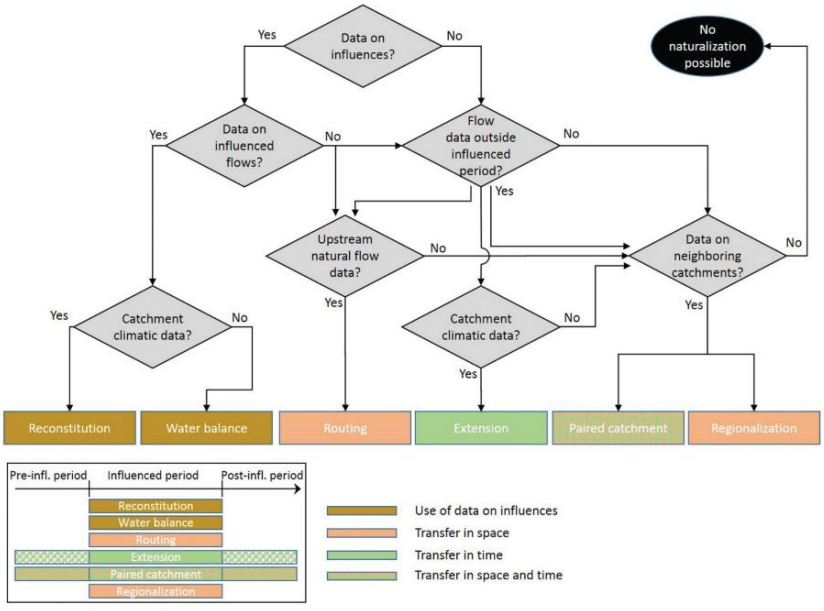

Figure 7-4. Diagram of naturalization method selection based on the available input data (Terrier et al., 2021)

Based on the availability of the input data on the influences, catchment climatic data and the calibrated hydrological model, the reconstitution method was chosen as a naturalization method in the scope of this thesis study. The reconstitution method involves usage of the influenced observed streamflow and the information available on influences during the influenced period and a hydrological model which is calibrated on the influenced period. The first step in the reconstitution method is calibrating the hydrological model on the influenced observed streamflow. The anthropogenic influences are also taken into account. Then, the naturalized streamflow is obtained by using the calibrated set of parameters and by excluding the anthropogenic effects (Figure 7-5).

The naturalized streamflow needed in many studies in the literature have been obtained by the reconstitution method (De Girolamo et al., 2015; Gosain et al., 2005; Kim et al., 2012; Maheshwari et al., 1995; Nobert, 2012; Shi et al., 2013; Yin et al., 2017; Zhang et al., 2016). These studies differ from each other in terms of the influence taken into account as input such as reservoirs and associated withdrawals, irrigation, crop model, land use/land cover, withdrawal for domestic and industrial purposes etc.

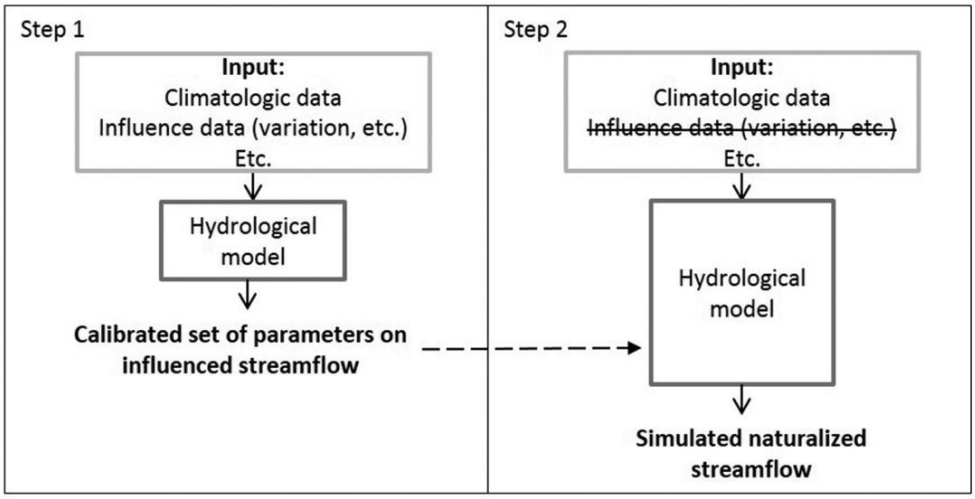

Figure 7-5. Steps of the application of the reconstitution method (Terrier et al., 2021)

7.3 Streamflow naturalization results for the Sakarya Basin

As it was explained in Section 7.2, the reconstitution method was used to naturalize the streamflow in Sakarya Basin. For this purpose, the calibrated and validated WEAP-LEAP model on the influenced period between October 2003 and September 2017 was used. All anthropogenic influences such as reservoirs and associated withdrawals, irrigational activities, withdrawals for domestic and industrial purposes, and all types of power plants were removed from the system to obtain the naturalized streamflow. The only influence not included in the scope of the study was land use and land cover changes. Then, the model was run for the baseline period, i.e., October 2003 – September 2017, and also for the future period, i.e., January 2022 – December 2030; January 2057 – December 2065; January 2092 - September 2100 in each scenario. Since the first two years at the beginning of each 10-year future period were determined as the warm-up period, those years were not

included in the evaluation (details in Chapter 8). The naturalized streamflow results were obtained at each subbasin's outlet. Figure 7-6 shows the naturalized streamflow in the model calibration period at each subbasin. There are three scenarios, i.e., RCP4.5_SSP1, RCP4.5_SSP2, and RCP 8.5_SSP5, simulated in the 21st century in the scope of this study (details in Section 8.3.7 in Chapter 8). Thus, there are three different naturalized streamflow projections in the 21st century in each subbasin. These projections are shown in Figure 7-7. In Figure 7-8, Figure 7-9, Figure 7-10, Figure 7-11, Figure 7-12, Figure 7-13, and Figure 7-14, the box and whisker plots of the naturalized streamflow in Upper Sakarya, Porsuk, Ankara, Kirmir, Middle Sakarya, Göksu, and Lower Sakarya subbasins, respectively, are given for each future period, i.e., near, mid-, and far century.

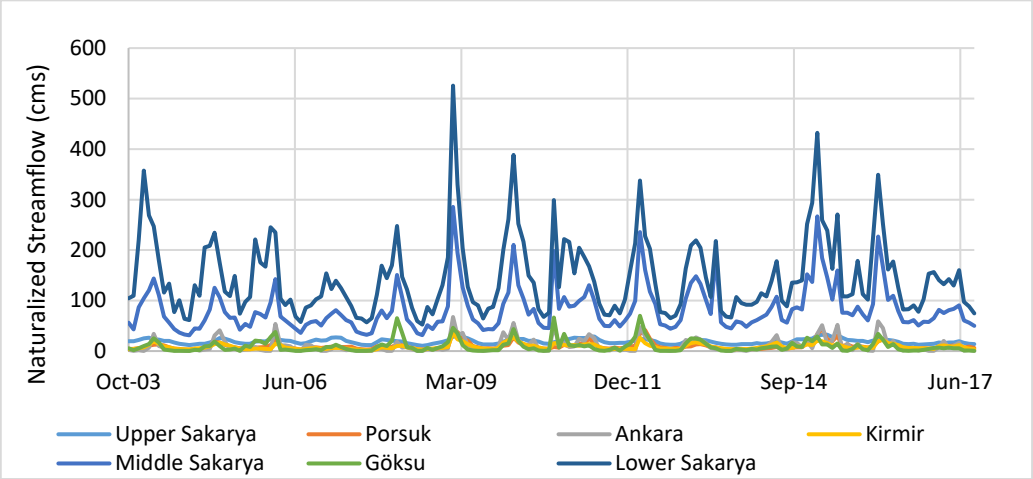

Figure 7-6. Naturalized streamflow of each subbasin in the baseline period (October 2003 – September 2017)

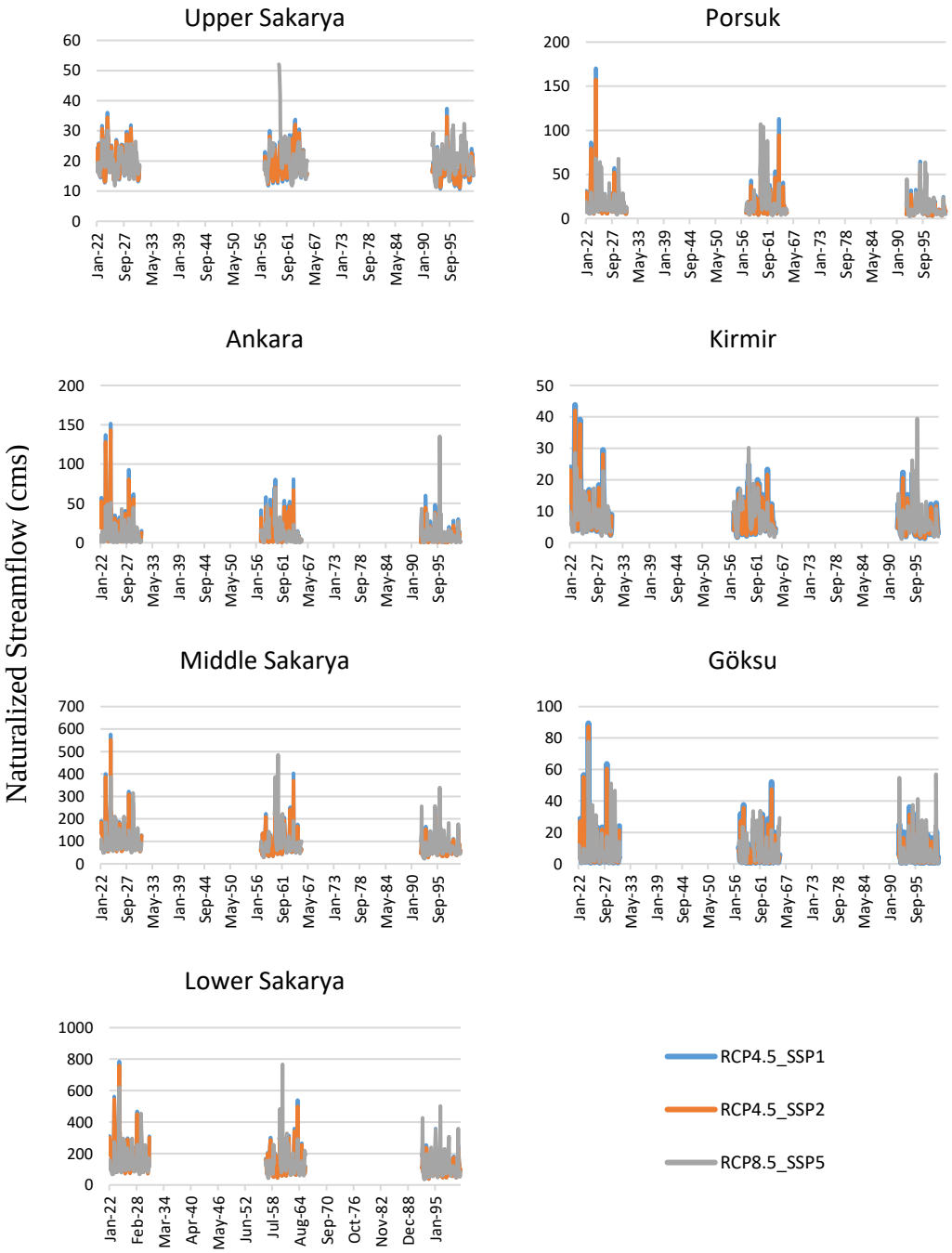

Figure 7-7. Time series of naturalized streamflow in each subbasin in each future scenario, i.e., RCP4.5_SSP1, RCP4.5_SSP2, and RCP8.5_SSP5

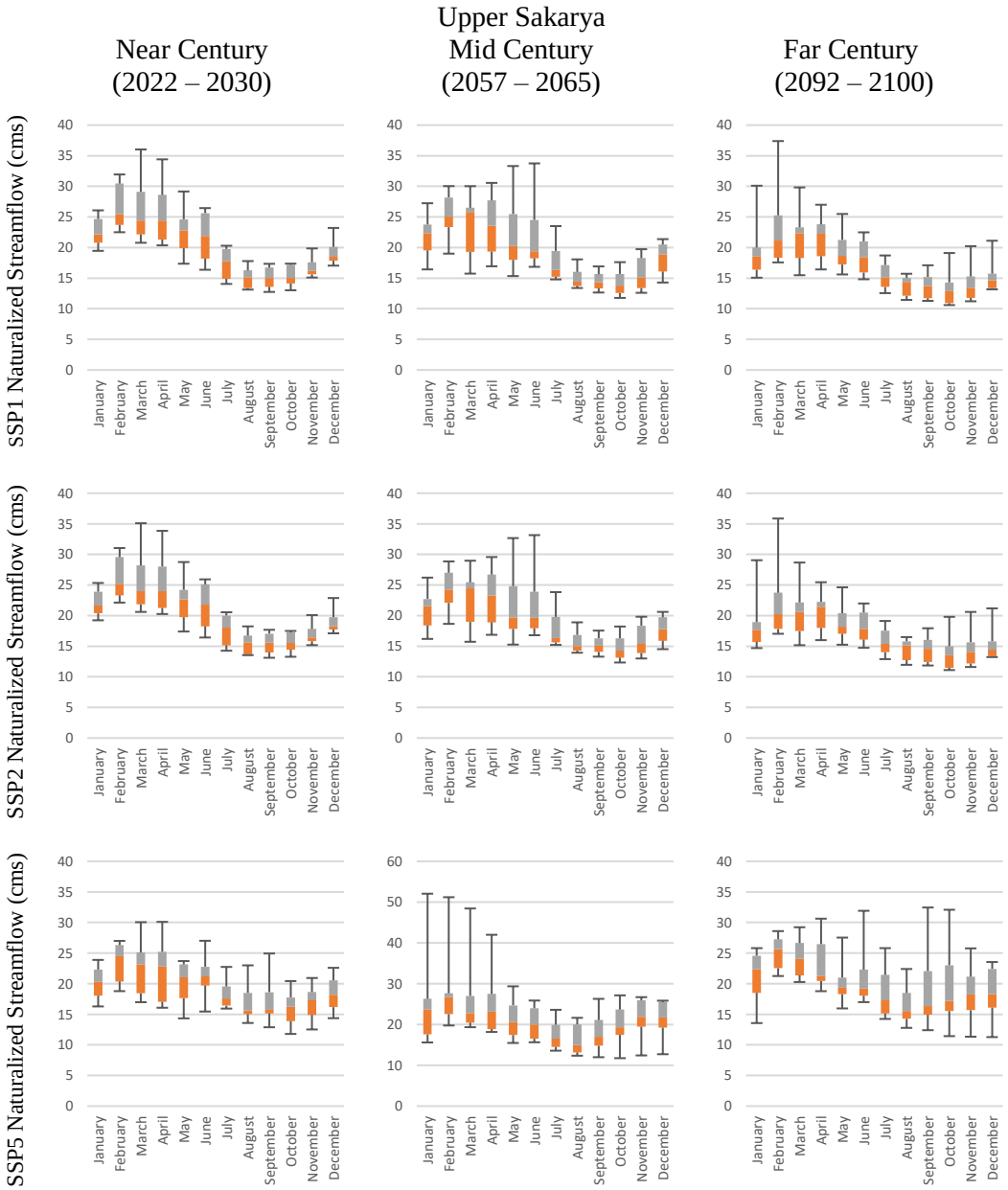

Figure 7-8. Upper Sakarya subbasin: Box and whisker plot of the naturalized streamflow results. Orange box: Lower quartile of naturalized streamflow; Grey box: Upper quartile of naturalized streamflow

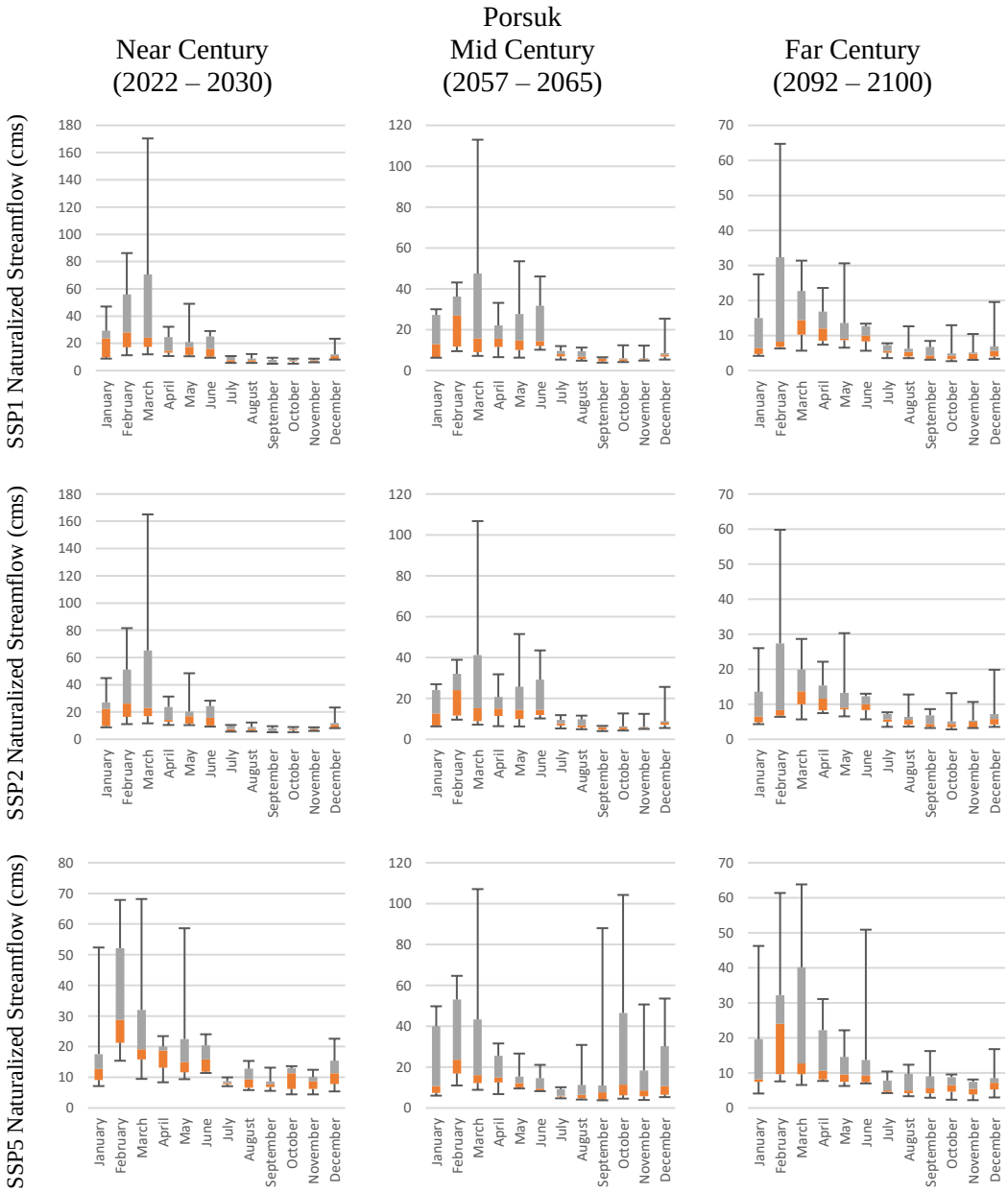

Figure 7-9. Porsuk subbasin: Box and whisker plot of the naturalized streamflow results. Orange box: Lower quartile of naturalized streamflow; Grey box: Upper quartile of naturalized streamflow

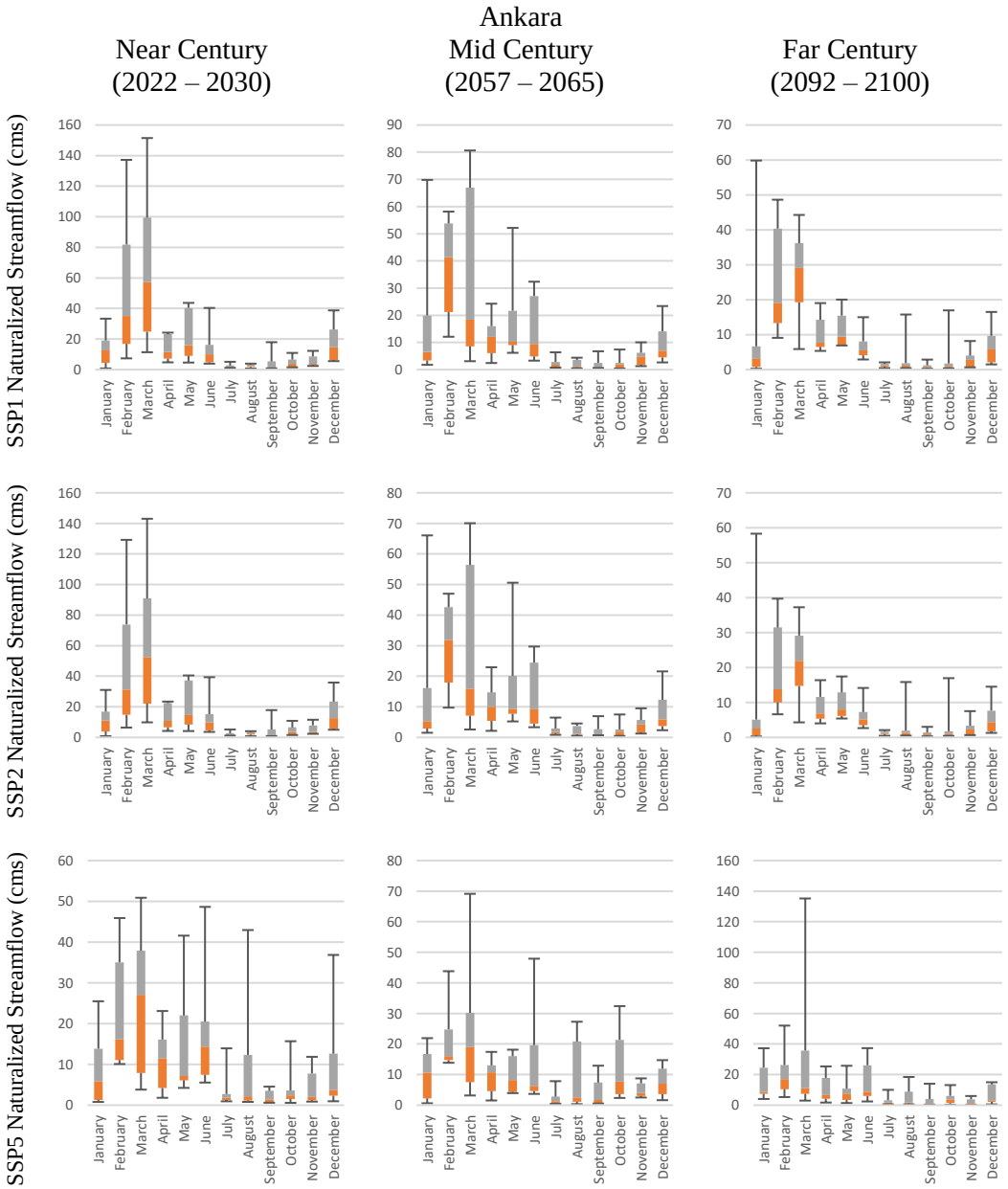

Figure 7-10. Ankara subbasin: Box and whisker plot of the naturalized streamflow results. Orange box: Lower quartile of naturalized streamflow; Grey box: Upper quartile of naturalized streamflow

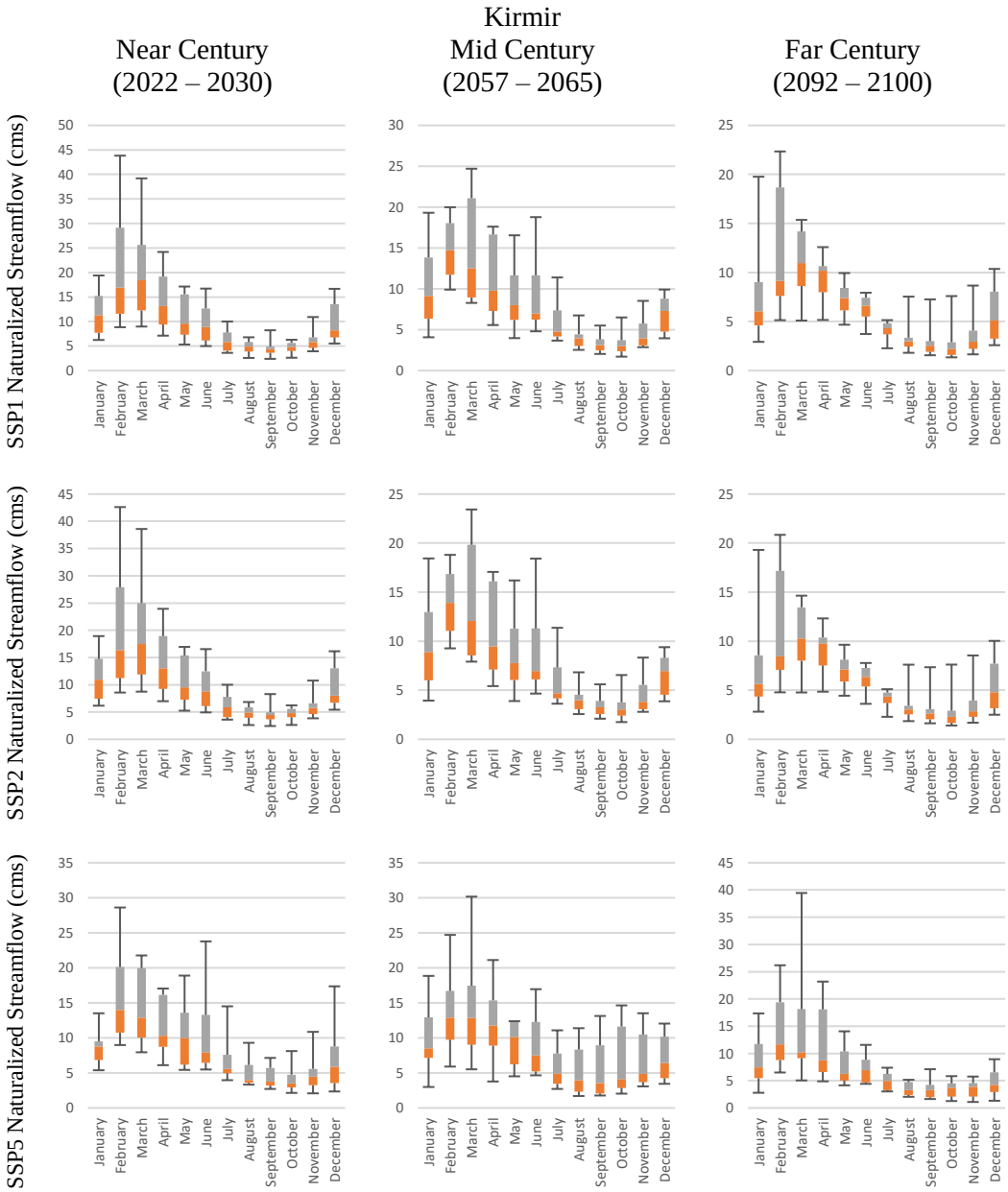

Figure 7-11. Kirmir subbasin: Box and whisker plot of the naturalized streamflow results. Orange box: Lower quartile of naturalized streamflow; Grey box: Upper quartile of naturalized streamflow

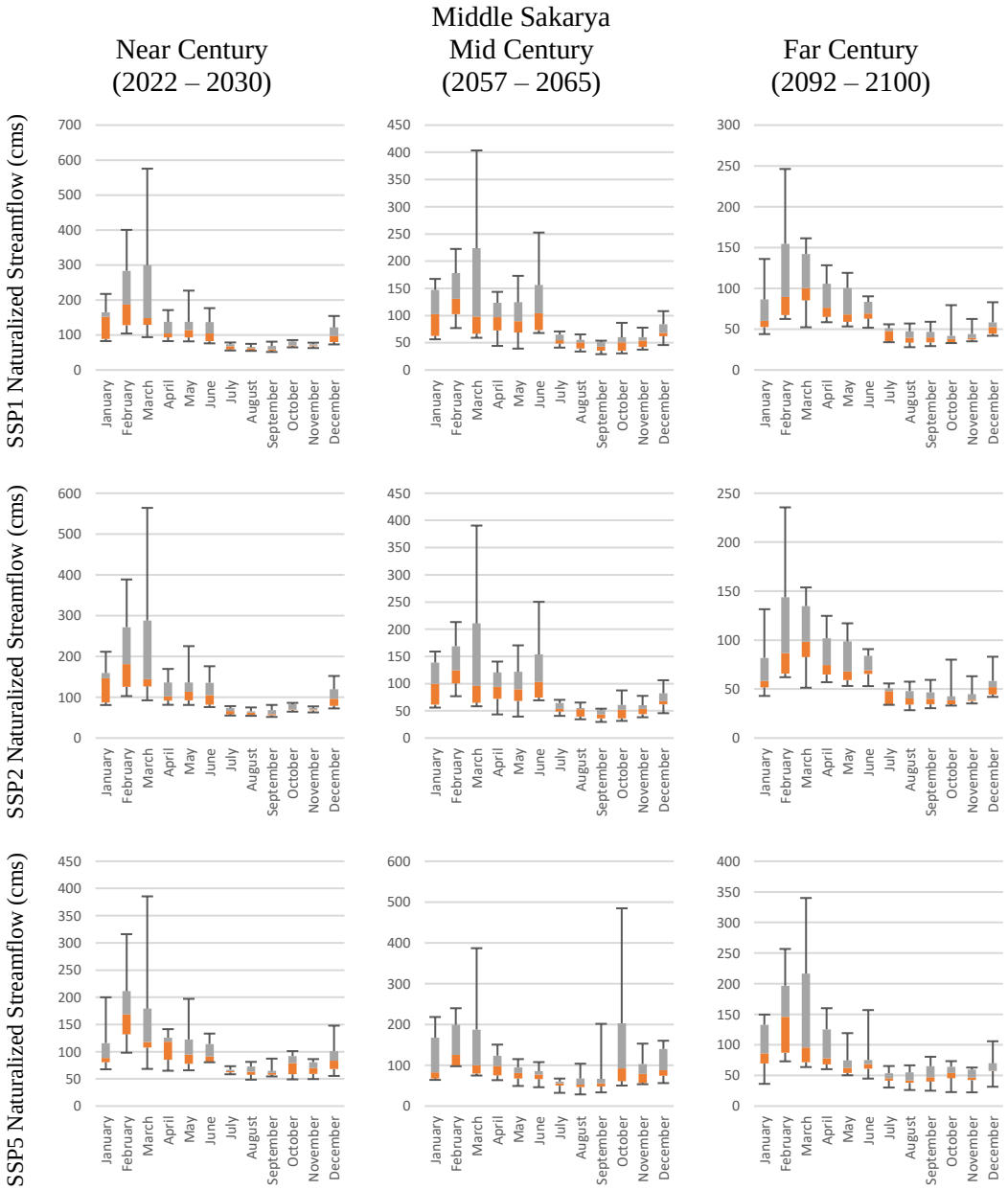

Figure 7-12. Middle Sakarya subbasin: Box and whisker plot of the naturalized streamflow results. Orange box: Lower quartile of naturalized streamflow; Grey box: Upper quartile of naturalized streamflow

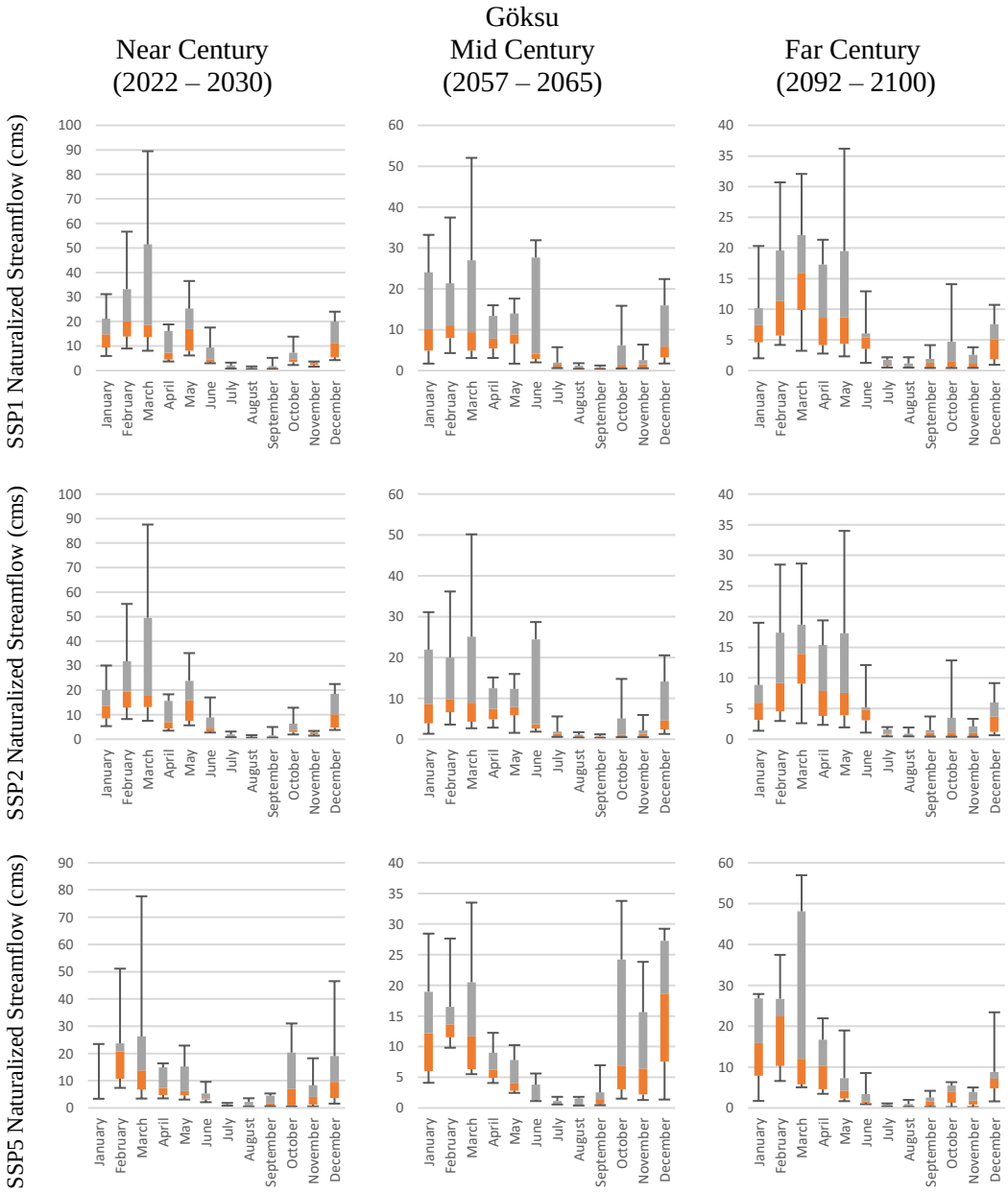

Figure 7-13. Göksu subbasin: Box and whisker plot of the naturalized streamflow results. Orange box: Lower quartile of naturalized streamflow; Grey box: Upper quartile of naturalized streamflow

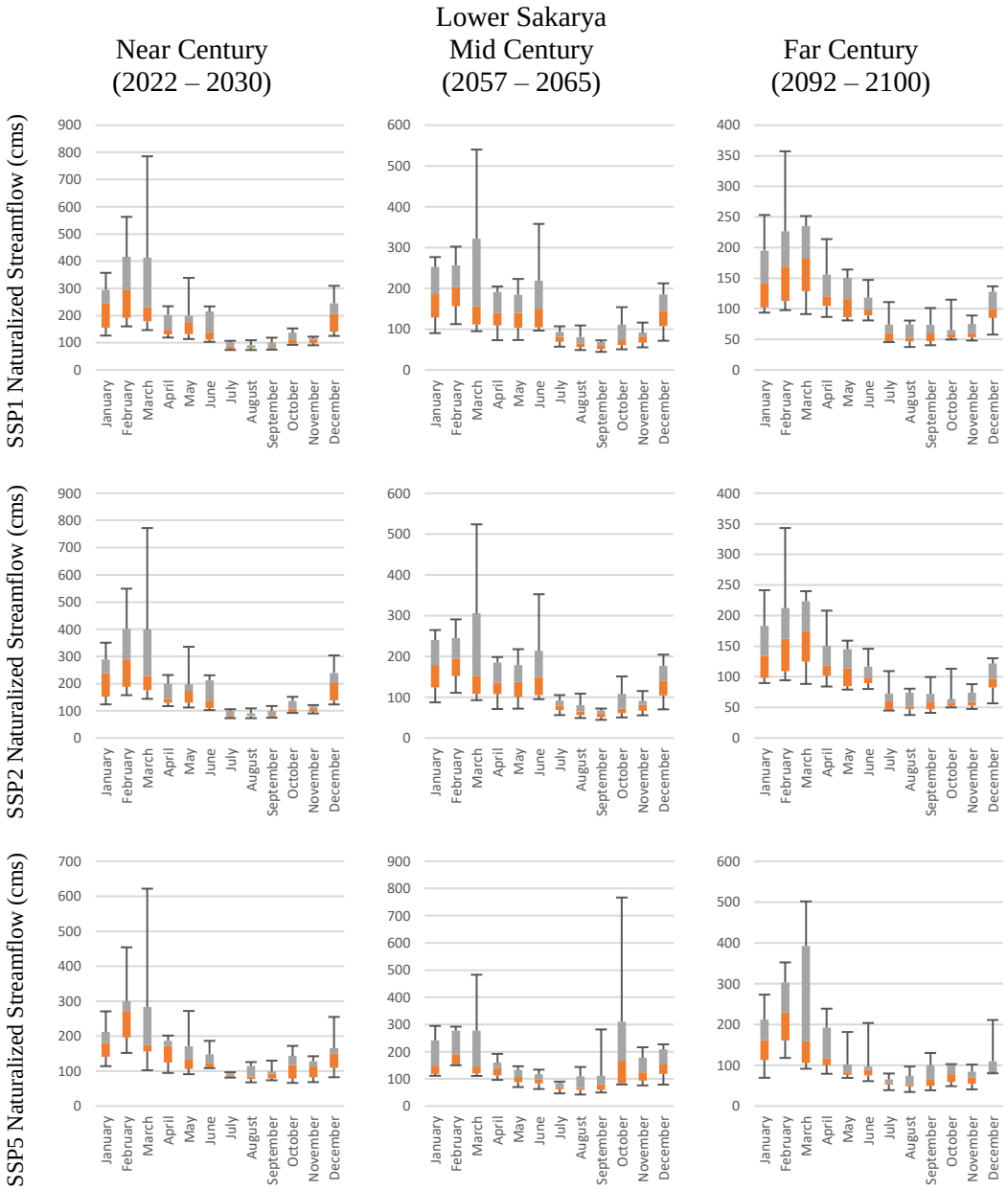

Figure 7-14. Lower Sakarya subbasin: Box and whisker plot of the naturalized streamflow results. Orange box: Lower quartile of naturalized streamflow; Grey box: Upper quartile of naturalized streamflow

7.4 Indicators of Hydrological Alteration (IHA) / Range of Variability Approach (RVA)

The natural variability of the flow regime in river ecosystems is crucial for maintaining its ecological integrity. Streamflow is considered a "master variable" that impacts the distribution and abundance of riverine species (Poff et al., 1997). Several hydrological indices have been developed to analyze the flow regime, including the Indicators of Hydrological Alteration (IHA) which is part of the Range of Variability Approach (RVA) developed by Richter et al. (1996, 1997). This method is widely used in the literature (Bai et al., 2017; Gierszewski et al., 2020; Guo et al., 2022; Lu et al., 2022; Reichold et al., 2010).

The RVA for assessing hydrologic alteration involves comparing the streamflow characteristics between two defined time periods at a given stream gauge. The difference in the streamflow regime between a period of more natural or less altered conditions and a period of more altered conditions is used to measure the degree of alteration that has taken place. The RVA is used as a management tool for regulated or developed rivers. The goal of RVA is to restore or maintain the natural flow regime of a river by using the range of natural variability in 33 different ecologically relevant flow parameters to set management targets. The RVA target range for each hydrologic parameter is typically based on selected percentile levels or a multiple of the parameter standard deviations for the natural or pre-development streamflow regime. A range of variation in each of these parameters are then used as initial flow management targets (Richter et al., 1998).

IHA parameters, referred to as indicators, are grouped into five categories based on their regime characteristics (Table 7-1). The explanations of the five categories are given below:

Group 1 of IHA parameters includes 12 indicators that measure the central tendency (mean) of the daily water conditions for a specific month. The monthly mean provides an indication of the general water conditions for the month, including habitat availability and suitability. The similarity of monthly means within a year indicates relative hydrologic constancy, while inter-annual variation in the mean water condition for a specific month reflects environmental contingency.

The 10 parameters in *Group 2* measure the magnitude of extreme annual water conditions of various durations, including daily to seasonal. These durations follow natural or human-imposed cycles and include 1-day, 3-day, 7-day (weekly), 30-day (monthly), and 90-day (seasonal) extremes. The magnitude of high and low water extremes provides measures of environmental stress and disturbance, which may be necessary for certain species' reproduction. The variation in the magnitude of these extremes provides an expression of contingency.

Group 3 includes two parameters, one measuring the Julian date of the 1-day annual minimum water condition and the other measuring the Julian date of the 1-day maximum water condition. The parameters provide information on the timing of the highest and lowest water conditions within the annual cycle, which serves as another measure of environmental disturbance or stress by describing the seasonal nature of these stresses. Changes in timing caused by human activities may result in reproductive failure, stress, or mortality. The inter-annual variation in the timing of extreme events reflects environmental contingency.

Group 4 of the IHA method includes four parameters, two of which measure the number of times per year that the water condition exceeds an upper threshold or falls below a lower threshold and two that measure the average duration of these high and low water conditions. These parameters describe the pulsing behavior of water variation within a year and provide a measure of the shape of these water conditions. The IHA method defines water pulses as periods within a year in which the daily

average water condition rises above the 75th percentile (high pulse) or falls below the 25th percentile (low pulse) of all daily values for the pre-impact time period.

The four parameters in *Group 5* measure the number and average rate of changes in water conditions from one day to the next, both positive and negative. These parameters describe the rate and frequency of intra-annual cycles of environmental variation and provide a measure of the rate and frequency of intra-annual environmental change (Richter et al., 1996).

Table 7-1. Hydrologic parameters used in the IHA method and their characteristics (Richter et al., 1996)

IHA Statistics Group	**Regime Characteristics**	**Hydrologic Parameters**
Group 1: Magnitude of monthly water conditions	Magnitude Timing	1-12. Mean or median value for each calendar month
Group 2: Magnitude and duration of annual extreme water conditions	Magnitude Duration	13. Annual minima 1-day mean 14. Annual maxima 1-day mean 15. Annual minima 3-day means 16. Annual maxima 3-day means 17. Annual minima 7-day means 18. Annual maxima 7-day means 19. Annual minima 30-day means 20. Annual maxima 30-day means 21. Annual minima 90-day means 22. Annual maxima 90-day means 23. Number of zero-flow days 24. Base flow index: 7-day minimum flow/mean flow for year
Group 3: Timing of annual extreme water conditions	Timing	25. Julian date of each annual 1-day maximum 26. Julian date of each annual 1-day minimum
Group 4: Frequency and duration of high and low pulses	Magnitude Frequency Duration	27. Number of high pulses within each water year 28. Number of low pulses within each water year 29. Mean or median duration of high pulses (days) 30. Mean or median duration of low pulses (days)
Group 5: Rate and frequency of water condition changes	Frequency Rate of change	31. Rise rates: Mean or median of all positive differences between consecutive daily values 32. Fall rates: Mean or median of all negative differences between consecutive daily values 33. Number of hydrologic reversals

The goal of IHA method is to determine whether the state of the perturbed system has changed significantly from what it would have been without the perturbation, particularly by testing whether the central tendency or inter-annual variation of an attribute has been altered. To provide the consistency in IHA studies, the cause of the impact being evaluated should be clearly identified and pre- and post-impact time periods should be defined. The results of the IHA method should be presented in terms of the magnitude of differences between pre- and post-impact periods along with confidence limits, instead of p values for the null hypotheses. Hypothesis testing may be valuable if biologically relevant thresholds can be identified, in which case an equivalence test can be used to test the null hypothesis that the observed difference is greater than a biologically significant value (Richter et al., 1996)

The RVA is a process for managing a river or river reach that has 6 steps (Richter et al., 1997):

Step 1 characterizes the natural range of streamflow variation using the Indicators of Hydrologic Alteration (IHA) method.

Step 2 selects management targets based on the IHA parameters, aiming to have the annual value of each IHA parameter fall within the range of natural variation.

Step 3 designs management rules to attain the targeted flow conditions.

Step 4 implements the management system and assesses its ecological effects through monitoring and research.

Step 5 compares actual streamflow variation to the RVA target values.

Step 6 revises the management system or RVA targets based on the results of previous years and new information.

7.5 Methodology to Assess Hydrological Alteration

Hydrological alteration assessment was carried out in the river segments, which are the outlets of the Sakarya Basin subbasins. Thus, there are total of seven river segments where the IHA assessment were performed. The method for evaluating potential changes in the hydrological regime is similar to the IHA-RVA method and involves a five-step procedure:

1) *Defining data series for pre-impact and post-impact conditions:*

   The hydrological assessment methodology followed in this study is based on a combination of hydrological-water allocation model, i.e., WEAP, and the assessment and comparison of set of IHA parameters under the pre-impact and post-impact conditions in the baseline and future periods. In this study, pre-impact conditions represent hydrological conditions obtained by subtracting all anthropogenic effects (except land use changes) from the hydrological model. Thus, each of the scenarios simulated in the study, i.e., baseline, SSP1, SSP2 and SSP5 (details in Section 8.3.7), has its own pre-impact hydrological conditions. Post-impact conditions, on the other hand, refer to the hydrological condition obtained when anthropogenic effects are included in all the scenarios mentioned. In many studies, the natural and altered regimes are defined based on the presence of infrastructure such as reservoirs. However, in the present study, the natural regime is simulated using a hydrological model and the altered regimes for different management scenarios are produced using a water allocation model. Another point that distinguishes this study from most studies in the literature is the use of monthly data in the present study.

2) *Calculating annual values of hydrological attributes for each year of the natural and post-impact conditions:*

Monthly mean streamflow values were calculated for each year in both natural and post-impact conditions.

3) *Computing interannual statistics (measures of central tendency and dispersion) for the hydrological attributes of the two periods,*

In this study, the extent of hydrological alteration in water systems is determined by analyzing the interannual statistical data between the natural and altered flow regimes. Data between the following dates were used to calculate interannual statistics: Baseline period October 2003 - September 2017; Near century January 2022 - December 2030; Mid-century January 2057 - December 2065; Far century January 2092 - December 2100. The indicators used in this work are the Group 1 parameters, i.e., magnitude of monthly water conditions, of the IHA method. Because of the nature of the data available, it's not feasible to use all the original parameters of the IHA method and it's necessary to use those that can be adapted to a monthly scale. Thus, the 12 indicators of Group 1 were adopted as indicators. The ecosystem influences of Group 1 IHA parameters include impacts on habitat availability for aquatic organisms, soil moisture availability for plants, water availability for terrestrial animals, food and cover for fur-bearing mammals, reliability of water supplies, access by predators to nesting sites, and water temperature, oxygen levels, and photosynthesis in the water column (Richter et al., 1998).

4) *Measuring the difference between the interannual statistics of the post-impact periods and a target range based on the natural period's interannual statistics (Figure 7-15)*

The natural and altered regimes were obtained in each of the seven outlets of the Sakarya Basin subbasins. IHA parameters can be calculated using parametric (mean/standard deviation) or nonparametric (percentile) statistics. In this study, non-parametric statistics were preferred. That is, the initial flow management targets were based on the median and the interquartile range (IQR) of the natural

flow conditions (pre-impact conditions), and the interannual statistics were obtained by calculating the median of the streamflow in each calendar month, i.e., MMS, under the related post-impact condition. The reason why median and IQR were chosen is because most of the time hydrologic datasets do not have a normal distribution which is the key assumption of parametric statistics. Moreover, they are less sensitive to outliers compared to mean ±1 standard deviation (Laize et al., 2014).

By comparing the median values of the indicators in the post-impact condition with the IQR in the pre-impact condition, the indicators adopt values ranging from 0 to 1 (see also Chapter 9 Section 9.2). Figure 7-15 shows schematically how the hydrological indicators take values ranging from 0 to 1. While the value of 1 refers to an unaltered or sustainable state, the value of zero refers to total alteration or unsustainable state. The indicator takes the value of one if MMS value is within the IQR. The indicator ranges between 0 and 1 according to a continuous linear function if MMS value is between Q_{min} and Q_{25} or Q_{75} and Q_{max}. The indicator is zero if MMS value is either less than or equal to Q_{min}; or greater than or equal to Q_{max}. Here Q_{min} and Q_{max} refer to the minimum and maximum streamflow rates occur under the pre-impact conditions.

5) *Computing a total index of hydrological alteration to summarize the information from the different indices.*

Finally, a total hydrological alteration indicator is calculated for each river segment by averaging the values of twelve indicators. This aggregated indicator is accepted as the indicator showing the status of the Ecosystem component of the WEFE Nexus. The results can be found in Chapter 9 Section 9.4.

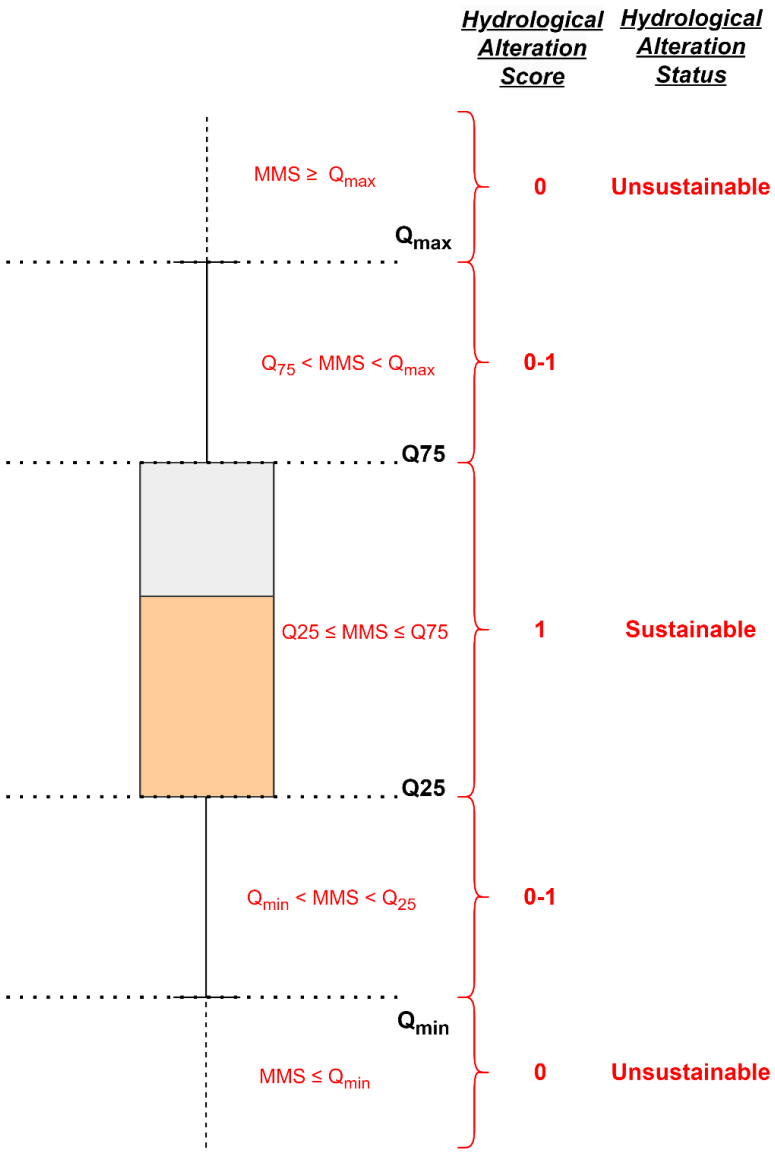

Figure 7-15. Schematic representation of indicators hydrological alteration score and status assessments

CHAPTER 8

BUILDING WEAP-LEAP MODEL FOR THE 21st CENTURY

This thesis aims to develop a methodology that enables the assessment of the sustainability of and the security provision for the WEFE Nexus components through the derivation of the indicators, which in turn will be aggregated into a WEFE Nexus index. In this context, the external factors affecting the WEFE Nexus were determined as the future climate conditions and the socio-economic parameters, i.e., population growth, economic development, and technological change (Figure 3-2). The period in which the effects of climate change and socioeconomic factors on WEFE Nexus is evaluated has been determined as a period of 33 years between 2020 – 2100, i.e., 2020 – 2030 (near 21st century); 2055 – 2065 (mid-21st century); 2090 – 2100 (far 21st century). The first two years of each future period segment were designated as the warm-up period. For this reason, the evaluations were made between 2022-2030 in the near century, 2057-2065 in the mid-century, and 2092-2100 in the far century.

In this chapter, the explanation begins with the determination of the warm-up period. The subsequent section describes the process of creating climate change scenarios in the WEAP-LEAP model. Finally, the method employed to incorporate socio-economic changes into the model is discussed.

8.1 Determination of Warm-up Period

Within the scope of this study, the future period covers the years between 2020 and 2100. However, as stated previously, the climate data available during this period is

not continuous. The available data are in 10-year periods as near century (2020 - 2030), mid-century (2055 - 2065), and late century (2090 - 2100). Therefore, for example, at the beginning of the 2055-2065 period, the dam volumes will be zeroed, the plant water needs will increase and the surface flow values will decrease in the period from 2030 to 2055. In order to evaluate what kind of problems this situation will cause; the initial storage values of the dams were reset at the calibration period (2004 – 2017). Then, the evolution of the dam volumes and the streamflow values at the flow observation stations located close to the dam were evaluated. The evaluations made at several different points in the basin are provided in Figure 8-1, Figure 8-2, Figure 8-3, and Figure 8-4. As it can be seen from these figures, the dam volumes and the streamflow reach the required level in about 2 years. Consequently, it was decided that 2-year warm-up period will be used in each period when evaluating the model results. The same evaluations were also made for the future period, and it was found that the model requires 2-year warm-up period to reach the realistic state.

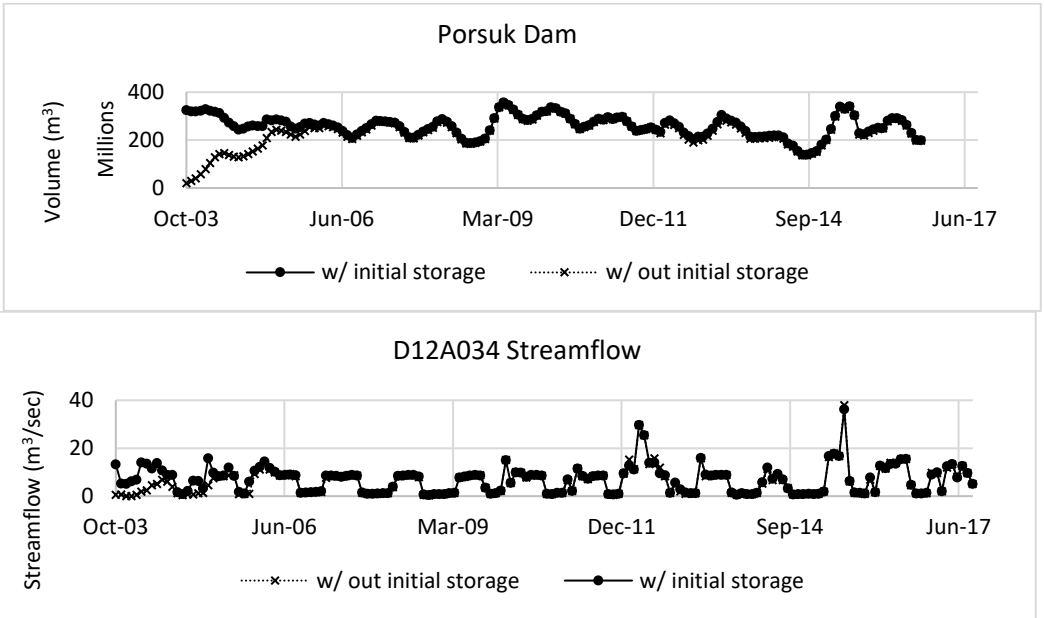

Figure 8-1. Volume of Porsuk Dam and the streamflow at D12A034 with and without initial storage

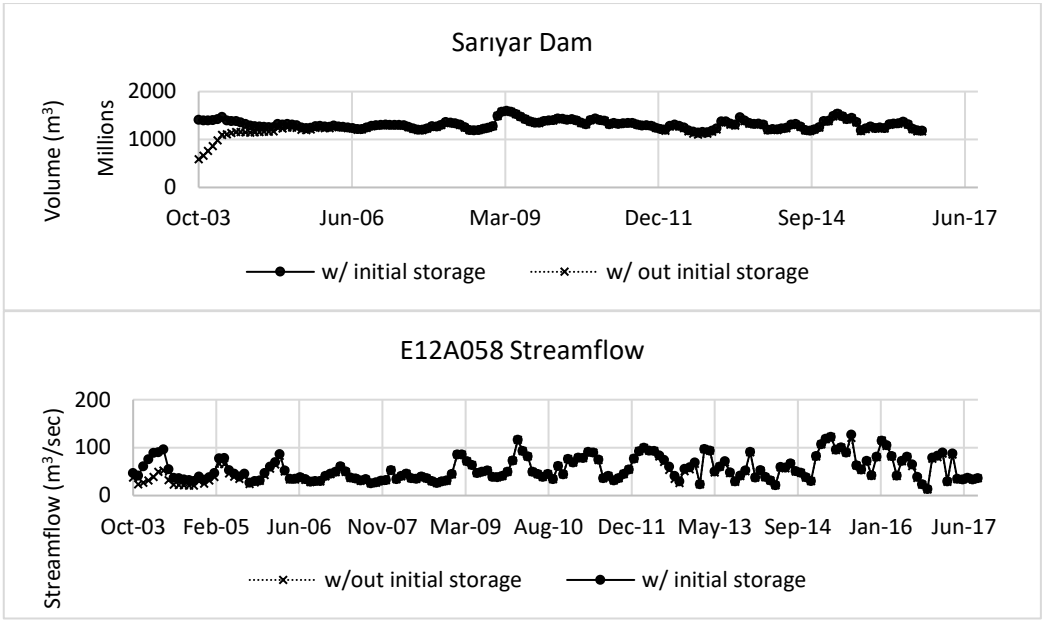

Figure 8-2. Volume of Sarıyar Dam and the streamflow at E12A058 with and without initial storage.

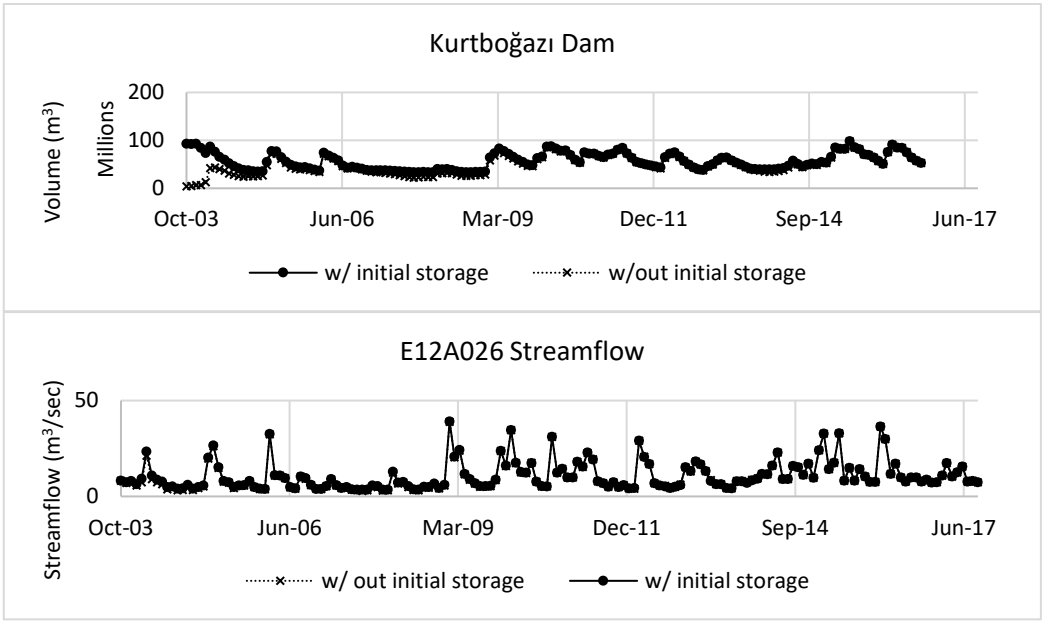

Figure 8-3. Volume of Kurtboğazı Dam and the streamflow at E12A026 with and without initial storage

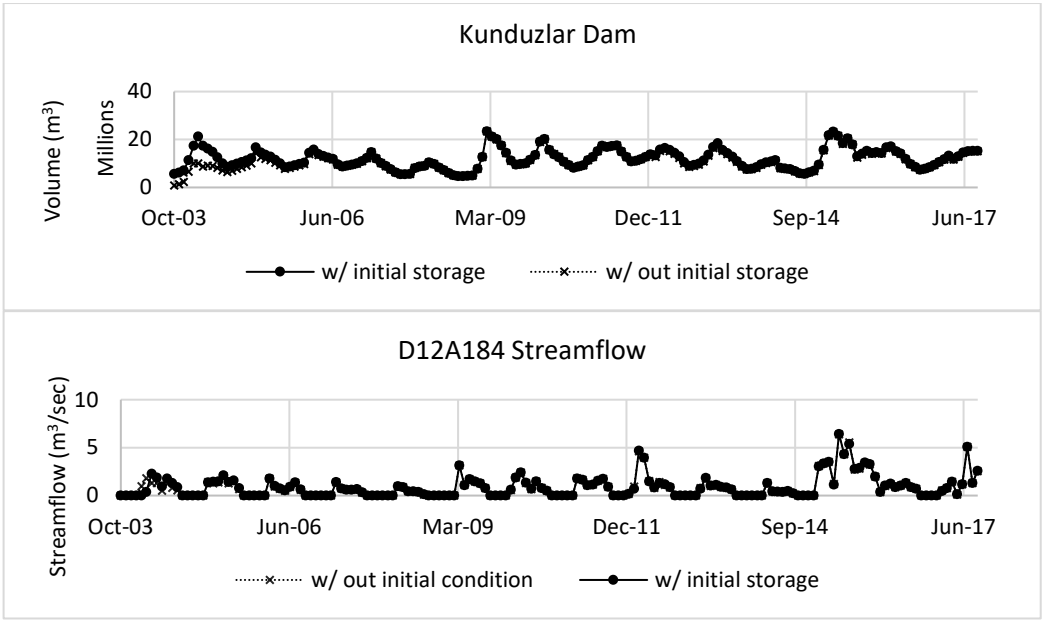

Figure 8-4. Volume of Kunduzlar Dam and the streamflow at D12A184 with and without initial storage

8.2 Introducing Climate Change Projections to the Model

As it was already explained in detail in the Chapter 6, impacts of future climate change on watershed-scale climate data were investigated over the Sakarya Basin based on future climate projections by means of a dynamical downscaling approach. For this purpose, four different future climate projection realizations from two general circulation models (GCMs: CCSM4 and MIROC5) based on two emission scenarios (RCP 4.5 and RCP 8.5) were dynamically downscaled to 18-km resolution grids over Sakarya Basin for a period of 33 years (2020 – 2030; 2055 – 2065; 2090 – 2100). Moreover, basin average climate data were investigated based on the ensemble average over future climate projection realizations for each subbasin in the Sakarya Basin. The ensemble averages were calculated for RCP 4.5 and RCP 8.5 realizations separately. Then, *the ensemble-averaged* RCP 4.5 and RCP 8.5 data

were introduced into the WEAP-LEAP model as two different climate scenarios. The ensemble-averaged precipitation, temperature, relative humidity, and wind speed data can be seen in Figure 6-5, Figure 6-6, Figure 6-7, Figure 6-8, and Figure 6-9 in Chapter 6.

8.3 Socio-Economic Scenarios (Shared Socioeconomic Pathways)

Representative Concentration Pathways (RCPs) are the greenhouse gas concentration trajectories adopted by the Intergovernmental Panel on Climate Change (IPCC). There are four pathways spanning a broad range of radiative forcing in 2100, i.e., 2.6, 4.5, 6.0, and 8.5 W/m^2. However, these pathways do not include any socioeconomic narratives which are consistent with them. Therefore, Shared Socioeconomic Pathways (SSPs) have been developed recently (O'Neill et al., 2017; Riahi et al., 2017). SSPs are alternative futures of societal development, providing a socio-economic dimension to the integrative work started by the RCPs (Rogelj et al., 2018). SSPs investigate the ways how the world might change without climate policies and to what extent climate change targets could be achieved when the mitigation targets of RCPs are combined with the SSPs. Thus, the RCPs and the SSPs are complementary to each other.

The SSPs describe alternative futures about the demographic, economic, technological, social, governance, and environmental aspects of society. They provide both qualitative descriptions (narratives) and quantification of key variables, which can be used as inputs to integrated assessment models (IAMs), large-scale impact models, and vulnerability assessments. The outcomes of SSPs are specific combinations of socioeconomic challenges to mitigation and socioeconomic challenges to adaptation (O'Neill et al., 2017). There are five different SSPs depending on the combinations of challenges to mitigation and adaptation (Figure 8-5). SSP1, a green growth paradigm, represents low challenges to mitigation and

adaptation. SSP2, a middle-of-the-road development along historical patterns, means medium challenges to mitigation and adaptation. SSP3, a regionally heterogeneous development, implies high challenges to mitigation and adaptation. SSP4, a development that results in both geographical and social inequalities, represents low challenges to mitigation, high challenges to adaptation. Lastly, SSP5, a development path that is dominated by high energy demand supplied by extensive fossil-fuel use, implies high challenges to mitigation, low challenges to adaptation. The summary of these SSPs is provided in the following subheadings.

Figure 8-5. Five shared socioeconomic pathways (SSPs) representing different combinations of challenges to mitigation and to adaptation (O'Neill et al., 2017)

8.3.1 SSP1: Sustainability – taking the green road

SSP1 describes a potential future scenario in which the world gradually shifts towards a more sustainable and inclusive path, prioritizing the preservation of

environmental boundaries and reducing environmental degradation and inequality. This shift is driven by an increasing awareness of the social, cultural, and economic costs of environmental degradation and inequality, and is facilitated by cooperation and collaboration between local, national, and international organizations and institutions, the private sector, and civil society. Investments in education and healthcare lead to a demographic transition and reduced population growth. Economic growth is increasingly balanced with human well-being, and inequality is reduced. Environmental technology and tax changes improve resource efficiency and reduce energy and resource use. Renewable energy becomes more attractive, and consumption is oriented towards low material growth and lower resource and energy intensity. The combination of environmentally-friendly technology, renewable energy, and strong global institutions results in relatively low challenges to mitigation and adaptation (O'Neill et al., 2017).

8.3.2 SSP2: Middle of the road

SSP2 describes a potential future scenario in which social, economic, and technological trends continue along historical patterns. Some countries make progress in development and income growth while others fall short. Most economies are politically stable, but global and national institutions make slow progress towards achieving sustainable development goals. Technological development continues without fundamental breakthroughs. Environmental systems experience some degradation, but resource and energy use decline. Fossil fuel dependency decreases slowly but unconventional fossil resources are still used. Global population growth is moderate and levels off in the second half of the century. Education investments are not high enough to accelerate the demographic transition in low-income countries, and income inequality persists or improves slowly, maintaining challenges to reducing vulnerability to societal and environmental changes. These moderate

development trends result in moderate challenges to mitigation and adaptation, with significant heterogeneities across and within countries. This scenario is consistent with historical patterns observed over the past century and is a dynamic pathway with changes in various elements consistent with middle-of-the-road expectations (O'Neill et al., 2017).

8.3.3 SSP3: Regional rivalry – a rocky road

The SSP3 scenario predicts a world characterized by resurgent nationalism, regional conflicts, and weak global institutions that focus on domestic or regional issues, leading to slow economic development, material-intensive consumption, and persistent inequality. Limited progress is made toward sustainability, with strong environmental degradation in some regions. Population growth is low in industrialized countries and high in developing countries. There is high difficulty in achieving international cooperation and slow technological change, implying high challenges to mitigation. The limited progress on human development, slow income growth, and lack of effective institutions implies high challenges to adaptation for many groups in all regions. This scenario is based on the assumption that current globalization trends could be reversed by regional conflict, reducing support for international institutions and development partners (O'Neill et al., 2017).

8.3.4 SSP4: Inequality – a road divided

SSP4 describes how unequal investments in human capital, economic opportunity, and political power lead to increasing inequalities and stratification both within and across countries. This leads to a widening gap between well-educated, globally-connected societies and lower-income, poorly educated societies. Economic growth is moderate in industrialized and middle-income countries, but low-income countries

struggle to provide basic services for the poor. Social cohesion deteriorates, conflict becomes common, and vulnerable groups have little representation in national and global institutions. Technology development is high in the high-tech sectors, but uncertainty in the fossil fuel markets leads to underinvestment in new resources. Environmental policies focus on local issues in middle and high-income areas. The challenges to adaptation are high for populations at low levels of development and with limited access to effective institutions for coping with economic or environmental stresses (O'Neill et al., 2017).

8.3.5 SSP5: Fossil-fueled development – taking the highway

The SSP5 scenario predicts that the world will continue to place its faith in competitive markets, innovation, and participatory societies to achieve sustainable development. Global markets will become more integrated, with efforts to remove institutional barriers and maintain competition. There will be strong investments in health, education, and institutions to enhance human and social capital. However, the reliance on fossil fuels and resource-intensive lifestyles will lead to potential global environmental impacts, with little effort to mitigate them due to a perceived tradeoff with economic progress. Global population will peak and decline in the 21st century, with increased international mobility. The SSP5 scenario also predicts accelerated globalization and rapid development of developing countries, including a significant improvement in institutions and economic participation. The emergence of a global middle class could stabilize global economic development, and the digital revolution could promote global coordination. Challenges to adaptation to climate change are relatively low for all but a few (O'Neill et al., 2017).

8.3.6 Translation of qualitative SSP narratives into quantitative projections

Riahi et al. (2017) states that the second step in developing the SSPs is the translation of qualitative SSP narratives into quantitative projections for the major socioeconomic drivers of the SSPs. These drivers are population, education (KC and Lutz, 2017), urbanization (Jiang and O'Neill, 2017), and economic development (Crespo Cuaresma, 2017; Dellink et al., 2017; Leimbach et al., 2017), and they were constructed at the country level. Then, the developments in the energy system, land use and greenhouse gas and air pollutant emissions of the SSP baseline scenarios and mitigation scenarios were elaborated via set of Integrated Assessment Models (IAMs). SSP baseline scenarios describe the future worlds that might occur due to the evolution of underlying factors like population, economic growth etc. without climate policy. The important point here is that there is only a single SSP baseline scenario (SSP5) which reaches the radiative forcing level of 8.5 W/m^2. Moreover, the lowest climate forcing value obtained among the SSP baseline scenarios (SSP1) is 5 W/m^2. That is, it is necessary to integrate climate mitigation policies in order to reach the radiative forcing levels below 5 W/m^2. Thus, the SSP mitigation scenarios were created. The quantitative estimates for population, economic growth, energy system parameters, land use, emissions, and concentrations are publicly available through the SSP web-database (IIASA, 2018). The comparison of key features of SSPs to show changes in population, economic growth, education, urbanization, and technological development is given in Table 8-1. In this table, the degree of change is represented by the number of arrows with more arrows indicating a higher degree of increase.

Table 8-1. Comparison of key features of shared socioeconomic pathways (SSPs) using arrows to show changes in population, economic growth, education, urbanization, and technological development

Shared Socioeconomic Pathways	Population	Economic Growth	Education	Urbanization	Technological Development
SSP1: Sustainability	↑ (Low)	↑↑ (Medium)	↑↑↑ (High)	↑↑↑ (High)	↑↑↑ (High)
SSP2: Middle of the Road	↑↑ (Medium)	↑↑ (Medium)	↑↑ (Medium)	↑↑ (Medium)	↑↑ (Medium)
SSP3: Regional Rivalry	↑↑↑ (High)	↑ (Low)	↑ (Low)	↑ (Low)	↑ (Low)
SSP4: Inequality	↑↑ (Medium)	↑ (Low)	↑ (Low)	↑↑↑ (High)	↑↑↑ (High)
SSP5: Fossil-fueled development	↑ (Low)	↑↑↑ (High)	↑↑↑ (High)	↑↑↑ (High)	↑↑↑ (High)

8.3.7 SSP scenarios evaluated in this study and creation of integrated climate and socio-economic scenarios

In the context of this thesis study, the socio-economic impacts on the WEFE Nexus are evaluated based on the SSPs. For this purpose, three different SSPs namely SSP1, SSP2, and SSP5 are selected. The reason why three of the SSPs are selected is to be able to comprise the uncertainties associated with the future changes in the economic and social aspects of the society. In addition, the SSPs are selected in way that they are consistent with RCP4.5 and RCP8.5 scenarios. SSP3 is not included in the analysis since it represents extreme conditions such that it is highly difficult to mitigate and adapt to climate change because of extreme poverty and a rapidly growing population (Hanasaki et al., 2013). Thus, it is thought that it is not a highly possible scenario for the study area. SSP4, on the other hand, represents a highly unequal world both within and across countries. Therefore, the conditions foreseen in this SSP are not very relevant at the catchment scale (Momblanch et al., 2018). That is, it is also excluded from the analysis. SSP5 was included in the study as it is the only scenario where radiative forcing level 8.5 W/m^2 (RCP 8.5) can be achieved. In the scope of this study, the priority for the data acquisition is given to the national,

regional, or catchment scale sources. However, when the data is not available at the mentioned scales, the SSP web-database is used to obtain the relevant data per SSP.

In the light of the information given so far, the scenarios within the scope of this study were created as follows: First, there are two main climate change scenarios namely RCP 4.5 (Low Emission Climate Change Scenario) and RCP 8.5 (High Emission Climate Change Scenario). The socio-economic scenarios are created under these climate change scenarios according to the consistency of RCP and SSP scenarios (Figure 8-6). Thus, the socio-economic scenarios have the same climate data as the climate change scenario they are under. The RCP 8.5 scenario has only a single SSP scenario since the only SSP baseline scenario which reaches the radiative forcing level of 8.5 W/m^2 is SSP5. The socio-economic scenarios located under the RCP 4.5 scenario are the SSP mitigation scenarios. Thus, there are total of three future scenarios, i.e., RCP4.5_SSP1, RCP4.5_SSP2, and RCP8.5_SSP5.

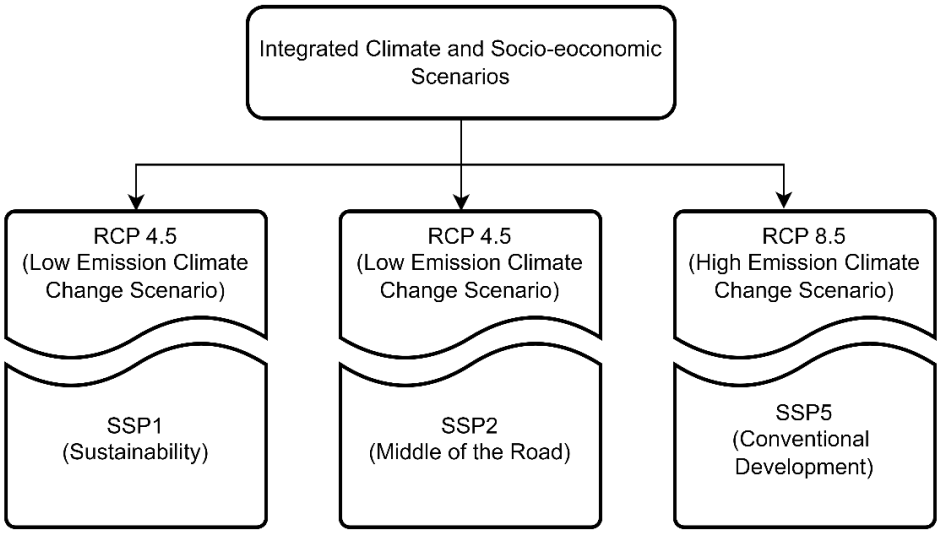

Figure 8-6. Hierarchy of the climate change and socio-economic scenarios in the WEAP-LEAP model

8.4 Data Categories Modified for the Future Period Model Building

The categories of data modified throughout the future period model building stage can be examined under five different headings as: (1) Climate, (2) Land Use Areas, (3) Municipal Water Demand, (4) Industrial Water Demand, (5) Energy Demand, (6) Cooling Systems in Thermal Power Plants, (7) Water Losses in Municipal Water Networks, (8) Reuse of Treated Wastewater, and (9) Environmental Flow Requirements.

8.4.1 Climate

The procedure for the introduction of future climate data into the model is explained in detail in Section 8.2. To summarize again, precipitation, temperature, relative humidity, and wind data for future period were obtained through dynamical downscaling using the WRF model. Then, the ensemble averages of the RCP 4.5 and RCP 8.5 scenarios were introduced into the WEAP-LEAP as two different scenarios.

8.4.2 Land Use (LU) Areas

Projections of future land use areas

The future evolution of five different land use classes namely Forest, Built-up Area, Pasture, Cropland, and Irrigated Areas based on SSPs are introduced into the model. The sources for the estimates of the future change in the land use areas are given in Table 8-2. In the SSP web-database (IIASA, 2018), the quantitative results for the SSP baseline and mitigation scenarios for the land use projections are given on the region level. In the database, there are five region levels, and Türkiye is included in the R5.2OECD level which includes the OECD 90 and EU member states and candidates. Thus, the results for the R5.2OECD level were downloaded within the

scope of this study. According to the land use area projections downloaded from the database, the percent change in the land use areas compared to the year 2005 were calculated. Then, these percent changes were reflected to the land use areas in the study area accordingly. The projection of irrigated area under SSPs are were obtained from another source, Hanasaki et al. (2013). In this study, SSP1, SSP2, and SSP5 are denoted as low, medium, and high growth, respectively. Thus, the irrigated area growth per each pathway changes accordingly (Table 8-3).

Table 8-2. Sources for the future land use area estimates

Land Use Class	**Reference**
Forest	SSP web-database (IIASA, 2018)
Built-up Area	SSP web-database (IIASA, 2018)
Pasture	SSP web-database (IIASA, 2018)
Cropland	SSP web-database (IIASA, 2018)
Irrigated Areas	Hanasaki et al. (2013)

Table 8-3. Irrigated area growth change per scenario (Hanasaki et al., 2013)

Scenario	**Irrigated area growth (%y^{-1})**
SSP1	0.06
SSP2	0.3
SSP5	0.6

Mass balance on land use areas in the future period

The future land use areas are projected according to the land use area projections downloaded from the SSP database. Then, the percent changes in the land use areas in the 2020 – 2100 period compared to the year 2005 were calculated. Then, these percent changes were reflected to the land use areas in the study area accordingly. Therefore, it is necessary to do the mass balance check for the percent changes in the land use/land cover areas in the SSP scenarios.

The methodology to perform a mass balance check is as follows. First of all, it was calculated how much of a change there was in the areas of land use classes as compared to the year 2005 due to the percent changes. In order for the entire catchment area not to change, the sum of the residual areas should be zero. Then, if any residual land area exists, it has been fed into other lower land use classes to which percentage changes do not apply such as natural grasslands, transitional woodland-shrub, bare rocks, and sparsely vegetated areas. The distribution of residual areas is based on the ratio of the areas of these land use classes. A sample screenshot for the calculation of the residual areas in each subbasin and distribution of them in Ankara subbasin for the SSP1 scenario is provided in Figure 8-7 and Figure 8-8, respectively. The same calculation methodology and procedure were applied to all subbasins for all SSP scenarios.

	SSP1_RCP4.5								
	Total Residual Area (ha)								
	2020	2030	2040	2050	2060	2070	2080	2090	2100
YS_Havza_AYDINLI	-18195.1	-38660.1	-42227.6	-46045.9	-51679.1	-57748.1	-63721.9	-69111.9	-70642.1
YS_Havza_AKTAS	-1940.65	-10848.4	-13425.5	-15930	-18764.9	-21633.7	-24485.5	-27050.4	-28269.1
YS_Havza_AYVALI	-23092.7	-50286.6	-56337.6	-62558	-70628.9	-79139.9	-87527.8	-95109.8	-97905.1
YS_Havza_CIKIS	-4164.43	-8300.83	-9689.82	-11044.4	-12521.3	-14011.4	-15521	-16925.6	-17784.5
ANK_Havza_ANKARA	-13236.5	-27213.7	-24116.2	-22409.1	-25765	-30394.2	-35878.5	-42085.5	-45390
KIR_Havza_KIRMIR	-1068.24	-6987.9	-6704.58	-6537.34	-7437.44	-8496.08	-9581.49	-10515.1	-10153.9
ORT_Havza_DOGANCAY	2111.505	-267.251	1433.74	3046.148	3578.209	4016.903	4364.065	4744.64	5831.461
ORT_Havza_KAYABELI	3353.59	-2036.67	685.4053	3297.342	3977.792	4518.891	4938.74	5506.208	7547.725
PR_Havza_ESENKARA	-510.611	-9350.13	-9189.97	-9249.04	-10932.9	-12887.7	-14960.5	-16900.1	-17051
PR_Havza_KIRANHARMANI	-4544.4	-13320.5	-14014	-14951.1	-17252.5	-19844.4	-22600.6	-25304.3	-26443.3
ASAK_Havza_MUDURNU	885.4828	504.5983	2062.53	3598.838	4447.282	5279.584	6041.664	6807.556	7834.952
ASAK_Havza_ADATEPE	-23.1519	-2241.22	-505.323	1003.755	1251.975	1295.599	1173.833	955.3185	1380.484
GOK_Havza_GOKSU	1410.957	-616.501	654.4992	1842.046	2153.395	2378.818	2520.645	2676.513	3397.152

Figure 8-7. A sample screenshot: Calculation of the residual areas in the RCP 4.5_SSP1 scenario

				Values to Add (ha)								
	Area in 2005 (ha)	Ratio		2020	2030	2040	2050	2060	2070	2080	2090	2100
Transitional woodland-shrub	29888.7	0.167694		2219.673	4563.571	4044.141	3757.872	4320.628	5096.917	6016.595	7057.475	7611.617
Bare rocks	5311.8	0.029802		394.4789	811.0349	718.7221	667.8465	767.8592	905.8208	1069.265	1254.25	1352.731
Natural grasslands	83485.3	0.468403		6200.005	12747	11296.12	10496.51	12068.41	14236.74	16805.59	19712.98	21260.81
Beaches, dunes, sands	224.2	0.001258		16.65013	34.23209	30.33576	28.18841	32.40974	38.23281	45.13146	52.93927	57.09598
Sparsely vegetated areas	54425.5	0.30536		4041.89	8309.985	7364.135	6842.856	7867.601	9281.176	10955.85	12851.23	13860.29
Water bodies	2324.5	0.013042		172.6281	354.9175	314.5204	292.2567	336.0233	396.3968	467.9218	548.873	591.9696
Wetlands	1753.9	0.00984		130.2527	267.7951	237.3144	220.5158	253.539	299.0924	353.06	414.14	446.6576
Fruit trees and berry plantations	819.9	0.0046		60.88957	125.1868	110.938	103.0851	118.5225	139.8175	165.0459	193.599	208.8001
SUM	178233.8			13236.47	27213.72	24116.23	22409.13	25764.99	30394.19	35878.46	42085.49	45389.98

Figure 8-8. A sample screenshot: Distribution of the residual areas in Ankara subbasin for the RCP4.5_SSP1 scenario

8.4.3 Municipal Water Demand

For the estimation of the changes in municipal water demand in the future period, the study conducted by Graham et al. (2018) was useful. In their study Graham et al. (2018), developed a set of qualitative and quantitative assumptions for future water sector technological advancements in different sectors, i.e. agricultural, electricity, manufacturing, and municipal, within the SSPs. The results of the scenarios were applied to an integrated assessment model, and then future water demand per sector was analyzed. The outcomes of this study as percent change as compared to the year 2010 are summarized in Table 8-4. For all years except 2050 and 2100, the municipal water demand was calculated by linear interpolation.

Table 8-4. Percent change in the global municipal water withdrawals as compared to the year 2010

2050			**2100**		
SSP1	***SSP2***	***SSP5***	***SSP1***	***SSP2***	***SSP5***
55.1	56.5	72.2	27.4	63.3	70.5

8.4.4 Industrial Water Demand

For the estimation of the changes in industrial water demand in the future period, the outcomes of the Graham et al. (2018)'s study were used. Percent change in the global industrial water withdrawals as compared to the year 2010 were reflected in the WEAP-LEAP model's future period (Table 8-5). After the industrial water demand in the years 2050 and 2100 was calculated, the industrial water demand rest of the years was calculated by linear interpolation.

Table 8-5. Percent change in the global industrial water withdrawals as compared to the year 2010 (Graham et al., 2018).

2050			**2100**		
SSP1	***SSP2***	***SSP5***	***SSP1***	***SSP2***	***SSP5***
6.0	52.4	38.9	-45.2	39.5	-9.9

8.4.5 Energy Demand

Within the scope of this study, the value expressed as "Electricity Demand" in the LEAP model represents the electricity generation in the basin. Therefore, the electricity demand entered into the LEAP model in the baseline period reflects the total electricity produced in the power plants located within the basin boundary. Similarly, in future scenarios, the electricity requirement was calculated by determining the average amount of electricity that can be produced from the power plants that are under construction or planned in the basin. In this context, a list of the power plants that are currently in operation, under construction and planned in the basin was prepared, and thus the total electricity expected to be produced in the basin

in the future was calculated. EPDK (Energy Market Regulatory Authority) progress reports were used for the installed power, project and reliable production values by years as of the date of commissioning of the private sector production facilities that are under construction and are expected to be put into operation in the projection period. In addition, the list of Türkiye's HPP projects prepared by DSİ (DSİ, 2021) and the Turkish Electricity 5-Year Generation Capacity Projection (2019-2023) prepared by TEİAŞ (TEİAŞ, 2019) were examined. The list of the power plants that are under construction or planned in the basin is given in Table 8-6.

Table 8-6. List of power plants under construction or planned to be built in the Sakarya Basin

Name of the power plant	Type	Province	District	Subbasin	Installed Power (MW)	Electricity Generation (GWh)	Actual Realization (%)
Gürsöğüt HPP	Hydroelectric	Eskişehir	Mihalıççık	Middle Sakarya	242.0	158.7	91
Kargı HPP	Hydroelectric	Ankara	Beypazarı	Middle Sakarya	100.0	203.0	100
Bozüyük WPP	Wind	Bilecik	Bozüyük	Middle Sakarya	90.0	323.0	90
Adapazarı WPP	Wind	Bolu	Göynük	Middle Sakarya	80.0	70.0	96
WPP YEKA-1	Wind	Eskişehir	Tepebaşı	Porsuk	50.0	175.0	No info
Kartal WPP	Wind	Eskişehir	Tepebaşı	Porsuk	39.0	136.5	93
Arıkçayırı BPP	Biomass	Bolu	Göynük	Middle Sakarya	30.0	208.2	96
Meryem WPP	Wind	Bilecik	Merkez	Middle Sakarya	30.0	73.0	20
Kırka FOPP	Fuel-oil	Eskişehir	Kırka	Upper Sakarya	26.9	177.0	100
Pamukova WPP	Wind	Sakarya	Geyve	Middle Sakarya	20.0	70.0	98
Kuyulukoyak WPP	Wind	Konya	Sarayönü	Upper Sakarya	16.0	57.0	96
İnegöl BPP	Biomass	Bursa	İnegöl	Göksu	14.1	60.5	57
Hisar HPP	Hydroelectric	Bilecik	İnhisar	Middle Sakarya	13.4	11.9	0
Ova HPP	Hydroelectric	Sakarya	Pamukova	Middle Sakarya	13.2	30.0	72
Gök HPP	Hydroelectric	Bilecik	Osmaneli	Middle Sakarya	12.6	20.0	100
İnönü NGPP	Natural Gas	Eskişehir	İnönü	Porsuk	12.6	73.7	100
Boğazköy HPP	Hydroelectric	Eskişehir	Mihalıççık	Göksu	10.0	20.0	100

NGPP:Natural Gas Power Plant; HPP: Hydroelectric Power Plant; BPP: Biogas Power Plant; WPP: Wind Power Plant; FOPP: Fuel Oil Power Plant

In the SSP2 and SSP5 scenarios, it is assumed that no other power plants will be built in the Sakarya Basin other than the ones currently under construction and planned. In the SSP1 scenario, it is assumed that all the renewable energy potential of the basin will be used until 2100, in line with the narrative of this scenario. In this context, solar and wind energy potential of Sakarya Basin was investigated. Figure 8-9 shows the total electricity generation in the Sakarya Basin in three future scenarios. As it can be seen from the figure, SSP2 and SSP5 scenarios have the same amount of electricity generation throughout the 21st century. The SSP1 scenario, on the other hand, has the highest electricity generation, as it aims to use renewable energy at full potential.

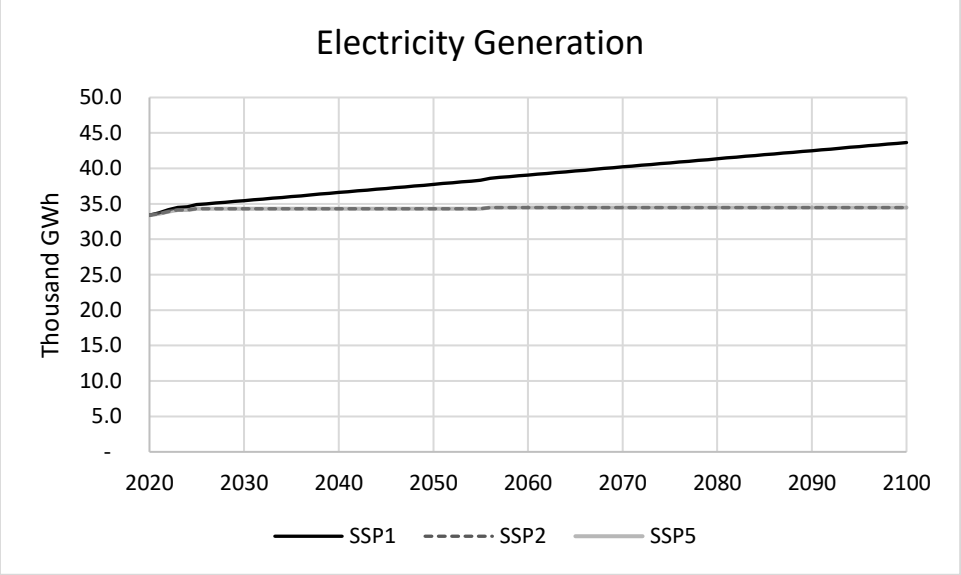

Figure 8-9. Total electricity generation in Sakarya Basin for the future scenarios

Sakarya Basin Solar Power Potential

Within the scope of the dissertation study carried out by Cebeci (2017), the installed solar power potential of Türkiye is stated as 56000 MW. Based on the ratio of the total drainage area of the Sakarya Basin to the total area of all the basins in Türkiye,

the Sakarya Basin's installed power potential was calculated with a rough assumption. As a result, the installed power potential of Sakarya Basin was calculated as 3681 MW. It is assumed that this potential will be fully utilized by 2100. Starting from 0 MW in 2020, it is assumed that the installed power will reach 3681 MW in 2100. This assumption does not exclude existing solar power plants. In addition to the existing power plants, there will be as much installed power as in this assumption. By using the average Specific photovoltaic power output (kWh/kWp) value obtained from Global Solar Atlas 2.0, a free, web-based application (World Bank Group, 2023a), for Türkiye, i.e., 4.27 kWh/kWp, how much electricity will be produced from the solar power plant installed power was calculated. This value was entered into the LEAP as electricity demand.

Sakarya Basin Wind Power Potential

Sakarya Basin's installed wind power potential is calculated by using the installed power potential values (Enerji Atlası, 2023) on a provincial basis. The areal percentage values of the provinces within the basin boundary are multiplied by the installed wind power potential values that can be established in these provinces. The potential of whole Sakarya Basin was obtained by summing the installed power potential calculated in this way in all provinces. While making this calculation, the process/theory ratios were also taken into consideration. The process/theory ratio expresses the ratio of the installed power currently in operation to the theoretical potential. For example, if the process/theory ratio is 100%, it is assumed that no more power plants can be built in that province. Accordingly, the total wind potential of Sakarya Basin was calculated as 1307.2 MW. Similar to the solar energy potential calculation, starting from 0 MW in 2020, the total installed power in 2100 was interpolated to 1307.2 MW. Considering that wind power plants operate with an average capacity factor of 30%, annual electricity generation is calculated. The average capacity factor of the wind power plants was calculated using the wind

power plants that are already in operation in the basin. These annual values are entered into the LEAP as electricity demand.

8.4.6 Cooling Systems in Thermal Power Plants

In the WEAP-LEAP model, the amount of water required for the thermal power plants' cooling systems are calculated based on the water consumption factors (WCF). The WCFs change depending on the type of the cooling system used in the power plant. Thus, shifting from wet cooling systems to either hybrid or dry cooling systems can be modeled in the proper scenarios. The water consumption factors of the thermal power plants modeled within the scope of the study are given in Table 8-7.

In SSP2 and SSP5 scenarios, it is assumed that there will be no change in the cooling system of thermal power plants. In SSP1 scenario, on the other hand, it is assumed that all thermal power plants with wet cooling system will switch to dry cooling system.

Table 8-7. Water consumption factors of the thermal power plants modeled in the study

Fuel Type	**Cooling Type**	**Water Consumption Factor (m^3/GWh)**	**Reference**
Lignite/Coal	Wet	2,600.6	(Macknick et al., 2012)
Lignite/Coal	Dry	97.2	(Spang et al., 2014)
Natural Gas	Wet	776.0	(Macknick et al., 2012)
Natural Gas	Dry	7.6	(Macknick et al., 2012)
Biogas	Wet	776.0	(Macknick et al., 2012)

8.4.7 Water Losses in Municipal Water Networks

In accordance with the Regulation on the Control of Water Losses in Drinking Water Supply and Distribution Systems published in the Official Gazette dated 8/5/2014 and numbered 28894, metropolitan and provincial municipalities will reduce their water losses to a maximum of 30% until 2023 and to a maximum of 25% until 2028.; other municipalities are obliged to reduce their water losses to a maximum of 35% until 2023, to a maximum of 30% until 2028, and to a maximum of 25% until 2033.

In line with the obligations of the regulation, it is assumed that the water loss/leakage will be maximum 30% until 2023 and 25% until 2028 in the SSP2 and SSP5 scenarios. This value is assumed to be constant for all years after 2028. In the SSP1 scenario, it is assumed that it will be at most 30% until 2023, and at most 25% until 2028, but until 2100, water losses will be reduced to zero (Table 8-8).

Table 8-8. Water losses in municipal water networks in the future scenarios

	2023	**2028**	**2100**
SSP1	30%	25%	0%
SSP2	30%	25%	25%
SSP5	30%	25%	25%

8.4.8 Reuse of Treated Wastewater

The Ministry of Environment, Urbanization and Climate Change aims to increase the reuse rate of treated wastewater to 5 percent in 2023 and 15 percent in 2030 (MoEUC, 2022a). Accordingly, in the SSP1 scenario, it is assumed that the reuse rate will be 5% in 2023, 15% in 2030 and this rate will be 30% until 2100.

8.4.9 Environmental Flow Requirements

In the WEAP model, the Minimum Flow Requirement establishes the lowest amount of water flow needed on a monthly basis in a river to fulfill various needs such as water quality, fish and wildlife preservation, navigation, recreation, and downstream requirements. Depending on its demand priority, the flow requirement will be met either before, after, or concurrently with other demands on the river. Thus, the priority refers to the level of importance of the flow requirement compared to all other demands in the system. The priorities are typically assigned a value between 1 to 99, with 1 being the most critical and 99 being the least important.

According to the "Regulation on the Right to Use Water" in Türkiye, companies building hydroelectric power plants (HPPs) must release a minimum amount of water into the stream bed to preserve natural life. The regulation requires companies to release at least 10% of the stream's last ten-year average flow, which is based on the HPP project. During the Environmental Impact Assessment (EIA) process, companies have the option to increase this amount based on their evaluation of ecological needs. However, during the field studies, it has been determined that these obligations regarding environmental flows are not fulfilled most of the time in Sakarya Basin. In addition, environmental flows are not considered as a priority. For this reason, no environmental flow requirement was imposed on the model in the SSP2 and SSP5 scenarios. In the SSP1 scenario, on the other hand, the environmental flow requirement was mandated at the outlet of each subbasin in the Sakarya Basin. Chapter 7 in Section 7.3 describes the flow naturalization approach used in the Sakarya Basin and presents its outcomes. The natural flow time series, generated using this methodology at each subbasin's outlet point, were employed to establish the environmental flow requirement. Additionally, a priority level of 1 was assigned to the environmental flow requirement.

CHAPTER 9

SELECTION, NORMALIZATION, WEIGHTING, AND AGGREGATION OF WEFE NEXUS INDICATORS

9.1 Selection and Calculation of Indicators

Within the scope of the WEFE Nexus security and sustainability assessment studies, the most relevant indicators in terms of availability, affordability, accessibility, quality, and safety are selected. This way, the status and security of WEFE Nexus components are analyzed (Endo et al., 2015; Giupponi and Gain, 2017; Momblanch et al., 2018). Indicators are methods used to quantitatively describe and operationalize any system regardless of its complexity (Endo et al., 2015). As Yi et al. (2020) state, indicator selection is always the first step to initiating a sustainability assessment. Giupponi and Gain (2017) state that a concise index developed from the aggregation of multiple indicators can significantly enhance scientific evidence's transformation into practical information for policy/decision-making.

Resource availability, accessibility, self-sufficiency, and productivity are the primary drivers of the securities of water, energy, and food from where indicators are defined. Thus, Nhamo et al. (2019) emphasize that indicators that are not related to these drivers should be excluded from the list of WEFE Nexus indicators. According to Saladini et al. (2018), the selected indicators for the assessment of water, energy, and food securities should cover the most sustainable development goals (SDGs), consider biophysical limits, highlight the linkages among all nexus components, consider both national and sectoral systems, and be limited in number. In addition, data availability should be guaranteed frequently enough to be

meaningful in the desired time horizon. Moreover, as Endo et al. (2015) state, the indicators should be strongly linked to the issue and objective for measurement and tailored specifically for the research area.

Literature review and related evaluations related to WEFE Nexus indicators are given in Chapter 2 in Section 2.6 in detail. The indicators used within the scope of this study are given in Table 9-1. While selecting the indicators, the major drivers of the security of the WEFE Nexus, the characteristics of the Sakarya Basin itself, and the WEAP-LEAP model's capability were also taken into account.

Table 9-1. Summary of the selected WEFE Nexus indicators

WEFE Nexus Components	**Indicator No**	**Indicator Name**	**Indicator Unit**	**Indicator Acronym**
Water	1	Municipal water demand coverage	%	MDC
Food (Agriculture)	2	Irrigation demand met	%	IDM
Energy	3	Hydropower production as % of maximum hydropower generation capacity	%	HPP_MGC
	4	Decrease in CO_2 Emissions	%	CO_2_EG
	5	Renewable Energy Share	%	RES
Ecosystem		*Median Discharge for Each Calendar Month*		
	6	January Median Monthly Streamflow	m^3/sec	Jan-MMS
	7	February Median Monthly Streamflow	m^3/sec	Feb-MMS
	8	March Median Monthly Streamflow	m^3/sec	Mar-MMS
	9	April Median Monthly Streamflow	m^3/sec	Apr-MMS
	10	May Median Monthly Streamflow	m^3/sec	May-MMS
	11	June Median Monthly Streamflow	m^3/sec	Jun-MMS
	12	July Median Monthly Streamflow	m^3/sec	Jul-MMS
	13	August Median Monthly Streamflow	m^3/sec	Aug-MMS
	14	September Median Monthly Streamflow	m^3/sec	Sep-MMS
	15	October Median Monthly Streamflow	m^3/sec	Oct-MMS
	16	November Median Monthly Streamflow	m^3/sec	Nov-MMS
	17	December Median Monthly Streamflow	m^3/sec	Dec-MMS

9.1.1 Municipal water demand coverage (MDC) (%)

Detailed information about the Sakarya Basin is given in Chapter 4. The 100% of Eskişehir, Sakarya, and Bilecik provinces, and some parts of the provinces of Kütahya, Ankara, Konya, Bursa, Afyonkarahisar, Bolu, Kocaeli, and Uşak are located in the Sakarya Basin. Among these cities, Ankara is Türkiye's second-largest city in terms of population; thus, there is a significant drinking water need. For instance, the total amount of water withdrawn for drinking and potable water networks in Ankara in 2020 was 502,458 thousand m^3/year (TÜİK, 2020). Ankara's drinking water is supplied from Kurtboğazı, Çamlıdere, Akyar, Çubuk, Kavşakkaya and Eğrekkaya Dams. However, it is known that from time to time, due to the difficulties experienced in meeting the municipal water demand, reinforcements were made from the Kızılırmak River. In this sense, the indicator of meeting the municipal water demand, which is expected to become even more important with the effects of climate change, is important for examining the safety of the WEFE Nexus in the basin. Moreover, MDC is related to SDG6, the water and sanitation goal, which aims to ensure the availability and sustainable management of water and sanitation for all. Thus, it will also guide the way toward achieving this goal.

To calculate MDC, the WEAP-LEAP model results and Equation 9.1 are used. First of all, the supply requirement (m^3) of and supply delivered (m^3) to each municipal demand site node in the relevant subbasin are obtained. Then, the total amount of supply requirement and supply delivered are calculated by summing up all demand site nodes. Finally, the whole watershed municipal water demand coverage is calculated as it is given in Equation 9.1.

$$Municipal\ water\ demand\ coverage\ (\%) = \frac{\sum_i \sum_t Supply\ delivered\ (m^3)}{\sum_i \sum_t Supply\ requirement\ (m^3)} * 100 \qquad 9.1$$

Where i represents the number of municipal demand site nodes, and t is the number of months for the related time period, i.e., 108 months for near century (2022 – 2030), mid-century (2057 – 2065), and far century (2092 – 2100).

9.1.2 Irrigation Demand Met (IDM) (%)

Sakarya Basin constitutes approximately 13% of Türkiye's surface area, and about 53% of the basin consists of agricultural areas. Moreover, irrigated agricultural activities are carried out in a significant part of the basin; therefore, agricultural water withdrawals constitute a large share of sectoral water allocations. That is, it is crucially important to include irrigation demand coverage among the WEFE Nexus indicators in Sakarya Basin. Furthermore, IDM is an indicator that can help determine how SDG 6, the goal to end hunger, referring to achieving food security and improved nutrition and promoting sustainable agriculture, is being impacted.

In the WEAP model, catchment processes such as evapotranspiration, runoff, infiltration, and irrigation demands are simulated with the Soil Moisture Method. Soil Moisture Method is one dimensional, 2-compartment (or "bucket") soil moisture accounting scheme, and it is based on empirical functions that describe evapotranspiration, surface runoff, sub-surface runoff (i.e., interflow), and deep percolation for a watershed unit. In the WEAP model, irrigation is required when rainfall is insufficient to compensate for the water lost by evapotranspiration. There occurs an irrigation shortfall when the theoretical catchment irrigation demand is higher than the sum of irrigation (supply delivered) to the catchment branch. To obtain the IDM (%), first, the sum of the total amount of irrigation shortfall (m^3) in all catchment branches in the watershed is calculated and it is divided by the sum of the total theoretical catchment irrigation demand (m^3) in all catchment branches in the study watershed. This calculation is performed on the catchments with irrigated

agriculture. In this calculation, an irrigation demand deficit is found. To calculate IDM, the calculation given in Equation 9.2 is employed:

$$Irrigation\ Demand\ Met\ (\%) = \left(1 - \frac{\sum_i \sum_t Irrigation\ Shortfall\ (m^3)}{\sum_i \sum_t Theo.Catchment\ Irrigation\ Demand\ (m^3)}\right) * 100 \quad 9.2$$

Where i represents the number of catchments with irrigated agriculture, and t is the number of years for the related time period, i.e., 9 years for near century (2022 – 2030), mid-century (2057 – 2065), and far century (2092 – 2100).

9.1.3 Hydropower production as % of maximum hydropower generation capacity (HPP_MGC)

There are 24 hydroelectric power plants in the Sakarya Basin with a total installed capacity of 684 MW. The installed capacities of the hydroelectric power plants range between 0.18 MW to 278 MW. The three hydroelectric power plants with the largest capacity namely Gökçekaya, Sarıyar and Yenice are located in the Middle Sakarya basin. Gökçekaya with an installed capacity of 278 MW is the Türkiye's 22nd largest hydroelectric power plant. Total annual electricity production of hydroelectric power plants in the Sakarya Basin is around 1600 GWh. In addition, there are number of hydroelectric power plants planned to be built in the basin (DSİ, 2022). These numbers imply that hydroelectricity has a significant contribution to electricity generation in the Sakarya Basin. For this reason, HPP_MGC should be among the indicators in the evaluation of energy security. In addition, HPP_MGC is also relevant to SDG 7 which is about ensuring access to affordable, reliable, sustainable and modern energy for all.

To calculate HPP_MGC, firstly, the maximum electricity generation that can be produced in a year from the hydropower plants is calculated by using their installed capacities. Then, the average annual value actually produced from the hydroelectric power plants during the simulation period is obtained. Finally, HPP_MGC is calculated as follows (Equation 9.3).

$$Hydro.prod.as\ \%\ of\ max.gen.capacity\ of\ HPPs = \frac{Ave.\ Total\ Hydro\ (GWh/year)}{Hydro.Max.Generation\ Capacity\ (GWh/year)} * 100 \quad 9.3$$

9.1.4 Decrease in CO_2 Emissions (CO_2_EG) (%)

The United Nations Framework Convention on Climate Change is the first and most important step in the international arena against the negative effects of global warming on climate change. The Paris Agreement was adopted at the 21st conference of the parties to this convention. Türkiye signed the Paris agreement in 2016 and ratified it in September 2021. The Paris agreement is based on the United Nations Framework Convention on Climate Change and aims to regulate the climate change regime after 2020, the expiration date of the Kyoto Protocol. The long-term goal of the Paris agreement is to keep the global temperature rise as low as 2°C (1.5°C if possible) compared to the pre-industrial era.

Another important feature of the agreement is that, unlike the Kyoto Protocol, developed and developing countries participate in the mitigation action with Nationally Determined Contribution/NDC. NDCs are contributions made up of voluntary, non-binding objectives that are determined by the parties' national conditions and self-determined. In this context, in 2015, Türkiye set its intended NDC as up to 21 percent reduction in GHG emissions from the Business as Usual

(BAU) level by 2030. However, this target was updated to 41% at the 27th parties conference (COP27) held in Sharm El Sheikh, Egypt in 2022 (MoEUC, 2022b).

In line with the Türkiye's NDC, it is important adopt policies reducing CO_2 emissions country wise. Accordingly, including the CO_2_EG indicator is important for assessing the security of the WEFE Nexus.

In the LEAP model it is possible to specify environmental loadings for a given technology by creating a link to one of the libraries of technologies in the accompanying Technology and Environmental Database (TED). TED contains emission factors for hundreds of energy consuming and energy producing technologies, including the default emission factors suggested by the IPCC for use in climate change mitigation analyses (SEI, 2005). In this study, IPPC Tier 1 emission factors are used, and the resulting CO_2 emissions from the electricity generation are calculated accordingly.

To calculate CO_2_EG, first, the annual average CO_2 emissions in the baseline period (2004 – 2017) was calculated for each subbasin. Next, the annual average CO_2 emissions in each future period segments, i.e., near, mid- and far century, were calculated in each subbasin. Finally, CO_2_EG is calculated as follows (Equation 9.4):

$$\text{Decrease in } CO_2 \text{ emissions (CO2\_EG)} = \frac{Ave.CO_2(baseline) - Ave.CO_2\ (future\ period)}{Ave.CO_2(baseline)} * 100 \qquad 9.4$$

9.1.5 Renewable energy share (RES) (%)

Türkiye is the world's 19th largest economy (World Bank Group, 2023b). With its growing economy and increasing population, Türkiye's energy demand is increasing rapidly. This situation, for electricity and other primary energy sources, brought

energy supply security to the top of the country's agenda. Türkiye is a country whose economy is dependent on imported energy resources. It is foreseen that Türkiye's economic development process will continue in the coming years, and therefore, it is expected that the energy demand will continue to increase. Thus, it is important to encourage alternative solutions based on renewable energy in order to prevent the risks arising from high level of external dependency in energy and to develop a sustainable energy model (MoENR, 2014).

According to the national renewable energy action plan (MoENR, 2014), Türkiye aims to create a generation portfolio in which renewable energy meets at least 30 percent of the total electrical energy demand by 2023. Moreover, Sakarya Basin has a high installed capacity potential in terms of renewable energy. Considering the national target and the basin's potential, it is important for the evaluation of WEFE security that the share of renewable energy in total electricity production is included as an indicator.

To calculate RES, first, the average annual electricity generation from the renewable energy plants throughout the relevant time period is calculated based on the LEAP model results. Then, average annual total electricity generation for the same time period is calculated. Finally, RES is calculated as follows (Equation 9.5):

$$Renewable\ energy\ share\ (RES)(\%) = \frac{Ave.\ annual\ electricity\ generation\ (renewable\ plants)}{Ave.\ annual\ electricity\ generation\ (all\ power\ plants)} * 100 \qquad 9.5$$

9.1.6 Median streamflow for each calendar month (MMS) (m^3/sec)

The relationship between ecological integrity and hydrological variation is detailed in Chapter 7. In river ecosystems the natural variability of the flow regime was

recognized as a key controlling variable in sustaining ecological integrity. Poff et al. (1997) states that streamflow is a "master variable" that limits the distribution and abundance of riverine species and regulates the ecological integrity of flowing water systems. In the literature, there are several hydrological indices developed and employed to reveal the characteristics of the flow regime (Poff et al., 1997). One of the most commonly used methods is Indicators of Hydrological Alteration (IHA) used for the Range of Variability Approach (RVA) which was developed by Richter et al. (1996, 1997). RVA uses daily hydrological data to obtain 33 hydrological parameters such as mean annual maximum and minimum flows; 7-day, 30-day maximum and minimum flows. These statistics are categorized into five groups depending on their hydrological features. RVA defines initial, interim river management targets that are based on the natural flow regime. These targets serve as a starting point to begin adaptive management efforts. The details are given in Chapter 7.

In order to evaluate the ecosystem pillar of the WEFE Nexus, twelve different indicators were selected (Table 9-2). These indicators are actually the Group 1 parameters, i.e., magnitude of monthly water conditions, of the IHA method. In the original IHA method, there are a total of 33 parameters divided into 5 groups. The reason why partial IHA analysis is performed within the scope of this study is that the WEAP model has a monthly timestep. IHA method requires daily streamflow data for a full analysis. However, the methodology followed to evaluate the potential changes in the hydrological regime is similar to the IHA-RVA method (details in Chapter 7).

IHA parameters can be calculated using parametric (mean/standard deviation) or nonparametric (percentile) statistics. In this study, non-parametric statistics were preferred. That is, the initial flow management targets were based on the median and the interquartile range (IQR) of the natural flow conditions (pre-impact period), and

the interannual statistics were obtained by calculating the median of the streamflow in each calendar month in the related post-impact period (details in Chapter 7). The reason why median and IQR were chosen is because most of the time hydrologic datasets do not have a normal distribution which is the key assumption of parametric statistics. Moreover, they are less sensitive to outliers compared to mean ±1 standard deviation (Laize et al., 2014).

Table 9-2. Ecosystem pillar indicators; regime characteristics, analogue IHA variables, pre-and post-impact inter-annual statistics

Intra-annual hydrological attributes (Mean MS)	**Regime characteristics**	**Analogue IHA variables (Mean MS)**	**Inter-annual statistics**	
			Pre-impact period	**Post-impact period**
January	Magnitude; Timing	January	IQR	Median
February		February	IQR	Median
March		March	IQR	Median
April		April	IQR	Median
May		May	IQR	Median
June		June	IQR	Median
July		July	IQR	Median
August		August	IQR	Median
September		September	IQR	Median
October		October	IQR	Median
November		November	IQR	Median
December		December	IQR	Median
MS: Monthly streamflow; IQR: Interquartile range				

9.2 Normalization Procedure

Following the selection of the indicators, all indicators are normalized prior to their aggregation since they have different measurement units. Normalization is required to transform the indicators into a uniform scale so that they can be comparable and aggregable. There are various normalization methods available such as ranking,

standardization, min-max, distance to reference, categorical scale, cyclical indicators, balance of opinions (details in OECD JRC, 2008).

Nardo et al. (2005) states that the normalization method should be chosen based on the data properties and the objectives of the composite indicator. In this study, the purpose of developing a WEFE Nexus Index is not only to determine the best- and worst-case scenarios but also identify its relative distance to the target or sustainability levels. For this purpose, employing normalization functions to normalize the values of the indicators given in Table 9-1 was determined as the most suitable method for the purpose of the study and the characteristics of the indicators. According to Castoldi and Bechini (2010), there are four different functions that determine the relationship between the indicator values and the sustainability scores. These functions are dichotomic judgement, step function, continuous linear function and continuous non-linear function. In this study, the value of an indicator is normalized by use of continuous linear functions. In this method, the normalization function gradually converts the indicator value into a score ranging from 0 to 1 based on the pre-defined sustainability thresholds. That is, the indicator takes the value of 1 if its value is within some range of optimal thresholds (S_{opt1} and S_{opt2} in Figure 9-1); it takes values between 0 and 1 for an indicator value between the optimal and anti-ideal thresholds (between S_{min} and S_{opt1} or S_{opt2} and S_{max} in Figure 9-1); and takes a value of zero at and outside of the anti-ideal thresholds, i.e., S_{min} and S_{max} in Figure 9-1 (Castoldi and Bechini, 2010; Pinar et al., 2014). The transition range for the left and the right side of the curve are described by Equation 9.6 and Equation 9.7, respectively. In these equations, V_i represents the value of an indicator.

$$S_i = \left(\frac{V_i - S_{min}}{S_{opt1} - S_{min}} \right) \quad 9.6$$

$$S_i = \left(\frac{V_i - S_{max}}{S_{opt2} - S_{max}} \right) \quad 9.7$$

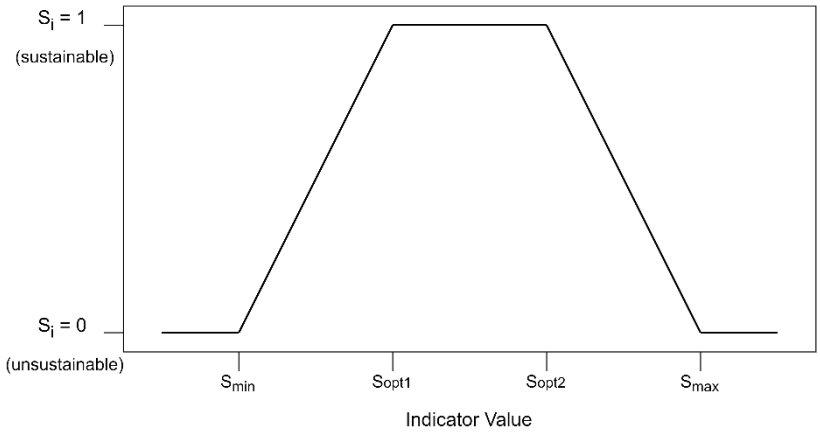

Figure 9-1. A general function used to transform indicator values into sustainability scores adopted from (Castoldi and Bechini, 2010)

The initial step of the normalization method adopted in this study is to define the optimal or the target levels for the selected indicators. For this purpose, Sustainable Development Goals Report (United Nations, 2022), the targets of the Paris Agreement, Türkiye's national renewable energy action plan (MoENR, 2014), and the natural flow regime characteristics in the study subbasins were benefited. The normalization functions and the optimal thresholds of each indicator selected in this study are detailed in the following paragraphs.

Water Nexus Component

For the Water component indicator, MDC, the target level was determined based on the SGD 6 which is Clean Water and Sanitation Goal. This goal has eight different targets and first target of this goal is to achieve universal and equitable access to safe and affordable drinking water ***for all*** by 2030. Considering this target, the sustainability score of 1 corresponds to 100% coverage of municipal water demand, and the normalization function is created accordingly (Figure 9-2).

Food Nexus Component

Approximately 44% of the Sakarya Basin consists of agricultural lands. Important agricultural activities are carried out in the basin, especially in large plains and areas with microclimate characteristics (Alp et al., 2020). Although the Sakarya Basin is industrialized at an increasing rate, it has not lost its feature of being an agricultural basin yet. Livestock and agricultural activities are carried out intensively throughout the basin. Although mainly field cultivation is done throughout the basin, there is also vegetable and fruit production. Thus, the need for agricultural water puts a significant pressure on the water resources in the basin. Knowing the fact that the increases in crop yield are directly and linearly correlated with increases in the consumption of water (Perry et al., 2009), meeting irrigational demand is important for agricultural productivity. In addition, the second sustainable development goal (SDG2) aims to ensure global food security and agricultural sustainability. In this context, one of the targets of this goal, i.e., 2.4, is to ensure sustainable food production systems and implement resilient agricultural practices that increase productivity and production. In line with all this information, the sustainability score of 1 corresponds to 100% coverage of irrigation demand in the basin. Thus, the normalization function of IDM is employed as shown in Figure 9-2.

Energy Nexus Component

There are three indicators of the Energy component of the WEFE Nexus Index (Table 9-1). The first one is HPP_MGC (%) which refers to the hydropower production as percent of the maximum hydropower generation capacity of the installed hydroelectric power plants in the basin. As mentioned previously in Section 9.1.3, Sakarya Basin has a high hydroelectric potential and there are currently 24 hydroelectric power plants installed. In addition, there are several hydroelectric power plants planned to be built in the coming years. Moreover, according to the Renewable Action Plan (MoENR, 2014), Türkiye's strategy is to utilize the

country's hydroelectric potential to the maximum extent. For all of these reasons, the target level for the HPP_MGC was identified as 100%. Thus, the sustainability score of 1 corresponds to 100% utilization of installed capacities of the hydroelectric power plants located in the basin (Figure 9-2).

The second indicator of the Energy component is CO_2_EG which refers to the percentage decrease in CO_2 emissions as compared to the baseline period. As previously mentioned in Section 9.1.4, Türkiye ratified the Paris Agreement in September 2021, and its most updated NDC is 41 percent reduction in GHG emissions from the Business as Usual (BAU) level by 2030. The Paris Agreement aims to reduce global carbon emissions by 50% by 2030 and to zero by 2050. In this study, the ultimate objectives of the Paris Agreement were adopted as the target levels for the CO_2_EG indicator, since the objectives are stricter. Thus, the target levels change in each future period segment accordingly. For the near century (2022 – 2030), the target level was set to 50% reduction in the CO_2 emissions, and for the mid- (2057 – 2065) and far century (2092 – 2100) the target level was set as 100%. The normalization functions created in line with these goals is shown in Figure 9-3.

The last indicator of the Energy component is RES (%) which refers to the share of the renewable energy in the total electricity production portfolio. The target level for this indicator directly comes from the Türkiye's national renewable action plan (MoENR, 2014) (details in Section 9.1.5). Thus, the sustainability score of 1 refers to the 30% in the normalization function (Figure 9-4).

Ecosystem Nexus Component

The target levels for the indicators of Ecosystem component of the nexus are adapted from the IHA-RVA method (Richter et al., 1997). In this method, the initial flow management targets, i.e., range of variation, of each of the 33 parameters of the IHA are selected either as mean ±1 standard deviation or the twenty-fifth to seventy-fifth percentile range (interquartile range). In this study, the median and the IQR were

selected (details in Section 9.1.6 and Chapter 7). The normalization function employed to transform MMS values into their normalized values is given in Figure 9-5. In this figure, Q_{25} and Q_{75} correspond to the twenty-fifth to seventy-fifth percentile flow ranges of the naturalized streamflow conditions, respectively. Q_{min} and Q_{max} refer to the the minimum and maximum flows, respectively. Thus, the sustainability score of the MMS is 1 if its value is within the IQR. It's normalized value or the sustainability score gradually decreases outside of the IQR. That is, the normalized value of MMS ranges between 0 and 1 if it is value is between Q_{min} and Q_{25} or Q_{75} and Q_{max}. The sustainability score is zero if the value of MMS is either less than or equal to Q_{min}; or greater than or equal to Q_{max}.

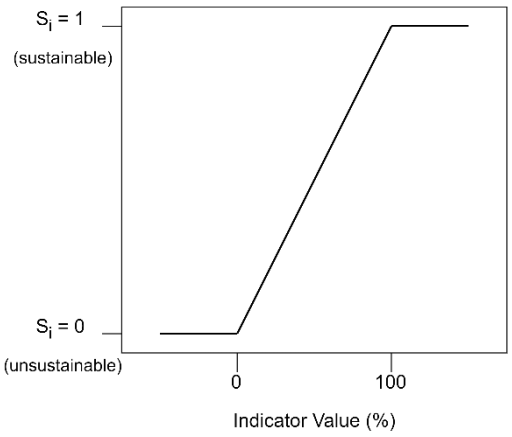

Figure 9-2. Normalization function used to transform MDC (%), IDM (%) and HPP_MGC (%) into sustainability scores

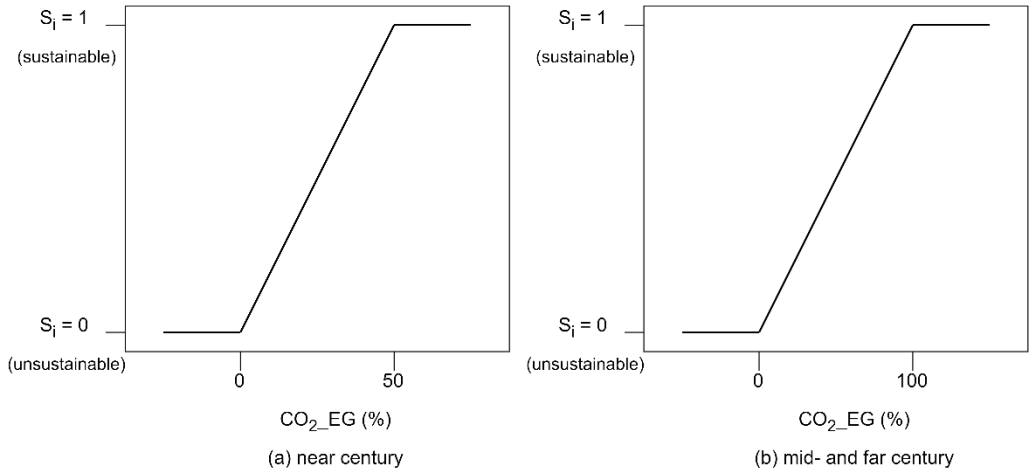

Figure 9-3. Normalization functions used to transform CO_2_EG (%) into sustainability scores: (a) near century; (b) mid- and far century

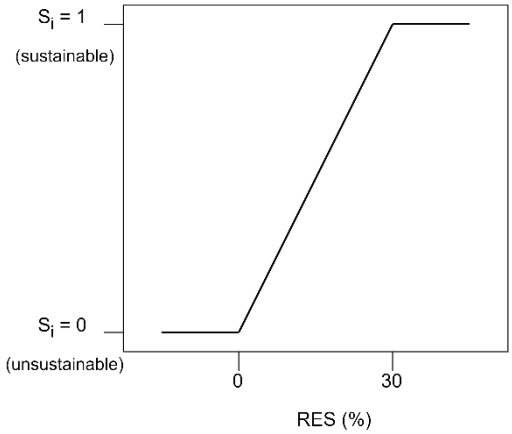

Figure 9-4. Normalization function used to transform RES (%) into sustainability scores

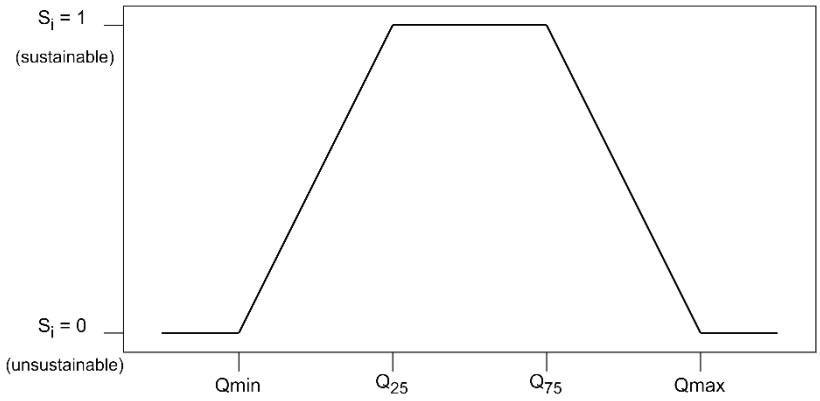

Figure 9-5. Normalization function used to transform MMS (m^3/sec) into sustainability scores

9.3 Weighting and Aggregation of Indicators and Pillars to the WEFE Nexus Index

There are several weighting methods that are derived from statistical models or from participatory models. Factor analysis, data envelopment analysis and unobserved component models (UCM) are the examples of the statistical models. The participatory models include budget allocation process (BAP), analytic hierarchy processes (AHP) and conjoint analysis (CA) (OECD, 2008). Nardo et al. (2005) discuss that an agreed methodology for weighting individual indicators does not exist. While some indicators are weighted based on the value judgments of the analyst or the weights derived from the principal component analysis to avoid double-counting problems, others could be based on the opinion of the experts.

In this study, equal weighting method was adopted due to several reasons. First of all, by adopting the equal weighting method, it is ensured that each component of the WEFE Nexus approach is given the same level of importance. As Benson et al. (2015) and Hoff (2011) state, the multi-centric nature of the approach highlights the

equal significance of each component. Thus, assigning an equal weight to each component aligns the fundamental philosophy of the WEFE Nexus approach. This approach ensures that the study's results are unbiased, fair, and representative of the complex interrelationships between water, energy, food, and ecosystem. Equal weighting has been preferred in many studies for the same reason (Gan et al., 2017; Momblanch et al., 2018; Simpson, 2020; Simpson et al., 2022). Secondly, this study evaluates the WEFE Nexus at a large watershed scale throughout the 21st century. The reason for not using value judgments, public or expert opinion for weighting the components of the WEFE Nexus in this study is due to the large temporal and spatial scale of the evaluation. Over long periods of time, the value judgments on each resource sector may change considerably, leading to biased or inaccurate results. Additionally, public or expert opinions can also be subjective and influenced by various factors such as personal biases, cultural background, and political views, which can further contribute to a lack of objectivity in the study. In addition, the participatory methods at local scales reflect local conditions, and they cannot be directly applied at larger scales (Gan et al., 2017). Lastly, it was preferred in terms of ease of use, being easily replicated by others, and ease of interpretation of the results. This is also why many other sustainability indices, such as Human Development Index (UNDP, 1990), the Living Planet Index (Loh et al., 1998), Genuine Saving Index (WorldBank, 1999), SDG Index (Sachs et al., 2018) used this method.

Since the equal weighting was employed at the pillar level, some indicators in a pillar have higher weighting as compared to the other. This is due to the fact that not all pillars have the same number of indicators. The final weight distribution of the indicators and the pillars of the WEFE Nexus Index is given in Table 9-3.

Table 9-3. Weight distribution of the WEFE Nexus indicators and pillars

Indicator no	Indicator code	Indicator weight in the index	Pillar	Pillar weight in the index
1	MDC	0.250	Water	0.25
2	IDM	0.250	Food	0.25
3	HPP_MGC	0.083	Energy	0.25
4	CO_2_EG	0.083		
5	RES	0.083		
6	Jan-MMS	0.021	Ecosystem	0.25
7	Feb-MMS	0.021		
8	Mar-MMS	0.021		
9	Apr-MMS	0.021		
10	May-MMS	0.021		
11	Jun-MMS	0.021		
12	Jul-MMS	0.021		
13	Aug-MMS	0.021		
14	Sep-MMS	0.021		
15	Oct-MMS	0.021		
16	Nov-MMS	0.021		
17	Dec-MMS	0.021		

Numerous aggregation methods exist in the literature. The arithmetic mean and the geometric mean are the most commonly used aggregation methods. However, both of these methods allow for compensability between the indicators. There is a higher degree of compensability in the arithmetic mean compared to the geometric mean (Simpson et al., 2022). Compensability means that a low score of one indicator can be compensated by the higher score of another indicator. According to OECD (2008), if an analyst is looking for a non-compensability, then neither arithmetic nor the geometric method can be used. A non-compensatory multi-criteria approach (MCA) is used in such cases. However, it is stated that this method can be computationally costly.

In this study, first the scores of each pillar were estimated using the arithmetic mean of the indicators for that pillar. Then, the pillar scores were averaged to obtain the WEFE Nexus Index score. The main reason for choosing arithmetic mean is because

it is easy to understand and communicate. Arithmetic mean method is also adopted in the development of SDG Index, and the advantage of simplicity in interpretation was stated as the reason for choosing this method (Sachs et al., 2016).

9.4 Results and Discussion

This study delves into the intricacies of the WEFE Nexus under different climatic projections and socioeconomic scenarios. There are two distinct climate projections and a total of three different scenarios evaluated under these climate projections, i.e., RCP4.5_SSP1, RCP4.5_SSP2, and RCP8.5_SSP5. Detailed information about these scenarios can be found in Chapter 8. In this section, WEFE Nexus Index, nexus pillar scores and nexus pillar indicator scores obtained in these scenarios are evaluated on a subbasin basis. The evaluation of these parameters in diverse scenarios offers valuable insights into the intricate interdependencies between water, energy, food, and ecosystem components and their vulnerability to the impacts of climate change and socioeconomic factors.

9.4.1 Upper Sakarya Subbasin

Table 9-4 provides a comparative analysis of the WEFE Nexus indicators for different scenarios representing climate and socioeconomic changes and for different time periods, i.e., near, mid-, and far century, in the Upper Sakarya subbasin. Figure 9-6 presents the same information as Table 9-4 in a visual format, using spider charts to illustrate the values of WEFE Nexus indicators for different time periods and scenarios. The charts provide a clear and concise comparison of the values for each scenario across the different time periods, highlighting the differences that exist between scenarios and time periods. By examining the values for each indicator, a deeper understanding of the complex interplay between water, energy, food, and the

ecosystem can be gained, and how this interplay may evolve over time can be understood. The pillar indices created using these indicators are evaluated in detail under the subtitles Water, Energy, Food, and Ecosystem below.

Table 9-4. WEFE Nexus indicators' comparative analysis for different scenarios in the 21st century: variations over multiple time periods in the Upper Sakarya subbasin

		RCP4.5_SSP1				RCP4.5_SSP2				RCP8.5_SSP5		
		NC	MC	FC		NC	MC	FC		NC	MC	FC
	MDC	0.96	0.96	0.96	MDC	0.99	0.97	0.96	MDC	0.98	0.98	0.95
	HPP_MGC	-	-	-	HPP_MGC	-	-	-	HPP_MGC	-	-	-
	RES	1.00	1.00	1.00	RES	0.00	0.00	0.00	RES	0.00	0.00	0.00
	CO2_EG	0.00	0.00	0.00	CO2_EG	0.00	0.00	0.00	CO2_EG	0.00	0.00	0.00
	IDM	0.36	0.36	0.35	IDM	0.75	0.70	0.60	IDM	0.74	0.68	0.56
	Jan-MMS	1.00	1.00	1.00	Jan-MMS	1.00	1.00	1.00	Jan-MMS	1.00	1.00	1.00
	Feb-MMS	1.00	1.00	1.00	Feb-MMS	1.00	1.00	1.00	Feb-MMS	1.00	1.00	1.00
	Mar-MMS	1.00	1.00	0.97	Mar-MMS	1.00	1.00	1.00	Mar-MMS	1.00	1.00	1.00
	Apr-MMS	1.00	1.00	1.00	Apr-MMS	0.00	0.00	0.00	Apr-MMS	0.00	0.00	0.00
	May-MMS	1.00	1.00	1.00	May-MMS	0.00	0.00	0.00	May-MMS	0.00	0.00	0.00
	Jun-MMS	1.00	1.00	1.00	Jun-MMS	0.00	0.00	0.00	Jun-MMS	0.00	0.00	0.00
	Jul-MMS	1.00	1.00	1.00	Jul-MMS	0.00	0.00	0.00	Jul-MMS	0.00	0.00	0.00
	Aug-MMS	1.00	1.00	1.00	Aug-MMS	0.00	0.00	0.00	Aug-MMS	0.00	0.00	0.00
	Sep-MMS	1.00	1.00	1.00	Sep-MMS	0.00	0.00	0.00	Sep-MMS	0.00	0.00	0.00
	Oct-MMS	1.00	1.00	1.00	Oct-MMS	1.00	1.00	1.00	Oct-MMS	1.00	1.00	1.00
	Nov-MMS	1.00	1.00	1.00	Nov-MMS	1.00	1.00	1.00	Nov-MMS	1.00	1.00	1.00
	Dec-MMS	1.00	1.00	1.00	Dec-MMS	1.00	1.00	1.00	Dec-MMS	1.00	1.00	1.00

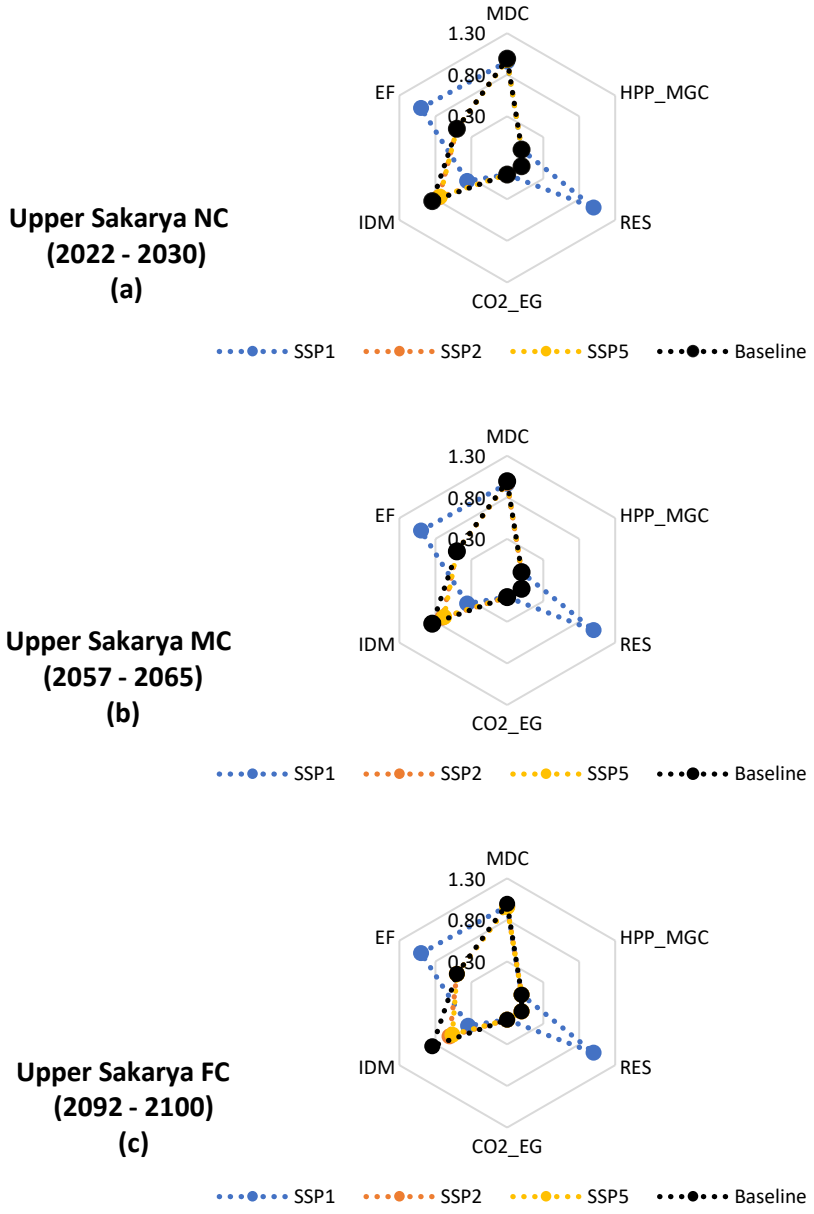

Figure 9-6. Upper Sakarya subbasin: The values of the WEFE Nexus Index Pillar Indicators in each scenario in each future period segment; near century (a), mid-century (b), far century (c). Note: Ecosystem indicator values are not provided in this figure. The parameter EF represents the average of ecosystem indicators, which is equivalent to the Ecosystem pillar value

Water

Figure 9-7 shows that the baseline Water pillar value (0.99) is higher than all scenarios at all times. That is, there will be some deficit in meeting the municipal water demand in the 21st century under all climate and all socioeconomic changes in the Upper Sakarya subbasin. Although the results are very close to each other in all scenarios, the lowest value of the Water pillar (around 0.96) is obtained in the SSP1 scenario in all time periods. The main reason for this is that meeting the environmental flow requirement has the highest priority in the SSP1 scenario which is at the expense of municipal and irrigational water demand coverage. Although it is not clearly seen from Figure 9-7, the Water pillar score increases slightly from the near century to the far century in the SSP1 scenario. This is owing to the improvements in water networks in the SSP1. In contrast to SSP1 scenario, the Water pillar value continuously decreases from the beginning to the end of the 21st century in the SSP2 scenario. The SSP5 scenario, on the other hand, starts with a score less than SSP2 in the near century, reaches a higher score than SSP2 in the mid-century, and reaches a lower score than SSP2 in the far century.

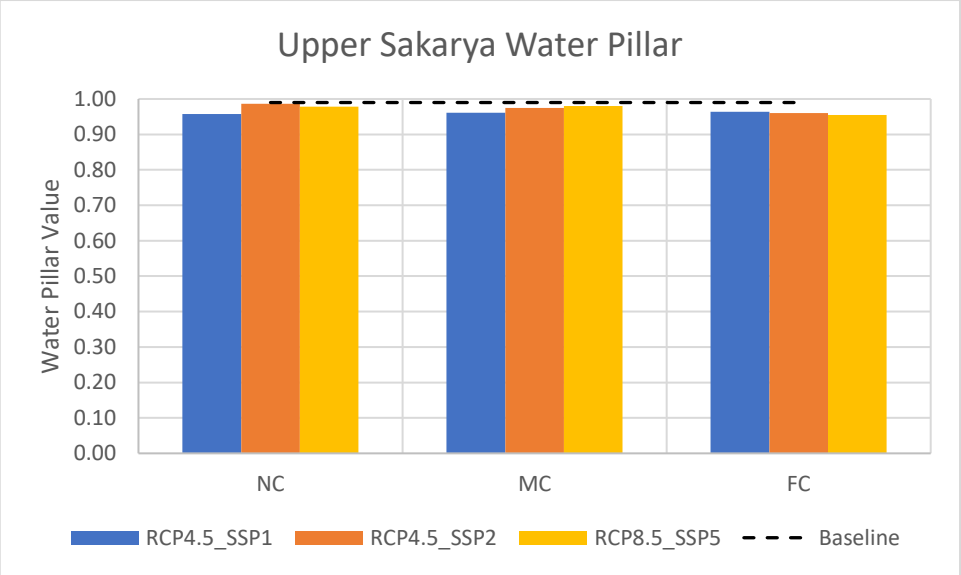

Figure 9-7. Water pillar value under climate and socioeconomic changes in the Upper Sakarya subbasin.

Energy

In the Upper Sakarya subbasin, the electricity is generated only by the thermal power plants in the baseline period. There is no renewable power plant in this period. Thus, the baseline Energy pillar value is zero (Figure 9-8). There are no renewable power plants planned to be built during the 21st century in the SSP2 and SSP5 scenarios. This causes the CO_2_EG and RES indicators to take the zero value (Figure 9-6) and which in turn results in the Energy Pillar value of zero. The highest and the only above zero value (0.50) of Energy pillar is obtained in the SSP1 scenario since the SSP1 scenario makes maximum use of the basin's renewable energy potential. The Energy pillar score is 0.50 throughout the 21st century. This is firstly due to the fact that there is no HPP currently built or planned to be built in the Upper Sakarya subbasin in any of the scenarios. Thus, the indicator HPP_MGC is not evaluated in the Upper Sakarya subbasin. In the SSP1 scenario, the indicator RES takes the value

of one in all time periods which means that the 30% renewable share target is met. However, while the indicator CO_2_EG always takes the value of 0.00. This means that the thermal power plants in the basin produce the same or more electricity than the base case. Therefore, the overall Energy pillar value is 0.50.

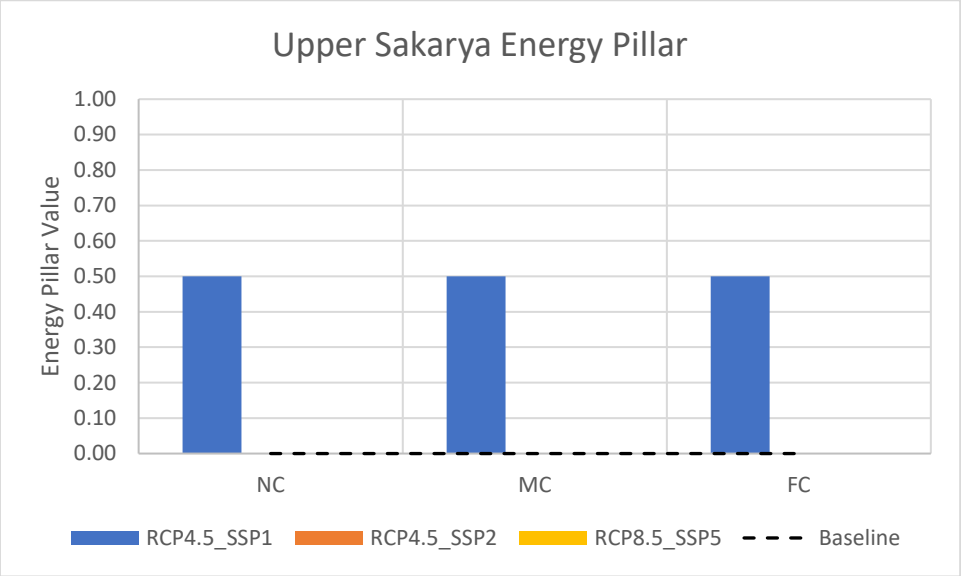

Figure 9-8. Energy pillar value under climate and socioeconomic changes in the Upper Sakarya subbasin.

Food

Figure 9-9 shows that the baseline value of the Food pillar (0.84) is higher than all scenarios at all times. This means that there will be more agricultural irrigation deficit in the Upper Sakarya subbasin in the future compared to the current situation. When the scores of each scenario are compared, it is seen that the SSP2 scenario achieves the highest score in all time periods. However, the SSP2 and SSP5 scenarios have close Food pillar value in each time period. Figure 9-9 also shows that there is a significant difference between the scores of the SSP1 and other scenarios which is mainly due to the strict environmental flow requirements imposed in the SSP1

scenario, as discussed previously. In the SSP2 and SSP5 scenarios, the value of the Food pillar decreases over time. In the SSP1 scenario, on the other hand, it remains almost constant around 0.36 throughout all time.

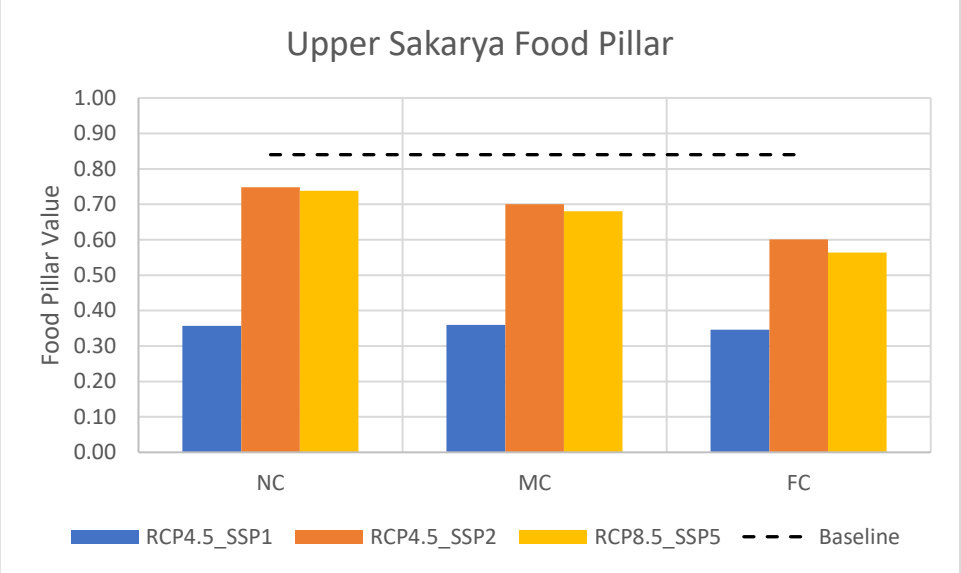

Figure 9-9. Food pillar value under climate and socioeconomic changes in the Upper Sakarya subbasin.

Ecosystem

The comparison of the simulated median monthly flows with the IQR of the naturalized streamflow in each scenario in each time period is given in Figure 9-10. The first, second, and the third row of this figure shows the results of the SSP1, SSP2, and SSP5 scenario, respectively. As it can be seen from Figure 9-10, the MMS values in all months in each time period is within the IQR in the SSP1 scenario. Thus, each indicator of the Ecosystem pillar takes the value of one. As a result, the score of the Ecosystem pillar is one. While the SSP1 scenario maximizes the Ecosystem pillar value, this creates deficits in other pillars, i.e., Water and Food. Especially the deficit in the Food pillar is at significant levels in the SSP1 scenario. In the SSP2 and SSP5

scenario, the score of the Ecosystem pillar is 0.50 in all time periods (Figure 9-11) which means that the MMS values in six months of the year, i.e., April, May, June, July, August, September, and October, are outside the IQR of the naturalized streamflow (Figure 9-11). These are the months when the need for agricultural irrigation is high. It is understood that the water that should be given for environmental flow in SSP2 and SSP5 scenarios is used in agricultural irrigation. In the SSP1 scenario, on the contrary, the water is first allocated to the environmental flow and this causes a deficit in agricultural irrigation.

When examining the Ecosystem pillar indicators' scores separately, a clear pattern emerged during the low (October – March) and high (April – September) flow periods. But how do these periods compare to each other in terms of the health of the ecosystem? To answer this question, a closer look is taken at the scores for each period, while also comparing each period for different scenarios. The results of this analysis are presented in Table 9-5. This table shows the 21st century average Ecosystem pillar scores for the low and high flow periods. As discussed earlier in Chapter 7, both high- and low-flow events can be critical to the survival and diversity of river biota. The results showed that there is no problem in terms of ecosystem health in both low and high flow periods in the SSP1 scenario. However, in the SSP2 and SSP5 scenarios, while the ecosystem pillar score is 1 in the low flow period, it is 0 in the high flow period. This shows that in these scenarios, high flow events that are critical for ecosystem productivity and diversity are unsustainably affected.

NF-Q1: Naturalized Streamflow Lower Quartile; NF-Q3: Naturalized Streamflow Upper Quartile; MMS: Simulated Median Monthly Streamflow

Figure 9-10. Upper Sakarya: The comparison of the simulated median monthly flows with the IQR of the naturalized streamflow in each scenario in each time period. First row: SSP1; Second row: SSP2; Last row: SSP5

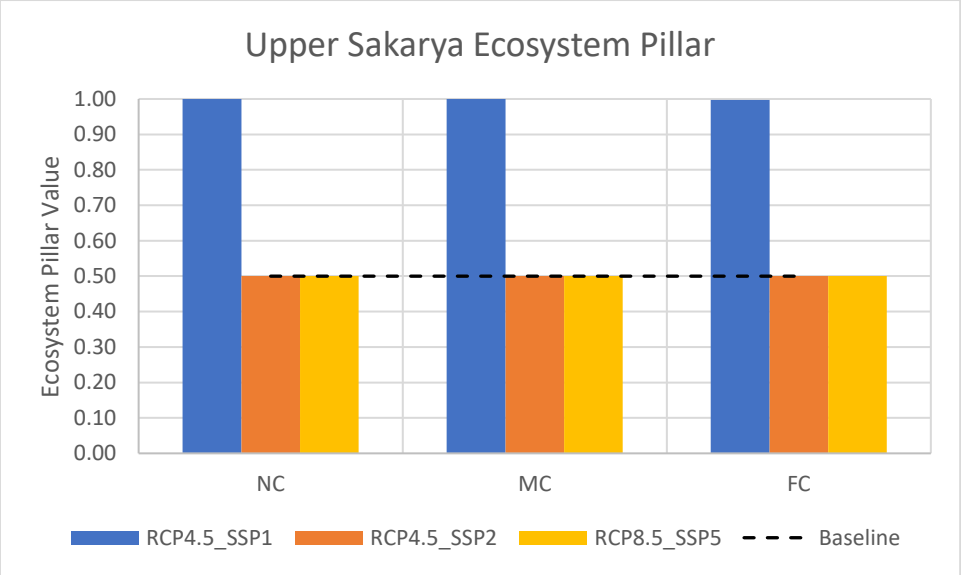

Figure 9-11. Ecosystem pillar value under climate and socioeconomic changes in the Upper Sakarya subbasin.

Table 9-5. 21st century average ecosystem pillar scores for low and high flow periods in Upper Sakarya subbasin

	SSP1	SSP2	SSP5
October – March (low flow period)	1.00	1.00	1.00
April -September (high flow period)	1.00	0.00	0.00

Aggregated WEFE Index

After scores of all nexus pillars are calculated and aggregated, the values of the WEFE Nexus Index given in Figure 9-12 are obtained. This figure shows that the baseline value of WEFE Nexus Index (0.58) is higher than the scores of SSP2 and SSP5 scenarios at all times. This is expected since each pillar value in these scenarios is lower compared to the baseline period. The highest score of the WEFE Nexus

Index, which is around 0.70 in all time periods, belongs to the SSP1 scenario. The lowest score of all time (0.50) belongs to the SSP5 scenario in the far century. However, the SSP2 and the SSP5 scenarios have close WEFE Nexus Index values in each time period. The most important reason why the SSP1 scenario has the highest WEFE Nexus Index value compared to other scenarios is that the Energy pillar value has the highest value in the SSP1 scenario. In the Upper Sakarya subbasin no significant electricity generation takes place in the baseline and, SSP2 and SSP5 scenarios. However, as the SSP1 scenario makes maximum use of the basin's renewable energy potential, the energy Pillar value is high in this scenario hence the high WEFE Nexus Index value difference between SSP1 and other scenarios. Furthermore, while the SSP1 scenario completely satisfies the ecosystem flow requirements, other scenarios have half of the score of the SSP1 scenario. Although there is a significant deficit in the Food pillar in the SSP1 scenario, this is compensated by the high scores in the Energy and Ecosystem pillars.

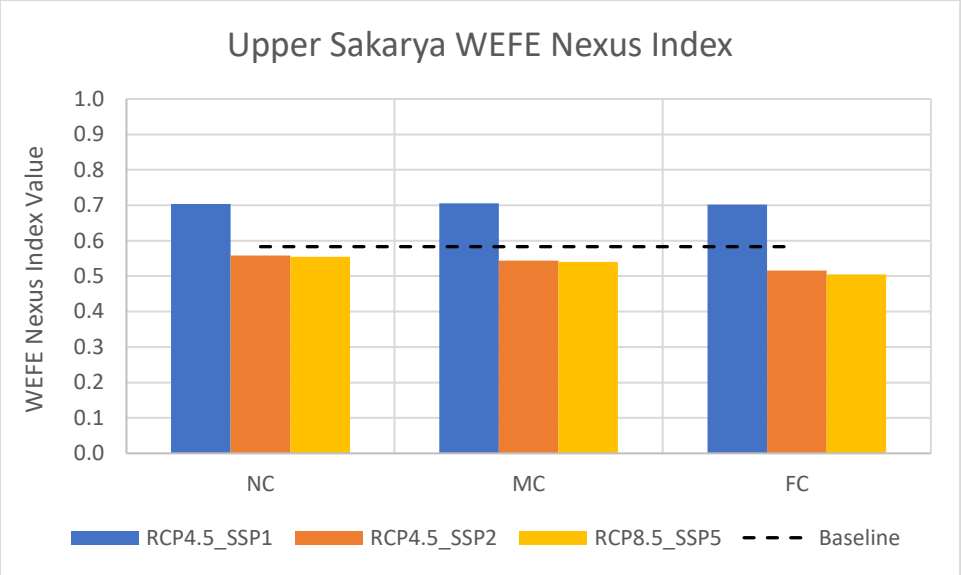

Figure 9-12. WEFE Nexus Index value under climate and socioeconomic changes in the Upper Sakarya subbasin.

The results indicate that the connections between the Water, Food and Ecosystem pillar come to the fore in the Upper Sakarya subbasin. Upper Sakarya is a subbasin where agricultural activities are intense. Based on the scenario results it is estimated that there will be significant irrigational demand deficit if strict environmental flow requirements are employed in the 21st century. Within the scope of this study, the techniques improving irrigation efficiency such as drip irrigation, crop rotation, and conservation tillage are not evaluated. However, such techniques would help to maintain the balance between the pillars. Furthermore, environmental flow requirements employed in the SSP1 scenario aim to achieve natural flow conditions. The results show that it is not realistic to aim for unmodified conditions in the subbasin. Thus, the initial flow management targets should be stretched to obtain more balanced results for all pillars. The results also show that even if there is no environmental flow requirement (SSP2 and SSP5 scenarios), there will be irrigational demand deficit, which is around %30, if current practices continue. This

is also valid for the municipal water demand coverage. In these scenarios, it is predicted that the deficit will be around 3% on average. As it can be understood from all these results, the most sustainable results will be obtained in the SSP1 scenario, in which applications that increase agricultural irrigation efficiency are included and the initial environmental flow management targets are stretched.

9.4.2 Porsuk Subbasin

Table 9-6 provides a comparative analysis of the WEFE Nexus indicators for different scenarios representing climate and socioeconomic changes and for different time periods, i.e., near, mid-, and far century, in the Porsuk subbasin. Figure 9-13 presents the same information as Table 9-6 in a visual format, using spider charts to illustrate the values of WEFE Nexus indicators for different time periods and scenarios. The charts provide a clear and concise comparison of the values for each scenario across the different time periods, highlighting the differences that exist between scenarios and time periods. By examining the values for each indicator, a deeper understanding of the complex interplay between water, energy, food, and the ecosystem can be gained, and how this interplay may evolve over time can be understood. The pillar indices created using these indicators are evaluated in detail under the subtitles Water, Energy, Food, and Ecosystem below.

Table 9-6. WEFE Nexus indicators' comparative analysis for different scenarios in the 21st century: variations over multiple time periods in the Porsuk subbasin

		NC	MC	FC			NC	MC	FC			NC	MC	FC
RCP4.5_SSP1	MDC	0.99	0.99	0.99	**RCP4.5_SSP2**	MDC	0.98	0.94	0.91	**RCP8.5_SSP5**	MDC	0.97	0.96	0.93
	HPP_MGC	-	-	-		HPP_MGC	-	-	-		HPP_MGC	-	-	-
	RES	0.16	0.64	0.93		RES	0.06	0.12	0.12		RES	0.06	0.12	0.12
	CO2_EG	0.12	0.05	0.03		CO2_EG	0.04	0.01	0.00		CO2_EG	0.03	0.02	0.01
	IDM	0.44	0.46	0.42		IDM	0.86	0.81	0.71		IDM	0.85	0.77	0.65
	Jan-MMS	1.00	1.00	1.00		Jan-MMS	1.00	1.00	1.00		Jan-MMS	1.00	1.00	1.00
	Feb-MMS	1.00	1.00	1.00		Feb-MMS	1.00	1.00	0.00		Feb-MMS	1.00	1.00	1.00
	Mar-MMS	1.00	1.00	1.00		Mar-MMS	1.00	1.00	1.00		Mar-MMS	1.00	1.00	1.00
	Apr-MMS	1.00	1.00	1.00		Apr-MMS	1.00	1.00	1.00		Apr-MMS	1.00	1.00	0.00
	May-MMS	1.00	1.00	1.00		May-MMS	0.00	0.00	0.00		May-MMS	0.00	0.00	0.00
	Jun-MMS	1.00	1.00	1.00		Jun-MMS	0.00	0.00	0.00		Jun-MMS	0.00	0.00	0.00
	Jul-MMS	1.00	1.00	1.00		Jul-MMS	0.00	0.00	0.00		Jul-MMS	0.00	0.00	0.00
	Aug-MMS	0.19	0.00	0.67		Aug-MMS	0.00	0.00	0.00		Aug-MMS	0.00	0.00	0.00
	Sep-MMS	1.00	1.00	1.00		Sep-MMS	0.00	0.00	0.00		Sep-MMS	0.00	0.00	0.00
	Oct-MMS	0.00	1.00	1.00		Oct-MMS	0.00	1.00	1.00		Oct-MMS	0.37	0.81	0.42
	Nov-MMS	1.00	0.78	0.89		Nov-MMS	0.00	0.88	1.00		Nov-MMS	0.61	1.00	1.00
	Dec-MMS	1.00	0.93	1.00		Dec-MMS	0.00	0.34	1.00		Dec-MMS	1.00	0.84	1.00

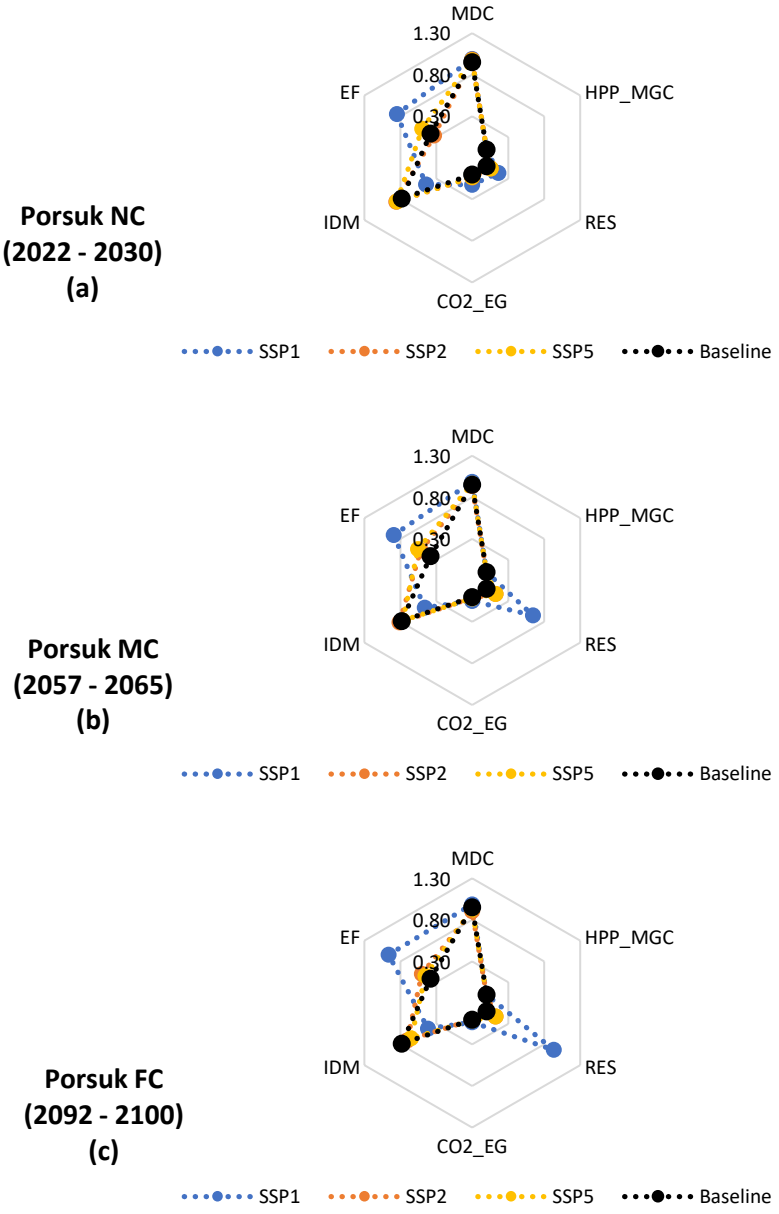

Figure 9-13. Porsuk subbasin: The values of the WEFE Nexus Index Pillar Indicators in each scenario in each future period segment; near century (a), mid-century (b), far century (c). Note: Ecosystem indicator values are not provided in this figure. The parameter EF represents the average of ecosystem indicators, which is equivalent to the Ecosystem pillar value

Water

Figure 9-14 shows that the value of the Water pillar ranges between 0.91 and 0.99 in the Porsuk subbasin. The highest Water pillar score (approximately 0.99) is obtained in the SSP1 scenario at all times. In addition, SSP1 is the only scenario which achieves higher scores than the baseline score of 0.95 in all time periods. The lowest Water pillar score (0.91) is obtained in the SSP2 scenario in the far century. In the SSP2 and SSP5 scenarios, the value of the Water pillar decreases over time. The values that are 0.98 and 0.97 respectively for the SSP2 and SPP5 at the beginning of the near century decrease to 0.91 and 0.93 in the far century. In the SSP1 scenario, the score remains nearly constant around 0.99. The most striking result is the fact that there is almost no deficit in the municipal water demand despite stringent environmental flow requirements in the SSP1 scenario. This proves that it is of great importance to prevent losses in the water supply network. In this way, it is possible to close the gaps that environmental flows may create in meeting the municipal water demand.

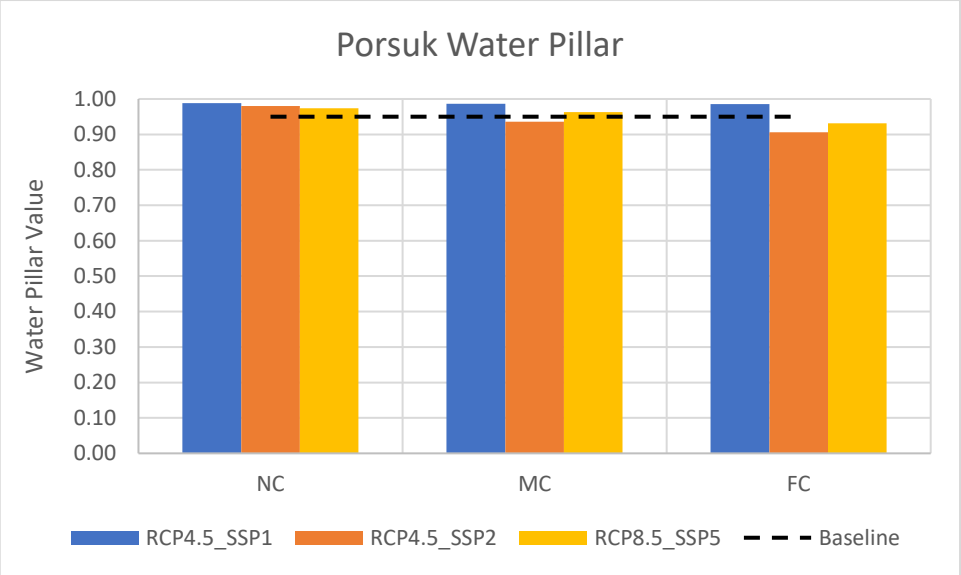

Figure 9-14. Water pillar value under climate and socioeconomic changes in the Porsuk subbasin

Energy

In the Porsuk subbasin, the electricity is produced by the thermal power plants in the baseline period. Thus, the renewable energy share is zero. In addition, there is no HPP currently built or planned to be built in the Porsuk subbasin. Hence, HPP_MGC indicator is not evaluated in this subbasin. As a result, the base case Energy pillar value is zero (Figure 9-15). All scenarios have higher scores of Energy pillar compared to the baseline. The highest Energy pillar value is obtained in the SSP1 scenario in all time periods. This is expected since SSP1 scenario aims to use renewable energy resources at the maximum. In the SSP1 scenario, it is seen that the Energy pillar value, which starts at the level of 0.14 in the near century, reaches the level of 0.48 at the end of the century. Towards the end of the century, the 30% renewable energy share target is almost reached with a RES value of 0.93 (Figure 9-13) in the SSP1 scenario. The value of the CO_2_EG ranges between 0.03 and 0.12.

The value of this indicator decreases in time since the sustainability target changes from 50% in near and mid-century to 100% in the far century. The results show that even the SSP1 scenario is far from the sustainability target for the CO_2_EG indicator. This implies that the thermal power plants need to be phased out while renewable power plants are being built. The results obtained in the SSP2 and SSP5 scenarios are very close to each other. The all-time average of Energy pillar is 0.06 in both scenarios which refers to an unsustainable state.

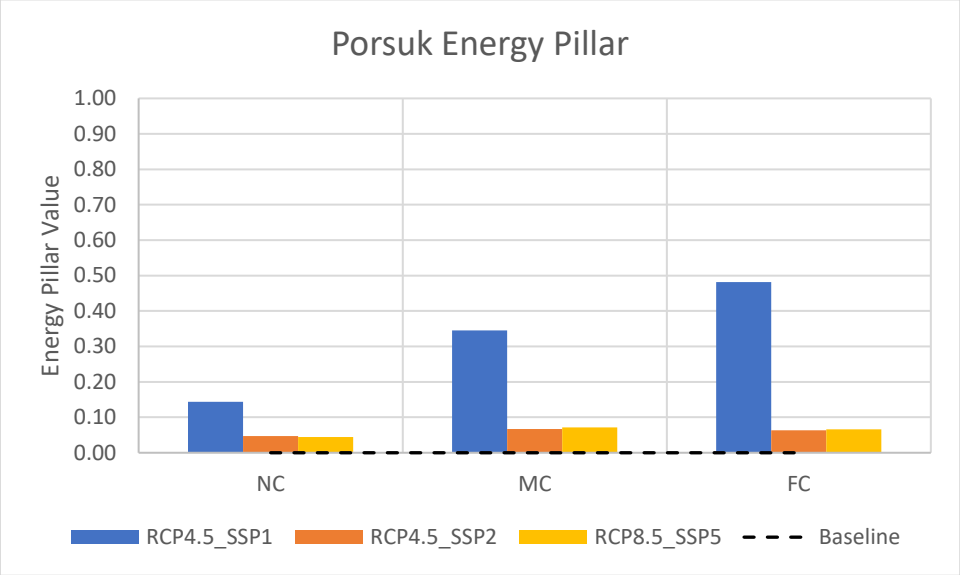

Figure 9-15. Energy pillar value under climate and socioeconomic changes in the Porsuk subbasin

Food

Figure 9-16 shows that the Food pillar value in the SSP1 scenario is the lowest among all scenarios at all times. Average Food pillar value in the 21st century is 0.44, 0.79 and 0.76 in SSP1, SSP2 and SSP5 scenarios, respectively. The fact that the environmental flow requirement has the highest priority in the SSP1 scenario creates

significant irrigation demand deficit in the Porsuk subbasin. It is seen that the deficit, which is approximately 22% in the baseline period, increases to an average of 56% in the SSP1 scenario. The Food pillar takes its highest value (0.86) in the SSP2 scenario in the near century. Although the Food pillar score is still higher than the score in the baseline period (0.78) in the mid-century, the score drops to 0.71 in the far century. SSP5 scenario shows similar results to the SSP2 scenario. The Food pillar value gradually decreases from 0.85 in the near century to 0.77 in the mid- and 0.65 in the far century.

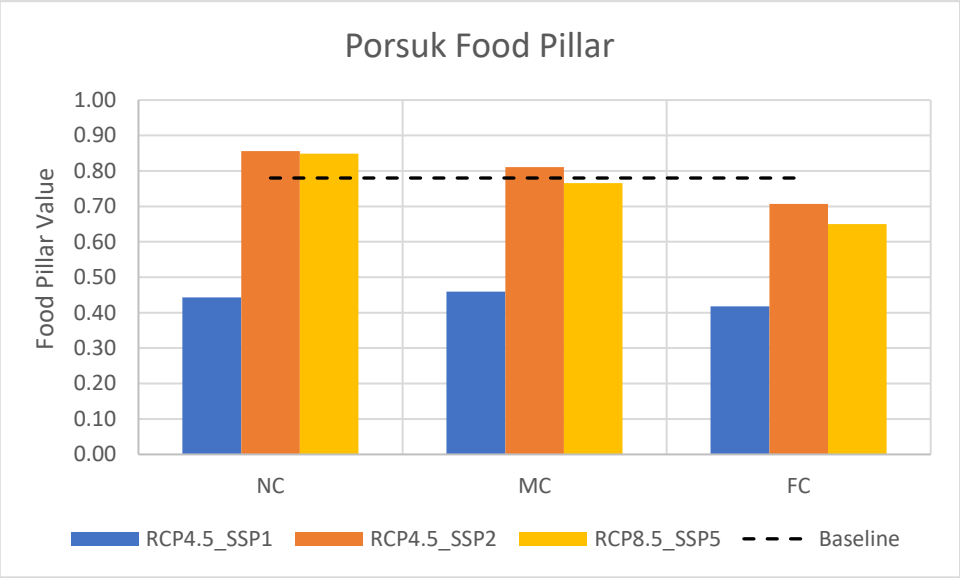

Figure 9-16. Food pillar value under climate and socioeconomic changes in the Porsuk subbasin

Ecosystem

The comparison of the simulated median monthly flows with the IQR of the naturalized streamflow in each scenario in each time period is given in Figure 9-17. The first, second, and the third row of this figure shows the results of the SSP1, SSP2, and SSP5 scenario, respectively. In the SSP1 scenario, the median monthly

streamflow in the near century is outside the IQR range only in August and October. In the mid-century, the number of months outside the IQR increases to three, i.e., August, November and December. In the far century, median streamflow values in August and November fall outside the IQR. Thus, the Ecosystem pillar value in the SSP1 scenario is 0.85, 0.89, and 0.96 in the near, mid- and far century, respectively (Figure 9-18). The Ecosystem pillar value takes its highest score in the SSP1 scenario at all time periods. In the SSP2 scenario, IQR target is achieved in just 4 months (January, February, March and April) in near century, and the Ecosystem pillar value is 0.33 in this period. In the mid-century, the Ecosystem pillar value increases to 0.52 which also corresponds to the highest score in the SSP2 scenario, and the median monthly streamflow falls inside the IQR in January, February, March, April, and October. The Ecosystem pillar score is calculated as 0.50 in the far century, and the streamflow is outside the IQR in six months. In the SSP5 scenario, the Ecosystem pillar value is 0.50, 0.55, and 0.45 in the near, mid- and far century, respectively. In the near century, IQR target is achieved in the months of January, February, March, April, and December. In the mid-century, the median streamflow values in the months of January, February, March, April and November are inside the IQR. Lastly, in the far century, the median streamflow values of January, February, March, November, and December satisfy the IQR target. The most sustainable Ecosystem pillar scores are obtained in the SSP1 scenario at the expense of deficit in the irrigational demand coverage. On the other hand, it is seen that the environmental flows, having the highest priority in the SSP1, do not cause any problems in terms of the municipal water demand coverage, but better results are obtained compared to other scenarios. The fact that there is no hydroelectric power plant in the Porsuk subbasin prevents potential hydroelectric generation problems that may occur due to strict environmental flow practices. In addition, the dependence on water availability in energy production decreases significantly towards the end of the century, thanks

to solar and wind power plants with almost zero water consumption, and this allows the value of Energy pillar to gradually improve.

By examining the scores of each Ecosystem pillar indicators, a distinct pattern was observed during the low (October - March) and high (April - September) flow periods. However, to evaluate the relative health of the ecosystem during these periods, a closer examination of the scores for each period and comparisons across different scenarios is necessary. The results of this analysis are presented in Table 9-7, which illustrates the 21st century average Ecosystem pillar scores for the low and high flow periods. As mentioned earlier in Chapter 7, both high- and low-flow events are crucial for the survival and diversity of river biota. As can be seen from Table 9-7, the Ecosystem pillar score obtained in the high flow period is lower than the score obtained in the low flow period especially in the SSP2 and SSP5 scenarios. The results show that the occurrence of high flow events is significantly affected, which can have detrimental effects on the ecosystem's productivity and diversity.

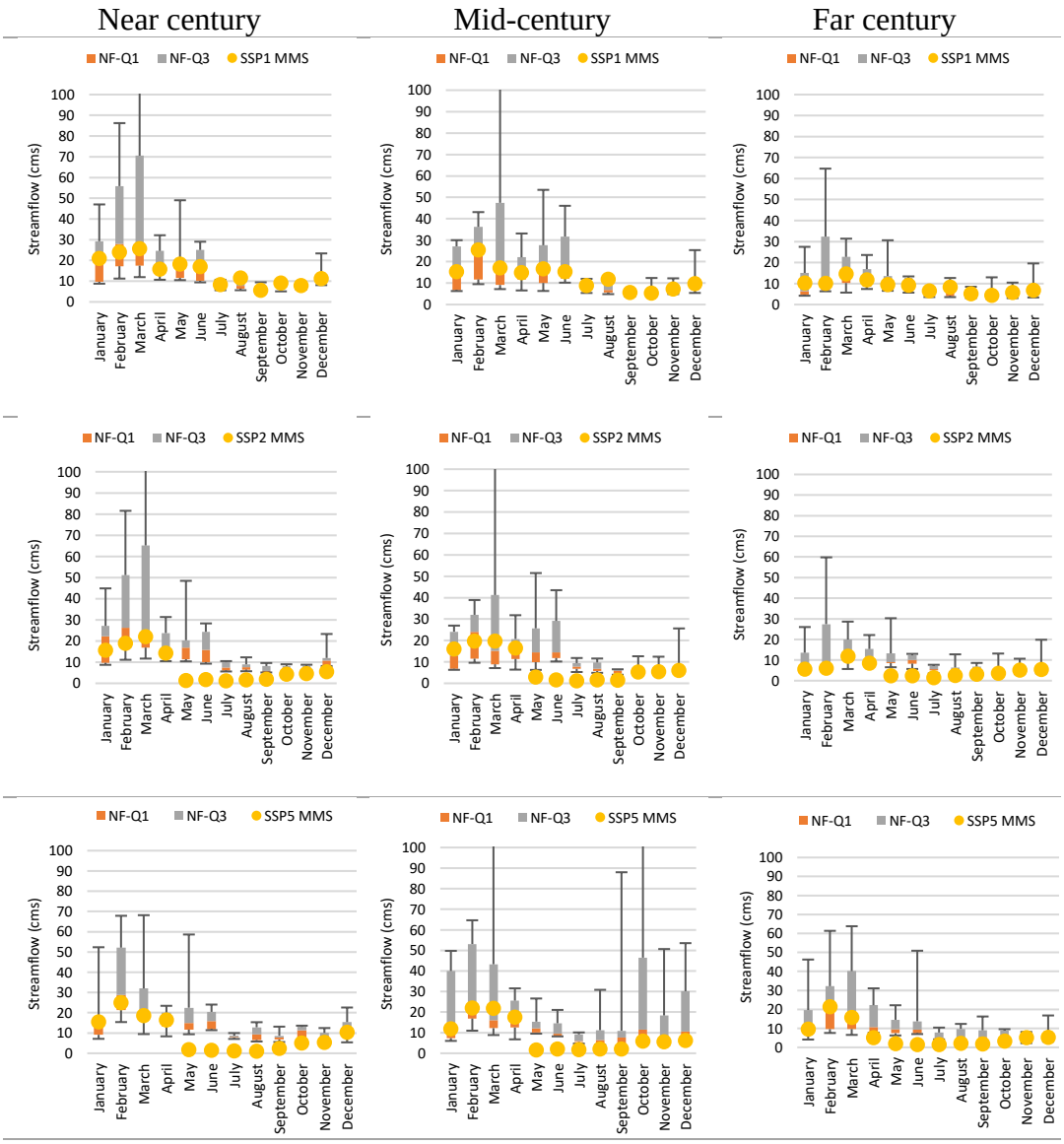

NF-Q1: Naturalized Streamflow Lower Quartile; NF-Q3: Naturalized Streamflow Upper Quartile; MMS: Simulated Median Monthly Streamflow

Figure 9-17. Porsuk: The comparison of the simulated median monthly flows with the IQR of the naturalized streamflow in each scenario in each time period. First row: SSP1; Second row: SSP2; Last row: SSP5

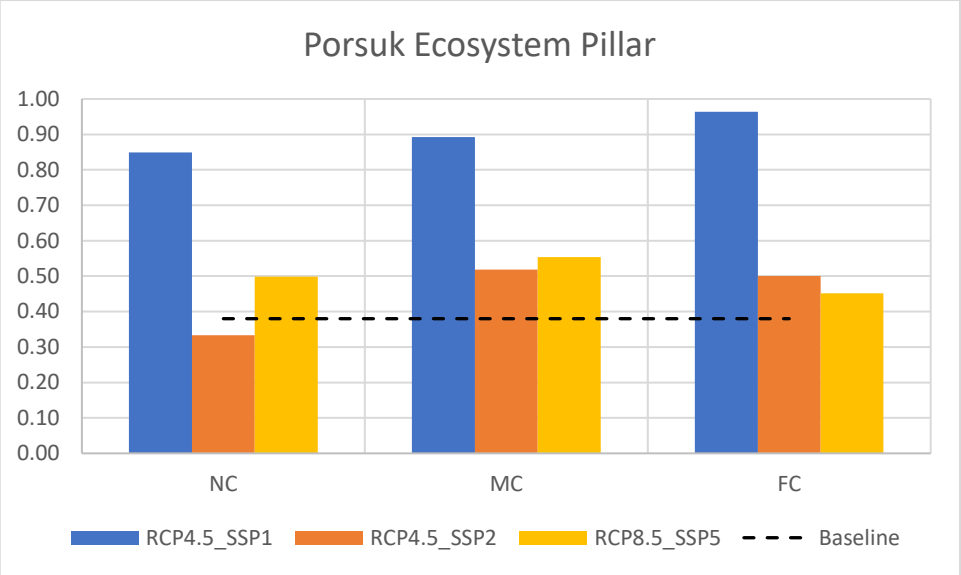

Figure 9-18. Ecosystem pillar value under climate and socioeconomic changes in the Porsuk subbasin

Table 9-7. 21st century average ecosystem pillar scores for low and high flow periods in Porsuk subbasin

	SSP1	SSP2	SSP5
October – March (low flow period)	0.92	0.73	0.89
April -September (high flow period)	0.88	0.17	0.11

Aggregated WEFE Index

After scores of all pillars are calculated and aggregated, the values of the WEFE Nexus Index given in Figure 9-19 are obtained. This figure shows that all scenarios have higher scores of WEFE Nexus Index compared to the baseline score of 0.53, except the SSP5 scenario in the far century. The highest scores are obtained in the SSP1 scenario in all time periods. This is expected since the highest scores of three

pillars namely Water, Energy and Ecosystem are calculated in the SSP1 scenario in each future period segment. The lowest score of all time (0.52) belongs to the SSP5 scenario in the far century. However, the SSP2 and SSP5 scenarios have close WEFE Nexus Index values in each time period. The major difference between SSP1 and other scenarios is due to the scores obtained for the Ecosystem pillar. Moreover, the fact that SSP1 scenario makes maximum use of the basin's renewable energy potential contributes to the highest score of WEFE Nexus Index in the SSP1 scenario. In addition, there is almost no municipal water demand deficit in the SSP1 scenario.

The results highlight especially the Water-Food-Ecosystem relationship in the Porsuk subbasin. Agricultural activities are intense especially in the downstream side of the subbasin. In addition, during the field studies (Alp et al., 2020), the authorities reported that too many illegal wells were detected for agricultural irrigation in this region. The SSP1 scenario results show that if strict environmental flow requirements are adopted in the watershed, there will be serious deficits in agricultural irrigation (56% on average). However, even in the SSP2 scenario with the highest Food pillar score, where no environmental flow is released, a deficit of around 21% is calculated on average. This actually reveals the importance of techniques to increase irrigation efficiency. For this purpose, it is important to adopt agricultural best management practices such as efficient irrigation techniques and planting products that require less water, both in terms of protecting the environment and not affecting the agricultural productivity. Moreover, environmental flow requirements adopted in the SSP1 scenario aim to upgrade the environmental status to unmodified conditions. In the baseline period, the Ecosystem pillar value is 0.38 which implies that the current environmental status of the river is already far from the natural conditions. Therefore, it seems that adopting slightly or moderately modified status instead of natural flow conditions in the SSP1 scenario can achieve the most sustainable condition for all pillars. The results also indicate that the average municipal water demand deficit in the SSP2 and SSP5 scenarios is 6% and 4%,

respectively. This reveals the importance of sustainable practices in the SSP1 scenario, where almost no municipal water demand deficit is calculated. In addition, the climate projections in the Porsuk basin show that the average precipitation in the 21st century will be less than the historical average. Furthermore, statistically significant increasing trends are detected in all temperature projections. Decreased rains and increasing temperatures mean that water availability in the basin will decrease compared to the base case. Therefore, practices that will increase productivity in drinking water and agricultural irrigation are of great importance in terms of the security of the WEFE Nexus components.

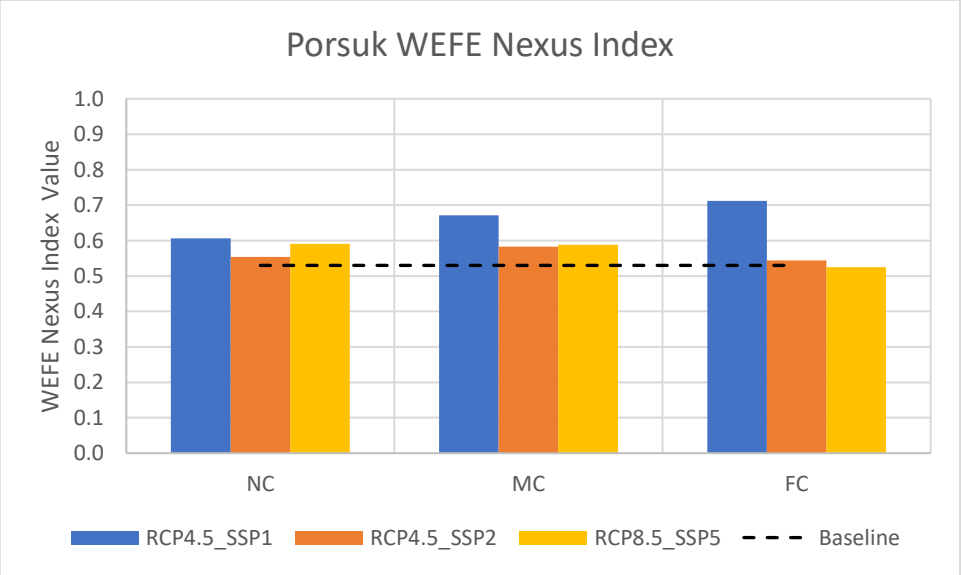

Figure 9-19. WEFE Nexus Index value under climate and socioeconomic changes in the Porsuk subbasin.

9.4.3 Ankara Subbasin

Table 9-8 provides a comparative analysis of the WEFE Nexus indicators for different scenarios representing climate and socioeconomic changes and for different time periods, i.e., near, mid-, and far century, in the Ankara subbasin. Figure 9-20 presents the same information as Table 9-8 in a visual format, using spider charts to illustrate the values of WEFE Nexus indicators for different time periods and scenarios. The charts provide a clear and concise comparison of the values for each scenario across the different time periods, highlighting the differences that exist between scenarios and time periods. By examining the values for each indicator, a deeper understanding of the complex interplay between water, energy, food, and the ecosystem can be gained, and how this interplay may evolve over time can be understood. The pillar indices created using these indicators are evaluated in detail under the subtitles Water, Energy, Food, and Ecosystem below.

Table 9-8. WEFE Nexus indicators' comparative analysis for different scenarios in the 21st century: variations over multiple time periods in the Ankara subbasin

		NC	MC	FC			NC	MC	FC			NC	MC	FC
RCP4.5_SSP1	MDC	0.96	0.90	0.97	**RCP4.5_SSP2**	MDC	0.98	0.94	0.91	**RCP8.5_SSP5**	MDC	0.97	0.96	0.93
	HPP_MGC	-	-	-		HPP_MGC	-	-	-		HPP_MGC	-	-	-
	RES	0.32	0.51	0.68		RES	0.06	0.12	0.12		RES	0.06	0.12	0.12
	CO2_EG	0.11	0.04	0.02		CO2_EG	0.04	0.01	0.00		CO2_EG	0.03	0.01	0.00
	IDM	0.53	0.48	0.51		IDM	0.86	0.81	0.71		IDM	0.85	0.77	0.65
	Jan-MMS	1.00	1.00	0.98		Jan-MMS	1.00	1.00	0.90		Jan-MMS	1.00	1.00	1.00
	Feb-MMS	1.00	1.00	1.00		Feb-MMS	1.00	1.00	1.00		Feb-MMS	1.00	1.00	1.00
	Mar-MMS	1.00	1.00	1.00		Mar-MMS	1.00	1.00	1.00		Mar-MMS	1.00	1.00	1.00
	Apr-MMS	1.00	1.00	1.00		Apr-MMS	1.00	1.00	0.19		Apr-MMS	1.00	0.26	1.00
	May-MMS	1.00	1.00	1.00		May-MMS	1.00	1.00	1.00		May-MMS	1.00	1.00	0.91
	Jun-MMS	1.00	1.00	0.80		Jun-MMS	1.00	1.00	0.21		Jun-MMS	1.00	1.00	1.00
	Jul-MMS	0.00	0.00	0.00		Jul-MMS	0.00	0.00	0.00		Jul-MMS	0.40	0.00	0.14
	Aug-MMS	0.00	0.00	0.67		Aug-MMS	0.00	0.00	0.50		Aug-MMS	1.00	1.00	0.94
	Sep-MMS	0.87	0.14	0.00		Sep-MMS	0.68	0.00	0.00		Sep-MMS	0.00	0.68	0.53
	Oct-MMS	0.52	0.05	0.70		Oct-MMS	0.00	0.00	0.50		Oct-MMS	0.51	1.00	0.35
	Nov-MMS	0.96	0.01	0.08		Nov-MMS	0.28	0.00	0.00		Nov-MMS	0.38	0.00	0.00
	Dec-MMS	1.00	1.00	1.00		Dec-MMS	1.00	1.00	0.55		Dec-MMS	1.00	0.42	1.00

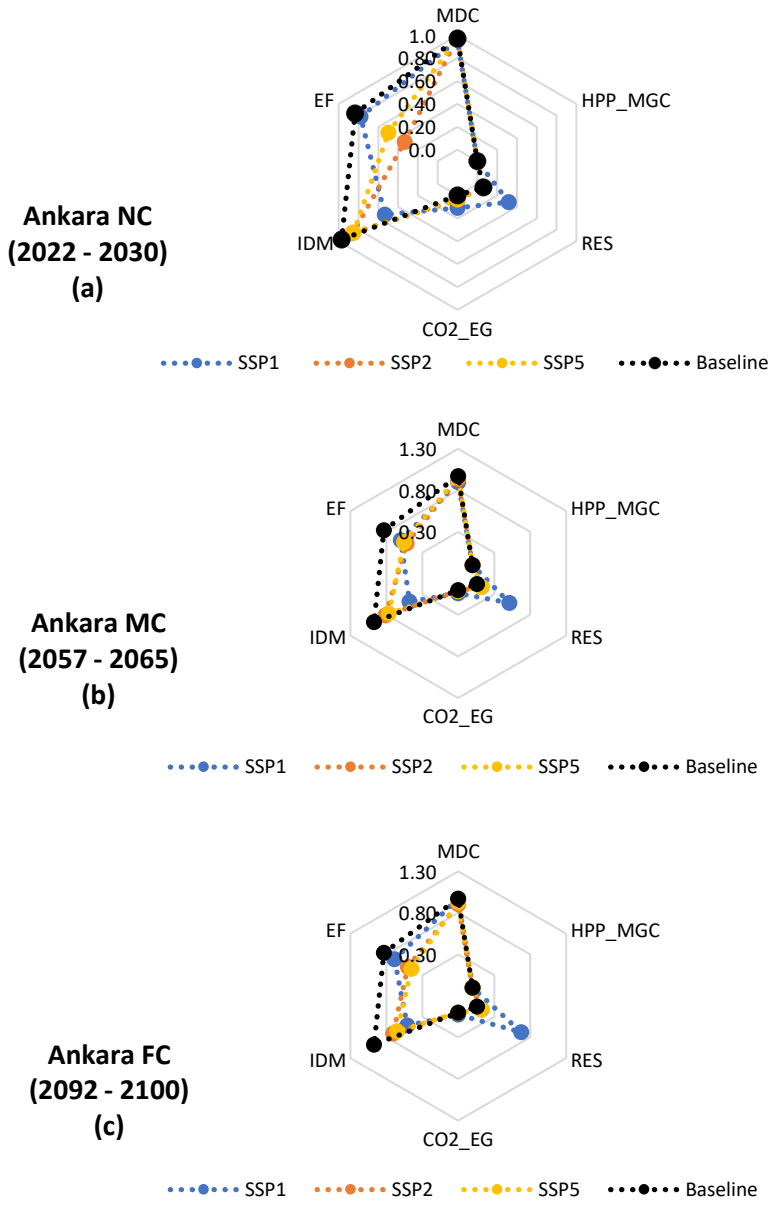

Figure 9-20. Ankara subbasin: The values of the WEFE Nexus Index Pillar Indicators in each scenario in each future period segment; near century (a), mid-century (b), far century (c). Note: Ecosystem indicator values are not provided in this figure. The parameter EF represents the average of ecosystem indicators, which is equivalent to the Ecosystem pillar value

Water

Figure 9-21 shows that the higher scores than the baseline Water pillar score of 0.97 were only achieved in near century SSP2 and SSP5 scenarios. In the near century, both SSP2 and SSP5 scenario have a score of one which corresponds to 100% coverage of municipal water demand. SSP1 scenario, on the other hand, has a score of 0.96. Average water pillar values of all times are 0.94, 0.83, and 0.83 for the SSP1, SSP2, and SSP5, respectively. Although the SSP2 and SSP5 scenarios appear to be best performing scenarios at the beginning of the 21st century, towards the end of the century SSP2 and SSP5 scores decreases to 0.70 and 0.73, respectively. The lowest value of the Water pillar (0.70) is obtained in the SSP2 scenario in the far century. This means that current policies will not be sufficient to meet the demand for municipal water in the Ankara subbasin, which hosts a city like Ankara with significant water needs. SSP1 scenario seems to be the most sustainable scenario in this sense. However, even in the SSP1 scenario, there will be an average deficit of 6%. The main reason for this is the environmental flow demand in the SSP1 scenario. The environmental flow demand creates nexus tension especially in terms of the Water and Food (Figure 9-23) pillars.

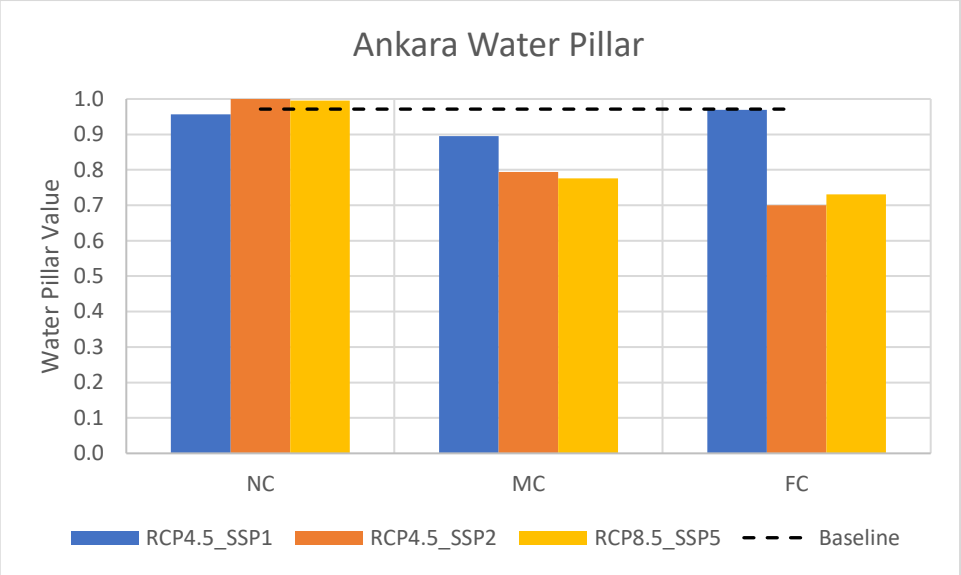

Figure 9-21. Water pillar value under climate and socioeconomic changes in the Ankara subbasin

Energy

All of the power plants that produce significant levels of electricity in the Ankara subbasin are thermal power plants. There is no HPP currently built or planned to be built in the Ankara subbasin. As a result, HPP_MGC indicator is not evaluated in this subbasin. There are biomass fueled power plants as well as fossil fuel power plants. Most of these plants have a wet cooling system. Therefore, water consumption is at significant levels. The baseline Energy pillar value is 0.06 (Figure 9-22). All of the scenarios have higher scores of Energy pillar than the baseline. The best Energy pillar score belongs to the SSP1 scenario in all time periods. This is because of the fact that the SSP1 scenario aims to benefit as much as possible from the renewable energy potential of the basin. In the SSP1 scenario, the Energy pillar value starts with a score of 0.21 in the near century, and it increases to 0.35 at the end of the century. Moreover, the 30% renewable energy target is almost achieved

with a RES score of 0.92 towards the end of the century. The value of the CO_2_EG ranges between 0.02 and 0.1. CO_2_EG has its highest value in the near century, and its value decreases towards the far century. This shows that even the most sustainable scenario, SSP1, is far from the Paris agreement targets. This highlights the importance of gradually reducing the dependence on thermal power plants in energy production and investing more in renewable energy power plants. Although, there are no renewable power plants planned to be built during the 21st century in the SSP2 and SSP5 scenarios, they have better RES scores (Figure 9-20) than the baseline since the already existing biomass power plants operated more compared to the baseline in these scenarios. The results obtained in the SSP2 and SSP5 scenarios are very close to each other. The all-time average of Energy pillar obtained in the SSP2 and SSP5 scenarios is 0.10 and 0.11, respectively. Thus, the Energy pillar score in these scenarios is very close to the unsustainability score of zero.

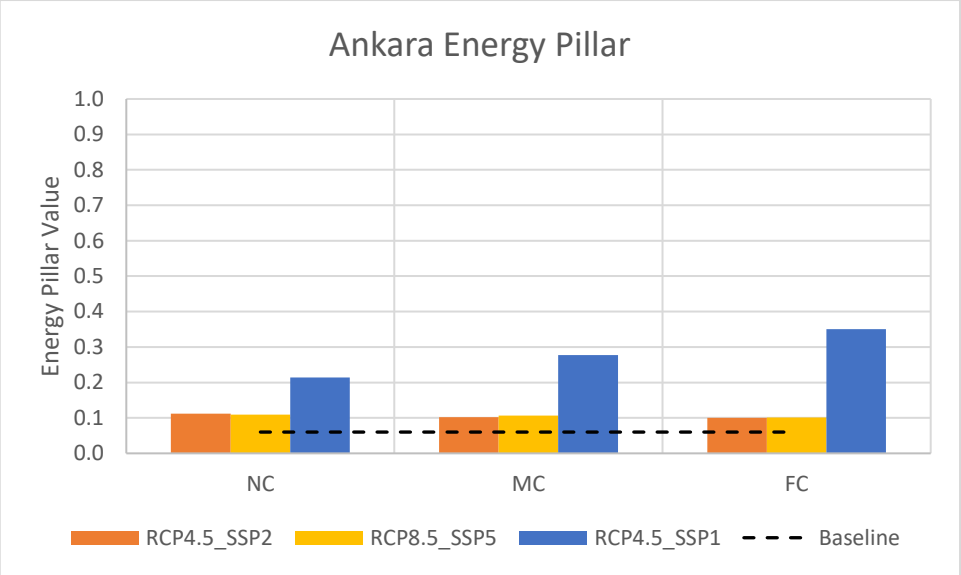

Figure 9-22. Energy pillar value under climate and socioeconomic changes in the Ankara subbasin

Food

Figure 9-23 shows that the baseline value of the Food pillar (0.97) is higher than other scenarios at all periods, and the lowest score of the pillar is obtained in the SSP1 scenario at all times. Average Food pillar value in the 21st century is 0.51, 0.69, and 0.67 in the SSP1, SSP2, and SSP5 scenarios, respectively. The results show that SSP2 and SSP5 scenarios have very close Food pillar value in each time period. The difference between the scores of the SSP1 and other scenarios are significant especially in the near and mid-century. The main reason behind the low SSP1 Food pillar scores is the strict environmental flow requirements. The average deficit which is nearly 3% in the baseline period increases to 49% in the SSP1 scenario. However, even in the SSP2 scenario in which the highest Food pillar score is obtained, there is an average deficit of almost 31%.

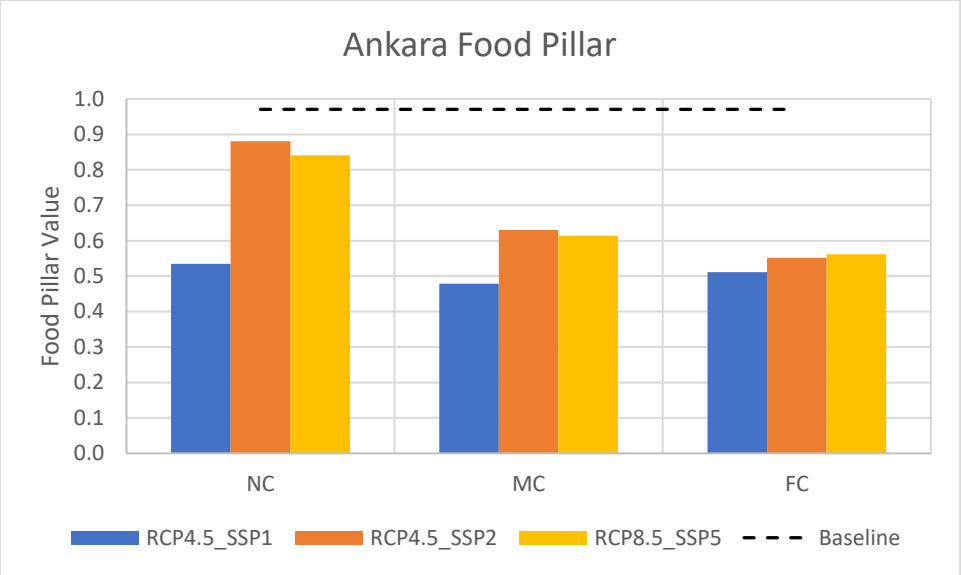

Figure 9-23. Food pillar value under climate and socioeconomic changes in the Ankara subbasin

Ecosystem

Figure 9-25 shows that the Ecosystem pillar score of all scenarios is lower than the baseline score (0.83) at all times in the Ankara subbasin. The reason for obtaining a lower score than the baseline, even in the SSP1 scenario which gives the highest priority to the Ecosystem requirement, can be explained only by water availability. In the Ankara subbasin, the average precipitation in the historical period is 417.1 mm. The climate projections show that near, middle and far century RCP 4.5 ensemble average precipitation values are 455.9 mm, 392.1 mm and 364.5 mm, respectively. In short, although there is a slight increase in the near century, the precipitation gradually falls below the historical averages. In addition, it is expected that the average temperature, which is around 12˚C in the baseline period, will increase to 15˚C towards the end of the century. It is evident that water availability for human uses and aquatic ecosystems will decrease in the basin compared to

baseline due to low rainfall and high temperatures. Another interesting result that can be seen from Figure 9-25 is the fact that in the mid- and far century, the SSP5 scenario has better scores compared to the SSP1 scenario. The ensemble average of the precipitation in the entire 21st century in the RCP4.5 and RCP8.5 scenarios is 404.1 and 412.6 mm, respectively. Therefore, the amount of precipitation received by the basin is less in the RCP 4.5 scenario than in the RCP 8.5 scenario. This, in turn, results in less water available for the environmental flow in the RCP 4.5 scenario. In the SSP2 scenario, which has the climatic conditions of the RCP 4.5 scenario, on the other hand, the Environment pillar score is decreasing over time, and the pillar gets its lowest score in the SSP2 scenario at all times. The comparison of the simulated median monthly flows with the IQR of the naturalized streamflow in each scenario in each time period is given in Figure 9-24. The first, second, and the third row of this figure shows the results of the SSP1, SSP2, and SSP5 scenario, respectively. In the SSP1 scenario, the IQR target is not met in five months, i.e., July, August, September, October, November, and December, in the near and mid-century. The number of months not meeting the IQR target increases to seven in the far century. The target is only met in the months of February, March, April, May, and December. In the SSP1 scenario, the Ecosystem pillar score is 0.78, 0.60, and 0.69 in the near, mid- and far century, respectively. In the SSP2 scenario, the IQR is not met in five months, i.e., July, August, September, October, and November, in the near century. In the mid-century, the number of months with MMS values outside the IQR is still five but this time different months (May, June, July, August, and September). In the far century, the target is achieved at six months which are January, February, March, October, November, and December. In the SSP2 scenario, the Ecosystem pillar gets scores of 0.66, 0.52, and 0.50, in the near, mid- and far century, respectively. In the SSP5 scenario, the MMS values are outside the IQR only in four months, i.e., July, September, October, November, in the near century. The number of months not meeting the IQR target increases to five in the mid-century, and these

months are April, July, September, November, and December. Lastly, in the far century, the IQR target is not met in the months of May, July, August, September, October, and November. In the SSP5 scenario, the Ecosystem pillar score is 0.77, 0.70, and 0.74, in the near, mid-, and far century, respectively.

Regular seasonal changes in river flow are crucial for the survival of river organisms as high and low-flow events provide both challenges and opportunities (details in Chapter 7). The ecosystem pillar scores for low (October – March) and high-flow (April – September) periods were assessed accordingly. Table 9-9 shows the 21st century average Ecosystem pillar scores for low and high flow periods in Ankara subbasin. Based on the table, it can be seen that SSP1 has the highest Ecosystem pillar indicator value across both low and high flow periods. This suggests that in this scenario, the ecosystem is expected to be the most sustainable. In comparison, SSP2 and SSP5 have lower Ecosystem pillar indicator values across both low and high flow periods, indicating a less sustainable situation for the ecosystem. It is also worth noting that the Ecosystem pillar indicator values for all scenarios are lower during the high flow period compared to the low flow period, suggesting that the ecosystem may face greater challenges during periods of higher flow. Thus, it may reflect the negative impacts on certain ecosystem functions, such as habitat quality and species diversity.

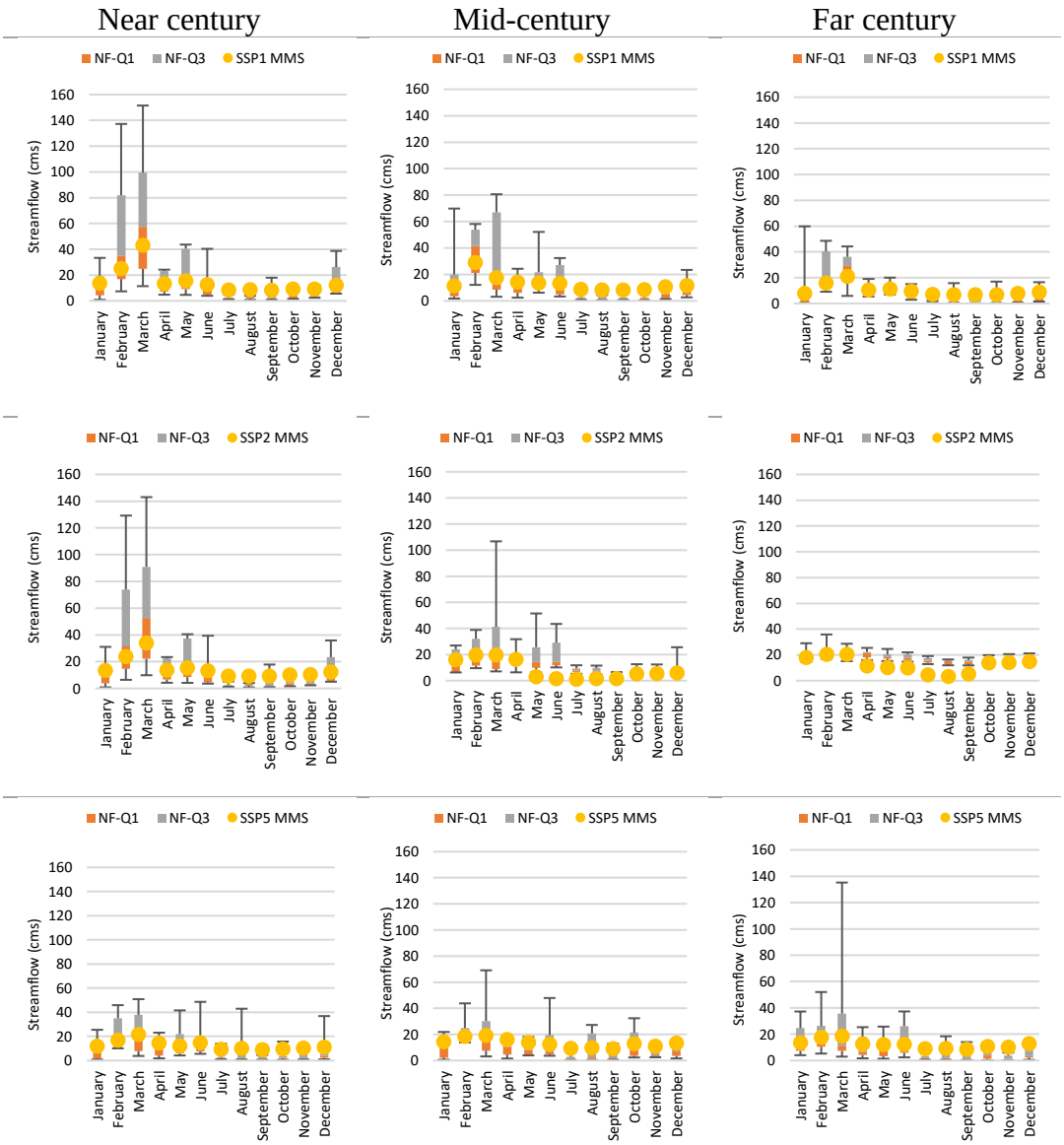

NF-Q1: Naturalized Streamflow Lower Quartile; NF-Q3: Naturalized Streamflow Upper Quartile; MMS: Simulated Median Monthly Streamflow

Figure 9-24. Ankara: The comparison of the simulated median monthly flows with the IQR of the naturalized streamflow in each scenario in each time period. First row: SSP1; Second row: SSP2; Last row: SSP5

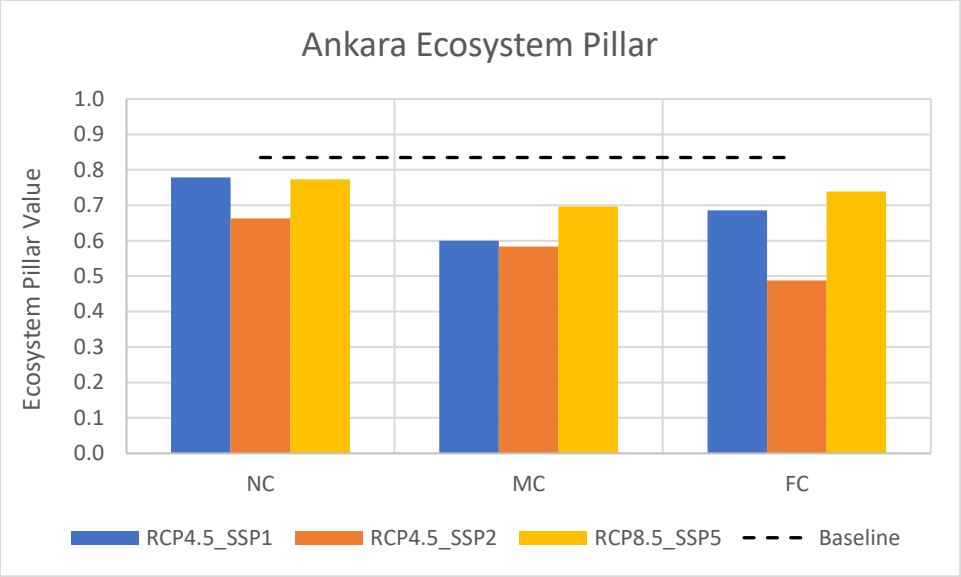

Figure 9-25. Ecosystem pillar value under climate and socioeconomic changes in the Ankara subbasin

Table 9-9. 21st century average ecosystem pillar scores for low and high flow periods in Ankara subbasin

	SSP1	SSP2	SSP5
October – March (low flow period)	0.79	0.68	0.76
April -September (high flow period)	0.58	0.48	0.71

Aggregated WEFE Nexus Index

After scores of all nexus pillars are calculated and aggregated, the values of the WEFE Nexus Index given in Figure 9-26 are obtained. The baseline value of the WEFE Nexus Index (0.71) is higher than the values obtained in all other scenarios. The main reason for this is that the Food and Ecosystem pillars have lower values compared to the baseline in all scenarios. Among the scenarios, the highest value of

the WEFE Nexus index (0.68) is obtained in the SSP5 scenario in the near century. However, this value gradually decreases to 0.55 and 0.53 in mid- and far century, respectively. WEFE Nexus index values are close to each other in every period in SSP2 and SSP5 scenarios. As in the SSP5 scenario, the value of the index decreases over time in the SSP2 scenario. In the SSP1 scenario, on the other hand, the index value, which decreases from near to mid-century, reaches its highest level (0.63) in the far century since the Water and the Energy pillars have their highest values in the SSP1 scenario in the far century.

The Ankara subbasin differs from other subbasins in that all nexus pillars are connected by much more complex relationships. First of all, the city of Ankara, the capital of Türkiye and the second largest city in terms of population, falls within the borders of the Ankara subbasin. There are many dams built for drinking water purposes in the basin. Moreover, drinking water is delivered from the dams in the Kirmir subbasin to the Kurtboğazı dam in the Ankara subbasin. In addition, in cases where there is a shortage of drinking water, water is transferred from the Kızılırmak river. Therefore, there is water transfer between basins. Ankara subbasin also has an important place in terms of agricultural production. 60% of Ankara province consists of agricultural lands and Polatlı district, which is described as Türkiye's granary, is located in the Ankara subbasin (DSİ, 2017). There are also many organized industrial zones in the basin. Although there are not any HPP in the basin, water-energy nexus is still important since there are thermal power plants with wet cooling systems. Furthermore, Ankara subbasin has a continental climate. It is the second driest subbasin in the Sakarya Basin with an average precipitation of 417.1 mm per year calculated in the baseline period. Also, it is projected that average precipitation will decrease in the 21st century. Hence, the basin will get drier which will increase the pressure on all sectors and nexus pillars. The results clearly show that if the current municipal water policies continue (SSP2), the deficit in drinking water demand will increase to about 30% towards the end of the 21st century. In addition, according to

the results of SSP2 scenario, the deficit in agricultural irrigation demand will reach serious levels (approximately 45%) and at the same time, the aquatic conditions will become much more critical than it is today. The SSP5 scenario shows similar results to the SSP2 scenario. One of the most important differences between these two scenarios is that the average precipitation in the RCP8.5 scenario is higher than in the RCP4.5 scenario, and therefore the availability of water for environmental flows is somewhat higher in the RCP 8.5 scenario. The results of the SSP1 scenario show that natural flow conditions cannot be targeted in the Ankara subbasin. This is because in the SSP1 scenario, although environmental flows are the first priority, worse Ecosystem pillar values are obtained compared to both the baseline and the SSP5 scenario. That is, the water availability is restricted due to climatic conditions. In addition, targeting natural environmental flows causes serious deficits in meeting the need for agricultural irrigation. However, in the SSP1 scenario, it is seen that sustainable applications significantly reduce the municipal water demand deficit compared to the SSP2 and SSP5 scenarios. All these results show that in the SSP1 scenario, if slightly or moderately modified is targeted instead of natural flow conditions, and sustainable practices that will increase efficiency in agricultural irrigation are adopted, the most balanced situation among nexus components and thus the highest overall WEFE Nexus index can be achieved in the Ankara subbasin.

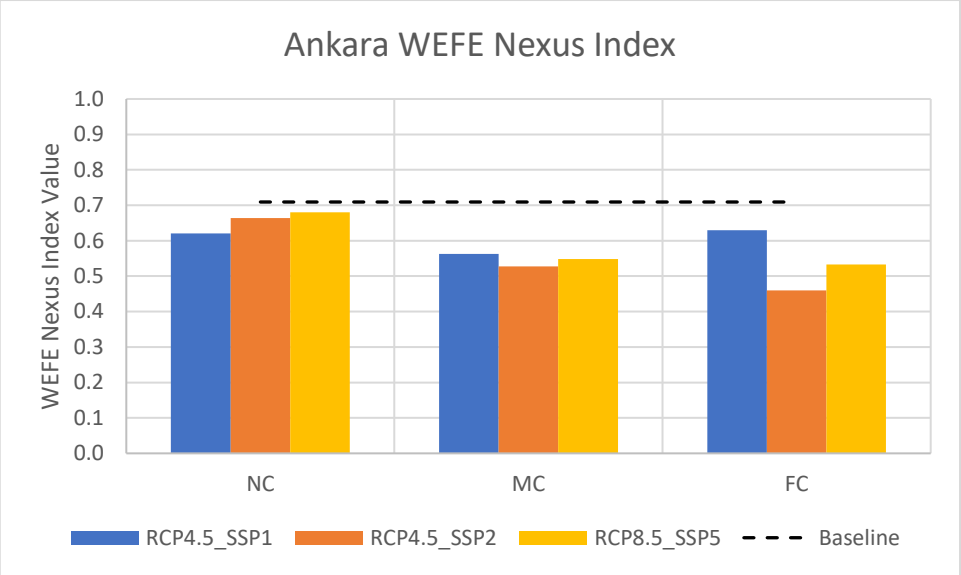

Figure 9-26. WEFE Nexus Index value under climate and socioeconomic changes in the Ankara subbasin

9.4.4 Kirmir Subbasin

Table 9-10 provides a comparative analysis of the WEFE Nexus indicators for different scenarios representing climate and socioeconomic changes and for different time periods, i.e., near, mid-, and far century, in the Kirmir subbasin. Figure 9-27 presents the same information as Table 9-10 in a visual format, using spider charts to illustrate the values of WEFE Nexus indicators for different time periods and scenarios. The charts provide a clear and concise comparison of the values for each scenario across the different time periods, highlighting the differences that exist between scenarios and time periods. By examining the values for each indicator, a deeper understanding of the complex interplay between water, energy, food, and the ecosystem can be gained, and how this interplay may evolve over time can be

understood. The pillar indices created using these indicators are evaluated in detail under the subtitles Water, Energy, Food, and Ecosystem below.

Table 9-10. WEFE Nexus indicators' comparative analysis for different scenarios in the 21st century: variations over multiple time periods in the Kirmir subbasin

		NC	MC	FC			NC	MC	FC			NC	MC	FC
RCP4.5_SSP1	MDC	0.60	0.67	0.86	**RCP4.5_SSP2**	MDC	0.99	0.99	0.99	**RCP8.5_SSP5**	MDC	0.99	0.99	0.98
	HPP_MGC	-	-	-		HPP_MGC	-	-	-		HPP_MGC	-	-	-
	RES	1.00	1.00	1.00		RES	-	-	-		RES	-	-	-
	CO2_EG	-	-	-		CO2_EG	-	-	-		CO2_EG	-	-	-
	IDM	0.48	0.47	0.46		IDM	0.89	0.77	0.68		IDM	0.85	0.75	0.67
	Jan-MMS	1.00	1.00	1.00		Jan-MMS	0.50	0.59	0.31		Jan-MMS	0.05	0.44	0.61
	Feb-MMS	1.00	1.00	1.00		Feb-MMS	0.40	0.00	0.09		Feb-MMS	0.00	0.39	0.10
	Mar-MMS	1.00	1.00	0.94		Mar-MMS	0.31	0.00	0.36		Mar-MMS	0.00	0.53	0.21
	Apr-MMS	1.00	0.99	1.00		Apr-MMS	0.06	0.00	0.14		Apr-MMS	0.00	0.50	0.06
	May-MMS	1.00	0.97	0.77		May-MMS	0.00	0.14	0.00		May-MMS	0.00	0.56	0.00
	Jun-MMS	1.00	0.77	0.77		Jun-MMS	0.00	0.00	0.00		Jun-MMS	0.00	0.00	0.00
	Jul-MMS	1.00	0.74	0.96		Jul-MMS	0.00	0.00	0.07		Jul-MMS	0.00	0.00	0.00
	Aug-MMS	1.00	1.00	1.00		Aug-MMS	0.14	0.00	0.00		Aug-MMS	0.00	0.73	0.00
	Sep-MMS	1.00	1.00	1.00		Sep-MMS	0.37	0.00	0.00		Sep-MMS	0.00	0.93	0.91
	Oct-MMS	1.00	0.72	1.00		Oct-MMS	0.40	0.37	0.64		Oct-MMS	0.33	0.51	0.83
	Nov-MMS	1.00	1.00	1.00		Nov-MMS	0.00	0.00	0.62		Nov-MMS	0.76	0.00	1.00
	Dec-MMS	1.00	1.00	1.00		Dec-MMS	0.00	0.33	0.15		Dec-MMS	1.00	0.35	0.88

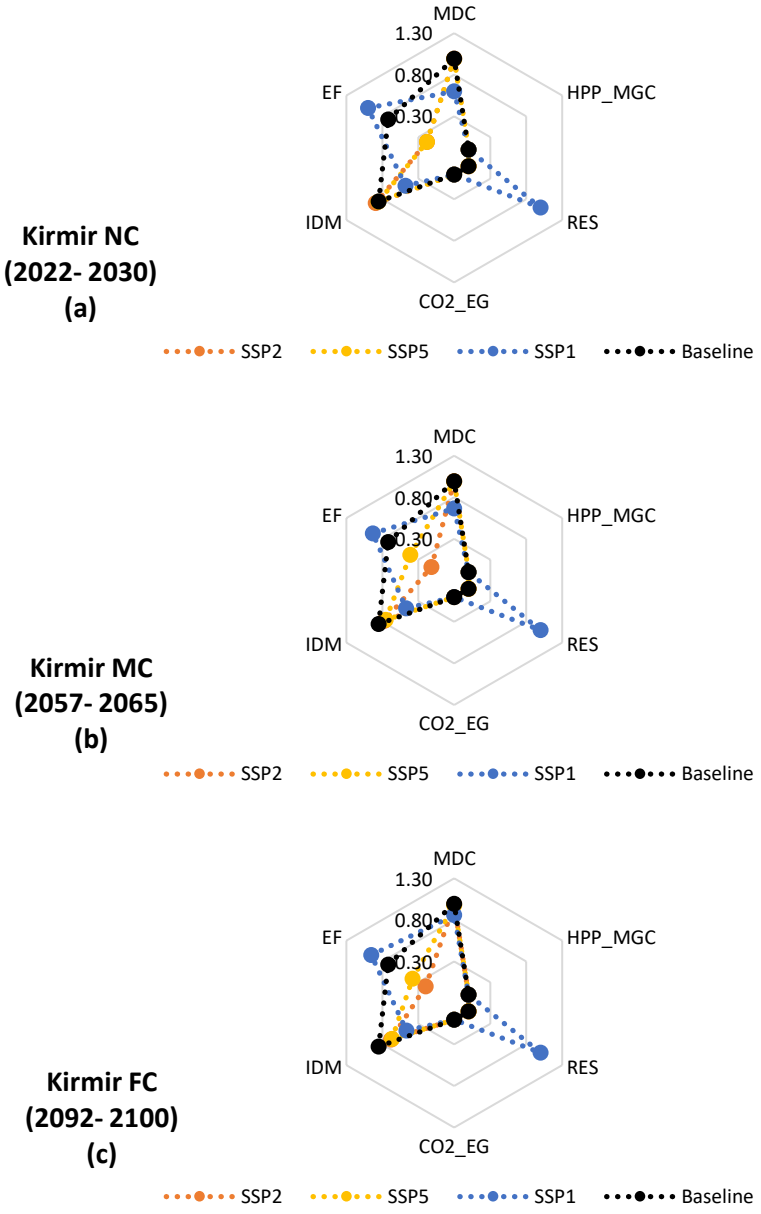

Figure 9-27. Kirmir subbasin: The values of the WEFE Nexus Index Pillar Indicators in each scenario in each future period segment; near century (a), mid-century (b), far century (c). Note: Ecosystem indicator values are not provided in this figure. The parameter EF represents the average of ecosystem indicators, which is equivalent to the Ecosystem pillar value

Water

Figure 9-28 shows that the Water pillar scores of the baseline, SSP2 and SSP5 are almost one at all times. However, in SSP1 scenario, it is seen that there is some deficit in all periods. Deficit gradually decreases towards the end of the century. The water pillar score is calculated as 0.60, 0.67, and 0.86 in the near, mid-, and far century, respectively. Therefore, in the SSP1 scenario, an average deficit of approximately 30% is calculated in the 21st century. Although some districts of Ankara province are included in the Kirmir subbasin, the municipal water demand in the Kirmir subbasin is not as high as in the Ankara subbasin, since these are the districts with low population density. The main reason for the municipal water demand deficit in the SSP1 scenario is the strict environmental flow requirement applied in this scenario.

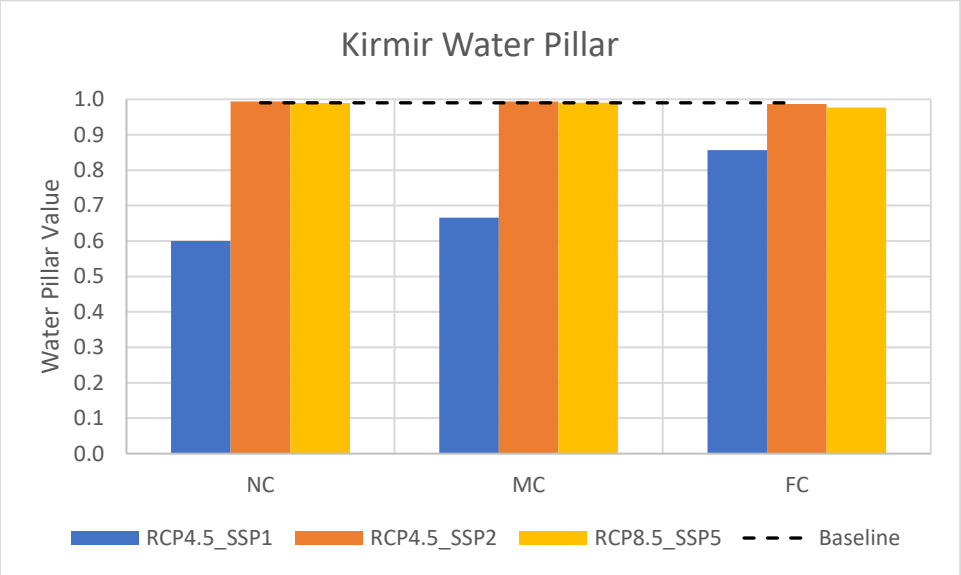

Figure 9-28. Water pillar value under climate and socioeconomic changes in the Kirmir subbasin

Energy

In Kirmir subbasin, there is no electricity production in the baseline period. There are also no hydroelectric or thermal power plants planned. Thus, none of the Energy pillar indicators were included in the evaluation of the baseline, SSP2 and SSP5 scenarios (Figure 9-27). Consequently, in these scenarios, Energy pillar is not included when calculating the overall WEFE Nexus Index. The SSP1 scenario, on the other hand, aims to benefit from the entire renewable energy potential of the basin until the end of the 21st century. Therefore, starting from the beginning of the century and increasing towards the end of the century, electricity is produced from solar and wind power plants. Accordingly, the Energy pillar score in the SSP1 scenario is calculated using only the RES indicator and included in the overall WEFE Nexus Index evaluation. In addition, since electricity is produced only from renewable energy plants, the RES indicator takes the value of one at all times, and therefore the Energy pillar score is calculated as one at all times in the SSP1 scenario (Figure 9-29).

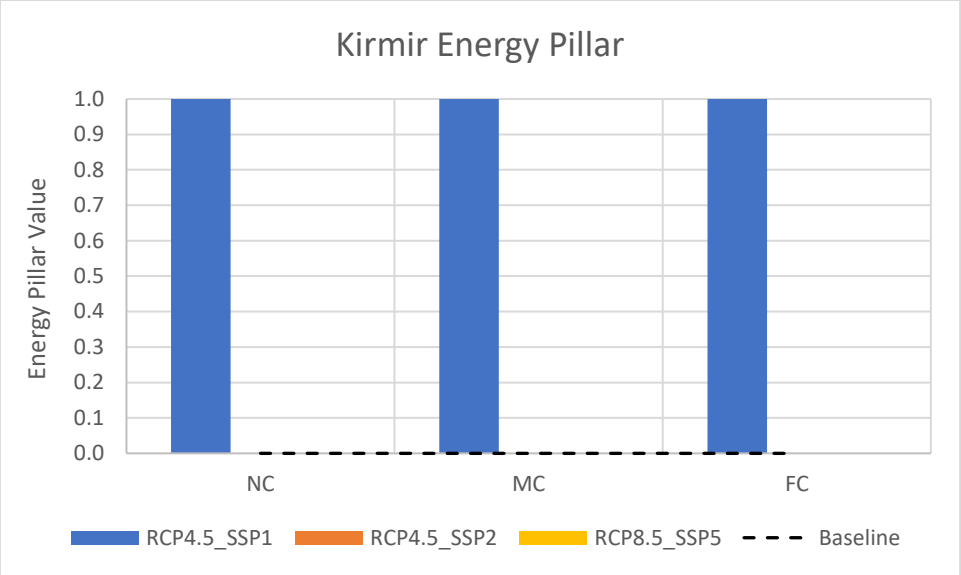

Figure 9-29. Energy pillar value under climate and socioeconomic changes in the Kirmir subbasin

Food

Figure 9-30 shows that there is approximately 15% irrigation demand deficit, i.e., IDM score of 0.85, in the baseline period in the Kirmir subbasin. Less or close deficit than baseline calculated only in near century SSP2 (IDM score of 0.89) and SSP5 (IDM score of 0.85) scenario. However, the Food pillar score appears to decrease over time in the SSP2 and SSP5 scenarios, and the results obtained in these two scenarios are very close to each other. In the SSP1 scenario, the Food pillar score is around 0.47 in all periods. There is a significant difference between the Food pillar score obtained in the SSP1 and the other scenarios. The main reason for this is the targeting of natural flow conditions in the SSP1 scenario, and therefore the inability to provide enough water to agriculture. An average deficit of approximately 53% is calculated in the SSP1 scenario. However, even in the SSP2 scenario representing

business as usual and the SSP5 scenario representing fossil-fueled development, an average of 22% and 24% deficit is calculated in the 21st century, respectively.

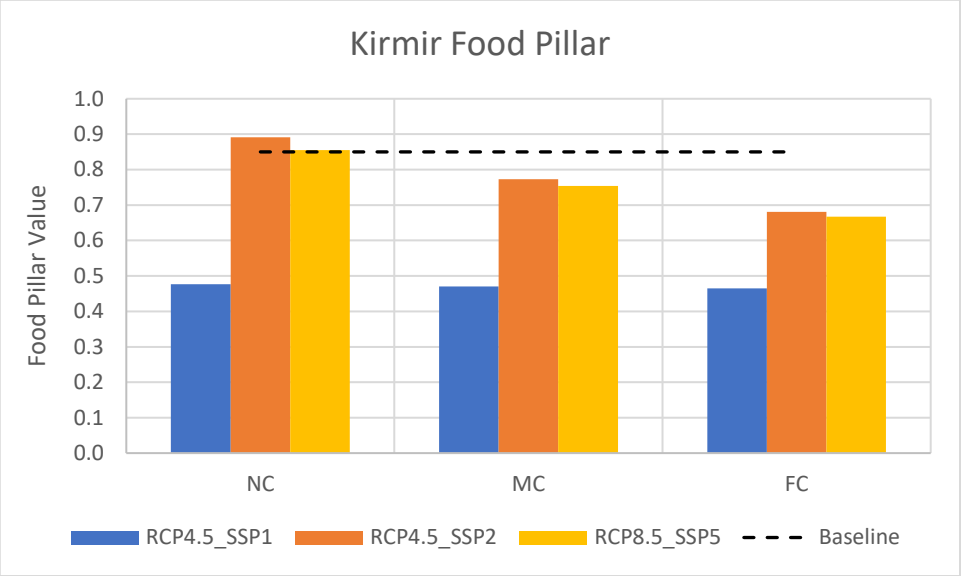

Figure 9-30. Food pillar value under climate and socioeconomic changes in the Kirmir subbasin

Ecosystem

The comparison of the simulated median monthly flows with the IQR of the naturalized streamflow in each scenario in each time period is given in Figure 9-31. The first, second, and the third row of this figure shows the results of the SSP1, SSP2, and SSP5 scenario, respectively. The near-century SSP1 scenario results show that the IQR target is met in all months. Thus, the Ecosystem Pillar value is one in this period in the SSP1 scenario (Figure 9-32). Mid-century SSP1 scenario results show that IQR target cannot not be achieved at 5 months (April, May, June, July, and October). However, the scores obtained in April and May are 0.99 and 0.97, and they are very close to the lower quartile of the IQR. The overall Ecosystem pillar score in the mid-century is calculated as 0.93 in the SSP1 scenario (Figure 9-32). In the far

century, there are five months (March, April, May, June, and July) in which the median simulated streamflow values are outside the IQR. However, the median March and July streamflow values are very close to lower quartile and hence their scores are 0.94 and 0.96, respectively. In the SSP1 scenario, the overall Ecosystem pillar value is calculated as 0.95 in the far century. As it can be seen from Figure 9-32, SSP1 is the only scenario which gets higher scores compared to the baseline Ecosystem pillar score of 0.72 in all time periods. Figure 9-31 shows that IQR target can never be met in any time period in the SSP2 scenario. The median streamflow values in all months are lower than the lower quartile and often even lower than the minimum natural flow value. The Ecosystem pillar scores in the SSP2 scenario are calculated as 0.18, 0.12, and 0.20 in the near, mid- and far century, respectively (Figure 9-32). These numbers imply that the SSP2 scenario results in severely unsustainable ecosystem conditions in the Kirmir subbasin. Similar to the SSP2 scenario, the SSP5 scenario almost never achieves the IQR target in any period. The MMS value is within the IQR only in December in the near century and in November in the far century. In all periods, all MMS values outside the IQR have values lower than the lower quartile. In the SSP5 scenario, the overall Ecosystem pillar scores are calculated as 0.18, 0.41, and 0.38 in the near, mid- and far century, respectively. Although the results obtained in the SSP5 scenario are better than the SSP2 results, they are still far from sustainability. In addition to socioeconomic differences, the main reason for the difference between these two scenarios is the difference in climatic conditions. In the Kirmir subbasin, the RCP 8.5 scenario projects higher average precipitation compared to the RCP 4.5 scenario.

Seasonal changes in river flow play a critical role in shaping the ecology of river systems. High- and low-flow events present both challenges and opportunities for river organisms, and the regularity of these events is essential for their survival (details in Chapter 7). Looking at the Ecosystem pillar indicator values for the low flow period (October – March) and the high flow period (April – September), it can

be seen that there are notable differences between the two. Table 9-11 shows the comparison of SSP1, SSP2, and SSP5 in terms of their 21st century average Ecosystem pillar scores in the low and high flow periods. During the low flow period, SSP1 has the highest Ecosystem pillar score of 0.98, indicating that it has the strongest sustainability performance among the three scenarios. SSP5 has the second-highest value of 0.44, while SSP2 has the lowest value of 0.28. During the high flow period, SSP1 still has the highest Ecosystem pillar indicator value, but its value decreases to 0.94. SSP5 has the second-highest value of 0.21, while SSP2 has the lowest value of 0.05. Comparing the two periods, it can be seen that the Ecosystem pillar scores are generally higher during the low flow period compared to the high flow period for all three scenarios. The fact that the Ecosystem pillar score is lower in the high flow period, especially in the SSP2 and SSP5 scenarios, indicates that the ecosystem faces greater challenges during this period. Thus, processes that are critical for the functioning of the ecosystem, such as sediment transport and nutrient cycling, which occur due to high flows, may be unsustainably affected.

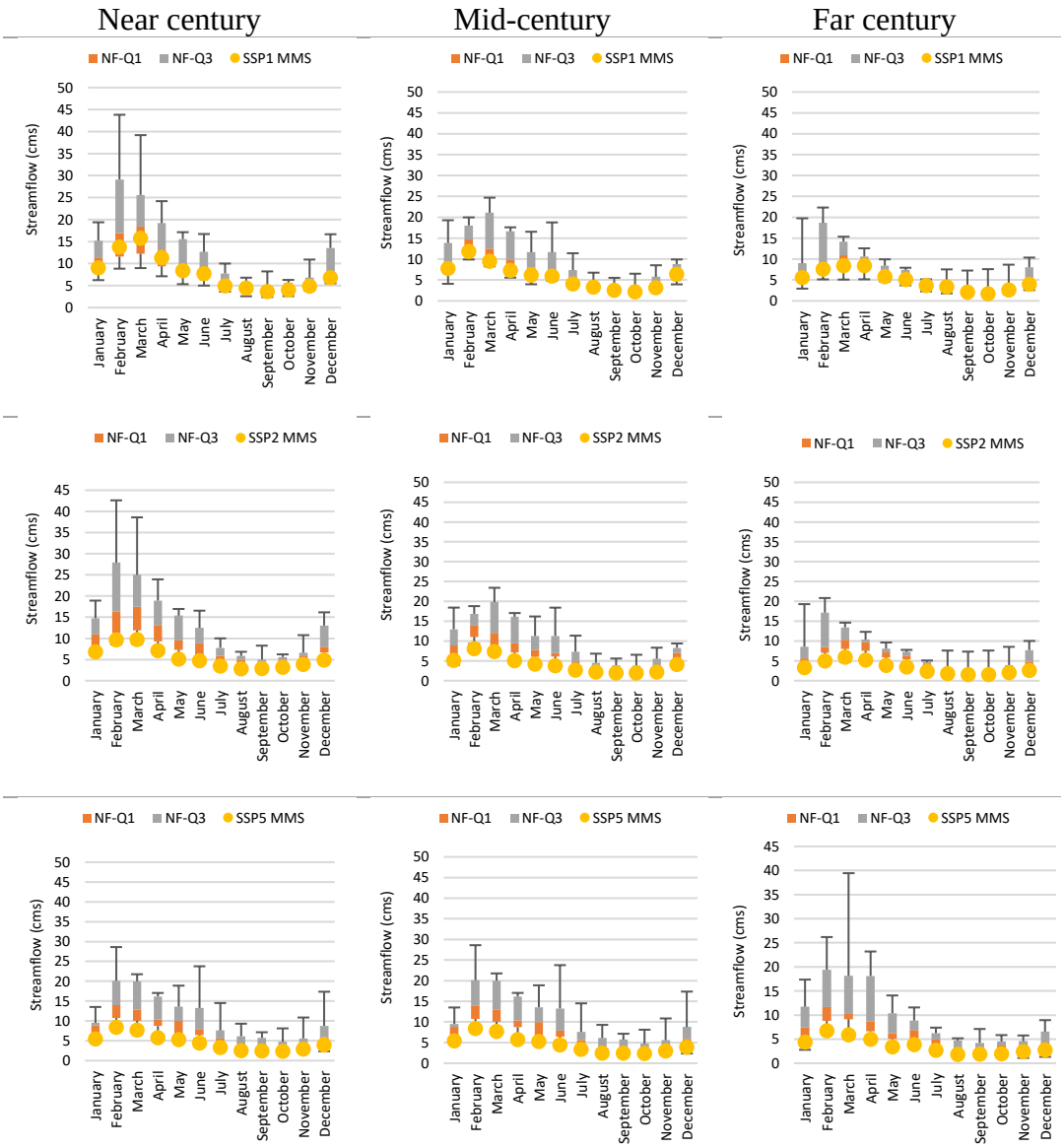

NF-Q1: Naturalized Streamflow Lower Quartile; NF-Q3: Naturalized Streamflow Upper Quartile; MMS: Simulated Median Monthly Streamflow

Figure 9-31. Kirmir: The comparison of the simulated median monthly flows with the IQR of the naturalized streamflow in each scenario in each time period. First row: SSP1; Second row: SSP2; Last row: SSP5

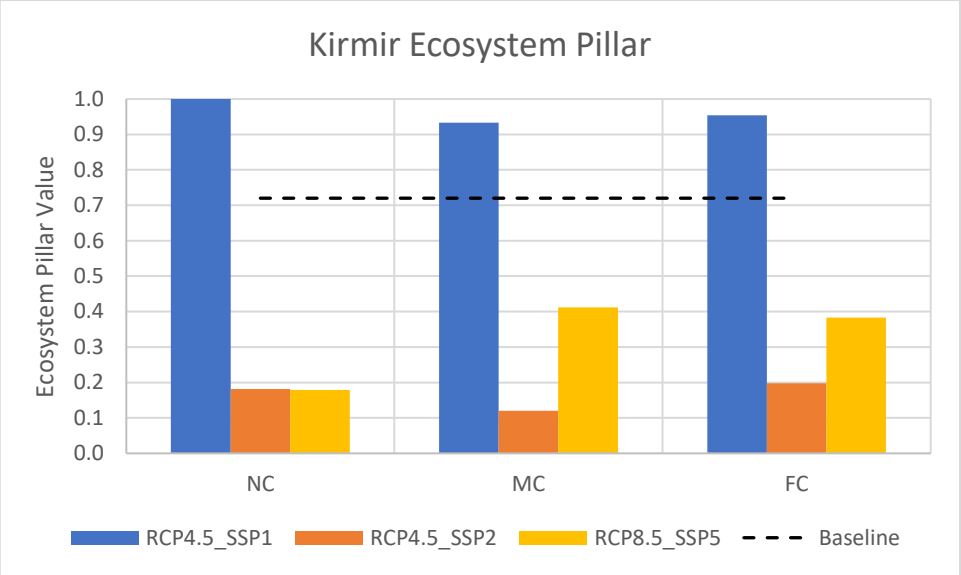

Figure 9-32. Ecosystem pillar value under climate and socioeconomic changes in the Kirmir subbasin

Table 9-11. 21st century average ecosystem pillar scores for low and high flow periods in Kirmir subbasin

	SSP1	SSP2	SSP5
October – March (low flow period)	0.98	0.28	0.44
April -September (high flow period)	0.94	0.05	0.21

Aggregated WEFE Nexus Index

After scores of all pillars are calculated and aggregated, the values of the WEFE Nexus Index given in Figure 9-33 are obtained. This figure shows that all scenarios have higher scores of WEFE Nexus Index compared to the baseline score of 0.61. The highest scores are obtained in the SSP1 scenario in all time periods. This is expected since the highest scores of Energy and Ecosystem pillars are obtained in

the SSP1 scenario. The lowest WEFE Nexus Index is calculated in the SSP2 scenario in the near century. The major difference between SSP1 and other scenarios is due to the scores obtained for the Ecosystem pillar. In addition, the Energy pillar is not included in the overall WEFE Nexus Index calculation in the SSP2 and SSP5 scenarios since there is no electricity production in these scenarios. In the SSP1 scenario, on the other hand, solar and wind power plants generate electricity in the basin. This is the second reason for the difference between SSP1 and other scenarios. Although the worst-scoring scenario for Water and Food pillars is SSP1, in the overall WEFE Nexus score this is compensated by good scores for Energy and Ecosystem pillars. This highlights the need to consider not only the overall WEFE Nexus Index score, but also all pillar scores when evaluating and comparing scenarios.

In the Kirmir subbasin, connections between Water, Food and Ecosystem pillars come to the fore. One of the most important features that distinguishes the Kirmir subbasin from other subbasins is that some of the water collected in this basin is transferred to the Ankara subbasin in order to meet the municipal water demand of the city of Ankara. For this purpose, the water collected in the Akyar Dam located in the Kirmir subbasin is first transferred to the Eğrekkaya Dam located in this subbasin. It is then transferred to Kurtboğazı Dam, located in the Ankara subbasin, by a transmission line. In addition, Çamlıdere Dam located in the Kirmir subbasin is also used to meet Ankara's drinking water. 78% of the drinking water of the municipalities in the Kirmir basin is met from groundwater and 22% from surface water. In villages, 27% of drinking water is met from groundwater, while 73% is from surface water (DSİ, 2017). According to the scenario results, the municipal water demand deficit in the Kirmir subbasin in the 21st century is almost zero in the SSP2 and SSP5 scenarios. However, targeting natural flow conditions in the basin creates problems in terms of sustainability in other pillars. In the SSP1 scenario, an average of 29% and 53% deficit is calculated to meet the municipal water demand

and agricultural water demand, respectively. Although almost no municipal demand deficit is calculated in SSP2 and SSP5 scenarios, the deficit in agricultural irrigation is calculated as 22% and 24% on average, respectively, in these scenarios. Also, the 21st century average Ecosystem pillar scores in the SSP2 and SSP5 scenarios are 0.17 and 0.32, respectively. Therefore, in these scenarios, the Ecosystem Pillar is far from the full sustainability score of one. All these results show that in order to achieve a more balanced situation for all pillars in the basin, while adopting the SSP1 scenario, it would be more appropriate to target slightly or moderately modified conditions instead of natural flow conditions in the basin. In this way, while maintaining the sustainability of the Ecosystem to a significant extent, the deficits in Water and Food pillar will also be reduced.

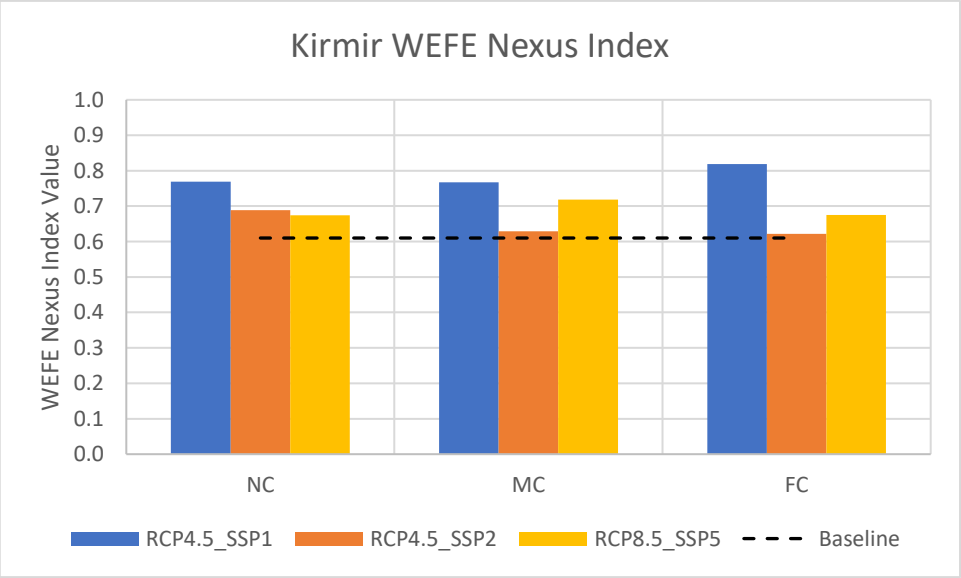

Figure 9-33. WEFE Nexus Index value under climate and socioeconomic changes in the Kirmir subbasin

9.4.5 Middle Sakarya Subbasin

Table 9-12 provides a comparative analysis of the WEFE Nexus indicators for different scenarios representing climate and socioeconomic changes and for different time periods, i.e., near, mid-, and far century, in the Middle Sakarya subbasin. Figure 9-34 presents the same information as Table 9-12 in a visual format, using spider charts to illustrate the values of WEFE Nexus indicators for different time periods and scenarios. The charts provide a clear and concise comparison of the values for each scenario across the different time periods, highlighting the differences that exist between scenarios and time periods. By examining the values for each indicator, a deeper understanding of the complex interplay between water, energy, food, and the ecosystem can be gained, and how this interplay may evolve over time can be understood. The pillar indices created using these indicators are evaluated in detail under the subtitles Water, Energy, Food, and Ecosystem below.

Table 9-12. WEFE Nexus indicators' comparative analysis for different scenarios in the 21st century: variations over multiple time periods in the Middle Sakarya subbasin

		NC	MC	FC			NC	MC	FC			NC	MC	FC
RCP4.5_SSP1	MDC	0.94	0.91	0.90	**RCP4.5_SSP2**	MDC	1.00	0.99	0.97	**RCP8.5_SSP5**	MDC	1.00	0.99	0.98
	HPP_MGC	0.32	0.30	0.23		HPP_MGC	0.18	0.16	0.12		HPP_MGC	0.17	0.21	0.15
	RES	1.00	1.00	1.00		RES	0.74	0.69	0.62		RES	0.71	0.80	0.68
	CO2_EG	0.00	0.00	0.00		CO2_EG	0.00	0.00	0.00		CO2_EG	0.00	0.00	0.00
	IDM	0.62	0.49	0.39		IDM	0.92	0.70	0.50		IDM	0.85	0.71	0.52
	Jan-MMS	1.00	1.00	1.00		Jan-MMS	1.00	1.00	1.00		Jan-MMS	1.00	1.00	1.00
	Feb-MMS	1.00	1.00	1.00		Feb-MMS	0.73	0.70	1.00		Feb-MMS	0.84	1.00	1.00
	Mar-MMS	1.00	1.00	1.00		Mar-MMS	1.00	1.00	1.00		Mar-MMS	1.00	1.00	1.00
	Apr-MMS	1.00	1.00	1.00		Apr-MMS	1.00	1.00	1.00		Apr-MMS	1.00	1.00	1.00
	May-MMS	1.00	1.00	0.81		May-MMS	0.00	0.80	0.00		May-MMS	0.00	0.49	0.00
	Jun-MMS	1.00	1.00	0.98		Jun-MMS	0.73	1.00	0.00		Jun-MMS	0.00	0.84	0.42
	Jul-MMS	1.00	0.82	0.23		Jul-MMS	1.00	1.00	1.00		Jul-MMS	0.74	0.30	1.00
	Aug-MMS	0.00	0.00	0.00		Aug-MMS	0.00	0.00	0.38		Aug-MMS	0.28	0.76	0.51
	Sep-MMS	1.00	1.00	1.00		Sep-MMS	0.13	1.00	1.00		Sep-MMS	0.00	1.00	1.00
	Oct-MMS	1.00	1.00	1.00		Oct-MMS	0.00	0.82	0.00		Oct-MMS	0.05	0.00	0.64
	Nov-MMS	0.53	1.00	1.00		Nov-MMS	0.00	0.09	0.00		Nov-MMS	0.32	0.00	0.88
	Dec-MMS	1.00	1.00	1.00		Dec-MMS	0.34	0.90	1.00		Dec-MMS	1.00	0.60	1.00

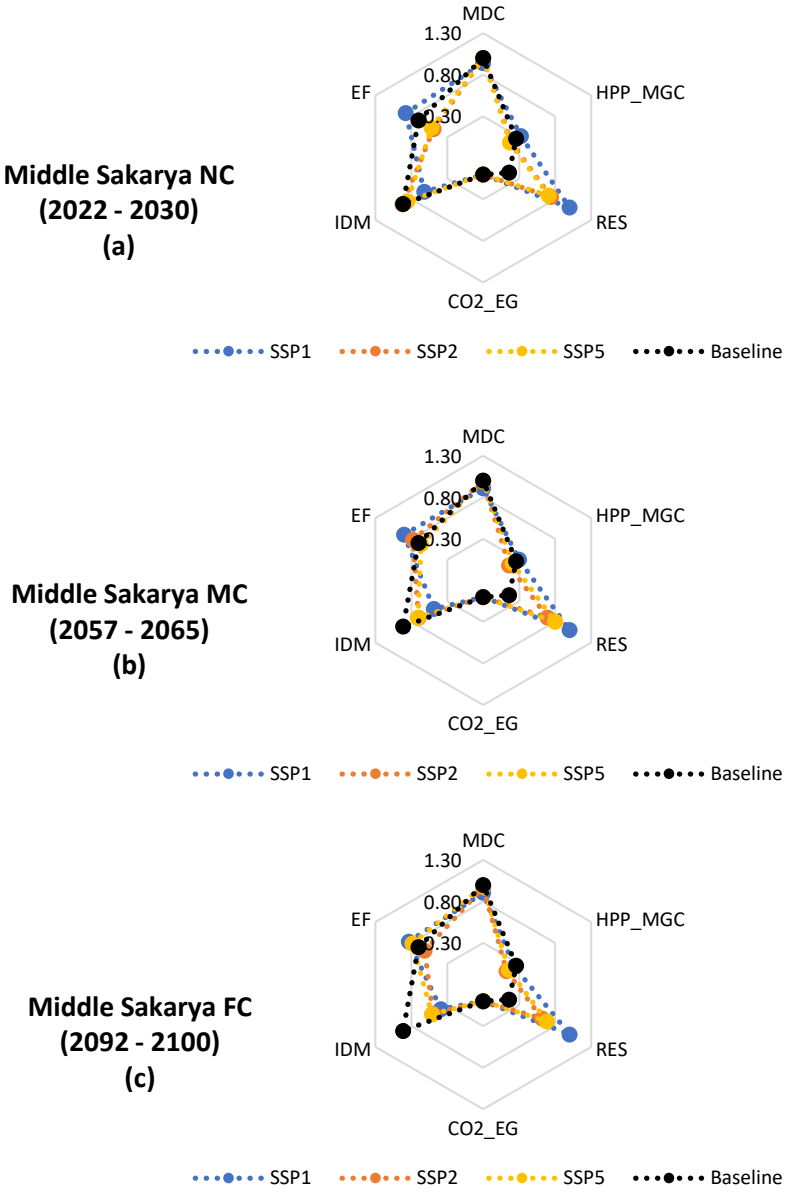

Figure 9-34. Middle Sakarya subbasin: The values of the WEFE Nexus Index Pillar Indicators in each scenario in each future period segment; near century (a), mid-century (b), far century (c). Note: Ecosystem indicator values are not provided in this figure. The parameter EF represents the average of ecosystem indicators, which is equivalent to the Ecosystem pillar value

Water

Figure 9-35 shows that Water pillar score in the baseline period (1.00) is higher than the scores obtained in other scenarios at all periods except the scores of SSP2 and SSP5 in the near century. The scores of Water pillar in the SSP2 and SSP5 are very close to each other. All-time average scores of the 21st century in these scenarios is calculated as 0.99. In the SSP1 scenario, on the other hand, the Water pillar values are 0.94, 0.91, and 0.90 in the near, mid-, and far century, respectively. That is, an average of 8% deficit is calculated in the 21st century and the lowest scores of the Water pillar are always calculated in the SSP1 scenario. This points out that the stringent environmental flow requirements employed in the SSP1 scenario results in municipal water demand deficit.

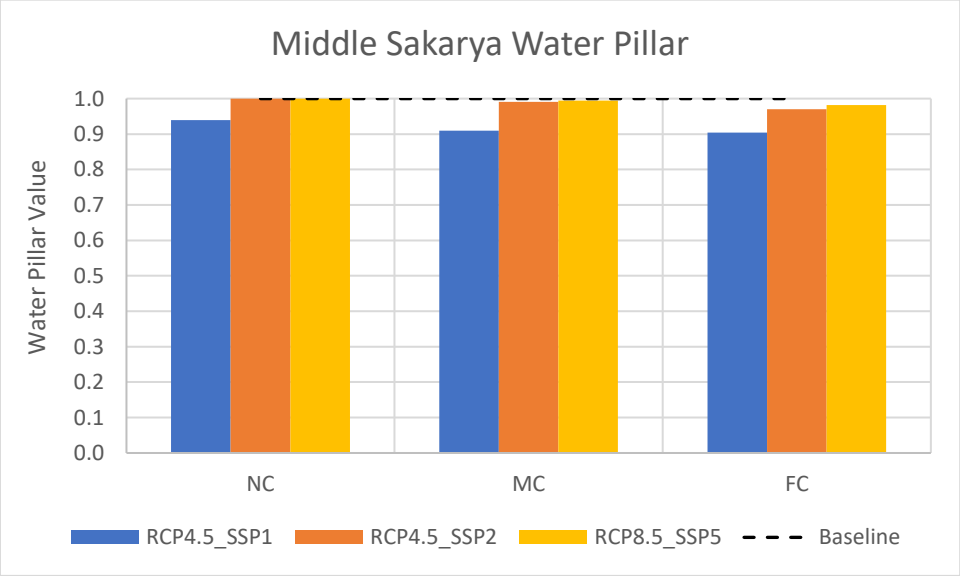

Figure 9-35. Water pillar value under climate and socioeconomic changes in the Middle Sakarya subbasin

Energy

The Middle Sakarya subbasin has high energy demand and it has the second highest energy production among the seven subbasins in the Sakarya Basin. In the baseline period, the total number of power plants within the Middle Sakarya subbasin is 25, with a total installed capacity of 1,742 MW. Out of these 25 power plants, 13 are HPPs with a total installed capacity of 593.8 MW (34% of the total). The installed capacities of the HPPs range between 0.36 MW and 160 MW. Also, there are seven fossil-fueled power plants in the region with a total installed capacity of 1106.6 MW. The largest installed capacity belongs to a 620 MW lignite-fired power plant. The number of power plants with wet cooling water systems is higher than those with dry cooling systems. The total installed capacities of the power plants with dry and wet cooling systems are 71.6 MW and 1038 MW, respectively. The annual total evaporation in the three largest hydroelectric power plants in the basin is 1189.3 mm. These numbers emphasize the importance of water-energy nexus in the subbasin. In the baseline period, the amount of hydropower production as a percentage of the maximum hydropower generation capacity and the renewable energy share are 26% and 16%, respectively (Figure 9-34). This in turn results in the Energy pillar score of 0.21 (Figure 9-36). In the 21st century, all scenarios have higher Energy pillar scores as compared to the base case. This is mainly owing to the substantial increase in renewable energy share in other scenarios compared to the baseline scenario. The renewable energy share is also increasing in SSP2 and SSP5 scenarios because there are already power plants under construction or planned in the basin. The CO_2_EG indicator takes the value 0.00 in all scenarios and all periods. This shows that in all scenarios, the CO_2 emission reduction targets of the near, mid- and far century are far from being achieved. This shows that it is not possible to reach these targets unless the thermal power plants are closed gradually. HPP_MGC indicator gets its highest value in SSP1 scenario in all scenarios and all periods. This is because renewable power plants are given the highest priority in electricity generation in the

SSP1 scenario. Since the HPP_MGC and RES indicators have their highest values in the SSP1 scenario, the highest values of the overall Energy pillar score are always calculated in the SSP1 scenario. All-time average Energy pillar scores are calculated as 0.43, 0.28, and 0.30 in the SSP1, SSP2, and SSP5 scenario, respectively. These numbers show that even in the SSP1 scenario, which takes the green road, the Energy pillar score is significantly away from the full sustainability score of one. The reason for this is that fossil fuel thermal power plants are active in all scenarios, even if priority is given to renewable power plants in the SSP1 scenario. Therefore, fossil fuel thermal power plants should be closed or, if these power plants cannot be closed, serious investments should be made in research and application of technologies that will reduce carbon emissions, e.g., carbon capture and storage (CCS).

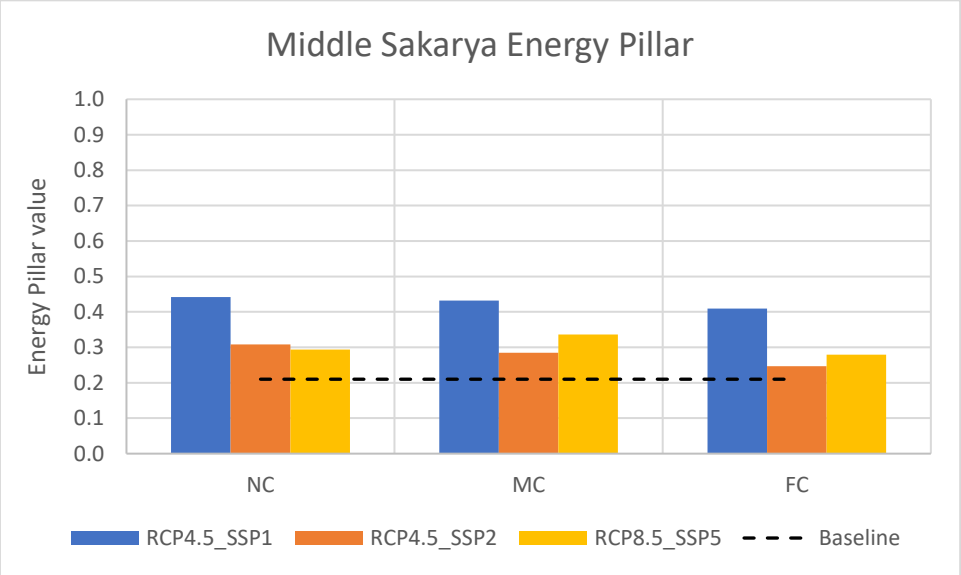

Figure 9-36. Energy pillar value under climate and socioeconomic changes in the Middle Sakarya subbasin

Food

Figure 9-37 shows that the Food pillar scores of all scenarios are always lower than the base case score of 0.92, except the SSP2 scenario in the near century. In addition, it is seen that the Food pillar score decreases over time in all scenarios. SSP2 and SSP5 scenario results are very close to each other. SSP2 scenario results show that if the current practices continue in the basin, irrigation demand deficit will be 8% in the near century, and it will gradually increase to 30% in the mid-century and to 50% in the far century. In SSP5 scenario, the irrigation demand deficit is calculated as 15%, 29%, and 48% in the near, mid- and far century, respectively. The worst Food pillar scores are obtained in the SSP1 scenario. Irrigation demand deficit, which is calculated as 38% in the near century, increases to 51% in the mid-century and to 61% in the far century. The main reason for the difference between the SSP1 scenario and the other scenarios is the strict environmental flow requirements applied in the SSP1 scenario.

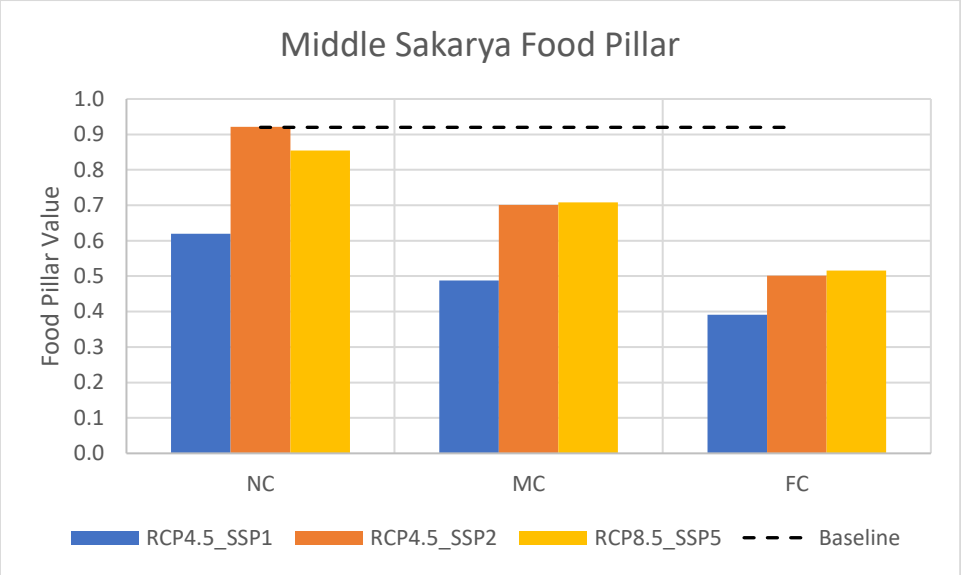

Figure 9-37. Food pillar value under climate and socioeconomic changes in the Middle Sakarya subbasin

Ecosystem

The comparison of the simulated median monthly flows with the IQR of the naturalized streamflow in each scenario in each time period is given in Figure 9-38. The first, second, and the third row of this figure shows the results of the SSP1, SSP2, and SSP5 scenario, respectively. In the SSP1 scenario, MMS of the months of August and November are outside the IQR in the near century, and the Ecosystem pillar score is calculated as 0.88 in this period (Figure 9-39). In the mid-century, the number of months with MMS values outside the IQR increases to five (April, May, June, July and October) but the Ecosystem pillar score (0.93) is still higher as compared to the near century. This is because the MMS values in this period are much closer to either lower or upper quartile of the IQR than the values in the near century. In the far century, the Ecosystem pillar score increases to 1.00 with only one month (March) in which the MMS values is outside the IQR, and in this month

the normalized MMS value is calculated as 0.97. In the SSP2 scenario, there are only four months (January, March, April and July) with MMS values inside the IQR in the near century. In addition, the MMS value in four months (May, August, October and November) is even lower than the minimum value of the naturalized flow, so the normalized MMS values in these months are zero. As a result, the Ecosystem pillar score of the SSP2 scenario in the near century is calculated as 0.49. In the mid-century, the number of months with MMS values inside the IQR increases to five (January, March, April, June and July), and August is the only month which has an MMS value even below the minimum of the naturalized flow. Thus, the Ecosystem pillar score increases to 0.78 in the mid-century. In the far century, the IQR target is met in six months (January, February, March, April, July and December). There are four months with normalized MMS value of zero. Therefore, the Ecosystem pillar value is 0.61 in the far century. The SSP5 scenario results show that there are four months (January, March, April and December) with MMS values inside the IQR and there are three months (May, June and September) that have MMS values even lower than the minimum flow. The Ecosystem pillar score of SSP5 in the near century is calculated as 0.52. In the mid-century, the IQR target is met in five months (January, February, March, April and September) and there are two months (October and November) with a normalized MMS value of zero. Thus, the Ecosystem pillar score is 0.67. In the far century, the Ecosystem pillar gets a higher score (0.79) than near and mid-century. There are seven months that have MMS values remain within the IQR, and only in the month of May the MMS value is lower than the minimum flow. Among all scenarios, the highest Ecosystem score in all periods is obtained in SSP1 scenario. In addition, the scores obtained in this scenario are always higher than the base case.

The changing flow patterns of rivers are fundamental to the survival and health of river ecosystems. High and low-flow events present both challenges and opportunities for different types of riverine species (details in Chapter 7). Given this

information, the 21st century average Ecosystem pillar scores for the low (October – March) and high flow (April – September) periods for three different scenarios SSP1, SSP2, and SSP5 were compared (Table 9-13). As can be seen from Table 9-13, the highest Ecosystem pillar score (0.97) in the low flow period belongs to the SSP1 scenario. The second-best score (0.74) is in the SSP5 scenario. The lowest score (0.64) was calculated in the SSP2 scenario. In the high flow period, although the highest score is in the SSP1 scenario, the score (0.77) decreases compared to the high flow period. Similarly, SSP2 (0.61) and SSP5 (0.57) scenarios also have lower Ecosystem pillar scores during the high flow period. The fact that the scores obtained in the high flow period are lower than the low flow periods in all scenarios indicates that high flow events, which are critical for ecosystem reproductivity and diversity, are more affected.

NF-Q1: Naturalized Streamflow Lower Quartile; NF-Q3: Naturalized Streamflow Upper Quartile; MMS: Simulated Median Monthly Streamflow

Figure 9-38. Middle Sakarya: The comparison of the simulated median monthly flows with the IQR of the naturalized streamflow in each scenario in each time period. First row: SSP1; Second row: SSP2; Last row: SSP5

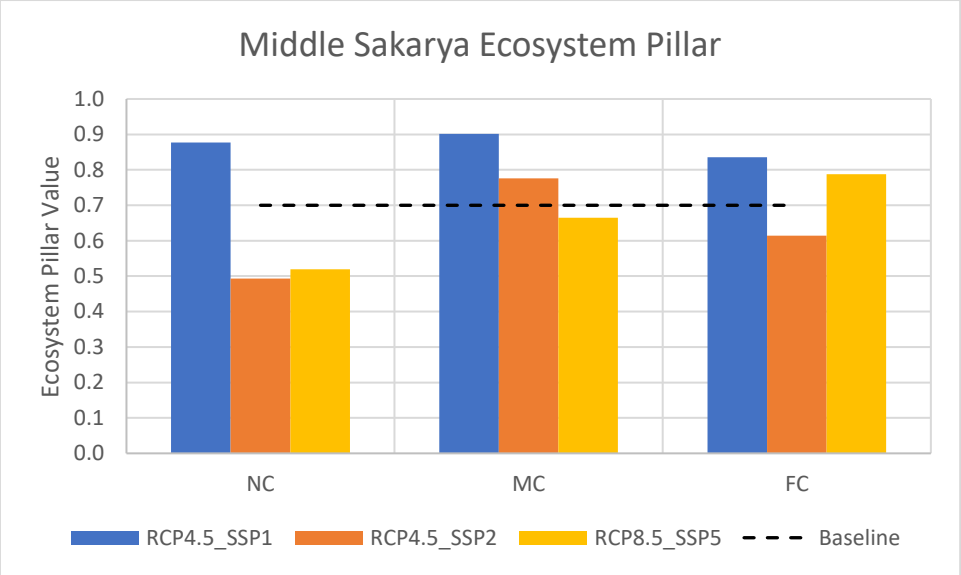

Figure 9-39. Ecosystem pillar value under climate and socioeconomic changes in the Middle Sakarya subbasin

Table 9-13. 21st century average ecosystem pillar scores for low and high flow periods in Middle Sakarya subbasin

	SSP1	SSP2	SSP5
October – March (low flow period)	0.97	0.64	0.74
April -September (high flow period)	0.77	0.61	0.57

Aggregated WEFE Nexus Index

After scores of all nexus pillars are calculated and aggregated, the values of the WEFE Nexus Index given in Figure 9-40 are obtained. As can be seen from the figure, there is no big difference between the index values calculated in the scenarios. The highest score is obtained in the near century in the SSP1 scenario (0.72). This value is very close to the baseline score (0.71). The lowest WEFE Nexus Index value

(0.58) is calculated in the SSP2 scenario in the far century. The all-time average WEFE Nexus Index values are 0.68, 0.65, and 0.66 for SSP1, SSP2, and SSP5, respectively. Considering the Pillar scores obtained in the SSP1 scenario, it is seen that the lowest score in the Water and Food pillars is obtained in the SSP1 scenario. However, in the overall WEFE Nexus assessment, high scores on Energy and Ecosystem pillars compensate for low scores on other pillars.

In the Middle Sakarya subbasin, all nexus pillars are interconnected by complex relationships. First of all, there are four subbasins (Upper Sakarya, Porsuk, Ankara, and Kirmir) located upstream of Middle Sakarya. The total drainage area and population of these subbasins are 43,945 km^2 and 6,102,000, respectively. All of these subbasins have intense agricultural, industrial, and urban activities. Therefore, the sustainability and security of WEFE Nexus components in the Middle Sakarya subbasin actually depends on the activities carried out in the upstream basins. Secondly, Middle Sakarya is a semi-arid basin with high energy demand and production. In the subbasin, electricity generation is highly dependent on water availability since 34% of the total installed capacity belongs to HPPs, and there are TPPs with wet cooling systems. The water shortages experienced from time to time due to climatic conditions and also due to upstream pressures, threaten energy security. In a fieldwork conducted in the basin in mid-July 2022, revealing the severity of the situation showed that the two headwaters of the Middle Sakarya subbasin were completely dry. This strong evidence suggests that an integrated approach considering upstream-downstream interaction in the basin is essential to evaluate the WEFE Nexus to provide sustainable solutions. Thirdly, the agricultural sector also has an important place in the Middle Sakarya subbasin. In the basin, there are several provinces, such as Bolu and Bilecik, whose economy is based on agriculture and animal husbandry. For this reason, there are many dams and ponds built for agricultural irrigation purposes in the basin. Lastly, in the Middle Sakarya subbasin, there are many hydroelectric power plants with dams built on the Sakarya

River main branch. Therefore, there are significant and clearly visible disturbances associated with basin and water resources development. As a result, natural habitat, biota and basic ecosystem functions have modified to a significant extent. In this study, the baseline Ecosystem pillar score in the Middle Sakarya subbasin is calculated as 0.70. In the 21st century, the highest scores of the Ecosystem pillar are obtained in the SSP1 scenario. However, this is at the expense of the agricultural irrigation and municipal water. Therefore, it is not reasonable to aim for a return to natural flow conditions in the Middle Sakarya subbasin, where significant modifications have already taken place. For this reason, it would be more realistic to target slightly or moderately modified conditions in the basin. In addition, even in scenarios where there is no environmental flow requirement, i.e., SSP2 and SSP5, an average of approximately 30% irrigation demand deficit is calculated and the amount of electricity produced in hydroelectric power plants in these scenarios is less than in the SSP1 scenario. Therefore, targeting slightly or moderately modified conditions in the SSP1 scenario and implementing agricultural BMPs will ensure that the basin reaches the most balanced and sustainable level in terms of all pillars. In addition, each application that will contribute to the sustainability of WEFE Nexus pillars in the Upper Sakarya, Porsuk and Ankara subbasins will result in higher WEFE Index scores in the Middle Sakarya subbasin.

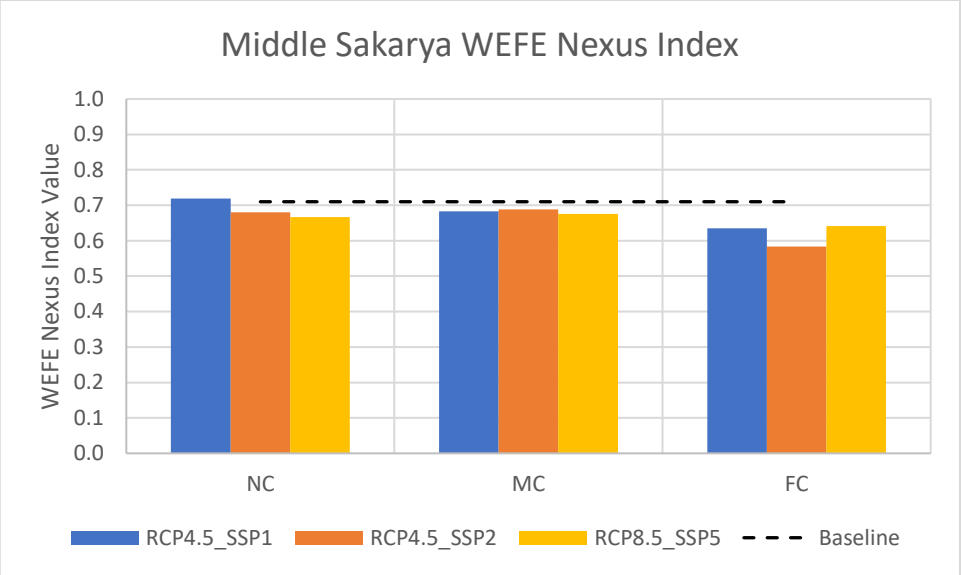

Figure 9-40. WEFE Nexus Index value under climate and socioeconomic changes in the Middle Sakarya subbasin

9.4.6 Göksu Subbasin

Table 9-14 provides a comparative analysis of the WEFE Nexus indicators for different scenarios representing climate and socioeconomic changes and for different time periods, i.e., near, mid-, and far century, in the Göksu subbasin. Figure 9-41 presents the same information as Table 9-14 in a visual format, using spider charts to illustrate the values of WEFE Nexus indicators for different time periods and scenarios. The charts provide a clear and concise comparison of the values for each scenario across the different time periods, highlighting the differences that exist between scenarios and time periods. By examining the values for each indicator, a deeper understanding of the complex interplay between water, energy, food, and the ecosystem can be gained, and how this interplay may evolve over time can be

understood. The pillar indices created using these indicators are evaluated in detail under the subtitles Water, Energy, Food, and Ecosystem below.

Table 9-14. WEFE Nexus indicators' comparative analysis for different scenarios in the 21st century: variations over multiple time periods in the Göksu subbasin

		NC	MC	FC			NC	MC	FC			NC	MC	FC
RCP4.5_SSP1	MDC	0.97	0.98	0.97	**RCP4.5_SSP2**	MDC	1.00	1.00	1.00	**RCP8.5_SSP5**	MDC	1.00	1.00	1.00
	HPP_MGC	0.11	0.08	0.07		HPP_MGC	0.06	0.05	0.04		HPP_MGC	0.06	0.07	0.06
	RES	1.00	1.00	1.00		RES	1.00	1.00	1.00		RES	1.00	1.00	1.00
	CO2_EG	0.00	0.00	0.00		CO2_EG	0.00	0.00	0.00		CO2_EG	0.00	0.00	0.00
	IDM	0.57	0.57	0.56		IDM	0.94	0.90	0.87		IDM	0.92	0.83	0.80
	Jan-MMS	1.00	1.00	1.00		Jan-MMS	1.00	1.00	1.00		Jan-MMS	1.00	1.00	1.00
	Feb-MMS	1.00	1.00	1.00		Feb-MMS	1.00	1.00	1.00		Feb-MMS	1.00	1.00	1.00
	Mar-MMS	1.00	1.00	1.00		Mar-MMS	1.00	1.00	1.00		Mar-MMS	1.00	1.00	1.00
	Apr-MMS	1.00	1.00	1.00		Apr-MMS	1.00	1.00	1.00		Apr-MMS	1.00	1.00	1.00
	May-MMS	1.00	1.00	1.00		May-MMS	1.00	1.00	1.00		May-MMS	1.00	1.00	1.00
	Jun-MMS	1.00	1.00	0.96		Jun-MMS	1.00	1.00	1.00		Jun-MMS	1.00	1.00	1.00
	Jul-MMS	0.59	0.76	0.27		Jul-MMS	1.00	0.84	0.00		Jul-MMS	0.00	0.00	0.00
	Aug-MMS	0.00	0.00	0.23		Aug-MMS	0.00	0.00	0.00		Aug-MMS	1.00	0.00	0.00
	Sep-MMS	0.77	0.00	0.78		Sep-MMS	0.92	0.00	0.51		Sep-MMS	1.00	0.99	0.93
	Oct-MMS	1.00	1.00	1.00		Oct-MMS	1.00	1.00	1.00		Oct-MMS	1.00	1.00	1.00
	Nov-MMS	0.00	1.00	1.00		Nov-MMS	1.00	1.00	0.94		Nov-MMS	1.00	1.00	1.00
	Dec-MMS	1.00	1.00	1.00		Dec-MMS	1.00	1.00	1.00		Dec-MMS	1.00	1.00	0.99

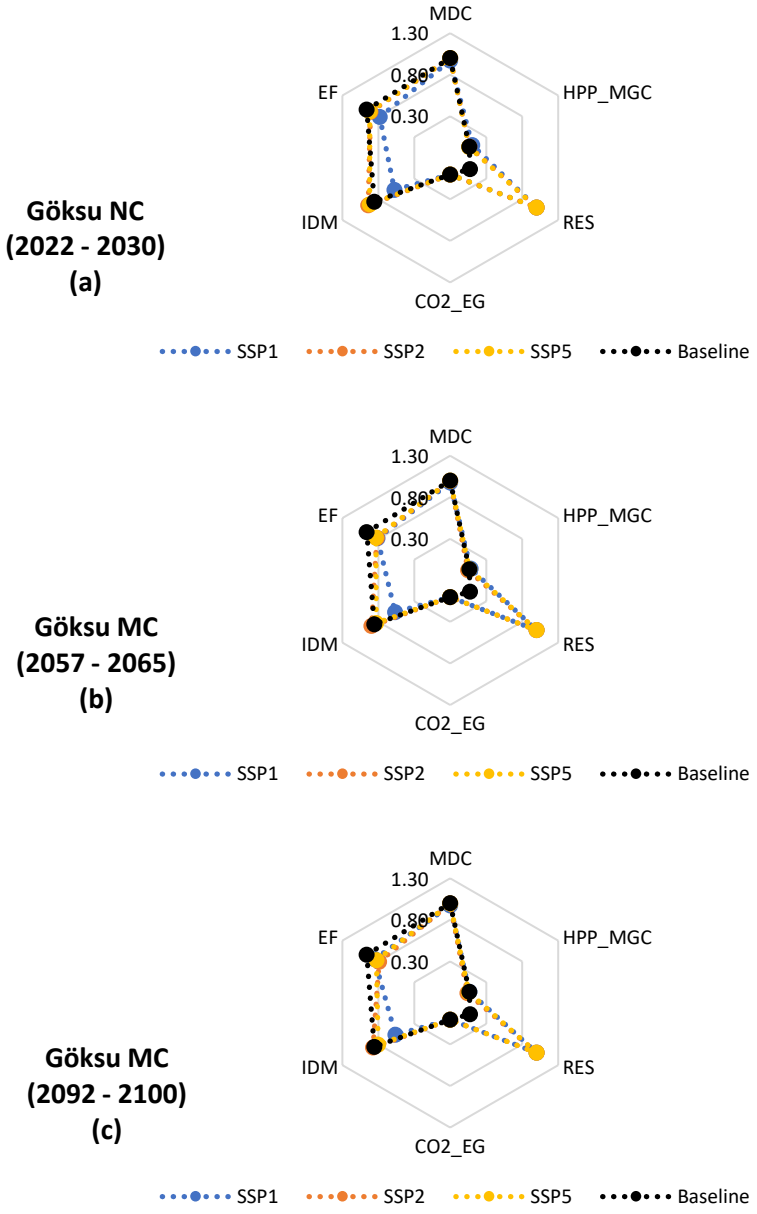

Figure 9-41. Göksu subbasin: The values of the WEFE Nexus Index Pillar Indicators in each scenario in each future period segment; near century (a), mid-century (b), far century (c). Note: Ecosystem indicator values are not provided in this figure. The parameter EF represents the average of ecosystem indicators, which is equivalent to the Ecosystem pillar value

Water

Figure 9-42 shows that the municipal water demand coverage is 100% in the base case, SPP2 and SSP5 scenario. The only scenario in which there is some municipal water demand deficit is the SSP1 scenario. However, the deficit amount calculated in the SSP1 scenario is not at critical levels either; the 21st century average of the Water pillar score is 0.97, which means an average deficit of 3%. The reason for the deficit calculated in the SSP1 scenario is the strict environmental flow requirements.

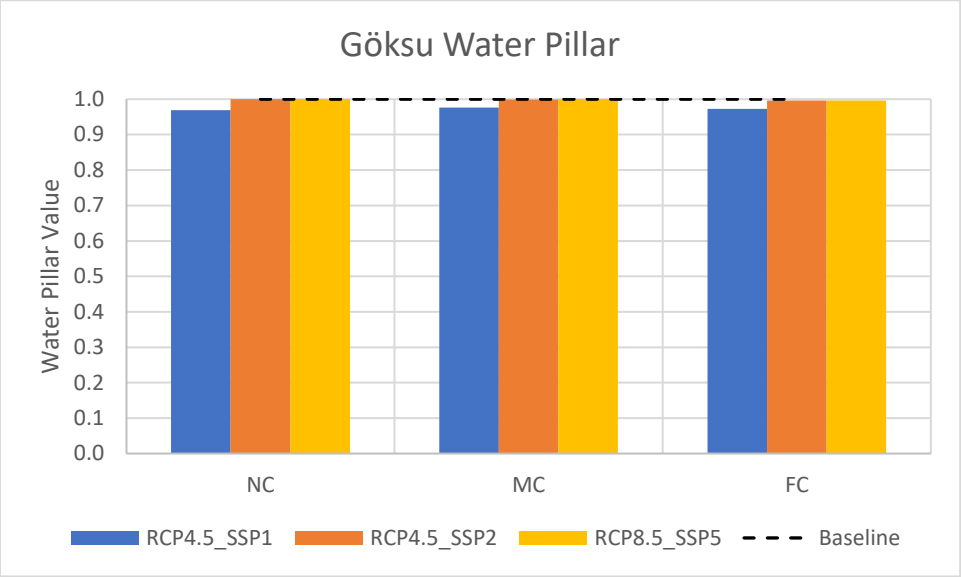

Figure 9-42. Water pillar value under climate and socioeconomic changes in the Göksu subbasin

Energy

Göksu subbasin is the second subbasin with the lowest electricity generation among the subbasins in the Sakarya Basin where electricity is produced. In the Göksu subbasin, there are only two power plants in the baseline period with an installed capacity of over 10 MW. One of them is hydroelectric and the other is natural gas fired thermal power plant. Figure 9-43 indicates that the Energy pillar has a score of

0.07 in the baseline period, and all scenarios have higher Energy pillar scores than the base case. As it can be seen from Figure 9-41, the value of the indicator RES is one in all scenarios in all periods. This means that the target of 30% of total electricity production from renewable sources is met in all scenarios. The value of the indicator CO_2_EG, on the other hand, is 0.00 in all scenarios in all periods. That is, the amount of CO_2 emissions in the scenarios is either equal to or greater than the baseline. The 21st century average value of the HPP_MGC indicator is 0.08, 0.05, and 0.06 in SSP1, SSP2 and SSP5 scenarios, respectively. This means that SSP1 is the only scenario where the hydroelectric potential is used more than the base case which has an HPP_MGC score of 0.07. The overall average Energy pillar score in the 21st century is 0.36 in the SSP1 scenario, and 0.35 in the SSP2 and SSP5 scenarios. Göksu is the subbasin with the lowest drainage area among the Sakarya Basin subbasins. Therefore, due to the strategy followed within the scope of this study, the potential for solar and wind power plants to be established is lower compared to other subbasins. This explains why the Energy pillar score of SSP1 and other scenarios is not very different from each other.

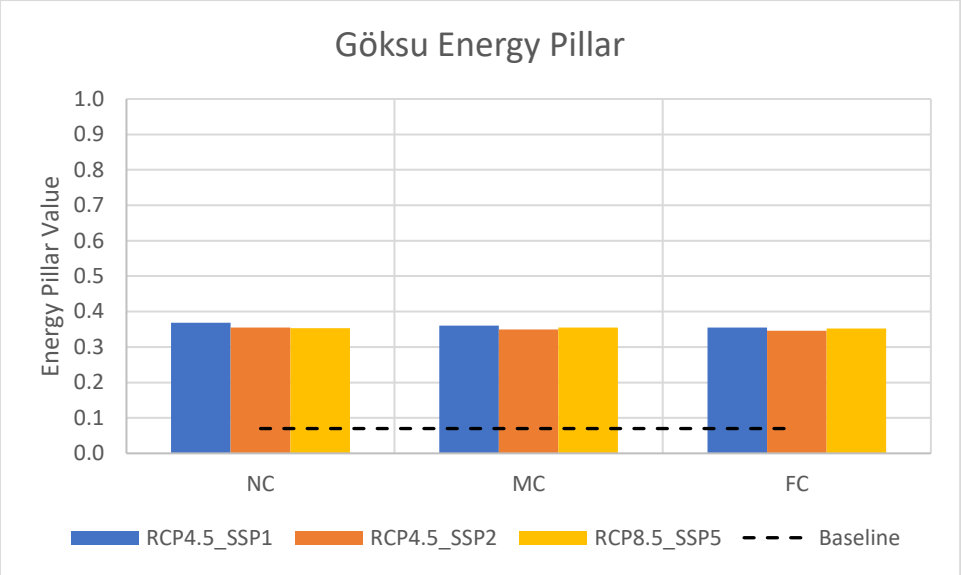

Figure 9-43. Energy pillar value under climate and socioeconomic changes in the Göksu subbasin

Food

Approximately 50% of Göksu subbasin consists of agricultural areas and about 20% of agricultural areas are irrigated. In the Göksu subbasin, the Food pillar score in the base case is 0.86 which means that there is an average of 14% irrigation demand deficit (Figure 9-44). The highest Food pillar scores in all future periods are obtained in the SSP2 scenario. The 21st century average Food pillar score in the SSP2 scenario is 0.90. Although the scores of the SSP2 and SSP5 scenarios are very close to each other, the scores of SSP5 scenario are always lower than SSP2. In the SSP1 scenario, on the other hand, there is a significant difference between its Food pillar score and the scores of other scenarios. The Food pillar score obtained in all periods in the SSP1 scenario is around 0.57. This means an average of 43% deficit in agricultural irrigation in the 21st century. The results show that the strict environmental flow

requirements applied in the SSP1 scenario cause a deficit in agricultural irrigation as well as municipal water demand deficit.

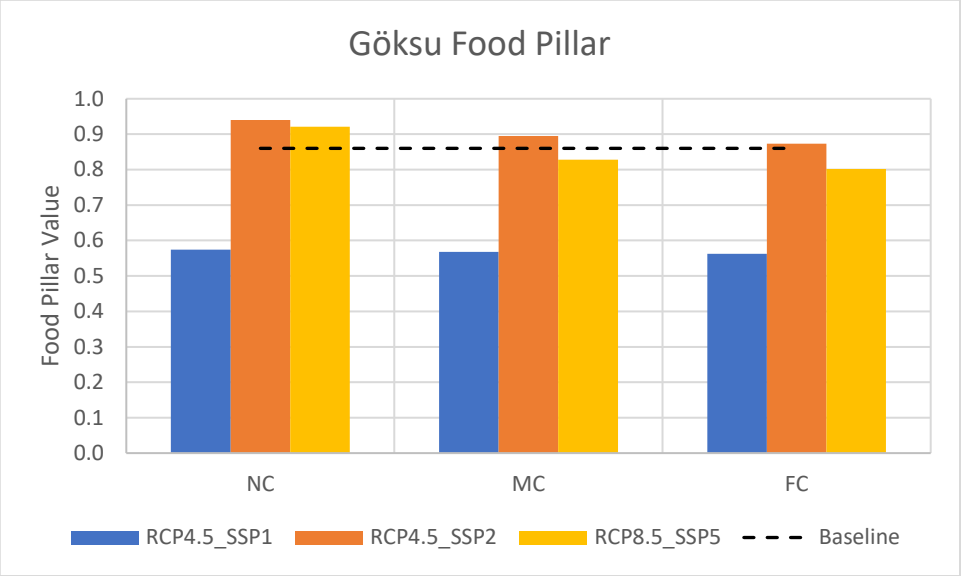

Figure 9-44. Food pillar value under climate and socioeconomic changes in the Göksu subbasin

Ecosystem

The comparison of the simulated median monthly flows with the IQR of the naturalized streamflow in each scenario in each time period is given in Figure 9-45. The first, second, and the third row of this figure shows the results of the SSP1, SSP2, and SSP5 scenario, respectively. In the SSP1 scenario, the MMS values in the months of July, August, September, and November are outside the IQR in the near century. Furthermore, the MMS values in August and November are even higher than the maximum naturalized streamflow occurring in these months. Thus, the normalized streamflow values in these months are zero. The overall Ecosystem pillar value is calculated as 0.78 in the near century (Figure 9-46). In the mid-century, the Ecosystem pillar value increases to 0.81, and there are three months (July, August

and September) with MMS values outside the IQR. Two of these months have a normalized value of zero since their medians are above the maximum naturalized streamflow. In the far century, the Ecosystem pillar value is 0.85 which is the highest score among the three future period segments. Therefore, in the SSP1 scenario, the Ecosystem pillar score increases from the near century to the far century. Although the number of months with an MMS value outside the IQR in the far century is higher than near and mid-century, the score is better since none of these months has a normalized value of zero. In the SSP2 scenario, the Ecosystem pillar score is 0.91 in the near century. There are only two months (August and September) in which the IQR target is not met. However, the median streamflow in September is very close to the upper quartile of the IQR and hence the normalized value is 0.92. In August, on the other hand, the normalized value is zero. In the mid-century, the Ecosystem pillar score decreases to 0.82. There are three months (July, August, and September) with an MMS value outside the IQR and two of them (August and September) have a normalized value of zero. In the SSP2 scenario, it is seen that the Ecosystem pillar score decreases from the near century to the far century. The lowest Ecosystem score is calculated in the far century with a value of 0.79. In the far century, there are four months (July, August, September, and November) in which the IQR target is not met, and two of them (July and August) have a normalized value of zero. In the SSP5 scenario, the Ecosystem pillar score in the near century is 0.92, and there is a single month (July) not meeting the IQR target. In this month, the normalized value is zero. In the mid-century, Ecosystem pillar score decreases to 0.83. In the months of July, August and September, the MMS values are outside the IQR. In July and August, the MMS value is above the maximum naturalized streamflow and hence the normalized values are zero. In September, on the other hand, the MMS is very close to the upper quartile of IQR, and the normalized value is 0.99. In the far century, the Ecosystem pillar score is the same as it is in the mid-century with a value of 0.83. Similar to mid-century, the normalized MMS values in July and August are zero. In

September and December, the MMS value is almost at the upper quartile of the IQR. The results show that, similar results are obtained in all scenarios in Göksu subbasin. The main difference is that in the SSP1 scenario, the Ecosystem pillar score is in an increasing trend from the near to the far century, whereas a decreasing trend is observed in the other scenarios. The most striking result is that the Ecosystem pillar score obtained in all scenarios is lower than the base case.

As mentioned in Chapter 7, both high and low-flow periods are essential for the survival and diversity of river organisms. To assess the ecosystem's relative health during these periods, it is necessary to analyze the scores for each period and make comparisons across the scenarios. Table 9-15 displays the results of this analysis, presenting the average Ecosystem pillar scores for the low and high flow periods in the 21st century. The results show that, in the low flow period, all three scenarios have Ecosystem pillar scores above 0.9, indicating a relatively high level of sustainability. However, during the high flow period, the scores are lower, ranging from 0.68 to 0.72, which suggests a decrease in the sustainability of the ecosystem during this period. It is important to note that high flow events can have numerous benefits for the ecosystem, such as nutrient cycling and sediment transport. In this case, the lower scores during the high flow period suggest that certain ecosystem functions may be more affected, potentially indicating negative impacts on the overall health and sustainability of the ecosystem.

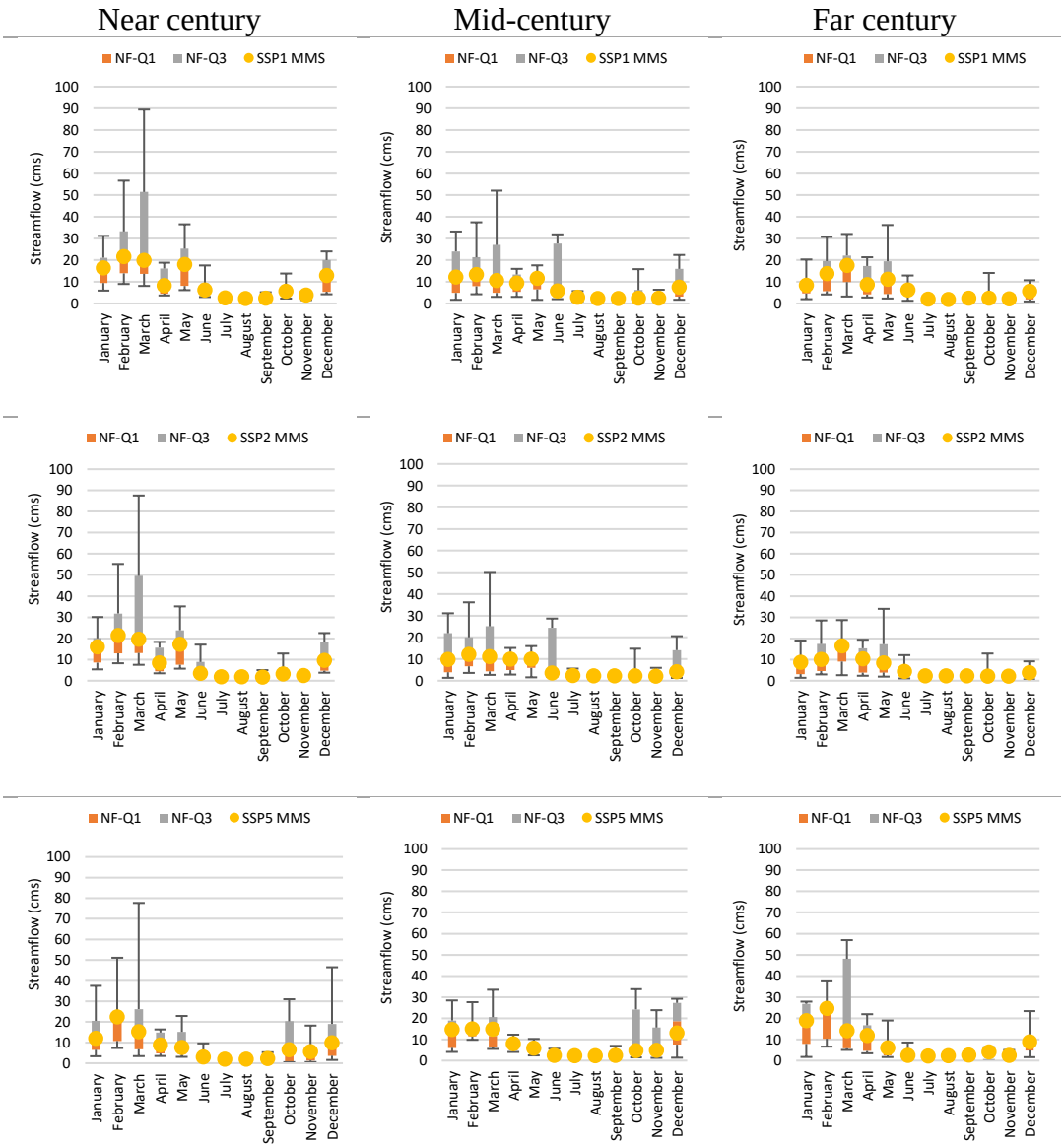

NF-Q1: Naturalized Streamflow Lower Quartile; NF-Q3: Naturalized Streamflow Upper Quartile; MMS: Simulated Median Monthly Streamflow

Figure 9-45. Göksu: The comparison of the simulated median monthly flows with the IQR of the naturalized streamflow in each scenario in each time period. First row: SSP1; Second row: SSP2; Last row: SSP5

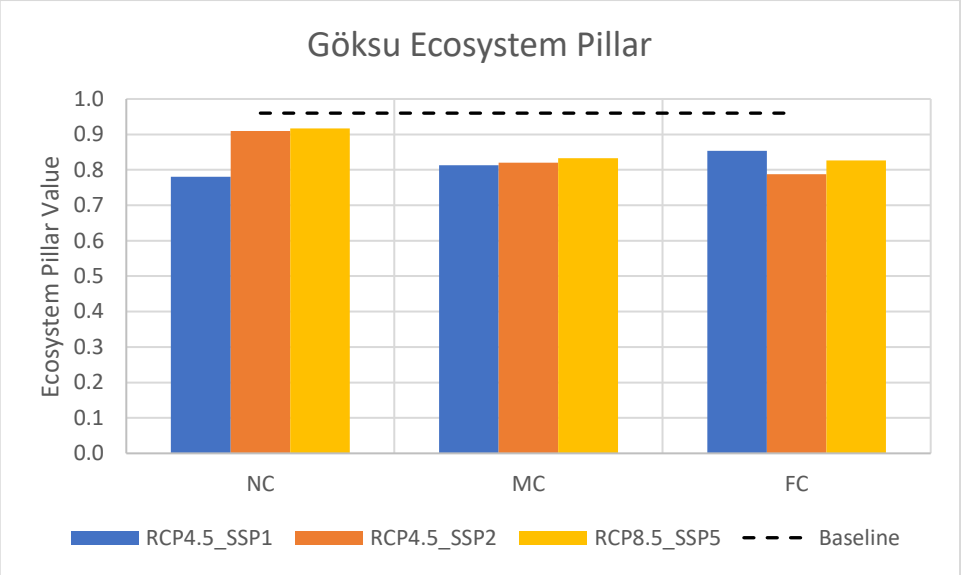

Figure 9-46. Ecosystem pillar value under climate and socioeconomic changes in the Göksu subbasin

Table 9-15. 21st century average ecosystem pillar scores for low and high flow periods in Göksu subbasin

	SSP1	SSP2	SSP5
October – March (low flow period)	0.94	1.00	1.00
April -September (high flow period)	0.69	0.68	0.72

Aggregated WEFE Nexus Index

After scores of all nexus pillars are calculated and aggregated, the values of the WEFE Nexus Index given in Figure 9-47 are obtained. This figure shows that while higher scores are obtained in SSP2 and SSP5 scenarios compared to the base case score of 0.72, the scores obtained in the SSP1 scenario are lower than the base case. The 21st century average WEFE Nexus Index value obtained in the SSP2 and SSP5

scenarios is the same, which is 0.77. In the SSP1 scenario, on the other hand, all-time average WEFE Nexus Index value is 0.68. In the Göksu subbasin, the scenario with the most balanced results in terms of all pillars and the highest overall WEFE Nexus Index score is the SSP2 scenario. That is, even if the social, economic, and technological trends do not shift markedly from historical patterns, the WEFE Nexus status will not be worser than today.

Göksu subbasin differs from other subbasins in Sakarya Basin with its future climatic conditions. While annual average precipitation is projected to decrease in other subbasins in the 21st century, no statistically significant decreasing trend is detected in precipitation in Göksu subbasin. On the contrary, when the historical period average is compared with the 21st century average, the average precipitation is higher than the historical average in almost all projections. Therefore, while a decrease in water availability is anticipated in WEFE Nexus sectors in other subbasins (except Lower Sakarya), this is not the case in Göksu subbasin. The results support this conclusion. In the Göksu subbasin, no significant deficit is detected in municipal water demand in any scenario. Furthermore, in the SSP2 scenario, the irrigation demand deficit decreases compared to the base case. Giving priority to the ecosystem in the SSP1 scenario causes a deficit in agricultural irrigation and municipal water demand, and it does not result in a significantly better ecosystem status than SSP2. In the Göksu subbasin, the Ecosystem pillar value in the base case is 0.96. This value is very close to full sustainability. Therefore, the current sectoral water allocation in Göksu subbasin does not cause any problems in terms of sustainability of WEFE Nexus pillars. The most critical recommendation for the Göksu subbasin may be to increase agricultural irrigation efficiency because, although the deficit in agricultural irrigation decreases in the SSP2 scenario than the base case, there is still an average of 10% deficit. To close this gap, investments should be made in sustainable agricultural practices that will increase productivity in agricultural irrigation. Thus, it will be possible to prevent the deterioration of the sustainability of the ecosystem

in the 21st century compared to the base case while decreasing irrigation demand deficit.

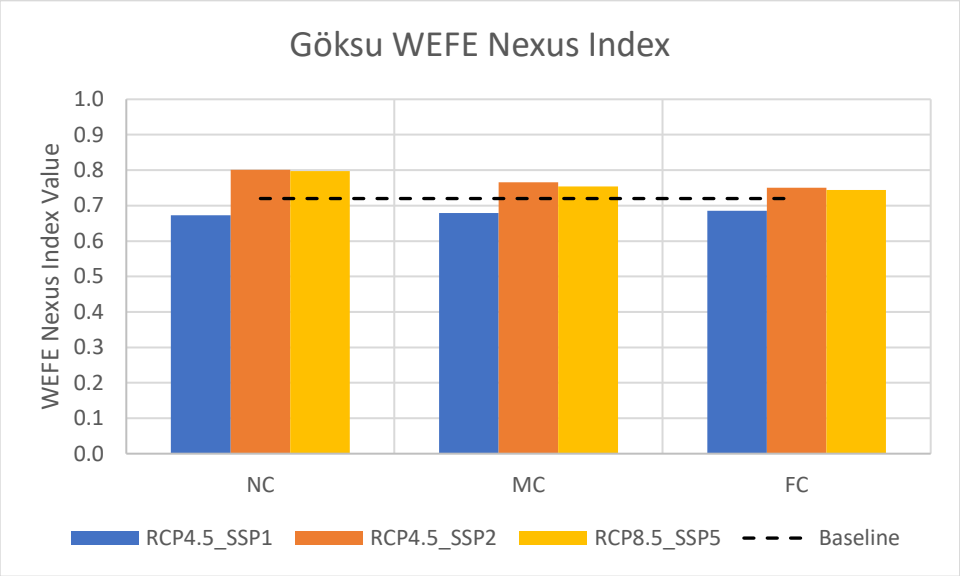

Figure 9-47. WEFE Nexus Index value under climate and socioeconomic changes in the Göksu subbasin

9.4.7 Lower Sakarya Subbasin

Table 9-16 provides a comparative analysis of the WEFE Nexus indicators for different scenarios representing climate and socioeconomic changes and for different time periods, i.e., near, mid-, and far century, in the Lower Sakarya subbasin. Figure 9-48 presents the same information as Table 9-16 in a visual format, using spider charts to illustrate the values of WEFE Nexus indicators for different time periods and scenarios. The charts provide a clear and concise comparison of the values for each scenario across the different time periods, highlighting the differences that exist

between scenarios and time periods. By examining the values for each indicator, a deeper understanding of the complex interplay between water, energy, food, and the ecosystem can be gained, and how this interplay may evolve over time can be understood. The pillar indices created using these indicators are evaluated in detail under the subtitles Water, Energy, Food, and Ecosystem below.

Table 9-16. WEFE Nexus indicators' comparative analysis for different scenarios in the 21st century: variations over multiple time periods in the Lower Sakarya subbasin

RCP4.5_SSP1		NC	MC	FC	RCP4.5_SSP2		NC	MC	FC	RCP8.5_SSP5		NC	MC	FC
	MDC	0.75	0.81	0.87		MDC	1.00	0.97	0.91		MDC	1.00	0.95	0.91
	HPP_MGC	0.54	0.45	0.38		HPP_MGC	0.35	0.29	0.25		HPP_MGC	0.33	0.32	0.28
	RES	0.07	0.13	0.18		RES	0.04	0.03	0.03		RES	0.04	0.04	0.03
	CO2_EG	0.12	0.05	0.03		CO2_EG	0.04	0.01	0.00		CO2_EG	0.03	0.02	0.01
	IDM	1.00	1.00	1.00		IDM	1.00	0.99	0.99		IDM	1.00	0.99	0.98
	Jan-MMS	1.00	1.00	1.00		Jan-MMS	1.00	1.00	1.00		Jan-MMS	1.00	1.00	1.00
	Feb-MMS	1.00	1.00	1.00		Feb-MMS	1.00	0.87	1.00		Feb-MMS	1.00	1.00	1.00
	Mar-MMS	1.00	1.00	1.00		Mar-MMS	1.00	1.00	1.00		Mar-MMS	1.00	1.00	1.00
	Apr-MMS	1.00	1.00	1.00		Apr-MMS	1.00	1.00	1.00		Apr-MMS	1.00	1.00	1.00
	May-MMS	1.00	1.00	1.00		May-MMS	1.00	1.00	0.86		May-MMS	0.20	0.42	0.00
	Jun-MMS	1.00	1.00	1.00		Jun-MMS	1.00	1.00	0.00		Jun-MMS	0.00	0.69	0.09
	Jul-MMS	1.00	1.00	1.00		Jul-MMS	1.00	1.00	1.00		Jul-MMS	0.00	1.00	0.96
	Aug-MMS	0.80	1.00	0.94		Aug-MMS	0.81	1.00	1.00		Aug-MMS	1.00	1.00	1.00
	Sep-MMS	1.00	1.00	1.00		Sep-MMS	0.00	1.00	0.58		Sep-MMS	1.00	1.00	1.00
	Oct-MMS	1.00	0.95	0.43		Oct-MMS	0.00	0.00	0.00		Oct-MMS	1.00	0.00	1.00
	Nov-MMS	1.00	1.00	1.00		Nov-MMS	0.00	0.30	0.00		Nov-MMS	1.00	0.22	1.00
	Dec-MMS	1.00	1.00	1.00		Dec-MMS	1.00	1.00	1.00		Dec-MMS	1.00	0.97	1.00

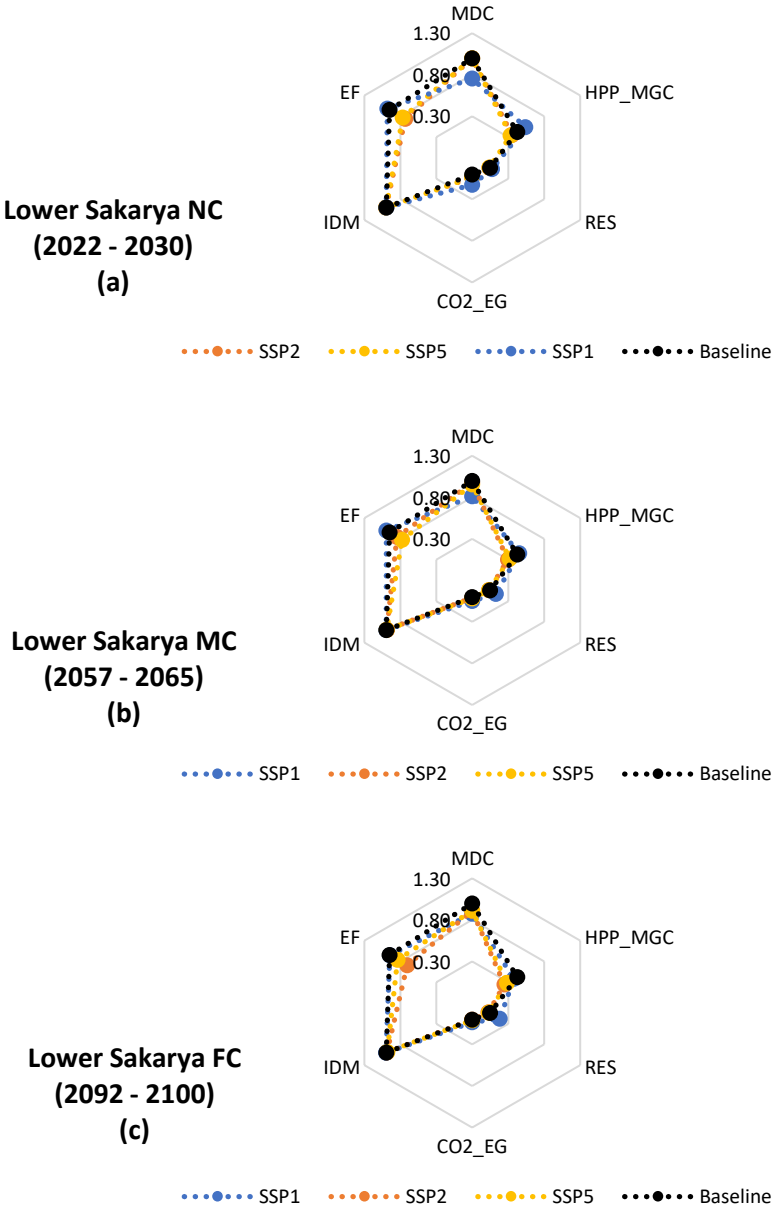

Figure 9-48. Lower Sakarya subbasin: The values of the WEFE Nexus Index Pillar Indicators in each scenario in each future period segment; near century (a), mid-century (b), far century (c). Note: Ecosystem indicator values are not provided in this figure. The parameter EF represents the average of ecosystem indicators, which is equivalent to the Ecosystem pillar value

Water

In Lower Sakarya subbasin, water use is mainly for drinking purposes since Sakarya city center is located in this subbasin. However, the water quality of the Sakarya River which constitutes a major part of the water potential, is not suitable for drinking water use. In order to use the river's water for drinking water purposes, it is necessary to install expensive treatment systems that require advanced treatment technology. Therefore, a significant part of the drinking water requirement is supplied from Sapanca Lake, whose water meets drinking water standards (DSİ, 2017). Figure 9-49 shows that there is no municipal water demand deficit in the base case in Lower Sakarya subbasin hence the Water pillar score is one. In the SSP2 and SSP5 scenarios, although municipal water demand coverage is 100% in the near century, the Water pillar score decreases from near century to far century. The 21st century average Water pillar score is 0.96 and 0.95 in the SSP2 and SSP5 scenario, respectively. In the SSP1 scenario, the Water pillar score is 0.71 in the near century, increasing to 0.81 in the mid-century and 0.87 in the far century. Thus, SSP1 scenario has an average of approximately 20% municipal water demand deficit in the 21st century. The main reason for this significant difference between SSP1 and other scenarios is the targeting of natural flow conditions in the SSP1 scenario.

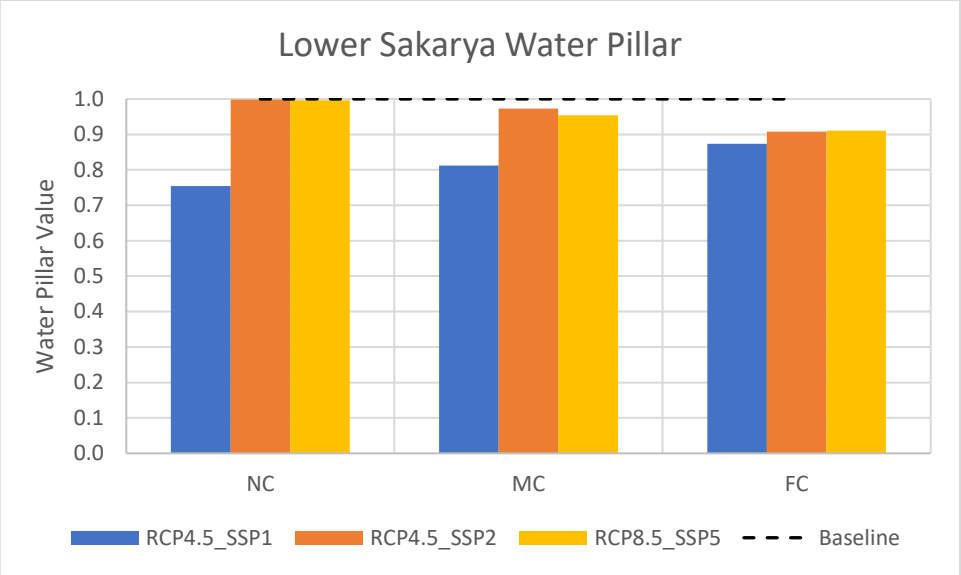

Figure 9-49. Water pillar value under climate and socioeconomic changes in the Lower Sakarya subbasin

Energy

Lower Sakarya subbasin has the highest electricity production among the seven subbasins in the Sakarya Basin. Türkiye's fourth largest and Sakarya Basin's largest thermal power plant which has an installed capacity of 1631 MW is located in this subbasin. In addition, there are four hydroelectric power plants in the basin, evaluated within this study's scope, and the installed capacities of these plants vary between 9.6 MW and 17 MW. The baseline energy pillar score is 0.23 (Figure 9-50), and the score closest or higher to this value is only in the SSP1 scenario. The Energy pillar scores obtained in the SSP2 and SSP5 scenarios are very close to each other. When the values of RES, one of the energy pillar indicators, are examined, it is seen that 30% renewable energy share cannot be reached in any scenario (Figure 9-48). In addition, the CO_2_EG indicator value shows that the thermal power plants in the basin are operated at the same level or more than the base case in the 21st century

scenarios. Even in the SSP1 scenario, taking the green road, the average CO_2_EG score obtained is 0.07, which means that the reduction in CO_2 emissions is far from the Paris agreement targets. This raises the issue of the need for gradual closure of thermal power plants in order to achieve emission reduction targets. If these power plants cannot be closed, serious investments should be made in research and application of technologies that will reduce carbon emissions, e.g., carbon capture and storage (CCS). The only scenario where hydroelectric power plants produce more electricity than the base case is again SSP1 (except for the far century). The average Energy pillar score in SSP1 and other scenarios is 0.22 and 0.12, respectively. In all scenarios, the Energy pillar score decreases from the near century to the far century.

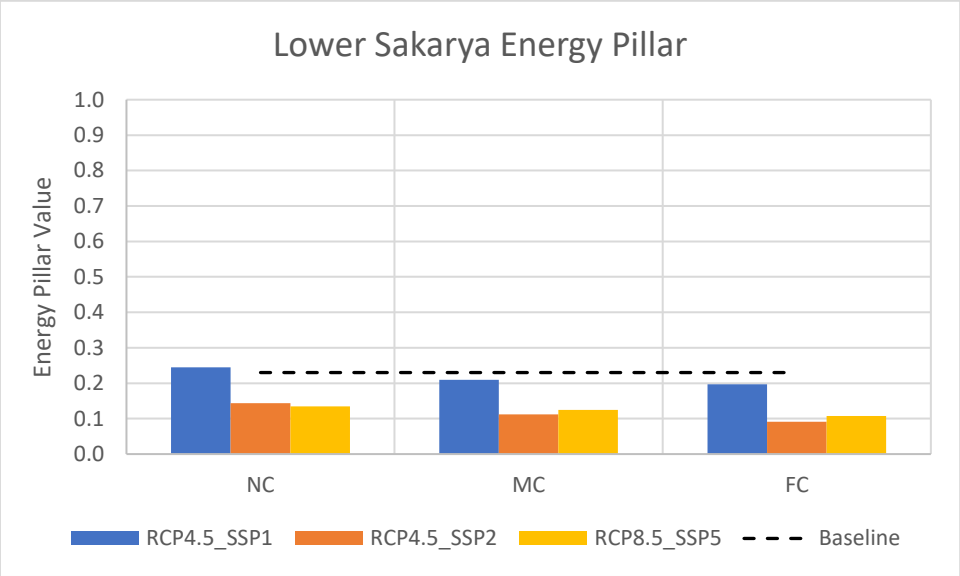

Figure 9-50. Energy pillar value under climate and socioeconomic changes in the Lower Sakarya subbasin

Food

Figure 9-51 shows that there is no problem in meeting the irrigation needs in the Lower Sakarya subbasin in the base case and in the 21st century scenarios. In the SSP1 scenario, the Food pillar score is one in all periods. The average Food pillar score calculated in the SSP2 and SSP5 scenarios is 0.99, hence there is only about 1% irrigation demand deficit.

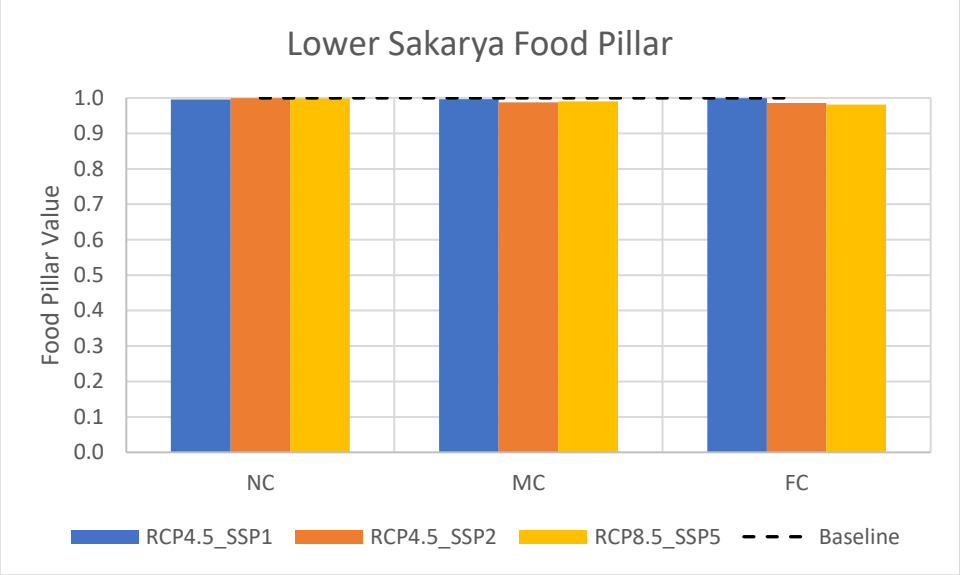

Figure 9-51. Food pillar value under climate and socioeconomic changes in the Lower Sakarya subbasin

Ecosystem

The comparison of the simulated median monthly flows with the IQR of the naturalized streamflow in each scenario in each time period is given in Figure 9-52. The first, second, and the third row of this figure shows the results of the SSP1, SSP2, and SSP5 scenario, respectively. In the SSP1 scenario, there is only one month in each period whose MMS value is outside the IQR. These months are August in the near century, October in the mid-century, and March in the far century. The overall

Ecosystem pillar scores in the near, mid-, and far century are 0.98, 1.00, and 0.95, respectively. In the SSP2 scenario, the MMS value in four months fails to meet IQR target in the near century. These months are August, September, October, and November. Three of these months have an MMS value lower than the minimum naturalized flow, and hence their normalized MMS value is zero. In the mid-century, there are three months (February, October, November) whose MMS value is outside the IQR. The MMS value of all these months are below the lower quartile of the IQR, and MMS value in October is even below the minimum naturalized flow. In the far century, the number of months whose MMS value is outside the IQR increases to five, and three of them have a normalized MMS value of zero. In the SSP2 scenario, the overall Ecosystem pillar score is 0.73, 0.85, and 0.70 in the near, mid- and far century, respectively. In the SSP5 scenario, there are three months (May, June, and July) with an MMS value outside the IQR in the near century. Two of these months (June and July) have a normalized value of zero. In the mid-century, the MMS value in the months of May, June, July, October, November, and December is outside the IQR. In October, the MMS is lower than the minimum naturalized flow thus the normalized MMS value is zero. In the months with an MMS value outside the IQR, the MMS value is lower than the lower quartile. Lastly, there are three months in which the IQR target is not met in the far century and these months are May, June, and July. May is the only month with a normalized value of zero. In all of these months, the MMS value is below the lower quartile. In the SSP5 scenario, the overall Ecosystem pillar scores are 0.77, 0.77, and 0.84, in the near, mid- and far century, respectively. The results show that the highest Ecosystem pillar scores are obtained in the SSP1 scenario among all scenarios in all time periods. Furthermore, the scores in the SSP1 scenario are very close to one which refers to full sustainability. In the SSP2 and SSP5 scenarios, on the other hand, the Ecosystem pillars scores are lower than the base case.

Regular seasonal fluctuations in river flow are crucial for the survival of river organisms as they enable them to complete their life cycle. Both high and low flow events provide critical stresses and opportunities for various riverine species. Moderately high flows that occur frequently transport sediment through channels and help maintain ecosystem productivity and diversity, providing several ecological benefits. In contrast, low flows create recruitment opportunities for riparian plant species in areas where floodplains are frequently inundated (details in Chapter 7). In light of this information, 21st century average Ecosystem pillar scores in low flow (October – March) and high flow (April – September) periods in all three scenarios were calculated. The results of this analysis are given in Table 9-17. Looking at the Ecosystem pillar scores for the low and high flow periods, it can be observed that in the SSP5 scenario, the low flow period score is higher than the high flow period score, indicating a more sustainable ecosystem during the low flow period. However, in the SSP1 and SSP2 scenario, the high flow period score is higher than the low flow period score, which is the only subbasin where this is the case. Additionally, the difference in scores between the two periods is relatively small in the SSP1 scenario, whereas in the SSP2 and SSP5 scenarios, the difference is more significant.

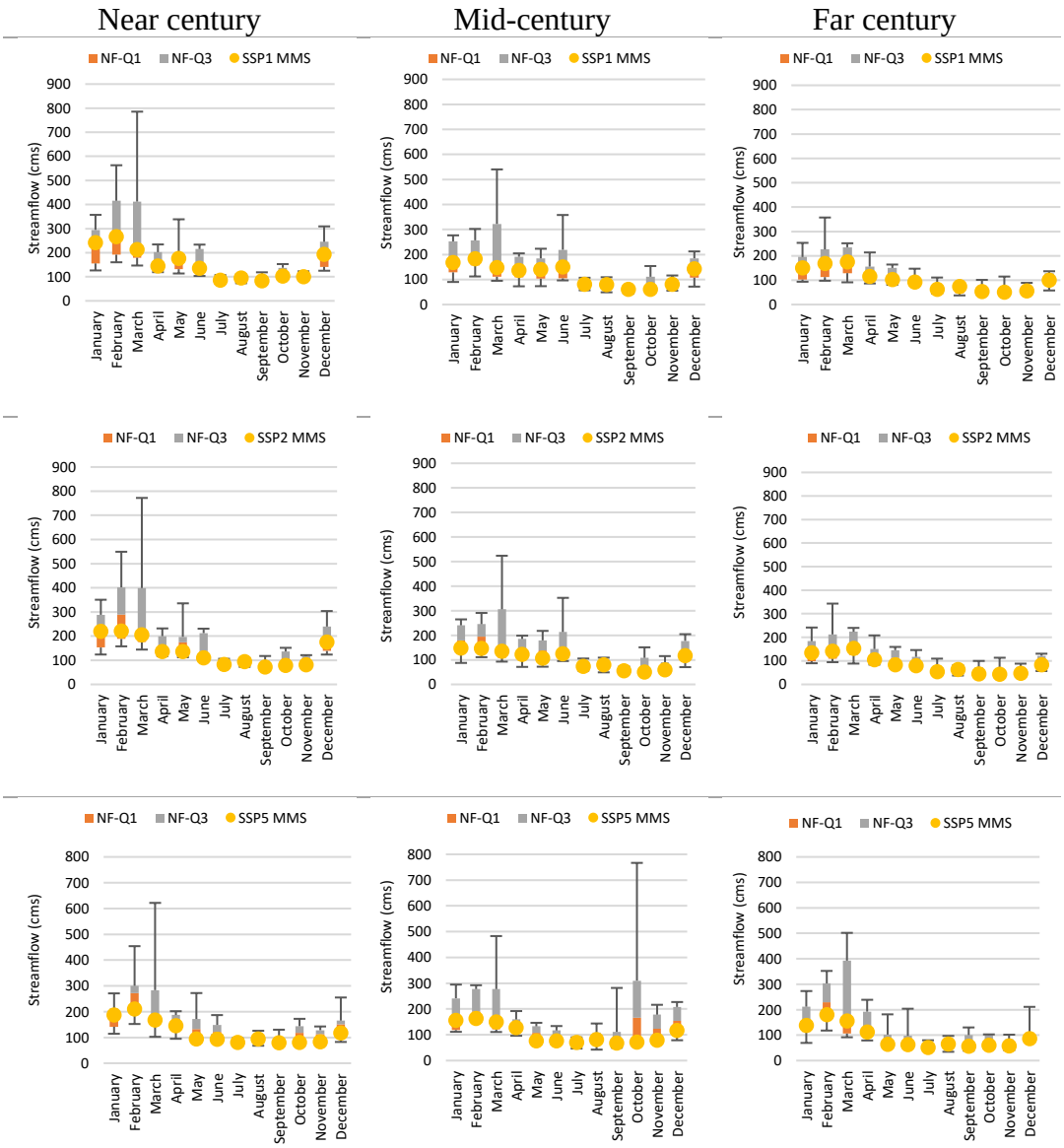

NF-Q1: Naturalized Streamflow Lower Quartile; NF-Q3: Naturalized Streamflow Upper Quartile; MMS: Simulated Median Monthly Streamflow

Figure 9-52. Lower Sakarya: The comparison of the simulated median monthly flows with the IQR of the naturalized streamflow in each scenario in each time period. First row: SSP1; Second row: SSP2; Last row: SSP5

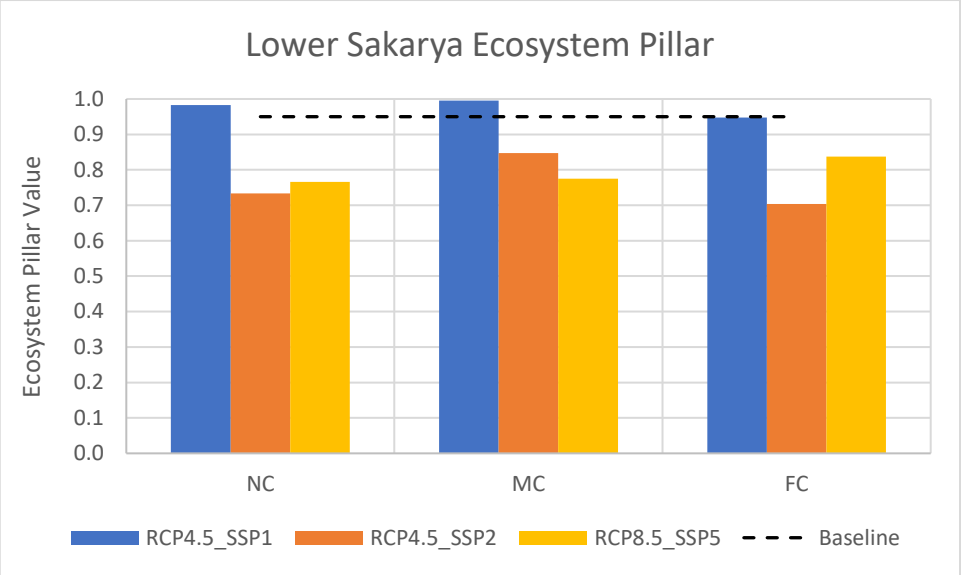

Figure 9-53. Ecosystem pillar value under climate and socioeconomic changes in the Lower Sakarya subbasin

Table 9-17. 21st century average ecosystem pillar scores for low and high flow periods in Lower Sakarya subbasin

	SSP1	SSP2	SSP5
October – March (low flow period)	0.97	0.68	0.90
April -September (high flow period)	0.99	0.85	0.69

Aggregated WEFE Nexus Index

After scores of all nexus pillars are calculated and aggregated, the values of the WEFE Nexus Index given in Figure 9-54 are obtained. This figure shows that WEFE Nexus Index value obtained in all scenarios is lower than the value obtained in the base case. In addition, the index values obtained in all scenarios are very close to each other. The highest values are obtained in the SSP1 scenario. The 21st century

average WEFE Nexus Index values are 0.75, 0.71 and 0.71 in SSP1, SSP2 and SSP5 scenarios, respectively. The reason for the difference between SSP1 and other scenarios is that the SSP1 scenario has a higher score in Energy and Ecosystem pillars than the other scenarios. In addition, although more municipal water demand deficit is calculated in the SSP1 scenario than in other scenarios, this is compensated by the good scores obtained in the Energy and Ecosystem pillars in the overall WEFE Nexus Index evaluation.

Lower Sakarya is the most downstream of the Sakarya Basin and the subbasin where the Sakarya River empties into the Black Sea. Therefore, it is affected by the management practices in all other subbasins of the Sakarya Basin. For this reason, every step taken for the sustainability of WEFE Nexus components in the upstream basins will contribute to obtaining higher WEFE Nexus Index values in the Lower Sakarya Basin. Among all the subbasins in the Sakarya Basin, the subbasin that receives the highest average precipitation in both the base case and the 21st century is the Lower Sakarya subbasin. Moreover, similar to Göksu subbasin (Section 9.4.6), there is no statistically significant decreasing trend in precipitation in the 21st century. In almost all climate projections, the average precipitation increases according to the historical period. This is also reflected in the pillar scores. All scenarios show that there will be little or no deficit in agricultural irrigation. In the SSP2 scenario, which expresses business as usual, the average municipal water demand deficit in the 21st century is 4%. A significant part of the drinking water in the Lower Sakarya subbasin is supplied from Sapanca Lake. However, increasing population and anthropogenic pollution sources around the lake put pressure on both lake water quantity and quality (Duman et al., 2007). Sapanca Lake is also important in terms of aquatic ecosystem. Therefore, it is important to develop a management plan for drinking water in order to meet the future drinking water demand and to prevent the deterioration of the ecological balance of the lake due to excessive water withdrawals from Sapanca Lake. Currently, there are dams under construction in the

Lower Sakarya Basin that will serve as an alternative drinking water source to Sapanca Lake. These dams are the Ballıkaya Dam being built by DSİ and the Akçay Dam being built by SASKİ (DSİ, 2017). These dams are not included in the scope of this study. However, when they are included, it is obvious that they will reduce the municipal water demand deficit calculated in the scenarios in the 21st century. In the SSP1 scenario, the municipal water demand deficit, which is calculated around 20% on average, will also decrease when these dams start to operate. Therefore, it can be predicted that the SSP1 scenario, in which the highest score is obtained in Energy, Food and Ecosystem pillars, will give the most balanced results for all nexus components in the Lower Sakarya Basin when the dams planned for drinking water are completed. Therefore, it seems possible to target natural flow conditions in the Lower Sakarya Basin without threatening the safety of other WEFE Nexus components.

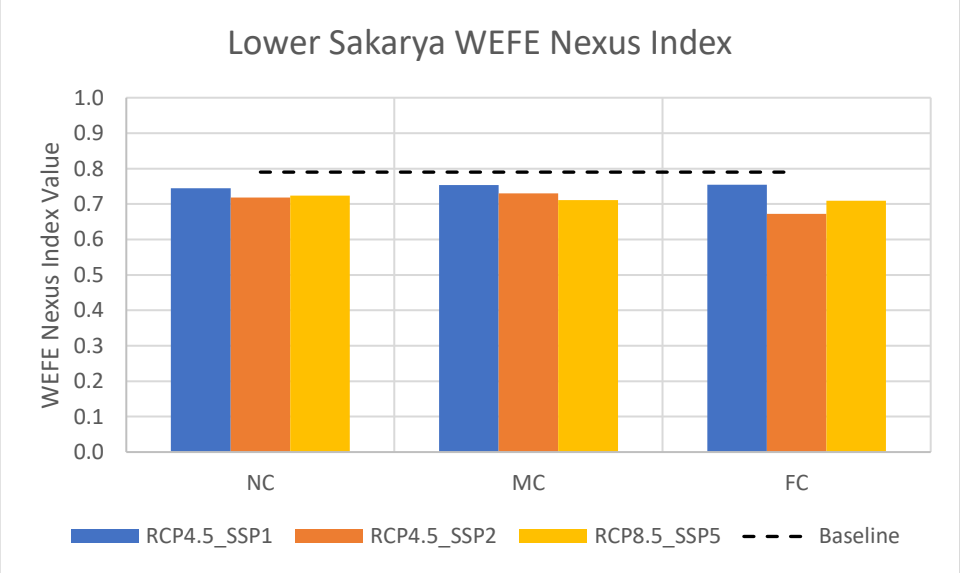

Figure 9-54. WEFE Nexus Index value under climate and socioeconomic changes in the Lower Sakarya subbasin

9.4.8 Overall Evaluation of the Results

The pillar and the WEFE Nexus Index scores of each scenario in each subbasin are given in Table 9-18. In this table, the pillar and the WEFE Nexus Index scores given for SSP1, SSP2, and SSP5 are the averages of near, mid- and far century. Except for the Göksu subbasin, the highest WEFE Nexus Index score is obtained in the SSP1 scenario in all subbasins. WEFE Nexus Index score in SSP2 and SSP5 scenarios in Göksu subbasin is the same and the score is higher than in SSP1 scenario. Although the WEFE Nexus Index value gives an idea of the general situation, this does not mean that the scenario with the highest WEFE Nexus Index score is the most sustainable scenario for all pillars. Therefore, pillar scores should also be considered while evaluating the WEFE Nexus Index value. For example, targeting natural flow conditions in the SSP1 scenario in almost all subbasins except Lower Sakarya causes serious deficits in agricultural irrigation. In addition, strict environmental flow applications in SSP1 scenario cause higher municipal water demand deficit compared to other scenarios, except for Porsuk and Ankara subbasins. The results show that the most balanced results in terms of all WEFE Nexus pillars in most subbasins, except Göksu and Lower Sakarya subbasins, are the SSP1 scenario where efficiency in agricultural irrigation is increased and slightly or moderately modified environmental management status is targeted instead of natural flow conditions. The main reason why different results are obtained in Göksu and Lower Sakarya subbasins compared to other subbasins is that the climatic conditions in the 21st century are different compared to other subbasins. While average precipitation increases in Göksu and Lower Sakarya subbasins, average precipitation decreases in other subbasins. In Göksu subbasin, the SSP1 scenario does not make a significant difference in terms of ecosystem condition compared to the SSP2 scenario. Even though the difference is small, the SSP2 scenario gives better results. The results of the Lower Sakarya subbasin show that SSP1 is the most sustainable scenario. Hence,

natural flow conditions can be targeted. However, this is possible only if alternative drinking water sources other than Sapanca Lake are created in the basin.

The results obtained in the SSP2 and SSP5 scenarios show that the WEFE Nexus Index values obtained in these scenarios are either equal to each other or the SSP5 scenario value is higher. This shows that the SSP2 scenario representing business as usual is not much different in terms of societal trends from the SSP5 scenario representing fossil fuel development. In the SSP2 scenario, excluding the Göksu and Lower Sakarya subbasins, the deficit in agricultural irrigation in the subbasins ranges between 21% and 32%. In the SSP5 scenario, this value varies between 24% and 34%. In both scenarios, an average of 17% municipal water demand is calculated in the Ankara subbasin, which hosts Türkiye's second largest city in terms of population. This highlights the importance of sustainable practices in the SSP1 scenario, where only 6% municipal water demand deficit is calculated on average, although environmental flows are a priority. In the base case, the Ecosystem pillar score, which varies between 0.38 and 0.96 in the subbasins, varies between 0.17 - 0.84 in the SSP2 scenario and 0.32 - 0.86 in the SSP5 scenario. Therefore, in most subbasins, the ecosystem quality status declines according to the base case.

The scenario in which the highest scores are obtained in all subbasins in the Energy pillar is the SSP1 scenario. Kirmir is the only subbasin where a score of one is obtained, representing full sustainability in the Energy pillar. The reason for this is that there is no thermal power plant in the Kirmir subbasin and in the SSP1 scenario, electricity is produced only by renewable energy plants. In line with the Paris Agreement targets, the target determined as 50% reduction in average emissions in the near century compared to the base case, and 100% in the mid- and far century, cannot be achieved in any subbasin in any scenario, and the results are far from these targets. In the SSP1 scenario, which gives priority to renewable energy in electricity generation, it is not possible to meet the emission targets even if the thermal power

plants are operated less than in the base case. However, it is understood that it is necessary to operate thermal power plants in order to meet the electricity need. Within the scope of this study, CO_2 emissions originating only from the energy sector are evaluated. Therefore, it can be argued that the emissions from other sectors can also be reduced to achieve the Paris Agreement targets. However, according to TÜIK, the energy sector ranks first in terms of emissions by sector in Türkiye (TÜİK, 2022). For example, the energy sector accounts for 70% of total emissions in 2020. Therefore, the most critical sector for CO_2 emission reduction targets is the energy sector. Any policy proposal to achieve the 2053 net-zero target would therefore suggest no more coal-fired power plants. However, since not building a new coal-fired power plant will not be enough to reach this target, existing coal capacity will also have to be phased out gradually until 2053. In case of a possible retirement, a retirement plan that prioritizes publicly operated power plants that have completed their economic life should be expected.

In all subbasins except Lower Sakarya, the lowest score in Food pillar belongs to the SSP1 scenario. The main reason for this is the targeting of natural flow conditions in the SSP1 scenario. In this study, the effect of different irrigation methods on the results was not modeled. However, field studies (Alp et al., 2020) and literature review (DSİ, 2017) have shown that open channel/canal systems with high leakages and evaporation losses in water distribution systems in the basin are the majority. Most of the irrigated areas use traditional flood irrigation. This results in low irrigation efficiency in the agricultural sector which has a large share in water consumption among all other sectors. That is, more water is consumed than is needed for agricultural irrigation. For this reason, it is of great importance to give priority to saving measures in the use of irrigation water. It is necessary to increase the irrigation efficiency by reducing the losses in irrigation, to apply limited irrigation, to increase the planting areas of crops that consume less water and to encourage agricultural best management practices. As a result, if the efficiency in agricultural irrigation is

increased, the Food pillar score can be increased while improving the ecosystem in the SSP1 scenario. Thus, the SSP1 scenario can be predicted to be the most sustainable for all pillars, when agricultural irrigation efficiency is included and slightly or moderately modified environmental status is targeted instead of unmodified conditions.

Except for Ankara and Göksu subbasins, the Ecosystem pillar gets its highest value in the SSP1 scenario. The lowest Ecosystem pillar score in all subbasins belongs to the SSP2 scenario. In accordance with the “Regulation on the Principles and Procedures for Signing Water Usage Rights Agreement for Operating in Electricity Market” in Türkiye, the companies that establish HPPs are obliged to release enough water to the stream bed to ensure the maintenance of natural life (The Ministry of Agriculture and Forestry, 2019). In the regulation, the amount of water to be released into the stream bed is determined as "at least 10% of the last ten-year average flow of the stream, which is based on the HPP project". In the EIA process, it is left to the initiative of the companies to determine the ecological needs and whether this amount should be increased or not. However, it is understood that this practice is not sufficient for the sustainability of the ecosystem. In the base case, the Ecosystem pillar value in the subbasins ranges from 0.38 to 0.96. Among the subbasins, the lowest Ecosystem pillar value belongs to the Porsuk subbasin. In the field study carried out on 18-22 July 2022 in the Porsuk subbasin within the scope of the project titled "A New Approach for Sustainable Water Management: Integration of the Circular Economy Approach to the Framework of the Water-Energy-Food-Ecosystem Nexus", hydrological and biological data were collected at 28 sampling points to determine the biological diversity of the aquatic habitats and the ecological quality status. All of the IBI classes (Karr, 1981) obtained at these sampling points are ‘Poor’ or ‘Very Poor’. This shows that the anthropogenic changes in the environment disrupts the ecosystem and threatens the survival of the species, and the results are compatible with the Ecosystem pillar score obtained within the scope of

this study. If the current policies regarding environmental flows continue in the 21st century (SSP2 scenario), the Ecosystem pillar score decreases to 0.17 (Kirmir subbasin), and the highest score obtained is 0.84 (Göksu subbasin). Therefore, it is predicted that the effect of anthropogenic stress factors on the ecosystem will increase further and the ecological quality will worsen rather than being preserved and restored. Consequently, it is crucially important that the necessary legal and scientific infrastructure should be completed and environmental flow practices should be implemented in order to preserve the health of rivers, natural life and the services offered by the rivers.

In Türkiye water availability varies greatly at the basin scale. However, water resources are allocated individually and demand-oriented. There is a lack of coordination caused by a dispersed structure in the sharing of duties and authorities (Ayten, 2014). However, water allocation should include economic, environmental and social factors. Policies that establish broad guidelines for significant water usage categories should incorporate provisions for meeting basic human water needs and protecting the environment. To promote sustainability, it is necessary to determine the maximum allowable water allocation for river basins and aquifers and take steps to ensure that these limits are not exceeded (UN, 2000). Within the scope of this study, the effects of both climate change and socioeconomic factors on water, energy, food and ecosystem sectors were studied holistically with the nexus approach. Depending on how the future might unfold in terms of broad societal trends and climatic conditions, three different scenarios were developed, and the overall WEFE Nexus Index values were calculated in the seven subbasins of Sakarya Basin. These three scenarios were compared in terms of nexus pillar scores, together with the overall WEFE Nexus Index values, and the security and sustainability of WEFE Nexus components were examined. It is believed that the index developed within the scope of this study will be a useful tool for policy making and information transfer for public communication. In addition, the fact that the method was applied

in seven different subbasins with very different characteristics proves the reproducibility of the study. Furthermore, the inclusion of seven distinct subbasins in the study facilitated the consideration of upstream-downstream interactions, thereby ensuring a comprehensive and holistic approach to the research.

Table 9-18. Pillar and WEFE Nexus Index scores of all subbasins

	Base Case					SSP1					SSP2					SSP5				
	Water	Energy	Food	Ecosystem	***WEFE Nexus Index***	Water	Energy	Food	Ecosystem	***WEFE Nexus Index***	Water	Energy	Food	Ecosystem	***WEFE Nexus Index***	Water	Energy	Food	Ecosystem	***WEFE Nexus Index***
Upper Sakarya	0.99	0.00	0.84	0.50	***0.58***	0.96	0.50	0.35	1.00	***0.70***	0.97	0.00	0.68	0.50	***0.54***	0.97	0.00	0.66	0.50	***0.53***
Porsuk	0.95	0.00	0.78	0.38	***0.53***	0.99	0.32	0.44	0.90	***0.66***	0.94	0.06	0.79	0.45	***0.56***	0.96	0.06	0.76	0.50	***0.57***
Ankara	0.97	0.20	0.97	0.83	***0.74***	0.94	0.28	0.51	0.69	***0.60***	0.83	0.10	0.69	0.58	***0.55***	0.83	0.11	0.67	0.74	***0.59***
Kirmir	0.99	-	0.85	0.72	***0.86***	0.71	1.00	0.47	0.96	***0.79***	0.99	-	0.78	0.17	***0.65***	0.99	-	0.76	0.32	***0.69***
Middle Sakarya	1.00	0.40	0.92	0.70	***0.75***	0.92	0.43	0.50	0.87	***0.68***	0.99	0.28	0.71	0.63	***0.65***	0.99	0.30	0.69	0.66	***0.66***
Göksu	1.00	0.16	0.86	0.96	***0.74***	0.97	0.36	0.57	0.82	***0.68***	1.00	0.35	0.90	0.84	***0.77***	1.00	0.35	0.85	0.86	***0.77***
Lower Sakarya	1.00	0.23	1.00	0.95	***0.79***	0.81	0.22	1.00	0.98	***0.75***	0.96	0.12	0.99	0.76	***0.71***	0.95	0.12	0.99	0.79	***0.71***

CHAPTER 10

CONCLUSIONS AND RECOMMENDATIONS

The last chapter of this thesis presents the findings of a comparative analysis of the categorized Water-Energy-Food-Ecosystem (WEFE) Nexus Index and pillar scores across different scenarios (Section 10.1), lists the assumptions and implementations adopted in this study to assist similar studies in the future (Section 10.2), and provides recommendations for future studies (Section 10.3). The analysis given in Section 10.1 sheds light on the interdependencies and trade-offs within the WEFE Nexus framework in the seven study subbasins. Based on these results, this section provides valuable insights into the managerial actions that can be taken to address the challenges and optimize the sustainability of each subbasin. Moreover, it presents the key conclusions derived from the analysis and offer practical recommendations for decision-makers and stakeholders to promote integrated and sustainable management of water, energy, food, and ecosystem resources in each subbasin.

10.1 Comparative Analysis of the Categorized Water-Energy-Food-Ecosystem (WEFE) Nexus Index and Pillar Scores Across Different Scenarios

The ultimate goal of this study is to guide decision-makers with the developed methodology. WEFE Nexus Index and Pillar scores were categorized (Table 10-1), and these categories were represented by smiling, neutral, and sad faces in order to express the results in a more understandable and clear manner to the decision-makers (Table 10-2). This method aims to obtain information quickly by simplifying complex data. A smiley face represents good results. This indicates a high

performance of the WEFE Nexus index or a pillar and positive progress toward targets. The neutral facial expression represents average results. In this case, there may be specific difficulties that need improvement or correction. A sad facial expression, on the other hand, represents low or negative results. This indicates that the index or related pillars are performing poorly or are experiencing severe problems. Using these expressions aims to enable decision-makers to evaluate the picture more quickly and effectively. As a visual representation, facial expressions help make strategic decisions by making the results easier to understand.

Table 10-1.Score ranges and corresponding symbols for categorization

Score Range	Corresponding Symbol
0.9 – 1	🙂
0.5 – 0.8	😐
0 – 0.4	😞

Table 10-2. Comparative analysis of categorized WEFE Nexus Index and pillar scores under different scenarios (SSP1, SSP2, SSP5)

		Water			Energy			Food			Ecosystem		
		NC	MC	FC	NC	MC	FC	NC	MC	FC	NC	MC	FC
Upper Sakarya	SSP1	🙂	🙂	🙂	😐	😐	😐	😞	😞	😞	🙂	🙂	🙂
	SSP2	🙂	🙂	🙂	😞	😞	😞	😐	😐	😐	😐	😐	😐
	SSP5	🙂	🙂	🙂	😞	😞	😞	😐	😐	😐	😐	😐	😐
Porsuk	SSP1	🙂	🙂	🙂	😞	😞	😞	😞	😞	😞	😐	😐	🙂
	SSP2	🙂	🙂	🙂	😞	😞	😞	😐	😐	😐	😞	😐	😐
	SSP5	🙂	🙂	🙂	😞	😞	😞	😐	😐	😐	😐	😐	😞
Ankara	SSP1	🙂	🙂	🙂	😞	😞	😞	😐	😞	😐	😐	😐	😐
	SSP2	🙂	😐	😐	😞	😞	😞	😐	😐	😐	😐	😐	😞
	SSP5	🙂	😐	😐	😞	😞	😞	😐	😐	😐	😐	😐	😐
Kirmir	SSP1	😐	😐	😐	🙂	🙂	🙂	😞	😞	😞	🙂	🙂	🙂
	SSP2	🙂	🙂	🙂	-	-	-	😐	😐	😐	😞	😞	😞
	SSP5	🙂	🙂	🙂	-	-	-	😐	😐	😐	😞	😞	😞
Middle Sakarya	SSP1	🙂	🙂	🙂	😞	😞	😞	😐	😞	😞	😐	🙂	😐
	SSP2	🙂	🙂	🙂	😞	😞	😞	🙂	😐	😐	😞	😐	😐
	SSP5	🙂	🙂	🙂	😞	😞	😞	😐	😐	😐	😐	😐	😐
Göksu	SSP1	🙂	🙂	🙂	😞	😞	😞	😐	😐	😐	😐	😐	😐
	SSP2	🙂	🙂	🙂	😞	😞	😞	🙂	🙂	😐	🙂	😐	😐
	SSP5	🙂	🙂	🙂	😞	😞	😞	🙂	😐	😐	🙂	😐	😐
Lower Sakarya	SSP1	😐	😐	😐	😞	😞	😞	🙂	🙂	🙂	🙂	🙂	🙂
	SSP2	🙂	🙂	🙂	😞	😞	😞	🙂	🙂	🙂	😐	😐	😐
	SSP5	🙂	🙂	🙂	😞	😞	😞	🙂	🙂	🙂	😐	😐	😐

Upper Sakarya

The most striking result in the Upper Sakarya subbasin is seen in the Food Pillar. As can be understood from the results, it is foreseen that there will be certain difficulties in the agricultural sector, whether it is a sustainable or fossil-fueled development scenario. For this reason, taking decisions to increase incentives for agricultural practices and technologies that increase food production efficiency and resilience; supporting local farmers, and promoting sustainable farming methods are critically important to ensure food security in this subbasin. Furthermore, it can clearly be observed that when practices promoting ecosystem health are encouraged, the challenges within the Food Pillar become more pronounced. This indicates a significant trade-off. Therefore, in the Upper Sakarya subbasin, it is crucial to address both the Food and Ecosystem pillars together to achieve balanced outcomes for both pillars. To this end, investing in research and innovation is necessary to develop and promote technologies, practices, and policies that can maximize food production efficiency without compromising ecosystem health. This includes evaluating and implementing practices such as sustainable irrigation methods, efficient water use, and crop diversification to enhance agricultural productivity while minimizing adverse environmental impacts. In the Upper Sakarya subbasin, neutral or sad faces are observed in all scenarios when examining the Energy Pillar. However, the relatively low electricity generation in the Upper Sakarya subbasin compared to other subbasins makes this issue less significant.

Porsuk

Similar comments can be made in the Porsuk subbasin to those made in the Upper Sakarya subbasin. The Food Pillar does not exhibit positive outcomes under any circumstances. This indicates that the agricultural sector in the Porsuk subbasin is confronted with significant challenges in the 21st century. In addition, it is observed that the ecosystem health is worse in the Porsuk subbasin, unlike the Upper Sakarya

subbasin. However, it is difficult to relate this to agriculture directly because the Porsuk basin is a subbasin where both agricultural and industrial activities are concentrated. These observations highlight the problematic state of the agricultural sector in the Porsuk subbasin during the 21st century. The Food Pillar, which encompasses factors such as agricultural productivity, sustainability, and food security, fails to demonstrate positive progress in this particular subbasin. This implies that there are formidable obstacles that hinder the growth and development of agriculture in the area. In the Porsuk subbasin, similar to other subbasins (excluding Kirmir), the Energy Pillar consistently falls short of achieving desired results across all scenarios, making it the most problematic sector. Currently, hydroelectricity production is absent in the Porsuk subbasin, and electricity is generated solely from thermal power plants. Even in the sustainability scenario, which prioritizes renewable energy generation, the unfavorable outcomes emphasize the necessity of a gradual closure of thermal power plants.

Ankara

Among the seven subbasins, the Ankara subbasin has the highest population density. Both agricultural and industrial productions play a significant role in the economy. A significant portion of the province of Ankara, which is the second most populous city in Türkiye and has the highest industrial gross domestic product among the cities in the Sakarya Basin, is located within this subbasin. Table 10-2 shows that in the business-as-usual and fossil fuel development scenarios in the Ankara subbasin, there will be difficulties in meeting the municipal water demand in the mid- and far century periods. The fact that this is not observed in the sustainability scenario reveals the importance of sustainable practices. In addition, it is obvious that there will be problems in agricultural production in the 21st century under all conditions in the Ankara subbasin, as in other subbasins where agricultural production is important. In addition, the fact that a good situation cannot be achieved in the

ecosystem in any period of the 21st century, even in the sustainability scenario where ecosystem health is the top priority, shows that the amount of water in the basin will decrease as a result of climate change. At this point, decision-makers especially have essential duties. In particular, measures need to be taken to adapt to climate change. In order for water resources to adapt to future changes, measures such as infrastructure development, increasing water storage capacity, and ensuring the efficient distribution of water should be taken. Moreover, managing water resources requires the cooperation and coordination of various stakeholders. Mechanisms should be established, and regular communication and coordination should be ensured to promote cooperation among decision-makers, local governments, the agriculture sector, industry, non-governmental organizations, and other relevant stakeholders. The Energy Pillar goals are not met in the Ankara subbasin as well. Similar to the Porsuk subbasin, there is no hydroelectric power plant in the Ankara subbasin, and a significant portion of electricity generation relies on thermal power plants. The outcomes underscore the challenges associated with achieving the set targets for the Energy Pillar, particularly due to the presence of thermal power plants.

Kirmir

The most significant feature of the Kirmir subbasin is that it is a drinking water basin. Significant amounts of water from the dams in this subbasin are transferred to the dams located in the Ankara subbasin. In the sustainability scenario of the Kirmir sub-basin, when ecosystem health is the primary priority, it is seen that it will be challenging to meet the municipal water demand and the agricultural irrigation need. As in other subbasins, it is seen that the agricultural sector will face difficulties under all circumstances in the 21st century. However, this is not as important as in other subbasins where agricultural production is much more intense because the density of agricultural areas is not high. There are currently no power plants in the Kirmir subbasin. The hyphens seen in Table 10-2 in the Energy Pillar mean that in these

scenarios the Energy Pillar is not included in the assessment as there is no electricity generation in the basin. In the sustainability scenario, the Energy Pillar has a smiley face that expresses good results, since electricity is only produced from renewable energy plants. It is easily seen from Table 10-2 that there is a tradeoff between meeting municipal water demand and ecosystem health. Various strategies can be considered to address the balance between these two sectors. Adopting an ecosystem-based approach to water management, including measures to protect and restore ecosystems, is essential. Additionally, policies should focus on protecting water resources, protecting habitats, and preventing pollution. Managing water demand through efficient water use practices and promoting water-saving technologies is crucial. Research, monitoring, and modeling are critical to understanding the relationship between ecosystem health and water demand. Multi-stakeholder cooperation should be encouraged to ensure inclusive decision-making and long-term planning for sustainable water management should be considered.

Middle Sakarya

The Middle Sakarya subbasin stands out with its hydroelectric production. There are tens of dam and river-type hydroelectric power plants on the Sakarya River main branch. In the Middle Sakarya subbasin, the share of agricultural areas is moderate, and the subbasin has a low population density compared to other subbasins. Even in the sustainability scenario where the ecosystem is prioritized, Table 10-2 demonstrates that changing climatic conditions prevent achieving the desired ecosystem conditions throughout the 21st century. Additionally, it is observed that agricultural activities will be significantly affected by changing climatic conditions, similar to other subbasins where there is a decreasing precipitation trend and agricultural production is significant, in the 21st century. In the Energy Pillar, which encompasses factors like the percentage of hydropower production relative to maximum capacity, the share of renewable energy, and the reduction in CO_2

emissions, there is a consistent presence of sad faces. Despite achieving the desired renewable energy share rate in the sustainability scenario, approximately 30% of hydroelectric power plants' maximum electricity generation capacity can be used. In addition, CO_2 emission reduction targets cannot be achieved. The water potential in the study area is expected to decline because of a decrease in precipitation and an increase in temperatures due to climate change. This demonstrates that improving drought resistance and ensuring the sustainability of the water-energy nexus requires reducing reliance on water to produce electricity. Therefore, diversifying the energy mix by encouraging the integration of other renewable energy sources, developing energy storage systems like pumped storage, or implementing efficient water management techniques in hydroelectric power plants to optimize water usage should be considered.

Göksu

The Göksu subbasin stands out as having the lowest population among the subbasins. However, Bursa, a province located within the boundaries of the subbasin and home to a significant portion of the population, is characterized by intense industrial production. The Göksu subbasin exhibits a roughly 50% ratio of agricultural areas, making it an important subbasin in terms of both agricultural and industrial productivity. One notable distinction of the Göksu subbasin from other subbasins (except the Lower Sakarya subbasin), is the absence of any statistically significant increasing or decreasing trend in precipitation during the 21st century. In fact, when comparing average precipitation across various projections to the historical period, it becomes evident that precipitation has generally increased. Nevertheless, the rising temperatures pose a significant challenge to water availability, as evident in the results of the Food Pillar. Similarly, the desired targets in the ecosystem cannot be achieved under any of the scenarios. A key recommendation for the Göksu subbasin is to improve agricultural irrigation efficiency. investments should focus on

implementing sustainable agricultural practices that enhance irrigation productivity. By doing so, it will be possible to prevent the degradation of ecosystem sustainability in the 21st century, while simultaneously reducing the deficit in irrigation demand. In all scenarios, the Energy Pillar also reflects a sense of concern. However, the Göksu subbasin stands out as the subbasin with the lowest production of both hydroelectricity and thermal electricity. As a result, this particular situation does not hold significant importance in the overall context

Lower Sakarya

Upon analyzing the results in the Lower Sakarya subbasin, one notable observation is the absence of any concerns regarding agricultural irrigation across all scenarios. This is primarily because Lower Sakarya is the subbasin with the highest average precipitation among all subbasins. Similar to the Göksu subbasin, no statistically significant decreasing or increasing trend in precipitation was observed in the 21st century for the Lower Sakarya subbasin. However, a tradeoff exists between the Ecosystem and Water Pillars in this subbasin. This is primarily attributed to Sapanca Lake, which serves as the primary drinking water source for the basin. As discussed in Chapter 9 Section 9.4.7, it is anticipated that this challenge will be resolved with the creation of alternative sources of drinking water. The Lower Sakarya subbasin is recognized as the subbasin that generates the highest amount of electricity from thermal power plants. When analyzing the results of the Energy Pillar, it becomes evident that sad faces are consistently observed in all scenarios. This signifies that the targets related to the energy sector are far from being achieved. In the Lower Sakarya subbasin, strategic actions can be taken to reduce CO_2 emissions and promote sustainability. For example, the integration of renewable energy technologies, such as wind and solar power, can be encouraged to gradually replace the reliance on thermal power generation. The feasibility of implementing carbon

capture and storage (CCS) technology in the existing thermal power plants can be explored to minimize their environmental impact.

10.2 Assumptions and Implementation Details: Supporting Future Studies

This section aims to provide a comprehensive overview of the assumptions and implementation details employed in this study, with the purpose of assisting future researchers and enabling the advancement of similar investigations. The following assumptions and implementations underlie this study:

- The crop pattern of the permanently irrigated lands was assumed to be constant throughout the simulation period.
- The Kc values of the crops were not calibrated, they were directly adopted from TAGEM and DSİ (2017)'s study.
- In the WEAP model, a separate catchment component was created for agricultural lands that use groundwater for irrigation in each unit within each subbasin. The crop pattern in these catchments reflects the specific crops grown using groundwater irrigation.
- The temperature, humidity, and wind speed data were sourced from the meteorology station that has the largest Thiessen polygon area within the respective subbasin.
- All transmission links have equal demand priority in the baseline simulation period.
- The runoff, calculated using the Soil Moisture method in the catchments, was allocated to the rivers based on the drainage areas of the significant dams within the subbasin.
- Groundwater-surface water interactions were specified directly, they were not modeled.

- To represent all the ponds within each subbasin, a reservoir component was created and positioned at the location of the largest pond in that particular subbasin.
- The water consumption percentage of industrial demand sites were accepted as 25% unless otherwise stated.
- Power plants with an installed capacity of less than 7 MW were not taken into consideration.
- For years in which total electricity generation information was unavailable, the average electricity generation value for that specific power plant was assumed to be equivalent to the electricity generation value for that year. Additionally, the total electricity generation derived from the power plants was entered into the LEAP model as the total electricity demand.
- Throughout the simulation period, the hourly load curve from the year 2017 is assumed to be applicable and representative.
- In this study, the future projection period spanning from 2020 to 2100 in the Sakarya Basin was examined. To cope with the high computational cost of the regional model and time constraints, the future climate projection realizations were downscaled to 18-km resolution grids over three 10-year segments: 2020-2030, 2055-2065, and 2090-2100.
- The relative humidity data for each catchment in each subbasin during the future period were derived using linear regression analysis with precipitation and temperature data as input variables.
- The process of streamflow naturalization in the Sakarya Basin excluded only one anthropogenic influence, which is the changes in land use and land cover.
- Due to data limitations, it was not feasible to utilize all the original parameters of the IHA (Indicators of Hydrologic Alteration) method. Therefore, the study had to select and utilize only those parameters that could

be adapted to a monthly scale. As a result, the decision was made to adopt the 12 indicators from Group 1 as the feasible indicators for the analysis.

- The analysis did not include SSP3 due to its representation of extreme conditions that are deemed highly challenging to mitigate and adapt to, primarily resulting from extreme poverty and a rapidly growing population. Consequently, SSP3 was considered an improbable scenario for the study area. Similarly, SSP4, which portrays a highly unequal world both within and across countries, was also excluded from the analysis as the conditions projected in this scenario were deemed less relevant at the catchment scale.
- Installed solar power potential of Türkiye is estimated to be 56,000 MW (Cebeci, 2017). By considering the ratio of the total drainage area of the Sakarya Basin to the total area of all basins in Türkiye, a rough calculation was performed to estimate the installed power potential of the Sakarya Basin. As a result, the installed power potential of the Sakarya Basin was estimated to be 3,681 MW.

10.3 Recommendations for Future Studies

In order to further advance the understanding and application of the study's findings, the following recommendations are proposed for future studies in the field of WEFE Nexus analysis:

1. Consider smaller-scale areas with higher data resolution: Due to the extensive temporal and spatial scope of the study, the resolution had to be reduced. Future studies should replicate the research in smaller-scale areas to enable a better reflection of the impact of diverse sustainable practices in each sector.

2. Enhance ecosystem assessment: As the study's large-scale nature limited the inclusion of components such as water quality and morphology, future studies should

apply the methodology in smaller-scale areas while considering these important factors. This will result in a more comprehensive assessment of ecosystem integrity.

3. Incorporate surface water-groundwater interactions: The modeling of surface water-groundwater interactions could not be accomplished due to the study's large-scale nature. It is recommended that future studies, conducted on smaller scales, specifically address and analyze the dynamics and interactions between surface water and groundwater.

4. Foster stakeholder engagement for practical implementation: The WEFE Nexus approach is a complex framework, and to bridge the gap between theoretical studies and practical implementation, the active participation of stakeholders from all sectors is crucial. Future studies should emphasize involving stakeholders to ensure the translation of WEFE Nexus study outputs into real-world applications.

REFERENCES

Abbott, M., Bazilian, M., Egel, D., & Willis, H. H. (2017). Examining the food–energy–water and conflict nexus. *Current Opinion in Chemical Engineering*, *18*, 55–60. https://doi.org/10.1016/j.coche.2017.10.002

Abera Abdi, D., & Ayenew, T. (2021). Evaluation of the WEAP model in simulating subbasin hydrology in the Central Rift Valley basin, Ethiopia. *Ecological Processes*, *10*(1). https://doi.org/10.1186/s13717-021-00305-5

Al-Ansari, T., Korre, A., Nie, Z., & Shah, N. (2015). Development of a life cycle assessment tool for the assessment of food production systems within the energy, water and food nexus. *Sustainable Production and Consumption*, *2*(March), 52–66. https://doi.org/10.1016/j.spc.2015.07.005

Albrecht, T. R., Crootof, A., & Scott, C. A. (2018). The Water-Energy-Food Nexus: A systematic review of methods for nexus assessment. *Environmental Research Letters*, *13*(4). https://doi.org/10.1088/1748-9326/aaa9c6

Allen, R. G., & Pereira, L. S. (2009). Estimating crop coefficients from fraction of ground cover and height. *Irrigation Science*, *28*(1), 17–34. https://doi.org/10.1007/s00271-009-0182-z

Alp, E., Özel, B., Özcan, C., Özcan, Z., Aydınalp Köksal, M., Demir, Y., Başkan, O., & Kentel Erdoğan, E. (2020). *Evaluation of Water, Energy and Food Nexus in Sakarya Watershed, Final Report, Project No: 116Y166*.

Amato, C. C., McKinney, D. C., Ingol-Blanco, E., & Teasley, R. L. (2006). CRWR Online Report 06-12 WEAP Hydrology Model Applied: The Rio Conchos Basin. *Center for Research in Water Resources, December*.

Arabi, M., Meals, D. W., & Hoag, D. L. (2012). Watershed Modeling: National

Institute of Food and Agriculture-Conservation Effects Assessment Project. In *How to Build Better Agricultural Conservation Programs to Protect Water Quality* (pp. 84–119). Soil and Water Conservation Society.

Ayten, N. (2014). *Sektörel Su Tahsisinin Esasları*. Ministry of Forestry and Water Affairs.

Bai, T., Ma, P. P., Kan, Y. Bin, & Huang, Q. (2017). Ecological risk assessment based on IHA-RVA in the lower Xiaolangdi reservoir under changed hydrological situation. *IOP Conference Series: Earth and Environmental Science*, *100*(012214). https://doi.org/10.1088/1755-1315/100/1/012214

Bazilian, M., Rogner, H., Howells, M., Hermann, S., Arent, D., Gielen, D., Steduto, P., Mueller, A., Komor, P., Tol, R. S. J., & Yumkella, K. K. (2011). Considering the energy, water and food nexus: Towards an integrated modelling approach. *Energy Policy*, *39*(12), 7896–7906. https://doi.org/10.1016/J.ENPOL.2011.09.039

Benson, D., Gain, A. K., & Rouillard, J. J. (2015). Water governance in a comparative perspective: From IWRM to a "nexus" approach? *Water Alternatives*, *8*(1), 756–773.

Bidoglio, G., & Brander, L. (2016). EDITORIAL: Enabling management of the Water-Food-Energy-Ecosystem Services Nexus. *Ecosystem Services*, *17*, 265–267. https://doi.org/10.1016/j.ecoser.2016.02.001

Bizikova, L., Roy, D., Swanson, D., David, H., & Mccandless, V. M. (2013). *The Water-Energy-Food Security Nexus: Towards a practical planning and decision-support framework for landscape investment and risk management*. www.iisd.org

Bonsch, M., Humpenöder, F., Popp, A., Bodirsky, B., Dietrich, J. P., Rolinski, S.,

Biewald, A., Lotze-Campen, H., Weindl, I., Gerten, D., & Stevanovic, M. (2016). Trade-offs between land and water requirements for large-scale bioenergy production. *GCB Bioenergy*, *8*(1), 11–24. https://doi.org/10.1111/gcbb.12226

Bunn, S. E., & Arthington, A. H. (2002). Basic principles and ecological consequences of altered flow regimes for aquatic biodiversity. *Environmental Management*, *30*(4), 492–507. https://doi.org/10.1007/s00267-002-2737-0

Castoldi, N., & Bechini, L. (2010). Integrated sustainability assessment of cropping systems with agro-ecological and economic indicators in northern Italy. *European Journal of Agronomy*, *32*(1), 59–72. https://doi.org/10.1016/j.eja.2009.02.003

Cebeci, S. (2017). Türkiye'de Güneş Enerjisinden Elektrik Üretim Potansiyelinin Değerlendirilmesi. In *T.C. Kalkınma Bakanlığı*. T.C. Kalkınma Bakanlığı.

Crespo Cuaresma, J. (2017). Income projections for climate change research: A framework based on human capital dynamics. *Global Environmental Change*, *42*, 226–236. https://doi.org/10.1016/j.gloenvcha.2015.02.012

Daccache, A., Ciurana, J. S., Rodriguez Diaz, J. A., & Knox, J. W. (2014). Water and energy footprint of irrigated agriculture in the Mediterranean region. *Environmental Research Letters*, *9*(12). https://doi.org/10.1088/1748-9326/9/12/124014

Daher, B., Lee, S.-H., Kaushik, V., Blake, J., Askariyeh, M. H., Shafiezadeh, H., Zamaripa, S., & Mohtar, R. H. (2019). Towards bridging the water gap in Texas: A water-energy-food nexus approach. *Science of The Total Environment*, *647*, 449–463. https://doi.org/10.1016/J.SCITOTENV.2018.07.398

Damerau, K., Patt, A. G., & van Vliet, O. P. R. (2016). Water saving potentials and possible trade-offs for future food and energy supply. *Global Environmental Change*, *39*, 15–25. https://doi.org/10.1016/j.gloenvcha.2016.03.014

De Girolamo, A. M., Lo Porto, A., Pappagallo, G., & Gallart, F. (2015). Assessing flow regime alterations in a temporary river - The River Celone case study. *Journal of Hydrology and Hydromechanics*, *63*(3), 263–272. https://doi.org/10.1515/johh-2015-0027

De Laurentiis, V., Hunt, D. V. L., & Rogers, C. D. F. (2016). Overcoming food security challenges within an energy/water/food nexus (EWFN) approach. *Sustainability (Switzerland)*, *8*(1). https://doi.org/10.3390/su8010095

De Strasser, L., Lipponen, A., Howells, M., Stec, S., & Bréthaut, C. (2016). A methodology to assess thewater energy food ecosystems nexus in transboundary river basins. *Water (Switzerland)*, *8*(2). https://doi.org/10.3390/w8020059

Dellink, R., Chateau, J., Lanzi, E., & Magné, B. (2017). Long-term economic growth projections in the Shared Socioeconomic Pathways. *Global Environmental Change*, *42*, 200–214. https://doi.org/10.1016/j.gloenvcha.2015.06.004

DSİ. (2017). *Sakarya Havzası Master Plan Nihai Raporu*.

DSİ. (2021). *HPP Water Use Agreements*. https://enerji.dsi.gov.tr/Sayfa/Detay/774

DSİ. (2022). *HES Su Kullanım Anlaşmaları*. https://enerji.dsi.gov.tr/Sayfa/Detay/774

Dudhia, J. (1989). Numerical Study of Convection Observed during the Winter Monsoon Experiment Using a Mesoscale Two-Dimensional Model. *Journal of The Atmospheric Sciences*, *46*(20). https://www.ptonline.com/articles/how-to-

get-better-mfi-results

Duman, F., Aksoy, A., & Demirezen, D. (2007). Seasonal variability of heavy metals in surface sediment of Lake Sapanca, Turkey. *Environmental Monitoring and Assessment*, *133*(1–3), 277–283. https://doi.org/10.1007/s10661-006-9580-3

El-Gafy, I. (2017). Water–food–energy nexus index: analysis of water–energy–food nexus of crop's production system applying the indicators approach. *Applied Water Science*, *7*(6), 2857–2868. https://doi.org/10.1007/s13201-017-0551-3

Endo, A., Burnett, K., Orencio, P. M., Kumazawa, T., Wada, C. A., Ishii, A., Tsurita, I., & Taniguchi, M. (2015). Methods of the water-energy-food nexus. *Water (Switzerland)*, *7*(10), 5806–5830. https://doi.org/10.3390/w7105806

Enerji Atlası. (2023). *Enerji Atlası*. http://www.enerjiatlasi.com/

FAO. (2014). Walking the Nexus Talk: Assessing the Water-Energy-Food Nexus in the Context of the Sustainable Energy for All Initiative. In *Fao* (Vol. 58). http://www.fao.org/publications/card/en/c/f065f1d5-2dda-4df7-8df3-4defb5a098c8/

FAO. (2023). *Ecosystem Services & Biodiversity (ESB)*. https://www.fao.org/ecosystem-services-biodiversity/en/

Foran, T. (2015). Node and regime: Interdisciplinary analysis of water-energy-food nexus in the Mekong region. *Water Alternatives*, *8*(1), 655–674.

Gan, X., Fernandez, I. C., Guo, J., Wilson, M., Zhao, Y., Zhou, B., & Wu, J. (2017). When to use what: Methods for weighting and aggregating sustainability indicators. *Ecological Indicators*, *81*(May), 491–502. https://doi.org/10.1016/j.ecolind.2017.05.068

Gao, B., Yang, D., Zhao, T., & Yang, H. (2012). Changes in the eco-flow metrics of the Upper Yangtze River from 1961 to 2008. *Journal of Hydrology*, *448–449*, 30–38. https://doi.org/https://doi.org/10.1016/j.jhydrol.2012.03.045

Gao, Y., Chen, L., Zhang, W., Li, X., & Xu, Q. (2021). Spatiotemporal variations in characteristic discharge in the Yangtze River downstream of the Three Gorges Dam. *Science of the Total Environment*, *785*(147343). https://doi.org/https://doi.org/10.1016/j.scitotenv.2021.147343

Garcia, D. J., Lovett, B. M., & You, F. (2019). Considering agricultural wastes and ecosystem services in Food-Energy-Water-Waste Nexus system design. *Journal of Cleaner Production*. https://doi.org/10.1016/j.jclepro.2019.04.314

Gent, P. R., Danabasoglu, G., Donner, L. J., Holland, M. M., Hunke, E. C., Jayne, S. R., Lawrence, D. M., Neale, R. B., Rasch, P. J., Vertenstein, M., Worley, P. H., Yang, Z. L., & Zhang, M. (2011). The community climate system model version 4. *Journal of Climate*. https://doi.org/10.1175/2011JCLI4083.1

Gierszewski, P. J., Habel, M., Szmańda, J., & Luc, M. (2020). Evaluating effects of dam operation on flow regimes and riverbed adaptation to those changes. *Science of the Total Environment*, *710*. https://doi.org/10.1016/j.scitotenv.2019.136202

Giupponi, C., & Gain, A. K. (2017). Integrated spatial assessment of the water, energy and food dimensions of the Sustainable Development Goals. *Regional Environmental Change*, *17*(7), 1881–1893. https://doi.org/10.1007/s10113-016-0998-z

Gorguner, M., Kavvas, M. L., & Ishida, K. (2019). Assessing the impacts of future climate change on the hydroclimatology of the Gediz Basin in Turkey by using dynamically downscaled CMIP5 projections. *Science of the Total Environment*, *648*, 481–499. https://doi.org/10.1016/j.scitotenv.2018.08.167

Gosain, A. K., Rao, S., Srinivasan, R., & Reddy, N. G. (2005). Return-flow assessment for irrigation command in the Palleru river basin using SWAT model. *Hydrological Processes*, *19*(3), 673–682.

Governorship of Ankara. (2022). *Ankara İli 2021 Yılı Çevre Durum Raporu*.

Governorship of Eskişehir. (2022). *Eskişehir İli 2021 Yılı Çevre Durum Raporu*.

Governorship of Sakarya. (2021). *Sakarya İli 2020 Yılı Çevre Durum Raporu*.

Graham, N. T., Davies, E. G. R., Hejazi, M. I., Calvin, K., Kim, S. H., Helinski, L., Miralles-Wilhelm, F. R., Clarke, L., Kyle, P., Patel, P., Wise, M. A., & Vernon, C. R. (2018). Water Sector Assumptions for the Shared Socioeconomic Pathways in an Integrated Modeling Framework. *Water Resources Research*, *54*(9), 6423–6440. https://doi.org/10.1029/2018WR023452

Grell, G. A., & Dévényi, D. (2002). A generalized approach to parameterizing convection combining ensemble and data assimilation techniques. *Geophysical Research Letters*, *29*(14), 10–13. https://doi.org/10.1029/2002GL015311

Guillaume, J. H. A., Kummu, M., Eisner, S., & Varis, O. (2015). Transferable principles for managing the nexus: Lessons from historical global water modelling of central Asia. *Water (Switzerland)*, *7*(8), 4200–4231. https://doi.org/10.3390/w7084200

Guo, W., Zhou, H., Jiao, X., Huang, L., & Wang, H. (2022). Analysis of Alterations of the Hydrological Situation and Causes of River Runoff in the Min River, China. *Water (Switzerland)*, *14*(7). https://doi.org/10.3390/w14071093

Halbe, J., Pahl-Wostl, C., A. Lange, M., & Velonis, C. (2015). Governance of

transitions towards sustainable development – the water–energy–food nexus in Cyprus. *Water International*, *40*(5–6), 877–894. https://doi.org/10.1080/02508060.2015.1070328

Han, X., Hua, E., Engel, B. A., Guan, J., Yin, J., Wu, N., Sun, S., & Wang, Y. (2022). Understanding implications of climate change and socio-economic development for the water-energy-food nexus: A meta-regression analysis. *Agricultural Water Management*, *269*(April), 107693. https://doi.org/10.1016/j.agwat.2022.107693

Hanasaki, N., Fujimori, S., Yamamoto, T., Yoshikawa, S., Masaki, Y., Hijioka, Y., Kainuma, M., Kanamori, Y., Masui, T., Takahashi, K., & Kanae, S. (2013). A global water scarcity assessment under Shared Socio-economic Pathways - Part 1: Water use. *Hydrology and Earth System Sciences*, *17*(7), 2375–2391. https://doi.org/10.5194/hess-17-2375-2013

Hanes, R. J., Gopalakrishnan, V., & Bakshi, B. R. (2018). Including nature in the food-energy-water nexus can improve sustainability across multiple ecosystem services. *Resources, Conservation and Recycling*, *137*(May), 214–228. https://doi.org/10.1016/j.resconrec.2018.06.003

Harmel, R. D., Smith, P. K., Migliaccio, K. W., Chaubey, I., Douglas-Mankin, K. R., Benham, B., Shukla, S., Munoz-Carpena, R., & Robson, B. J. (2014). Evaluating , interpreting , and communicating performance of hydrologic/water quality models considering intended use : A review and recommendations. *Environmental Modelling & Software*, *57*, 40–51. https://doi.org/http://dx.doi.org/10.1016/j.envsoft.2014.02.013

Hausfather, Z. (2018, April). Explainer: How ‘Shared Socioeconomic Pathways’ explore future climate change. *CarbonBrief*. https://www.carbonbrief.org/explainer-how-shared-socioeconomic-pathways-

explore-future-climate-change/

Heckl, I., Cabezas, H., & Friedler, F. (2015). Designing sustainable supply chains in the energy-water-food nexus by the P-graph methodology. *Chemical Engineering Transactions*, *45*, 1351–1356. https://doi.org/10.3303/CET1545226

Hoff, H. (2011). *Background paper for the Bonn 2011 Nexus Conference: THE WATER, ENERGY AND FOOD SECURITY NEXUS*. http://wef-conference.gwsp.org/fileadmin/documents_news/understanding_the_nexus.pdf

Hong, S. Y., Noh, Y., & Dudhia, J. (2006). A new vertical diffusion package with an explicit treatment of entrainment processes. *Monthly Weather Review*, *134*(9), 2318–2341. https://doi.org/10.1175/MWR3199.1

Howarth, C., & Monasterolo, I. (2016). Understanding barriers to decision making in the UK energy-food-water nexus: The added value of interdisciplinary approaches. *Environmental Science and Policy*, *61*, 53–60. https://doi.org/10.1016/j.envsci.2016.03.014

Howells, M., Hermann, S., Welsch, M., Bazilian, M., Segerström, R., Alfstad, T., Gielen, D., Rogner, H., Fischer, G., Van Velthuizen, H., Wiberg, D., Young, C., Alexander Roehrl, R., Mueller, A., Steduto, P., & Ramma, I. (2013). Integrated analysis of climate change, land-use, energy and water strategies. In *Nature Climate Change* (Vol. 3, Issue 7, pp. 621–626). https://doi.org/10.1038/nclimate1789

Hua, T., Zhao, W., Wang, S., Fu, B., & Pereira, P. (2020). Identifying priority biophysical indicators for promoting food-energy-water nexus within planetary boundaries. *Resources, Conservation and Recycling*, *163*(19), 105102. https://doi.org/10.1016/j.resconrec.2020.105102

IEA. (2021). World Energy Outlook 2021. In *IEA Publications*. www.iea.org/weo

IIASA. (2018). *SSP Public Database Version 2.0*. https://tntcat.iiasa.ac.at/SspDb/dsd?Action=htmlpage&page=20

Ingol-Blanco, E., & McKinney, D. C. (2012). Development of a Hydrological Model for the Rio Conchos Basin. *Journal of Hydrologic Engineering*, *18*(March), 410. https://doi.org/10.1061/(ASCE)HE.1943-5584.0000607

IPCC. (2000). *Summary for Policymakers Emission Scenarios*. https://www.ipcc.ch/site/assets/uploads/2018/03/sres-en.pdf

Irabien, A., & Darton, R. C. (2016). Energy–water–food nexus in the Spanish greenhouse tomato production. *Clean Technologies and Environmental Policy*, *18*(5), 1307–1316. https://doi.org/10.1007/s10098-015-1076-9

Ishida, K., Ercan, A., Trinh, T., Jang, S., Kavvas, M. L., Ohara, N., Chen, Z. Q., Kure, S., & Dib, A. (2018). Trend analysis of watershed-scale annual and seasonal precipitation in Northern California based on dynamically downscaled future climate projections. *Journal of Water and Climate Change*, *November*. https://doi.org/10.2166/wcc.2018.241

Jiang, L., & O'Neill, B. C. (2017). Global urbanization projections for the Shared Socioeconomic Pathways. *Global Environmental Change*, *42*, 193–199. https://doi.org/10.1016/j.gloenvcha.2015.03.008

Jones, K., Magliocca, N. R., & Hondula, K. (2017). *White Paper: an Overview of Conceptual Frameworks, Analytical Approaches and Research Questions in the Food-Energy-Water Nexus*. *March*, 1–35. https://doi.org/10.13016/M2BK10

Karabulut, A. A., Udias, A., & Vigiak, O. (2019). Assessing the policy scenarios for the Ecosystem Water Food Energy (EWFE) nexus in the Mediterranean

region. *Ecosystem Services*, *35*(November 2018), 231–240. https://doi.org/10.1016/j.ecoser.2018.12.013

Karabulut, A., Egoh, B. N., Lanzanova, D., Grizzetti, B., Bidoglio, G., Pagliero, L., Bouraoui, F., Aloe, A., Reynaud, A., Maes, J., Vandecasteele, I., & Mubareka, S. (2016). Mapping water provisioning services to support the ecosystem-water-food-energy nexus in the Danube river basin. *Ecosystem Services*, *17*(2016), 278–292. https://doi.org/10.1016/j.ecoser.2015.08.002

Karlberg, L., Hoff, H., Amsalu, T., Andersson, K., Binnington, T., Flores-López, F., de Bruin, A., Gebrehiwot, S. G., Gedif, B., zur Heide, F., Johnson, O., Osbeck, M., & Young, C. (2015). Tackling complexity: Understanding the food-energy-environment nexus in Ethiopia's lake TANA sub-basin. *Water Alternatives*, *8*(1), 710–734.

Karr, J. R. (1981). Assessment of Biotic Integrity Using Fish Communities. *Fisheries*, *6*(6), 21–27. https://doi.org/10.1577/1548-8446(1981)006<0021:aobiuf>2.0.co;2

KC, S., & Lutz, W. (2017). The human core of the shared socioeconomic pathways: Population scenarios by age, sex and level of education for all countries to 2100. *Global Environmental Change*, *42*, 181–192. https://doi.org/10.1016/j.gloenvcha.2014.06.004

Keairns, D. L., Darton, R. C., & Irabien, A. (2016). The Energy-Water-Food Nexus. *Annual Review of Chemical and Biomolecular Engineering*, *7*, 239–262. https://doi.org/10.1146/annurev-chembioeng-080615-033539

Kebede, A. S., Nicholls, R. J., Clarke, D., Savin, C., & Harrison, P. A. (2021). Integrated assessment of the food-water-land-ecosystems nexus in Europe: Implications for sustainability. *Science of the Total Environment*, *768*, 144461. https://doi.org/10.1016/j.scitotenv.2020.144461

Kessler, E. (1969). On the distribution and continuity of water substance in atmospheric circulations. *American Meteorological Society*, 1–84.

Kim, N. W., Lee, J. E., & Kim, J. T. (2012). Assessment of Flow Regulation Effects by Dams in the Han River, Korea, on the Downstream Flow Regimes Using SWAT. *Journal of Water Resources Planning and Management*, *138*(1), 24–35. https://doi.org/10.1061/(asce)wr.1943-5452.0000148

King, C. W., & Carbajales-Dale, M. (2016). Food–energy–water metrics across scales: project to system level. *Journal of Environmental Studies and Sciences*, *6*(1), 39–49. https://doi.org/10.1007/s13412-016-0390-9

Laize, C. L. R., Acreman, M. C., Schneider, C., Dunbar, M. J., Houghton-Carr, H. A., Flörke, M., & Hannah, D. M. (2014). PROJECTED FLOW ALTERATION AND ECOLOGICAL RISK FOR PAN-EUROPEAN RIVERS. *River Research and Applications*, *30*, 299–314. https://doi.org/10.1002/rra.2645

Lazaro, L. L. B., Bellezoni, R. A., Puppim de Oliveira, J. A., Jacobi, P. R., & Giatti, L. L. (2022). Ten Years of Research on the Water-Energy-Food Nexus: An Analysis of Topics Evolution. *Frontiers in Water*, *4*(May), 1–16. https://doi.org/10.3389/frwa.2022.859891

Lazarus, M., Hippel, D. Von, Hill, D., & Margolis, R. (1995). A Guide to Environmental Analysis For Energy Planners. *Environmental Protection*, *December*.

Leimbach, M., Kriegler, E., Roming, N., & Schwanitz, J. (2017). Future growth patterns of world regions – A GDP scenario approach. *Global Environmental Change*, *42*, 215–225. https://doi.org/10.1016/j.gloenvcha.2015.02.005

Loh, J., Randers, J., MacGillivray, A., Kapos, V., Jenkins, M., & Groombridge, B.

(1998). *Living Planet Report*.

Lu, M., Zhao, Q., Ding, S., Wang, S., Hong, Z., Jing, Y., & Wang, A. (2022). Hydro-geomorphological characteristics in response to the water-sediment regulation scheme of the Xiaolangdi Dam in the lower Yellow River. *Journal of Cleaner Production*, *335*(January). https://doi.org/10.1016/j.jclepro.2021.130324

Macknick, J., Newmark, R., Heath, G., & Hallett, K. C. (2012). Operational water consumption and withdrawal factors for electricity generating technologies: a review of existing literature. *Environmental Research Letters*, *7*(4), 1–10. https://doi.org/10.1088/1748-9326/7/4/045802

Maheshwari, B. L., Walker, K. F., & McMahon, T. A. (1995). Effects of regulation on the flow regime of the river Murray, Australia. *River Research and Applications*, *10*(1), 15–38.

Maraun, D. (2016). Bias Correcting Climate Change Simulations - a Critical Review. *Current Climate Change Reports*, *2*(4), 211–220. https://doi.org/10.1007/s40641-016-0050-x

Mbow, C., Rosenzweig, C., Barioni, L. G., Benton, T. G., Herrero, M., Krishnapillai, M., Liwenga, E., Pradhan, P., Rivera-Ferre, M. G., Sapkota, T., Tubiello, F. N., & Xu, Y. (2019). Food security. In P. R. Shukla, J. Skea, E. C. Buendia, V. Masson-Delmotte, H.-O. Pörtner, D. C. Roberts, P. Zhai, R. Slade, S. Connors, R. van Diemen, M. Ferrat, E. Haughey, S. N. S. Luz, M. Pathak, J. Petzold, J. P. Pereira, P. Vyas, E. Huntley, K. Kissick, … J. Malley (Eds.), *Climate Change and Land: an IPCC special report on climate change, desertification, land degradation, sustainable land management, food security, and greenhouse gas fluxes in terrestrial ecosystems*. https://doi.org/https://doi.org/10.1017/9781009157988.007

Mlawer, E. J., Taubman, S. J., Brown, P. D., Iacono, M. J., & Clough, S. A. (1997). Radiative transfer for inhomogeneous atmospheres: RRTM, a validated correlated-k model for the longwave. *Journal of Geophysical Research Atmospheres*, *102*(14), 16663–16682. https://doi.org/10.1029/97jd00237

MoENR. (2014). *Türkiye ulusal yenilenebilir enerji eylem plani*.

MoEUC. (2022a). *Haberler*. https://www.csb.gov.tr/aritilmis-atiksularin-yeniden-kullanim-oraninda-yuzde-4-olan-yil-sonu-hedefi-asildi-bakanlik-faaliyetleri-34168

MoEUC. (2022b). *Türkiye Ulusal Katkı Beyanı'nı COP27'de Açıkladı*. https://iklim.gov.tr/turkiye-ulusal-katki-beyani-ni-cop27-de-acikladi-haber-84

Mohtar, R. H., & Daher, B. (2010). Water, Energy, and Food: The Ultimate Nexus. In *Encyclopedia of Agricultural, Food, and Biological Engineering, Second Edition* (pp. 1–5). Taylor & Francis. https://doi.org/10.1081/E-EAFE2-120048376

Momblanch, A., Papadimitriou, L., Jain, S. K., Kulkarni, A., Ojha, C. S. p., Adeloye, A. J., & Holman, I. P. (2018). Untangling the water-food-energy-environment nexus for global change adaptation in a complex Himalayan water resource system. *Science of The Total Environment*, *655*, 35–47. https://doi.org/10.1016/j.scitotenv.2018.11.045

Moriasi, D. N., Arnold, J. G., Van Liew, M. W., Bingner, R. L., Harmel, R. D., & Veith, T. L. (2007). Model Evaluation Guidelines for Systematic Quantification of Accuracy in Watershed Simulations. *Transactions of the Asabe*, *50*(3), 885–900. https://doi.org/10.13031/2013.23153

Murrant, D. (2016). *The Water-Energy Nexus : Quantifying the Impact of Water Availability on Future UK Thermal Power Generation* (Issue September).

Nardo, M., Saisana, M., Tarantola, A., & Stefano, S. (2005). *Tools for Composite Indicators Building*. http://collection.europarchive.org/dnb/20070702132253/http://farmweb.jrc.ec.europa.eu/ci/Document/EUR 21682 EN.pdf

Nhamo, L., Mabhaudhi, T., Mpandeli, S., Nhemachena, C., Senzanje, A., Naidoo, D., Liphadzi, S., & Modi, A. T. (2019). *Sustainability indicators and indices for the water- energy-food nexus for performance assessment: WEF nexus in practice – South Africa case study* (Issue May).

Nilsson, C., & Malm Renofalt, B. (2008). Linking Flow Regime and Water Quality in Rivers: a Challenge to Adaptive Catchment Management. *Ecology and Society*, *13*(2). https://www.ecologyandsociety.org/vol13/iss2/art18/

Nobert, J. (2012). Hydrological Response of Watershed Systems to Land Use/Cover Change. A Case of Wami River Basin. *The Open Hydrology Journal*, *6*(1), 78–87. https://doi.org/10.2174/1874378101206010078

O'Neill, B. C., Kriegler, E., Ebi, K. L., Kemp-Benedict, E., Riahi, K., Rothman, D. S., van Ruijven, B. J., van Vuuren, D. P., Birkmann, J., Kok, K., Levy, M., & Solecki, W. (2017). The roads ahead: Narratives for shared socioeconomic pathways describing world futures in the 21st century. In *Global Environmental Change* (Vol. 42, pp. 169–180). https://doi.org/10.1016/j.gloenvcha.2015.01.004

O'Neill, B. C., Kriegler, E., Riahi, K., Ebi, K. L., Hallegatte, S., Carter, T. R., Mathur, R., & van Vuuren, D. P. (2014). A new scenario framework for climate change research: The concept of shared socioeconomic pathways. *Climatic Change*, *122*(3), 387–400. https://doi.org/10.1007/s10584-013-0905-2

OECD. (2008). *Handbook on Constructing Composite Indicators:*

METHODOLOGY AND USER GUIDE. OECD Publishing. https://www.oecd.org/sdd/42495745.pdf

OECD. (2012). *OECD Environmental Outlook to 2050: The Consequences of Inaction - Key Facts and Figures*. https://www.oecd.org/env/indicators-modelling-outlooks/oecdenvironmentaloutlookto2050theconsequencesofinaction-keyfactsandfigures.htm

Özcan, Z. (2016). *Evaluation of the Best Management Practices to Control Agricultural Diffuse Pollution in Lake Mogan Watershed with SWAT Model*. Middle East Technical University.

Özcan, Z., Başkan, O., Düzgün, H. Ş., Kentel, E., & Alp, E. (2017). A pollution fate and transport model application in a semi-arid region: Is some number better than no number? *Science of the Total Environment*, *595*. https://doi.org/10.1016/j.scitotenv.2017.03.240

Pastor, A. V., Palazzo, A., Havlik, P., Biemans, H., Wada, Y., Obersteiner, M., Kabat, P., & Ludwig, F. (2019). The global nexus of food–trade–water sustaining environmental flows by 2050. *Nature Sustainability*, *2*(6), 499–507. https://doi.org/10.1038/s41893-019-0287-1

Perry, C., Steduto, P., Allen, R. G., & Burt, C. M. (2009). Increasing productivity in irrigated agriculture: Agronomic constraints and hydrological realities. *Agricultural Water Management*, *96*(11), 1517–1524. https://doi.org/10.1016/j.agwat.2009.05.005

Pinar, M., Cruciani, C., Giove, S., & Sostero, M. (2014). Constructing the FEEM sustainability index: A Choquet integral application. *Ecological Indicators*, *39*, 189–202. https://doi.org/10.1016/j.ecolind.2013.12.012

Poff, N. L., Allan, J. D., Bain, M. B., Karr, J. R., Prestegaard, K. L., Richter, B. D., Sparks, R. E., & Stromberg, J. C. (1997). The Natural Flow Regime. *BioScience*, *47*(11), 769–784. https://doi.org/10.2307/1313099

Qin, J., Duan, W., Chen, Y., Dukhovny, V. A., Sorokin, D., Li, Y., & Wang, X. (2022). Comprehensive evaluation and sustainable development of water–energy–food–ecology systems in Central Asia. *Renewable and Sustainable Energy Reviews*, *157*(November 2021), 112061. https://doi.org/10.1016/j.rser.2021.112061

Reichold, L., Zechman, E. M., Brill, E. D., & Holmes, H. (2010). Simulation-Optimization Framework to Support Sustainable Watershed Development by Mimicking the Predevelopment Flow Regime. *Journal of Water Resources Planning and Management*, *136*(3), 366–375. https://doi.org/10.1061/(asce)wr.1943-5452.0000040

Riahi, K., Rao, S., Krey, V., Cho, C., Chirkov, V., Fischer, G., Georg, K., Nakicenovic, N., & Rafaj, P. (2011). RCP 8 . 5 — A scenario of comparatively high greenhouse gas emissions. *Climatic Change*, *109*, 33–57. https://doi.org/10.1007/s10584-011-0149-y

Riahi, K., van Vuuren, D. P., Kriegler, E., Edmonds, J., O'Neill, B. C., Fujimori, S., Bauer, N., Calvin, K., Dellink, R., Fricko, O., Lutz, W., Popp, A., Cuaresma, J. C., KC, S., Leimbach, M., Jiang, L., Kram, T., Rao, S., Emmerling, J., … Tavoni, M. (2017). The Shared Socioeconomic Pathways and their energy, land use, and greenhouse gas emissions implications: An overview. *Global Environmental Change*, *42*, 153–168. https://doi.org/10.1016/j.gloenvcha.2016.05.009

Richter, B. D., Baumgartner, J. V., Braun, D. P., & Powell, J. (1998). A spatial assessment of hydrologic alteration within a river network. *River Research*

and Applications, *14*(4), 329–340. https://doi.org/10.1002/(sici)1099-1646(199807/08)14:4<329::aid-rrr505>3.0.co;2-e

Richter, B. D., Baumgartner, J. V., Wigington, R., & Braun, D. P. (1997). How much water does a river need? *Freshwater Biology*, *37*(1), 231–249. https://doi.org/10.1046/j.1365-2427.1997.00153.x

Richter, B. D., Baumgartner, J. V, Powell, J., Braun, D. P., Richter, B. D., Baumgartner, J. V, Powell, J., & Braunt, D. P. (1996). A Method for Assessing Hydrologic Alteration within Ecosystems Published by : Wiley for Society for Conservation Biology All use subject to http://about.jstor.org/terms A Method for Assessing Hydrologic Alteration within E. *Conservation Biology*, *10*(4), 1163–1174.

Ringler, C., Willenbockel, D., Perez, N., Rosegrant, M., Zhu, T., & Matthews, N. (2016). Global linkages among energy, food and water: an economic assessment. *Journal of Environmental Studies and Sciences*, *6*(1), 161–171. https://doi.org/10.1007/s13412-016-0386-5

Rodriguez, B. M. (2017). *The Water-Energy-Food nexus: trends, trade- offs and implications for strategic energies* [UNIVERSIDAD COMPLUTENSE DE MADRID]. https://eprints.ucm.es/43443/1/T38965.pdf

Rogelj, J., Popp, A., Calvin, K. V., Luderer, G., Emmerling, J., Gernaat, D., Fujimori, S., Strefler, J., Hasegawa, T., Marangoni, G., Krey, V., Kriegler, E., Riahi, K., Van Vuuren, D. P., Doelman, J., Drouet, L., Edmonds, J., Fricko, O., Harmsen, M., … Tavoni, M. (2018). Scenarios towards limiting global mean temperature increase below 1.5 °c. *Nature Climate Change*, *8*(4), 325–332. https://doi.org/10.1038/s41558-018-0091-3

Sachs, J., Schmidt-Traub, G., Kroll, C., Lafortune, G., & Fuller, G. (2016). SDG Index and Dashboards - Global Report. *New York: Bertelsmann Stiftung and*

Sustainable Development Solutions Network (SDSN), *July*, 58. http://sdgindex.org/assets/files/sdg_index_and_dashboards_compact.pdf

Sachs, J., Schmidt-Traub, G., Kroll, C., Lafortune, G., & Fuller, G. (2018). SDG Index and Dashboards Report 2018: Global Responsibilities. In *BertelsmannStiftung*. www.pica-publishing.com

Saladini, F., Betti, G., Ferragina, E., Bouraoui, F., Cupertino, S., Canitano, G., Gigliotti, M., Autino, A., Pulselli, F. M., Riccaboni, A., Bidoglio, G., & Bastianoni, S. (2018). Linking the water-energy-food nexus and sustainable development indicators for the Mediterranean region. *Ecological Indicators*, *91*(December 2017), 689–697. https://doi.org/10.1016/j.ecolind.2018.04.035

SDG Indicators. (2021). United Nations. https://unstats.un.org/sdgs/indicators/indicators-list/

SEI. (2005). *User Guide for LEAP 2005* (Issue May). http://www.energycommunity.org/default.asp?action=41

Semertzidis, T. (2015). Can energy systems models address the resource nexus? *Energy Procedia*, *83*, 279–288. https://doi.org/10.1016/j.egypro.2015.12.182

Shi, P., Ma, X., Hou, Y., Li, Q., Zhang, Z., Qu, S., Chen, C., Cai, T., & Fang, X. (2013). Effects of Land-Use and Climate Change on Hydrological Processes in the Upstream of Huai River, China. *Water Resources Management*, *27*(5), 1263–1278. https://doi.org/10.1007/s11269-012-0237-4

Sieber, J., & Purkey, D. (2015). *Water Evaluation and Planing system (WEAP) User Guide*.

Simpson, G. B. (2020). *DEVELOPMENT OF WATER-ENERGY-FOOD NEXUS INDEX AND ITS APPLICATION TO SOUTH AFRICA AND THE SOUTHERN AFRICAN DEVELOPMENT COMMUNITY* (Issue February).

https://ukzn-dspace.ukzn.ac.za/handle/10413/19057

Simpson, G. B., Jewitt, G. P. W., Becker, W., Badenhorst, J., Masia, S., Neves, A. R., Rovira, P., & Pascual, V. (2022). The Water-Energy-Food Nexus Index: A Tool to Support Integrated Resource Planning, Management and Security. *Frontiers in Water*, *4*(March), 1–17. https://doi.org/10.3389/frwa.2022.825854

Skamarock, W., Klemp, J. B., Dudhia, J., Gill, D. O., Barker, D. M., Duda, M. G., Huang, X.-Y., Wang, W., & Powers, J. G. (2008). *A Description of the Advanced Research WRF Version 3* (Issue June).

Smirnova, T. G., Brown, J. M., & Benjamin, S. G. (1997). Performance of different soil model configurations in simulating ground surface temperature and surface fluxes. *Monthly Weather Review*, *125*, 1870–1884.

Spang, E. S., Moomaw, W. R., Gallagher, K. S., Kirshen, P. H., & Marks, D. H. (2014). The water consumption of energy production: An international comparison. *Environmental Research Letters*, *9*(10), 1–14. https://doi.org/10.1088/1748-9326/9/10/105002

Stucki, V., & Sojamo, S. (2012). Nouns and numbers of the water-energy-security nexus in Central Asia. *International Journal of Water Resources Development*, *28*(3), 399–418. https://doi.org/10.1080/07900627.2012.684304

SYGM. (2022). *Sakarya havzasi nehir havza yönetim plani hazirlanmasi projesi stratejik çevresel değerlendirme kapsam belirleme raporu*. https://webdosya.csb.gov.tr/db/scd/icerikler/sakarya-nhyp-kapsam-n-ha--raporu-20220131081815.pdf

TAGEM & DSİ. (2017). *Türkiye'de Sulanan Bitkilerin Bitki Su Tüketimleri*.

TEİAŞ. (2019). *Türkiye Elektrik Enerjisi 5 Yıllık Üretim Kapasite Projeksiyonu*

(2019-2023).

Terrier, M., Perrin, C., de Lavenne, A., Andréassian, V., Lerat, J., & Vaze, J. (2021). Streamflow naturalization methods: a review. *Hydrological Sciences Journal*, *66*(1), 12–36. https://doi.org/10.1080/02626667.2020.1839080

The Ministry of Agriculture and Forestry. (2019). *Regulation on the Principles and Procedures for Signing Water Usage Rights Agreement for Operating in Electricity Market [ELEKTRİK PİYASASINDA ÜRETİM FAALİYETİNDE BULUNMAK ÜZERE SU KULLANIM HAKKI ANLAŞMASI İMZALANMASINA İLİŞKİN USUL VE ESASLAR HAKKINDA YÖ*. https://www.resmigazete.gov.tr/eskiler/2019/06/20190615-5.htm

The Ministry of Forestry and Water Affairs. (2016). *Iklim Degisikliginin Su Kaynaklarina Etkisi Projesi*.

Thomson, A. M., Calvin, K. V., Smith, S. J., Kyle, G. P., Volke, A., Patel, P., Delgado-Arias, S., Bond-Lamberty, B., Wise, M. A., Clarke, L. E., & Edmonds, J. A. (2011). RCP4.5: A pathway for stabilization of radiative forcing by 2100. *Climatic Change*, *109*(1), 77–94. https://doi.org/10.1007/s10584-011-0151-4

TÜBİTAK MAM. (2013). *HAVZA KORUMA EYLEM PLANLARININ HAZIRLANMASI PROJESİ SAKARYA HAVZASI PROJE NİHAİ RAPORU*.

TÜİK. (2022). *Sera Gazı Emisyon İstatistikleri, 1990-2020*. https://data.tuik.gov.tr/Bulten/Index?p=Sera-Gazi-Emisyon-Istatistikleri-1990-2020-45862

UN. (2000). *Principles and Practices of Water Allocation Among Water-Use Sectors*.

UN Water. (2013). *What is Water Security? Infographic*.

https://www.unwater.org/publications/what-water-security-infographic

UN Water. (2015). *Water, Food and Energy*. http://www.unwater.org/water-facts/water-food-and-energy/

UNDP. (1990). *Human Development Report*.

United Nations. (2015). *A proposed approach to assessing the Water-Food-Energy-Ecosystems Nexus under the UNECE Water Convention Discussion paper*. 1–11.

United Nations. (2018). *The Sustainable Development Goals Report 2018*. https://unstats.un.org/sdgs/files/report/2018/TheSustainableDevelopmentGoalsReport2018-EN.pdf

United Nations. (2022). *The sustainable development goals report 2022*.

van Vuuren, D. P., Edmonds, J., Kainuma, M., Riahi, K., Thomson, A., Hibbard, K., Hurtt, G. C., Kram, T., Krey, V., Lamarque, J. F., Masui, T., Meinshausen, M., Nakicenovic, N., Smith, S. J., & Rose, S. K. (2011). The representative concentration pathways: An overview. *Climatic Change*, *109*(1), 5–31. https://doi.org/10.1007/s10584-011-0148-z

van Vuuren, D. P., Kok, M., Lucas, P. L., Prins, A. G., Alkemade, R., van den Berg, M., Bouwman, L., van der Esch, S., Jeuken, M., Kram, T., & Stehfest, E. (2015). Pathways to achieve a set of ambitious global sustainability objectives by 2050: Explorations using the IMAGE integrated assessment model. *Technological Forecasting and Social Change*, *98*, 303–323. https://doi.org/10.1016/j.techfore.2015.03.005

Venghaus, S., & Dieken, S. (2019). From a few security indices to the FEW Security Index: Consistency in global food, energy and water security assessment. *Sustainable Production and Consumption*, *20*, 342–355.

https://doi.org/10.1016/j.spc.2019.08.002

Veysey, J., & Wagner, C. (2021). *Training on Low Emissions Analysis Platform Introduction to LEAP* (Issue October).

Villamayor-Tomas, S., Grundmann, P., Epstein, G., Evans, T., & Kimmich, C. (2015). The water-energy-food security nexus through the lenses of the value chain and the institutional analysis and development frameworks. *Water Alternatives*, *8*(1), 735–755.

Vlotman, W. F., & Ballard, C. (2014). Water, food and energy supply chains for a green economy. *Irrigation and Drainage*, *63*(2), 232–240. https://doi.org/10.1002/ird.1835

Wada, Y., Flörke, M., Hanasaki, N., Eisner, S., Fischer, G., Tramberend, S., Satoh, Y., Van Vliet, M. T. H., Yillia, P., Ringler, C., Burek, P., & Wiberg, D. (2016). Modeling global water use for the 21st century: The Water Futures and Solutions (WFaS) initiative and its approaches. *Geoscientific Model Development*, *9*(1), 175–222. https://doi.org/10.5194/gmd-9-175-2016

Waheed, B., Khan, F., & Veitch, B. (2009). Linkage-based frameworks for sustainability assessment: Making a case for driving force-pressure-state-exposure-effect-action (DPSEEA) frameworks. *Sustainability*, *1*(3), 441–463. https://doi.org/10.3390/su1030441

Wang, K., Liu, J., Xia, J., Wang, Z., Meng, Y., Chen, H., Mao, G., & Ye, B. (2021). Understanding the impacts of climate change and socio-economic development through food-energy-water nexus: A case study of mekong river delta. *Resources, Conservation and Recycling*, *167*(June 2020), 105390. https://doi.org/10.1016/j.resconrec.2020.105390

Wang, S., Fath, B., & Chen, B. (2019). Energy–water nexus under energy mix

scenarios using input–output and ecological network analyses. *Applied Energy, 233–234*, 827–839. https://doi.org/10.1016/j.apenergy.2018.10.056

Watanabe, M., Suzuki, T., O'Ishi, R., Komuro, Y., Watanabe, S., Emori, S., Takemura, T., Chikira, M., Ogura, T., Sekiguchi, M., Takata, K., Yamazaki, D., Yokohata, T., Nozawa, T., Hasumi, H., Tatebe, H., & Kimoto, M. (2010). Improved climate simulation by MIROC5: Mean states, variability, and climate sensitivity. *Journal of Climate*. https://doi.org/10.1175/2010JCLI3679.1

Willis, H., Groves, D., Ringel, J., Mao, Z., Efron, S., & Abbott, M. (2016). Developing the Pardee RAND Food-Energy-Water Security Index: Toward a Global Standardized, Quantitative, and Transparent Resource Assessment. *Developing the Pardee RAND Food-Energy-Water Security Index: Toward a Global Standardized, Quantitative, and Transparent Resource Assessment*. https://doi.org/10.7249/tl165

Wolfe, M. L., Ting, K. C., Scott, N., Sharpley, A., Jones, J. W., & Verma, L. (2016). Engineering solutions for food-energy-water systems: it is more than engineering. *Journal of Environmental Studies and Sciences*, *6*(1), 172–182. https://doi.org/10.1007/s13412-016-0363-z

World Bank Group. (2023a). *Global Solar Atlas*. https://globalsolaratlas.info/map?c=11.609193,8.4375,3

World Bank Group. (2023b). *Overview*. https://www.worldbank.org/en/country/turkey/overview

World Economic Forum WEF. (2011). *Global Risks*. World Economic Forum.

WorldBank. (1999). *World Development Indicators*.

WWAP (United Nations World Water Assessment Programme). (2014). *The*

United Nations World Water Development Report 2014: Water and Energy (Vol. 1). https://doi.org/978-92-3-104259-1

WWF. (2022). *Living Planet Report 2022 - Building a nature-positive society*. https://wwflpr.awsassets.panda.org/downloads/living_planet_report__2022.pdf

Yates, D., Purkey, D., Sieber, J., Huber-Lee, A., & Galbraith, H. (2005). WEAP21 - A demand-, priority-, and preference-driven water planning model. Part 2: Aiding freshwater ecosystem service evaluation. *Water International*, *30*(4), 501–512. https://doi.org/10.1080/02508060508691894

Yi, J., Guo, J., Ou, M., Pueppke, S. G., Ou, W., Tao, Y., & Qi, J. (2020). Sustainability assessment of the water-energy-food nexus in Jiangsu Province, China. *Habitat International*, *95*(April 2019), 102094. https://doi.org/10.1016/j.habitatint.2019.102094

Yin, J., He, F., Jiu Xiong, Y., & Yu Qiu, G. (2017). Effects of land use/land cover and climate changes on surface runoff in a semi-humid and semi-arid transition zone in northwest China. *Hydrology and Earth System Sciences*, *21*(1), 183–196. https://doi.org/10.5194/hess-21-183-2017

Yuan, M. H., & Lo, S. L. (2020). Developing indicators for the monitoring of the sustainability of food, energy, and water. *Renewable and Sustainable Energy Reviews*, *119*(November 2019), 109565. https://doi.org/10.1016/j.rser.2019.109565

Zeiringer, B., Seliger, C., Greimel, F., & Schmutz, S. (2018). River Hydrology, Flow Alteration, and Environmental Flow. In S. Schmutz & J. Sendzimir (Eds.), *Riverine Ecosystem Management* (pp. 67–89). Springer, Cham. https://doi.org/10.1007/978-3-319-73250-3_4

Zhang, L., Nan, Z., Xu, Y., & Li, S. (2016). Hydrological impacts of land use change and climate variability in the headwater region of the Heihe River Basin, northwest China. *PLoS ONE*, *11*(6), 1–25. https://doi.org/10.1371/journal.pone.0158394

APPENDICES

A. WEAP-LEAP Model Inputs

Table A. 1. CORINE 2018 land classes areas and percentage distributions in each catchment and subbasin

	Catchment	Artificial surfaces	Agricultural areas	Forest and semi-natural areas	Wetlands	Water bodies	Total Area (ha)
Upper Sakarya	Aktaş	3954	231064	82344	-	-	317362
	Aydınlı	8524	434227	182003	3030	334	628118
	Ayvalı	10906	592381	256592	5485	193	865557
	Çıkış	3604	107298	43847	235	-	154984
	Total Area (ha)	***26988***	***1364970***	***564786***	***8750***	***527***	***1966021***
	Total Area (%)	***1.4***	***69.4***	***28.7***	***0.4***	***0.0***	
	Catchment	Artificial surfaces	Agricultural areas	Forest and semi-natural areas	Wetlands	Water bodies	Total Area (ha)
Porsuk	Eşenkara	12248	258324	279805	215	3003	553595
	Kıranharmanı	16599	281761	219530	69	668	518627
	Total Area (ha)	***28847***	***540084***	***499336***	***284***	***3671***	***1072222***
	Total Area (%)	***2.7***	***50.4***	***46.6***	***0.0***	***0.3***	
	Catchment	Artificial surfaces	Agricultural areas	Forest and semi-natural areas	Wetlands	Water bodies	Total Area (ha)
Ankara	Ankara	68572	461132	184017	1754	2325	717800
	Total Area (ha)	***68572***	***461132***	***184017***	***1754***	***2325***	***717800***
	Total Area (%)	***9.6***	***64.2***	***25.6***	***0.2***	***0.3***	
	Catchment	Artificial surfaces	Agricultural areas	Forest and semi-natural areas	Wetlands	Water bodies	Total Area (ha)
Kirmir	Kirmir	4541	149889	302235	42	3267	459974
	Total Area (ha)	***4541***	***149889***	***302235***	***42***	***3267***	***459974***
	Total Area (%)	***1.0***	***32.6***	***65.7***	***0.0***	***0.7***	

Table A. 1 (continued)

	Catchment	Artificial surfaces	Agricultural areas	Forest and semi-natural areas	Wetlands	Water bodies	Total Area (ha)
Middle Sakarya	Kayabeli	6626	245299	617705	190	9788	879608
	Doğançay	5190	137179	188323	-	188	330879
	Total Area (ha)	***11816***	***382478***	***806028***	***190***	***9976***	***1210487***
	Total Area (%)	***1.0***	***31.6***	***66.6***	***-***	***0.8***	
	Catchment	Artificial surfaces	Agricultural areas	Forest and semi-natural areas	Wetlands	Water bodies	Total Area (ha)
Göksu	Göksu	5029	121238	116874	-	403	243544
	Total Area (ha)	***5029***	***121238***	***116874***	***-***	***404***	***243545***
	Total Area (%)	***2.1***	***49.8***	***48.0***	***-***	***0.2***	
	Catchment	Artificial surfaces	Agricultural areas	Forest and semi-natural areas	Wetlands	Water bodies	Total Area (ha)
Lower Sakarya	Mudurnu	2442	84213	128609	-	70	215334
	Adatepe	11174	153905	85969	746	6656	258450
	Total Area (ha)	***13616***	***238118***	***214578***	***746***	***6726***	***473784***
	Total Area (%)	***2.9***	***50.3***	***45.3***	***0.2***	***1.4***	

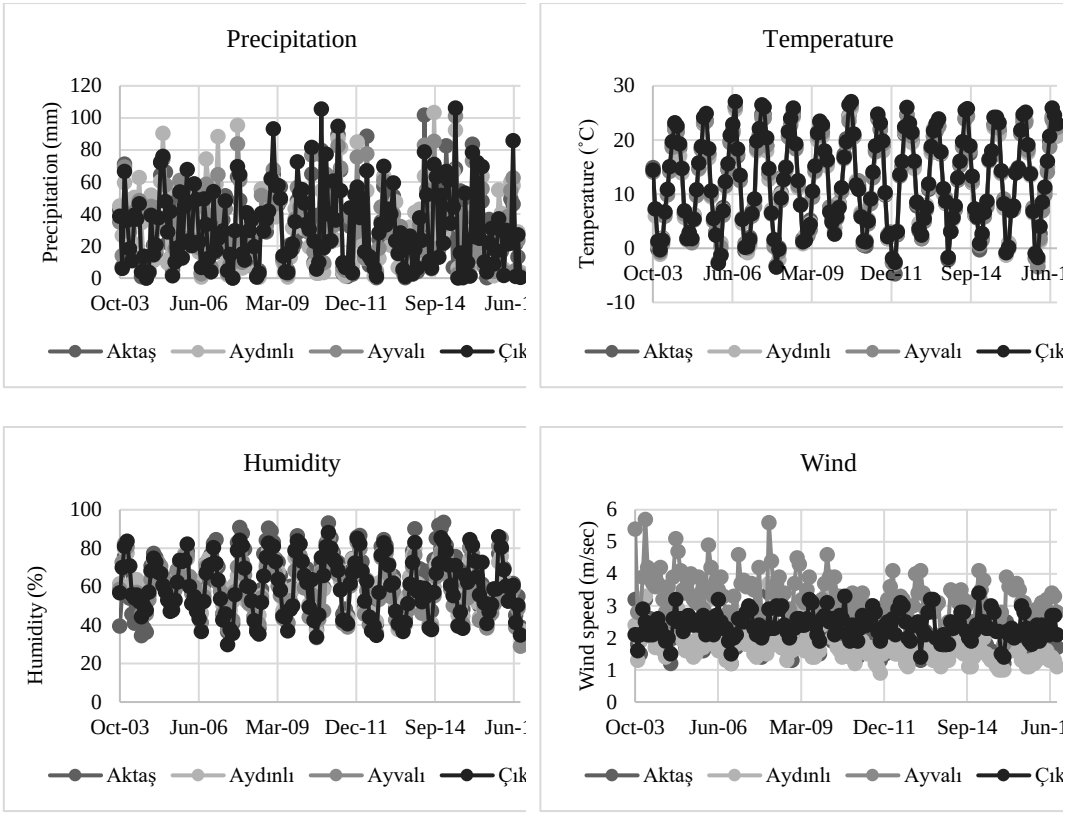

Figure A. 1. Upper Sakarya subbasin: The climate data of the catchments defined in the WEAP model

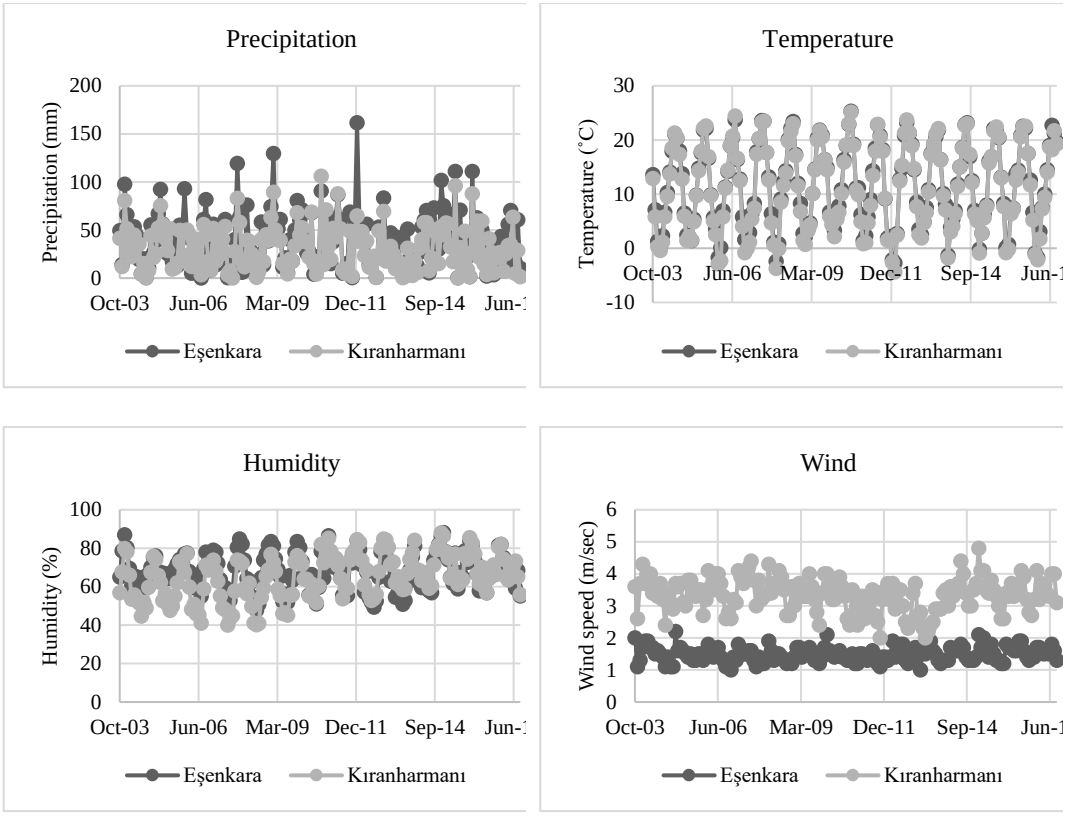

Figure A. 2. Porsuk subbasin: The climate data of the catchments defined in the WEAP model

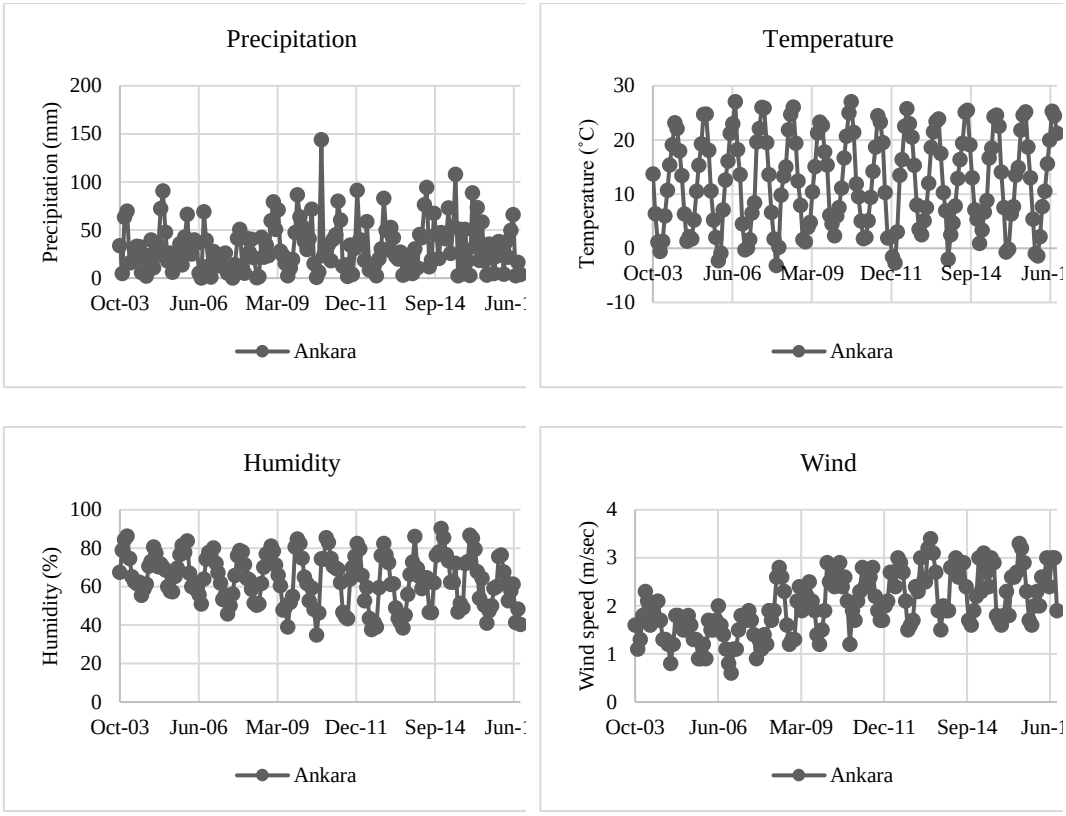

Figure A. 3. Ankara subbasin: The climate data of the catchments defined in the WEAP model

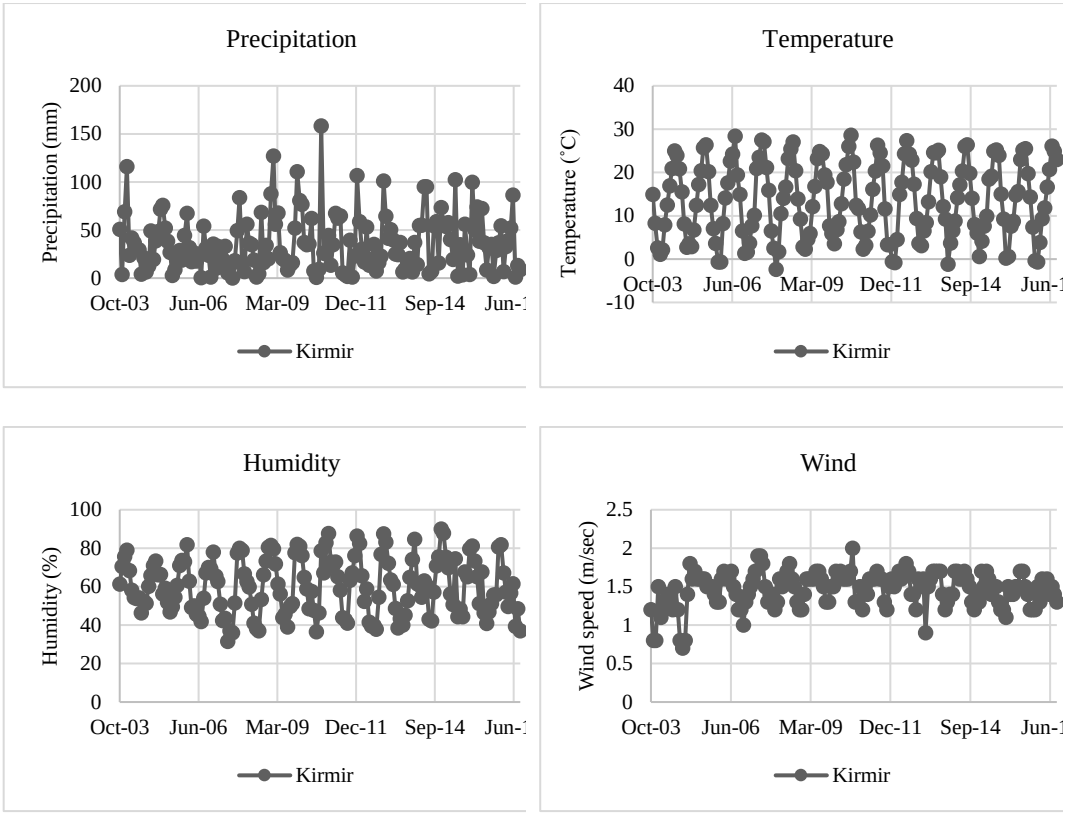

Figure A. 4. Kirmir subbasin: The climate data of the catchments defined in the WEAP model

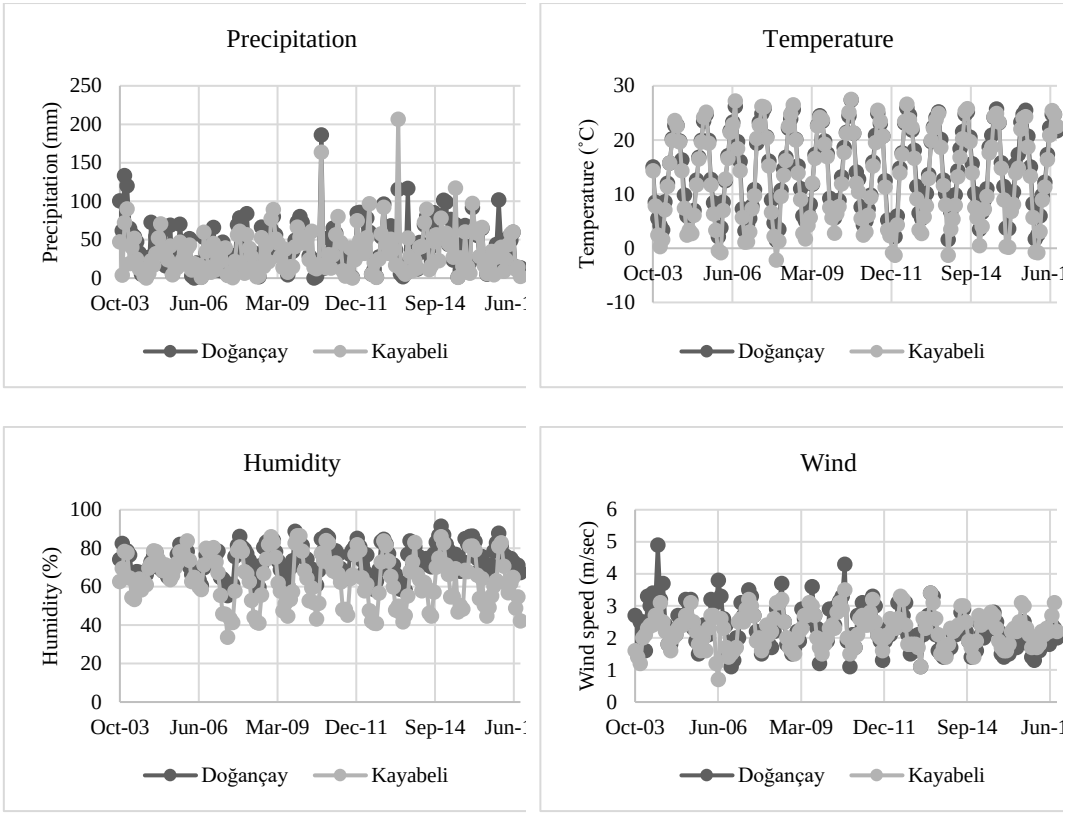

Figure A. 5. Middle Sakarya subbasin: The climate data of the catchments defined in the WEAP model

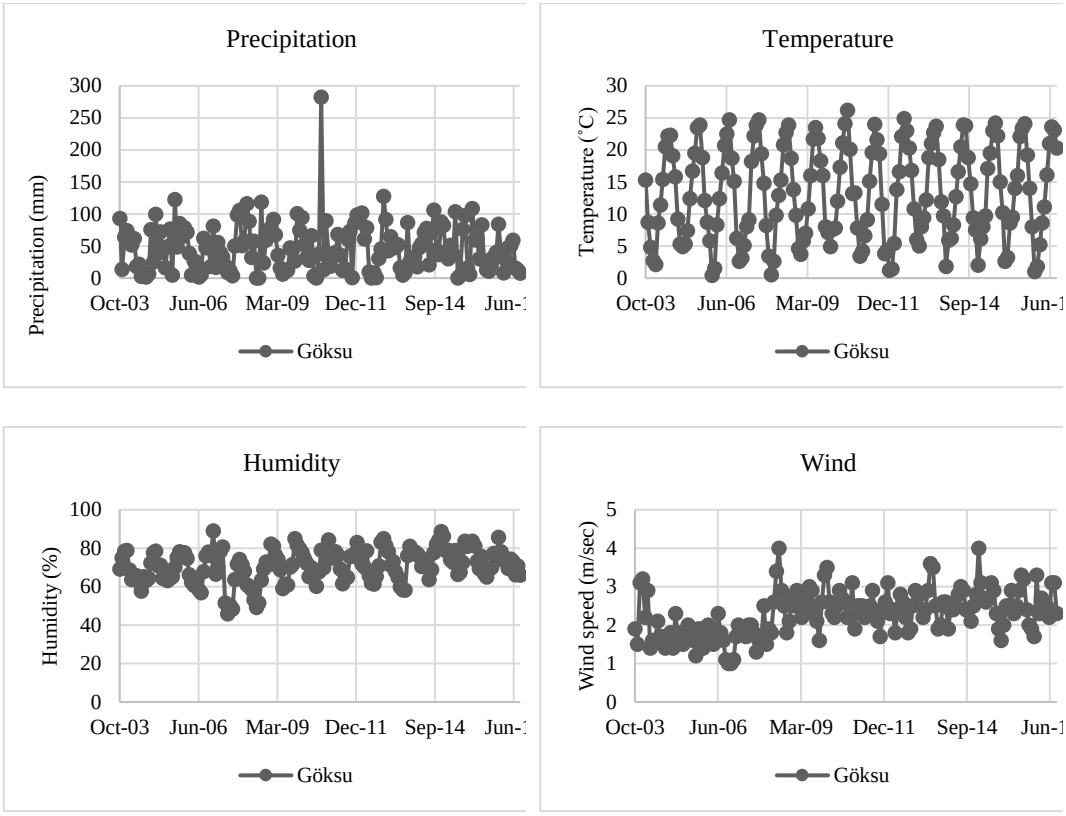

Figure A. 6. Göksu subbasin: The climate data of the catchments defined in the WEAP model

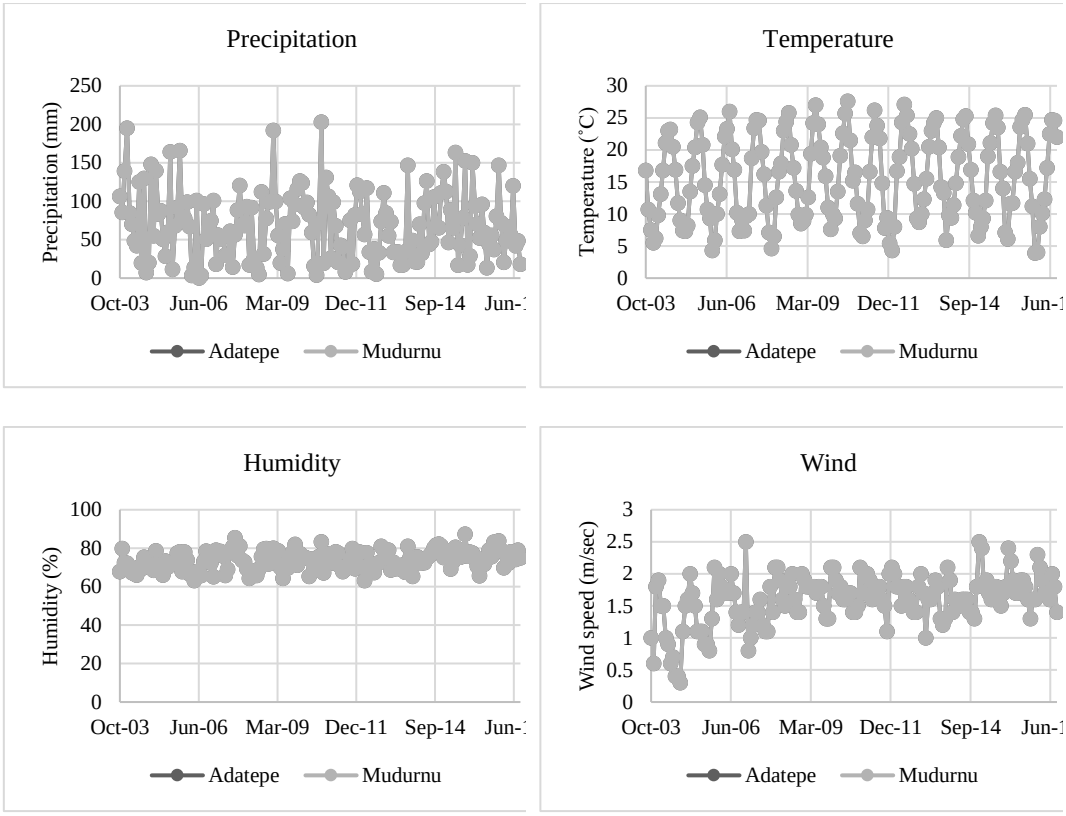

Figure A. 7. Lower Sakarya subbasin: The climate data of the catchments defined in the WEAP model

Table A. 2. Physical characteristics of the reservoirs and ponds in each subbasin

Name of the reservoir/pond	**Subbasin**	**Storage Capacity (hm^3)**	**Initial Storage (hm^3)**	**Inactive Volume (hm^3)**
Çatören Dam	Upper Sakarya	41	21	36
Kunduzlar Dam	Upper Sakarya	28	5	36
Çavuşçu Reservoir	Upper Sakarya	184	28	270
Aktaş Pond	Upper Sakarya	9	8	13
Aydınlı Pond	Upper Sakarya	26	23	38
Ayvalı Pond	Upper Sakarya	12	11	15
Çıkış Pond	Upper Sakarya	0	0	1
Aşağıkuzfındık Dam	Porsuk	21	0	14
Beşkarış Dam	Porsuk	76	0	25
Beylikova Reservoir	Porsuk	78	0	82
Dodurga Dam	Porsuk	19	8	23
Enne Dam	Porsuk	7	5	28

Table A. 2 (continued)

Eşenkaya Pond	Porsuk	16	7	18
Kıranharmanı Pond	Porsuk	26	5	23
Kureyşler Dam	Porsuk	26	0	16
Musaözü Dam	Porsuk	2	2	1
Porsuk Dam	Porsuk	449	344	1044
Çubuk I Dam	Ankara	7	2	0
Çubuk II Dam	Ankara	22	22	0
Ankara Pond	Ankara	244	133	338
Kavşakkaya Dam	Ankara	81	0	56
Kurtboğazı Dam	Ankara	98	92	71
Akyar Dam	Kirmir	56	16	108
Asartepe Dam	Kirmir	20	9	73
Çamlıdere Dam	Kirmir	1376	476	1791
Doğanözü Dam	Kirmir	35	0	28
Eğrekkaya Dam	Kirmir	112	62	330
Kirmir Pond	Kirmir	9	7	2
Doğançay Pond	Middle Sakarya	11	9	20
Kayabeli Pond	Middle Sakarya	11	9	20
Gökçekaya Dam	Middle Sakarya	954	915	8760
Günyurdu Dam	Middle Sakarya	7	7	2
Gürsöğüt Dam	Middle Sakarya	1103	0	0
Kargı Dam	Middle Sakarya	45	0	7
Kızıldamlar Dam	Middle Sakarya	12	10	16
Sarıyar Dam	Middle Sakarya	1699	1317	10288
Yenice Dam	Middle Sakarya	58	58	507
Babasultan Dam	Göksu	12	0	5
Boğazköy Dam	Göksu	39	0	97
Göksu Pond	Göksu	22	13	19
Adatepe Pond	Lower Sakarya	28	28	10
Sapanca Lake	Lower Sakarya	1050	1050	0

Table A. 3. Monthly average net evaporation values calculated by Pan Evaporation method in the reservoirs

Name of the Reservoir	Oct	Nov	Dec	Jan	Feb	Mar	Apr	May	Jun	Jul	Aug	Sep
Çubuk I	0.048	0.000	0.000	0.000	0.000	0.000	0.030	0.070	0.130	0.193	0.194	0.123
Çubuk II	0.026	-0.011	-0.027	-0.043	-0.032	-0.045	0.014	0.030	0.071	0.127	0.122	0.081
Kavşakkaya	0.021	-0.007	-0.021	-0.034	-0.025	-0.034	0.013	0.025	0.057	0.101	0.097	0.065
Kurtboğazı	0.031	-0.005	-0.027	-0.043	-0.032	-0.039	0.020	0.035	0.076	0.133	0.128	0.087
Babasultan	0.017	0.008	-0.014	-0.023	-0.019	-0.012	0.015	0.033	0.049	0.077	0.081	0.052

Table A. 3 (continued)

Boğazköy	0.019	0.010	-0.009	-0.018	-0.014	-0.008	0.017	0.032	0.047	0.072	0.075	0.049
Akyar	0.025	-0.012	-0.027	-0.043	-0.032	-0.045	0.014	0.029	0.070	0.126	0.122	0.080
Asartepe	0.033	-0.004	-0.027	-0.043	-0.032	-0.038	0.021	0.037	0.078	0.134	0.129	0.088
Çamlıdere	0.030	-0.007	-0.027	-0.043	-0.032	-0.041	0.018	0.034	0.075	0.131	0.126	0.085
Doğanözü	0.019	-0.002	-0.015	-0.024	-0.018	-0.021	0.013	0.022	0.045	0.077	0.075	0.051
Eğrekkaya	0.029	-0.008	-0.027	-0.043	-0.032	-0.042	0.017	0.033	0.073	0.130	0.125	0.084
Gökçekaya	0.027	0.021	-0.013	-0.025	-0.001	0.009	0.031	0.033	0.060	0.097	0.088	0.066
Günyurdu	0.023	0.008	-0.026	-0.035	-0.033	-0.023	0.020	0.048	0.073	0.116	0.121	0.077
Kızıldamlar	0.015	0.000	-0.031	-0.035	-0.035	-0.032	0.012	0.039	0.065	0.108	0.113	0.069
Sarıyar	0.028	0.009	-0.014	-0.027	-0.002	0.007	0.029	0.031	0.058	0.095	0.087	0.065
Yenice	0.029	0.023	-0.010	-0.023	0.002	0.011	0.033	0.035	0.062	0.099	0.091	0.069
Aşağıkuzfındık	0.041	0.003	-0.023	-0.054	0.003	-0.006	0.016	0.009	0.061	0.075	0.048	0.042
Beşkarış	0.028	0.000	-0.016	-0.041	0.001	-0.006	0.010	0.005	0.043	0.053	0.033	0.029
Dodurga	0.050	0.002	-0.029	-0.070	0.003	-0.009	0.019	0.009	0.076	0.094	0.059	0.052
Kureyşler	0.010	0.000	-0.006	-0.015	0.000	-0.002	0.004	0.002	0.016	0.020	0.012	0.011
Porsuk	0.054	0.005	-0.028	-0.067	0.006	-0.006	0.022	0.013	0.080	0.098	0.063	0.055
Çatören	0.051	0.002	-0.029	-0.070	0.003	-0.009	0.019	0.010	0.076	0.095	0.059	0.052
Kunduzlar	0.051	0.003	-0.029	-0.069	0.003	-0.009	0.019	0.010	0.077	0.095	0.060	0.052

Table A. 4. Annual average water use amount of the demand sites in the baseline simulation period

Name of the Demand Site	**Subbasin**	**Type**	**Source**	**Annual Average Water Use (hm^3)**
US_Aktaş_GW_Municipal	Upper Sakarya	Municipal	Groundwater	3.1
US_Aktaş_GW_Industrial	Upper Sakarya	Industry	Groundwater	5.8
US_Aktaş_SW_Municipal	Upper Sakarya	Municipal	Surface water	0.2
US_Aydınlı_GW_Municipal	Upper Sakarya	Municipal	Groundwater	35.2
US_Aydınlı_GW_Industrial	Upper Sakarya	Industry	Groundwater	3.4
US_Aydınlı_SW_Municipal	Upper Sakarya	Municipal	Surface water	7.2
US_Ayvalı_GW_Municipal	Upper Sakarya	Municipal	Groundwater	1.0
US_Ayvalı_GW_Industrial	Upper Sakarya	Industry	Groundwater	0.0
US_Ayvalı_SW_Municipal	Upper Sakarya	Municipal	Surface water	9.0
US_Çıkış_GW_Municipal	Upper Sakarya	Municipal	Groundwater	7.4
US_Çıkış_GW_Industrial	Upper Sakarya	Industry	Groundwater	0.0
US_Eskişehir_SW_Municipal	Upper Sakarya	Municipal	Surface water	3.2
US_OSB_Emirdağ	Upper Sakarya	Industry	Groundwater	0.5

Table A. 4 (continued)

US_OSB_Polatlı	Upper Sakarya	Industry	Groundwater	0.3
PR_Eşenkara_GW_Municipal	Porsuk	Municipal	Groundwater	8.7
PR_Eşenkara_GW_Industrial	Porsuk	Industry	Groundwater	19.4
PR_Eşenkara1_SW_Municipal	Porsuk	Municipal	Surface water	23.1
PR_Eşenkara2_SW_Municipal	Porsuk	Municipal	Surface water	2.8
PR_Kıranharmanı_Industrial	Porsuk	Industry	Groundwater	48.5
PR_Kıranharmanı_GW_Municipal	Porsuk	Municipal	Groundwater	22.1
PR_Kıranharmanı_SW_Municipal	Porsuk	Municipal	Surface water	22.8
PR_OSB2_Kutahya	Porsuk	Industry	Groundwater	3.2
ANK_OSB_Anadolu	Ankara	Industry	Groundwater	1.7
ANK_OSB_İvedik	Ankara	Industry	Surface water	7.7
ANK_OSB_Ostim	Ankara	Industry	Surface water	7.5
ANK_GW_Municipal	Ankara	Municipal	Groundwater	64.3
ANK_GW_Industry	Ankara	Industry	Groundwater	33.8
ANK_SW_Municipal	Ankara	Municipal	Surface water	248.8
KIR_GW_Municipal	Kirmir	Municipal	Groundwater	9.3
KIR_SW_Municipal	Kirmir	Municipal	Surface water	7.3
MS_Bilecik OSB\Bilecik 1. OSB	Middle Sakarya	Industry	Groundwater	2.8
MS_Bilecik OSB\Bilecik 2. OSB	Middle Sakarya	Industry	Groundwater	0.8
MS_Bilecik OSB\Bozuyuk OSB	Middle Sakarya	Industry	Groundwater	0.0
MS_Bilecik OSB\Osmaneli OSB	Middle Sakarya	Industry	Groundwater	0.5
MS_Bilecik OSB\Pazaryeri OSB	Middle Sakarya	Industry	Groundwater	0.0
MS_Bilecik OSB\Sogut OSB	Middle Sakarya	Industry	Groundwater	0.5
MS_Doğançay_GW_Municipal	Middle Sakarya	Municipal	Groundwater	4.0
MS_Doğançay_GW_Industry	Middle Sakarya	Industry	Groundwater	26.8
MS_Doğançcay_SW_Municipal	Middle Sakarya	Municipal	Surface water	26.1
MS_Kayabeli_GW_Municipal	Middle Sakarya	Municipal	Groundwater	7.7
MS_Kayabeli_GW_Industry	Middle Sakarya	Industry	Groundwater	6.0
MS_Kayabeli_SW_Municipal	Middle Sakarya	Municipal	Surface water	29.4
GOK_Inegol OSB	Göksu	Industry	Groundwater	1.1
GOK_GW_Municipal	Göksu	Municipal	Groundwater	36.0
GOK_GW_Industry	Göksu	Industry	Groundwater	10.0
GOK_Yenisehir OSB	Göksu	Industry	Groundwater	0.0
GOK_SW_Municipal	Göksu	Municipal	Surface water	11.7
LS_Adatepe_Sapanca_Municipal	Lower Sakarya	Municipal	Surface water	39.0
LS_Adatepe_GW_Municipal	Lower Sakarya	Municipal	Groundwater	5.1
LS_Adatepe_GW_Industrial	Lower Sakarya	Industry	Groundwater	14.4

Table A. 4 (continued)

LS_Adatepe_SW_Municipal	Lower Sakarya	Municipal	Surface water	17.8
LS_Adatepe_SW_Industrial	Lower Sakarya	Industry	Surface water	8.5
LS_Mudurnu_GW_Municipal	Lower Sakarya	Municipal	Groundwater	3.8
LS_Mudurnu_GW_Industrial	Lower Sakarya	Industry	Groundwater	7.9
LS_Mudurnu_SW_Municipal	Lower Sakarya	Municipal	Surface water	41.3
LS_Mudurnu_SW_Industry	Lower Sakarya	Industry	Surface water	3.6
LS_Sapanca_Municipal	Lower Sakarya	Municipal	Surface water	10.5
LS_Sapanca_Industry	Lower Sakarya	Industry	Surface water	10.8

Table A. 5. Power plants defined in the LEAP model

Name of PP	Plant Type	Subbasin	Installed Power (MW)	Water Consumption Factor (m^3/MWh)	Water Withdrawal Factor (m^3/MWh)	Year of Commissioning
Enka Gebze NGPP	Natural Gas	Lower S.	1540	0.10	0.16	2004
Baymina Ankara NGPP	Natural Gas	Ankara	798	0.66	1.32	2004
Enka Adapazarı NGPP	Natural Gas	Lower S.	770	0.10	0.18	2004
Çayırhan TPP	Lignite	Middle S.	620	2.60	3.80	2004
Seyitömer TPP	Lignite	Porsuk	600	2.60	3.80	2004
Gökçekaya HPP	Hydroelectric	Middle S.	278	-	-	2004
Aksa Bolu Göynük TPP	Lignite	Middle S.	270	2.85	2.96	2014
Sarıyar HPP	Hydroelectric	Middle S.	160	-	-	2004
Eskişehir OSB NGPP	Natural Gas	Porsuk	59	0.01	0.01	2004
Ostim NGPP	Natural Gas	Ankara	41	0.78	0.97	2004
Metristepe WPP	Wind	Middle S.	39	0.00	0.00	2012
Yenice HPP	Hydroelectric	Middle S.	38	-	-	2004
Meteksan NGPP	Natural Gas	Ankara	37	0.01	0.01	2006
Doğançay HPP	Hydroelectric	Lower S.	30	-	-	2014
Tekno Enerji Bilecik NGPP	Natural Gas	Middle S.	26	0.01	0.01	2012
Mamak Çöplüğü BPP	Biogas	Ankara	25	0.78	0.97	2004
Eti Soda TPP	Lignite	Ankara	24	0.10	0.10	2004
Çadırtepe BPP	Biogas	Ankara	23	0.01	0.01	2012
Ak Gıda NGPP	Natural Gas	Middle S.	23	0.78	0.97	2004
Ortadoğu Rulman NGPP	Natural Gas	Ankara	20	0.01	0.01	2005
Esgaz Kırka RM/A FOPP	Fuel oil	Upper S.	18	0.01	0.01	2004
HABAŞ Bilecik FOPP	Fuel oil	Middle S.	18	0.01	0.01	2004
Beyköy HPP	Hydroelectric	Middle S.	17	-	-	2004
Göksu HPP	Hydroelectric	Lower S.	17	-	-	2004

Table A. 5 (continued)

Kazım Taşkent		Porsuk				
Eskişehir Şeker						
Fabrikası NGPP	Natural Gas		16	0.01	0.01	2004
Ilgın şeker		Upper S.				
Fabrikası TPP	Lignite		14	0.10	0.10	2004
Bükor II HPP	Hydroelectric	Middle S.	13	-	-	2014
ITC Katı Atık		Ankara				
BPP	Biogas		11	0.78	0.97	2004
Sanko Tekstil		Göksu				
İnegöl NGPP	Natural Gas		11	0.01	0.01	2007
Doğançay II HPP	Hydroelectric	Lower S.	10.1	-	-	2014
Boğazköy HPP	Hydroelectric	Göksu	10	0.10	0.10	2010
Adapazarı Şeker		Lower S.				
Fabrikası TPP	Coal		10	-	-	2004
Darca HPP	Hydroelectric	Middle S.	9.6	-	-	2012
Adasu HPP	Hydroelectric	Lower S.	9.6	-	-	2013
Pamukova HPP	Hydroelectric	Middle S.	9.3	-	-	2013
Asaş Alüminyum		Lower S.				
NGPP	Natural Gas		8.6	0.01	0.01	2004
Akyazı NGPP	Natural Gas	Lower S.	7.52	0.01	0.01	2004

NGPP:Natural Gas Power Plant; TPP: Thermal Power Plant; HPP: Hydroelectric Power Plant; BPP: Biogas Power Plant; WPP: Wind Power Plant; FOPP: Fuel Oil Power Plant

CURRICULUM VITAE

Surname, Name: Özcan, Zeynep

EDUCATION

Degree	Institution	Year of Graduation
MS	METU Environmental Engineering	2016
BS	METU Environmental Engineering	2014
High School	Kalaba Anadolu High School, Ankara	2008

FOREIGN LANGUAGES

Advanced English, Basic Italian

PUBLICATIONS

1. Özcan, Z., Köksal, M.A., Alp, E., 2020, Evaluation of Water–Energy Nexus in Sakarya River Basin, Turkey. In: Naddeo, V., Balakrishnan, M., Choo, KH. (eds) Frontiers in Water-Energy-Nexus—Nature-Based Solutions, Advanced Technologies and Best Practices for Environmental Sustainability. Advances in Science, Technology & Innovation. Springer, Cham. https://doi.org/10.1007/978-3-030-13068-8_105
2. Özcan Z., Kentel, E. and Alp, E., 2017, Evaluation of the Best Management Practices in a Semi-Arid Region with High Agricultural Activity, Agricultural Water Management, Vol. 540, 40-49. https://www.sciencedirect.com/science/article/pii/S0378377417303025
3. Özcan Z., Başkan O., Düzgün, H.B, Kentel, E., and Alp, E., 2017, A pollution fate and transport model application in a semi-arid region: Is some number better than no number?, Science of the Total Environment, Vol. 595, 425–440. https://www.sciencedirect.com/science/article/pii/S0048969717307702